





This is to certify that the

thesis entitled

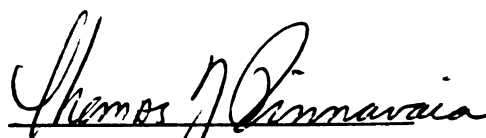
STRUCTURE DIRECTING ALKALI  
AND ALKALINE EARTH METAL IONS IN THE SOLUTION ORDERING  
OF GUANOSINE MONOPHOSPHATES

presented by

Elene Bouhoutsos-Brown

has been accepted towards fulfillment  
of the requirements for

Ph.D. degree in Chemistry

  
Major professor

Date May 15, 1980



OVERDUE FINES:

25¢ per day per item

RETURNING LIBRARY MATERIALS:

Place in book return to remove  
charge from circulation records

\_\_\_\_\_

\_\_\_\_\_

STRUCTURE DIRECTING ALKALI  
AND ALKALINE EARTH METAL IONS IN THE SOLUTION ORDERING  
OF GUANOSINE MONOPHOSPHATES

By

Elene Bouhoutsos-Brown

A DISSERTATION

Submitted to  
Michigan State University  
in partial fulfillment of the requirements  
for the degree of

DOCTOR OF PHILOSOPHY

Department of Chemistry

1980



I

(5'-3')

that a

The mos

multipl

dialkal

process

counter

size-se

orderin

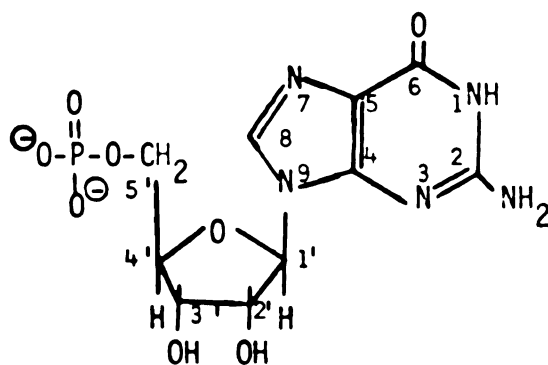
## ABSTRACT

### STRUCTURE DIRECTING ALKALI AND ALKALINE EARTH METAL IONS IN THE SOLUTION ORDERING OF GUANOSINE MONOPHOSPHATES

By

Elene Bouhoutsos-Brown

In aqueous solution, the dianion of guanosine-5'-monophosphate (5'-GMP<sup>2-</sup>) (shown below) is known to form regular ordered structures that are slow to exchange on the <sup>1</sup>H NMR time scale.<sup>1</sup>



The most compelling evidence for structure formation is the presence of multiple inequivalent H(8) resonances in the limiting spectra of dialkali metal ion salts in D<sub>2</sub>O solution near 0° C. This self-assembly process is dramatically dependent on the nature of the alkali metal counterion, which is believed to direct structure formation through a size-selective coordination mechanism.<sup>2</sup> Such metal ion dependent ordering is unprecedented in other nucleotide systems. All work to date

on alial  
systems  
the struc  
objective  
at metal  
different  
presence  
that does  
assembly.

Pro

TMA<sub>2</sub>GMP s  
generated  
contrast,  
distinctl  
metal ion  
pattern i  
that four  
"complex"  
as most u

Stud

ions are  
tetramer  
center of  
found for  
one type  
fraction

on alkali metal ion interactions with 5'-GMP has been done on pure salt systems with a metal ion to  $\text{GMP}^{2-}$  ratio of 2:1. Under these conditions, the structure directing metal ion is present in excess. Thus, the prime objective of this research was to examine the self-assembly phenomenon at metal ion to  $\text{GMP}^{2-}$  ratios between 0 and 2, since in this range different self-structures may be formed. Such ratios require the presence of a cation that is not a structure director by itself, and that does not inhibit the activity of cations capable of directing self-assembly. Tetramethylammonium ( $\text{TMA}^+$ ) was found to be such an ion.

Proton NMR studies of  $\text{Na}^+$  as the structure directing ion in the  $\text{TMA}_2\text{GMP}$  system have shown that only one set of sodium self-structures is generated, regardless of the metal ion to nucleotide ratio. In contrast, the addition of  $\text{K}^+$  or  $\text{Rb}^+$  to  $\text{TMA}_2\text{GMP}$  results in two sets of distinctly different NMR detectable self-structures, depending on the metal ion to  $\text{GMP}^{2-}$  ratio. At high  $\text{GMP}^{2-}/\text{M}^+$  ratio, a "simple" peak pattern is formed. At low  $\text{GMP}^{2-}/\text{M}^+$  ratio, the self-structure formed is that found for the homoionic  $\text{K}_2\text{GMP}$  system, and has been termed a "complex" structure. The  $\text{Na}^+$  self-structures are the simplest, as well as most unique of the alkali metal ions self-assembled  $\text{GMP}^{2-}$  complexes.

Studies of the structure-directing abilities of the alkali metal ions are not inconsistent with structure arising from stacking of tetramer units with  $\text{M}^+$  at the center of the tetramers ( $\text{Na}^+$ ) or at the center of two stacked tetramer sites ( $\text{K}^+$ ,  $\text{Rb}^+$ ). However, evidence was found for multiple equilibria resulting from the existence of more than one type of metal ion binding site per structured nucleotide unit. The fraction of structure present in solution as a function of  $\text{GMP}^{2-}$  to  $\text{Na}^+$

ratio shows a maximum at about  $1 \text{ GMP}^{2-}/\text{Na}^+$ . Furthermore, the addition of  $\text{Na}^+$  to  $\text{Na}_2\text{GMP}$  results in a decrease in the extent of self-assembly in solution, suggesting the blocking of sites which are necessary for self-assembly. These sites are concluded to be the phosphates on adjacent stacked tetramers which chelate the metal ion. The addition of  $\text{K}^+$ ,  $\text{Na}^+$  or  $\text{TMA}^+$  to  $\text{K}_2\text{GMP}$  results in a shift in the equilibrium concentrations of the self-assembled structures to favor those structures present normally only at very high  $\text{K}_2\text{GMP}$  concentrations. This is a nonspecific ion effect which is time dependent and has been attributed to a phosphate interaction.

Although  $\text{K}^+$  is a better stabilizing ion than  $\text{Na}^+$ , the latter ion was found to be the better structure director. This conclusion is based on the observation that the addition of  $\text{K}^+$  to a solution containing a high ratio of  $\text{GMP}^{2-}/\text{Na}^+$  results in the stabilization of the  $\text{Na}^+$  self-structure, and that the addition of  $\text{Na}^+$  to the "simple"  $\text{K}^+$  self-structure results in it being replaced by a  $\text{Na}^+$ -type of self-structure. On the other hand, the addition of  $\text{K}^+$  to ordered  $\text{Na}_2\text{GMP}$  results in the  $\text{Na}^+$  structure being replaced by a  $\text{K}^+$ -type structure, suggesting that once the phosphates are blocked by excess  $\text{Na}^+$ , the  $\text{K}^+$  is forced to compete for the structure directing position.

$\text{Li}^+$  is not a structure-inert cation. Although  $\text{Li}^+$  does not direct self-association of  $\text{GMP}^{2-}$ ,  $\text{Li}^+$  in solution can induce changes in the  $\text{Na}^+$  and  $\text{K}^+$  (but not  $\text{Cs}^+$ ) self-structured forms of the nucleotide. This is consistent with the phosphate being involved in structure formation, since  $\text{Li}^+$  would be expected to closely associate with the phosphate.

$\text{Cs}^+$ , on the other hand, can induce 5% NMR detectable self-structure

in the limiting case. The addition of small amounts of a strong structure directing ion such as  $\text{Na}^+$ ,  $\text{K}^+$  or  $\text{Rb}^+$  to  $\text{Cs}_2\text{GMP}$  dramatically increases the degree of self-structure formation. The self-assembled units are no longer those characteristic of the strong structure-directing cation, but are unique. Thus,  $\text{Cs}^+$  is active in structure formation when used in conjunction with a strong structure-directing cation.

The use of the  $\text{TMA}^+$  ion enabled an investigation of the alkaline earth cations.  $\text{Sr}^{2+}$  and  $\text{Ba}^{2+}$  were found to be capable of directing self-assembly. This is consistent with considerations of ionic radii applied to the alkali metal ions for the size selective mechanism.

A survey of the structure-forming properties of five other GMP derivatives (2'-GMP, 3'-GMP, 2',3'-cGMP, 3',5'-cGMP and 5'-dGMP) has shown that structure formation can occur in all cases in the presence of an appropriate structure-directing alkali or alkaline earth metal ion.

#### References

1. T. J. Pinnavaia, H. T. Miles, and E. D. Becker, J. Am. Chem. Soc., 97, 7198 (1975).
2. T. J. Pinnavaia, C. L. Marshall, C. M. Mettler, C. L. Fisk, H. T. Miles and E. D. Becker, J. Am. Chem. Soc., 100, 3625 (1978).

In memory of my brother,  
Constantine Dimitri Bouhoutsos

## ACKNOWLEDGEMENT

I would like to thank Houston for the love and understanding that he has shown throughout the years, as well as for typing this dissertation.

I would like to thank my parents, Drs. Jacqueline and Dimitri Bouhoutsos, for their constant love and enthusiastic encouragement throughout the years. I also acknowledge the love of my grandmothers, Bertha Cotcher and Eugenia Bouhoutsos.

Dr. T. J. Pinnavaia is both an able and patient teacher, as well as an excellent researcher and outstanding person. There are not enough words to express the respect and appreciation I hold for him as a research director and a friend. I am proud to have received my graduate training from Dr. Pinnavaia, and look forward to a continuing association with him.

The entire chemistry faculty at Michigan State University had an influence on my graduate career. In particular, I would like to thank my guidance committee, especially my second reader Dr. B.A. Averill, for the time they invested and the interest they expressed in me and my research.

I would like to acknowledge my closest friends and colleagues for making graduate school something special: Chris and Susan Marshall, Scott Sandholm, Walt Cleland, Tad and Laura Quayle, Barb Duhl-Emswiler, John Emswiler, Steve Christiano, Eileen Mason, Rich Barr and Paul Manis.

Finally, I would like to thank the faculty of the department of



chemistry at U.C.L.A., especially Drs. D. A. Evans, D. S. Eisenberg, M. Baur and M. F. Nicol, for cultivating my initial interest in chemistry.

## TABLE OF CONTENTS

	Page
INTRODUCTION	
I. Statement of General Objectives	2
II. Guanine and Its Derivatives	4
A. Guanine.	4
i. The Bases of DNA and RNA.	4
ii. Base Stacking Interactions.	4
B. Guanosine.	8
C. Guanosine Monophosphates.	9
i. Acyclic Mononucleotides.	9
ii. Cyclic Mononucleotides.	10
iii. Complementary Hydrogen Bonding and Self Association.	11
D. Polynucleotides.	14
III. Conformation Studies	15
A. Definition.	15
B. Syn vs. Anti Conformations.	20
C. Ribose Conformation.	25
D. The C(4')-C(5') and C(5')-O(5') Conformations.	25
E. Cyclic Nucleotide Conformations.	25

IV. The Interaction of Metal Ions with Guanine and Its Derivatives	27
A. X-ray Structure Determination.	28
i. Transition Metal Ions.	28
ii. Alkali and Alkaline Earth Metal Ions.	29
B. Nucleoside-Metal Ion Interaction in DMSO.	33
C. Guanosine Metal Ion Interactions in H <sub>2</sub> O.	37
D. 5'-GMP Alkali Metal Ion Interactions in Water.	40
E. Other Systems.	43
V. Specific Goals of this Research.	45
VI. Practical Considerations.	46
EXPERIMENTAL	
I. Materials, Techniques and Preparation	52
II. Instrumentation	53
A. Nuclear Magnetic Resonance Spectroscopy.	53
B. Ultraviolet Absorption Spectroscopy.	54
RESULTS	
I. Structure Forming Homoionic Salts of 5'-GMP	55
II. The Sodium-GMP Self-Structure	59
A. Tetramethylammonium as a Structure-Inert Cation.	59
B. TMA <sup>+</sup> /GMP <sup>2-</sup> Ion Pairing.	65
C. HDO/GMP <sup>2-</sup> Association.	72
D. Destabilization of the Na <sup>+</sup> Self-Structure by Excess Na <sup>+</sup> and K <sup>+</sup> .	72
E. Stabilization of the Na <sup>+</sup> Self-Structure by K <sup>+</sup> .	81
F. The Structure Directing Influence of Li <sup>+</sup> .	86



III.	The Potassium-GMP Self-Structure	91
A.	"Simple" and "Complex" $K^+$ /GMP <sup>2-</sup> Structure.	91
B.	Effect of Excess $K^+$ on the "Complex" $K_2$ GMP Self-Structure.	91
C.	Stability of the "Simple" $K^+$ Structure in the Presence of $Na^+$ .	105
D.	Effects of $Li^+$ on the $K^+$ Self-Structure.	112
IV.	The Rubidium-GMP Self-Structure	118
A.	Similarity of $K^+$ and $Rb^+$ Structuring Patterns.	118
B.	$Li^+$ - $Rb^+$ /GMP <sup>2-</sup> Gel Formation.	125
V.	The Cesium-GMP Self-Structure	126
A.	Effect of $Li^+$ on the Extent of the $Cs^+$ -GMP <sup>2-</sup> Self-Structure.	126
B.	Effect of Addition of $Na^+$ and $K^+$ to the $Cs^+$ Self-Structure.	126
VI.	Alkaline Earth Salts of 5'-GMP	136
VII.	<sup>1</sup> H Proton Resonances of GMP Self-Structures in Water	142
VIII.	A Survey of GMP Derivatives	154
A.	2'-M <sub>2</sub> GMP (M = $Na^+$ , $K^+$ ).	154
B.	3'-M <sub>2</sub> GMP (M = TMA <sup>+</sup> , $Na^+$ , $K^+$ ).	154
C.	2',3'-Cyclic GMP.	161
D.	3',5'-Cyclic GMP.	161
E.	Inosine-5'-Monophosphate.	171
F.	M <sub>2</sub> dGMP (M = TMA <sup>+</sup> , $Li^+$ , $Na^+$ , $K^+$ , $Rb^+$ , $Cs^+$ , $Sr^{2+}$ ).	171
i.	Sodium.	171
ii.	Potassium.	179
iii.	Rubidium.	184
iv.	Strontium.	189
v.	Summary.	192

DISCUSSION	
I. The Advantages of $\text{TMA}^+$ as a Counter-Ion	193
II. Specific and Non-Specific $\text{Na}^+$ and $\text{K}^+$ Ion Complexation Reactions	194
A. The Best Structural Model and Evidence for Specific Metal Ion Binding.	194
B. Other Models Which Have Been Proposed.	198
C. Evidence for Non-Specific Metal Binding Sites and a Suggested Model.	201
D. Features of the Outer Lines in a Sodium 5'-GMP Self-Structure.	219
E. Comparison to Polynucleotide and Nucleoside Systems.	222
III. Cesium "Structure Director" Systems	223
IV. The $\text{Sr}^{2+}$ and $\text{Ba}^{2+}$ Systems	227
V. Derivatives	228
CONCLUSIONS	231
RECOMMENDATIONS	
A. General Directions.	235
B. Suggested Experiments.	235
List of References	239
APPENDIX A	250
APPENDIX B	275

## LIST OF TABLES

	Page
Table 1. Molecular Conformation of Some Nucleotides.	23
Table 2. Crystallographically Determined Geometries of Metal-Nucleoside and Metal-Nucleotide Complexes.	30
Table 3. Alkali and Alkaline Earth Nucleotide and Dinucleotide Coordination.	36
Table 4. Dependence of $\text{Na}^+$ -Structure Formation on $\text{Na}^+/\text{GMP}^{2-}$ Concentration for Three Different $\text{TMA}^+/\text{Na}^+/\text{GMP}^{2-}$ Solutions.	62
Table 5. The Difference in the Percent Species Present Represented by a Peak as Determined by Integration at Two Different Field Strengths, both with and without Peak Suppression ( $0.56 \text{ M Na}_2\text{GMP}$ and $0.32 \text{ M TMACl}$ at $0^\circ \text{ C}$ ).	71
Table 6. Effective $\text{NH}/\text{H}(8)$ Ratios for Various Temperatures and Concentrations of Solutions Exhibiting a Sodium Self-Structure.	153

## LIST OF FIGURES

	Page
<p>Figure 1. The purine and pyrimidine parent compounds nucleosides and nucleotides.  denotes a point of ribose attachment.  denotes points of possible phosphate attachment.</p>	6
<p>Figure 2. The planar tetramer unit showing hydrogen bonding between N(1) and O(6) as well as N(2) and N(7) by dashed lines. R represents the ribophosphate group. Note the cavity formed in the center of the tetramer by the O(6) positions.</p>	13
<p>Figure 3. Newman projections showing the preferred nucleotide conformations and their nomenclature.</p>	17
<p>Figure 4. Four preferred conformations for the nucleotides: (a) C(3')-endo, anti, <i>gg</i>; (b) C(2')-endo, anti, <i>gg</i>; (c) C(3')-exo, anti, <i>gg</i>; (d) C(2')-exo, anti, <i>gg</i>. Taken from reference 55.</p>	19
<p>Figure 5. The pseudo rotation circle shows the relationship between the phase angle of pseudo rotation <math>P</math> and the 10 envelope <math>C_5</math> and 10 symmetric twist <math>C_2</math> conformations of the furanose ring. The pseudo mirror symmetry in the envelope conformations is indicated by the dashed lines and the pseudo twofold axis in the symmetric twist conformations is shown by the arrows. The signs of the torsional angles of the sugar ring are</p>	





indicated within the furanose ring. The preferred regions for the P values are 0-18 and 144-180 and they are generally referred to as C(3')-endo and C(2')-endo puckerings. Taken from reference 57.

22

Figure 6. The sodium ion environments in 5'-Na<sub>2</sub>dGMP. Taken from reference 88.

32

Figure 7. (A) The calcium ion environments in GpC. Taken from reference 90. (B) The sodium ion environments in GpC. Taken from reference 89.

35

Figure 8. A schematic representation of an idealized complete set of experiments to study each nucleotide system. The x-axis indicates all dimetal nucleotide systems of interest. For each set of divisions, concentration increases from left to right. The z-axis represents all metal ions of interest to be added to the dimetal nucleotide systems. A single anion should be used in all metal salts. Concentration within each division increased from bottom to top. The y-axis represents temperature from 0-100° C.

50

Figure 9. The H(8) regions of the self-assembled alkali metal 5'-GMP<sup>2-</sup> salts at low temperature.

57

Figure 10. Effect of adding aliquots of 4.0 M NaCl on the H(8) region of 0.76 M (TMA)<sub>2</sub>GMP at 2.8° C. Initial GMP<sup>2-</sup> concentration (upper spectrum) is 0.76 M. Final GMP<sup>2-</sup> concentration (lower spectrum) is 0.64 M.

61

Figure 11. Graphical representations showing the results of three different experiments. The results of integrating the H(8) resonances to determine the concentration of structured nucleotide in solution when: (a) solid NaCl is added to 0.64 M (TMA)<sub>2</sub>GMP at 1.0° C;

(b) solution NaCl is added to 0.78 M (TMA)<sub>2</sub>GMP at 2.8° C; (c) ratios of 0.76 M (TMA)<sub>2</sub>GMP and 0.76 M Na<sub>2</sub>GMP are mixed maintaining constant volume in the presence of 0.5 M TMAcI at 0.3° C.

64

Figure 12. The H(8) resonances of 0.55 M (TMA)<sub>2</sub>GMP with 0.31 M NaCl at 4° C (A) without peak suppression and (B) irradiating the methyl resonance of TMA<sup>+</sup> at 3.2 ppm.

67

Figure 13. The H(8) resonances of 0.56 M Na<sub>2</sub>GMP with 0.36 M TMAcI. The dashed line represents the spectrum without peak suppression. The solid line represents the spectrum when the methyl resonance of TMA<sup>+</sup> is irradiated at 3.2 ppm. These spectra were recorded at 100 MHz on a Varian instrument, and were provided courtesy of 3M.

70

Figure 14. The H(8) resonances of 0.36 M Na<sub>2</sub>GMP at 1.5° C where the solid line represents the spectrum without peak suppression and the dashed line represents the spectrum when the H<sub>2</sub>O resonance is irradiated.

74

Figure 15. Comparison of the H(8) region of 0.78 M Na<sub>2</sub>GMP (lower spectrum) with 0.78 M Na<sub>2</sub>GMP containing 0.38 M NaCl (upper spectrum). Note the relative intensities of the monomer line and the structure lines.

76

Figure 16. Effect of adding aliquots of 4.0 M NaCl on the H(8) resonances of 0.91 M Na<sub>2</sub>GMP at 4° C. The initial GMP<sup>2-</sup> concentration (lower spectrum) is 0.91 M. The final GMP<sup>2-</sup> concentration (upper spectrum) is 0.84 M. Note that the intensity of the monomer resonance increases slightly with increasing Na<sup>+</sup>/GMP<sup>2-</sup> ratio.

78

- Figure 17. Effect of varying the  $\text{GMP}^{2-}/\text{Na}^+$  ratios on the fraction of structured  $\text{GMP}^{2-}$  in 0.78 M  $(\text{TMA})_2\text{GMP}$  at 0.3° C;  $[(\text{TMA})\text{Cl}] = 0.5$  M. 80
- Figure 18. Effect of adding aliquots of 4.0 M KCl on the H(8) region of 0.9 M  $\text{Na}_2\text{GMP}$  at 3.4° C. Note the increase in monomer line intensity and the increase in  $\text{K}^+$  structure lines with the decrease in  $\text{Na}^+$  structure lines. 83
- Figure 19. Effect of adding aliquots of 4.0 M KCl on the H(8) lines of a solution containing the  $\text{Na}^+$  self-structure at a  $\text{Na}^+/\text{GMP}^{2-}$  ratio of 0.5. Note the dramatic increase in the Na self-structure lines that appear at the expense of the monomer line at low  $\text{K}^+/\text{Na}^+$  ratios.  $[(\text{TMA})_2\text{GMP}] = 0.63$  M,  $[\text{NaCl}] = 0.32$  M. Temperature is 2.9° C. 85
- Figure 20. The melting out of H(8) lines for two solutions containing the  $\text{Na}^+$  self-structure at a total alkali metal ion to  $\text{GMP}^{2-}$  ratio of 0.66:1. Solution A contains a mixture of  $\text{K}^+$  and  $\text{Na}^+$  ( $\text{K}^+/\text{GMP}^{2-} = 0.50$ ,  $\text{Na}^+/\text{GMP}^{2-} = 0.16$ ); solution B contains only  $\text{Na}^+$  ( $\text{Na}^+/\text{GMP}^{2-} = 0.66$ ).  $[(\text{TMA})_2\text{GMP}] = 0.57$  M. 88
- Figure 21. Effect on the H(8) region of mixing different volumes of 0.72 M  $\text{Li}_2\text{GMP}$  and 0.72 M  $\text{Na}_2\text{GMP}$  at 2° C and constant overall volume. Note that at high  $\text{Li}^+$  concentration (upper spectrum) the lines arising from a normal sodium self-structure are no longer present. 90

- Figure 22. H(8) resonances observed upon addition of aliquots of 4.19 M KCl to 0.85 M (TMA)<sub>2</sub>GMP at 3.2° C. The "simple" structure (and monomer) is seen at  $\text{GMP}^{2-}/\text{K}^+ = 12, 6$  and 2. The "complex" structure is represented  $\text{GMP}^{2-}/\text{K}^+ = 1$  and 0.5. The initial  $\text{GMP}^{2-}$  concentration (lower spectrum) is 0.85 M. The final  $\text{GMP}^{2-}$  concentration (upper spectrum) is 0.60 M. 93
- Figure 23. The melting out of H(8) resonances of the "complex"  $\text{K}^+ - \text{GMP}^{2-}$  self-structure at  $\text{GMP}^{2-}/\text{K}^+ = 1.0$ . [(TMA)<sub>2</sub>GMP] = 0.70 M. [KCl] = 0.70 M. 95
- Figure 24. The H(8) region of (A) 0.5 M K<sub>2</sub>GMP prepared at room temperature and stored at 0° C as a function of time expressed in minutes, and (B) 0.5 M K<sub>2</sub>GMP prepared and stored at room temperature as a function of time in minutes. Spectra obtained at 3.6° C. 97
- Figure 25. The time dependence of the H(8) region of (A) 0.5 M K<sub>2</sub>GMP containing 0.38 M KCl prepared at room temperature and stored at 0° C, and (B) 0.5 M K<sub>2</sub>GMP containing 0.38 M KCl prepared and stored at room temperature. Time is measured in minutes from the time the solution was prepared as zero minutes. Spectra measured at 3.6° C. 100
- Figure 26. The melting out of the H(8) region of (A) 0.5 M K<sub>2</sub>GMP prepared and stored at room temperature, and (B) 0.5 M K<sub>2</sub>GMP containing 0.38 M KCl prepared and stored at room temperature. 102
- Figure 27. The H(8) region of (A) 0.5 M K<sub>2</sub>GMP stored for 10 hours at 0° C and recorded at 3.6° C, (B) 0.5 M K<sub>2</sub>GMP containing 0.38 M KNO<sub>3</sub> stored for more than 10 hours at 0° C and recorded at 3.6° C, (C) 0.5 M K<sub>2</sub>GMP containing 0.38 M TMACl stored for more than 10 hours



at 0° C and recorded at 3.6° C, (D) 0.5 M K<sub>2</sub>GMP containing 0.38 M KCl stored for 10 hours at 0° C and recorded at 3.6° C, and (E) 0.5 M K<sub>2</sub>GMP heated to boiling and then cooled in ice to 0° C with the spectrum immediately recorded at 3.6° C.

104

Figure 28. Effect on the H(8) resonances of 0.92 M K<sub>2</sub>GMP on addition of aliquots of 4.01 M NaCl at 4° C. The initial concentration of GMP<sup>2-</sup> (lower spectrum) is 0.92 M and the final concentration of GMP<sup>2-</sup> (upper spectrum) is 0.83 M. Note the ratio 1:2:0.17, (A) was recorded 96 hours after (B). The sample was stored at room temperature. A definite change in the relative intensities of the inner and outer lines is apparent.

107

Figure 29. Effect on the H(8) resonances of 0.92 M K<sub>2</sub>GMP on addition of aliquots of 4.03 M KCl at 4° C. The initial concentration of GMP<sup>2-</sup> (lower spectrum) is 0.92 M and the final concentration of GMP<sup>2-</sup> (upper spectrum) is 0.59 M.

109

Figure 30. Effect on the H(8) resonance of adding aliquots of 4.0 M NaCl to the "simple" potassium self-structure at 2.3° C. [(TMA)<sub>2</sub>GMP] = 0.63 M. [KCl] = 0.32 M.

111

Figure 31. Effect on the H(8) region of adding aliquots of 4.0 M KCl to 0.72 M GMP<sup>2-</sup> containing 0.56 M TMA<sup>+</sup> and 0.88 M Li<sup>+</sup> at 2.3° C.

114

Figure 32. Effect on the H(8) resonance of adding LiCl to a "simple" K<sup>+</sup>-GMP self-structure at 0.3° C. [(TMA)<sub>2</sub>GMP] = 0.775 M. [KCl] = 0.36 M.

117

Figure 33. The H(8) resonances observed upon addition of aliquots of 4.15 M RbCl to 0.85 M (TMA)<sub>2</sub>GMP at 3.2° C. The final GMP<sup>2-</sup> concentration was 0.60 M.

120

- Figure 34. Melting out of the structure lines in the H(8) region of 0.60 M Rb<sub>2</sub>GMP containing 1.70 M (TMA)Cl. 122
- Figure 35. Effect on the H(8) resonance of 0.72 M Cs<sub>2</sub>GMP upon addition of aliquots of 4.15 M RbCl at 3.6° C. 124
- Figure 36. Effect on the H(8) resonance of 0.85 M (TMA)<sub>2</sub>GMP upon addition of 3.2 M CsCl at 3° C. The final GMP<sup>2-</sup> concentration was 0.57 M. 128
- Figure 37. Effect on the H(8) region of adding 4.0 M LiCl to 0.72 M Cs<sub>2</sub>GMP at 3.6° C. The final GMP<sup>2-</sup> concentration was 0.61 M. 130
- Figure 38. Effect on the H(8) resonances of 0.72 M Cs<sub>2</sub>GMP upon addition of 4.0 M NaCl at 3.3° C. The final GMP<sup>2-</sup> concentration was 0.58 M. 132
- Figure 39. Effect on the H(8) resonances of 1.19 M Cs<sub>2</sub>GMP upon addition of aliquots of 1.1 M KCl at 5° C. The final GMP<sup>2-</sup> concentration was 0.87 M. 135
- Figure 40. Effect on the H(8) resonance of 0.73 M (TMA)<sub>2</sub>GMP upon addition of aliquots of 4.74 M SrCl<sub>2</sub> at 3.2° C. Due to the presence of precipitate, exact solution ratios were unattainable. 138
- Figure 41. Effect on the H(8) resonance of 0.73 M (TMA)<sub>2</sub>GMP upon addition of aliquots of 2.0 M BaCl<sub>2</sub> at 3.2° C. Due to the presence of precipitate, exact solution ratios were unattainable. 141
- Figure 42. The NH and H(8) regions of (A) 0.3 M Na<sub>2</sub>GMP in H<sub>2</sub>O at 2° C, and (B) 0.7 M Na<sub>2</sub>GMP in H<sub>2</sub>O at 2° C. These spectra were provided courtesy of Jeol. Co. 144

- Figure 43. The H(8) and unstructured NH<sub>2</sub> resonances for (A) 0.7 M Na<sub>2</sub>GMP at 2° C in H<sub>2</sub>O, (B) 0.3 M Na<sub>2</sub>GMP at 2° C in H<sub>2</sub>O, and (C) 0.1 M Na<sub>2</sub>GMP at 2° C in H<sub>2</sub>O. These spectra were provided courtesy of Jeol. Co. 147
- Figure 44. The H(8) and NH resonances of 0.91 M K<sub>2</sub>GMP at 2° C in H<sub>2</sub>O containing NaTSP (1 wt%). 149
- Figure 45. A comparison of the NH and H(8) regions of two spectra of 0.79 M (TMA)<sub>2</sub>GMP in H<sub>2</sub>O with 0.13 M NaCl and 0.40 M KCl at 1° C. (A) was recorded on a Bruker WH-180 without H<sub>2</sub>O peak suppression. (B) was provided courtesy of Bruker and represents the same system with H<sub>2</sub>O peak suppression. Note the intensity of the 7.57 ppm peak relative to the 7.25 ppm peak in both cases. 152
- Figure 46. H(8) resonances of 0.64 M 2'<sup>1</sup>Na<sub>2</sub>GMP. 156
- Figure 47. A temperature dependence study (° C) of the H(8) resonances of 0.85 M 2'<sup>1</sup>K<sub>2</sub>GMP. 158
- Figure 48. A concentration study of the H(8) resonances of 2'<sup>1</sup>K<sub>2</sub>GMP at 1.3° C. 160
- Figure 49. The H(8) region of (A) 0.5 M 3'(TMA)<sub>2</sub>GMP containing 0.19 M KCl and (B) 0.5 M 3'(TMA)<sub>2</sub>GMP both at 0.7° C. Some precipitate is present in solution (A). 163
- Figure 50. A temperature study (° C) of the H(8) region of 0.74 M 3',5'-cyclic NaGMP. As the temperature increases the concentration decreases due to crystallization of the salt. 166



- Figure 51. A temperature study ( $^{\circ}\text{C}$ ) of the ribose region of  $0.74\text{ M } 3',5'\text{-cyclic GMP}$  as the sodium salt. As the temperature increases the concentration decreases due to crystallization of the salt. 168
- Figure 52. Effect on the H(8) resonance of  $0.58\text{ M Na}_2\text{GMP}$  upon addition of aliquots of  $0.74\text{ M Na-}3',5'\text{-cGMP}$  at  $5^{\circ}\text{C}$ . An impurity in the system is marked with an X. 170
- Figure 53. The H(8) and H(1)' regions of a  $0.9\text{ M}$  solution of 2'deoxy-5'-GMP at neutral pH (A) with  $1.5\text{ Na}^+/\text{dGMP}^{1.5-}$  at  $0.7^{\circ}\text{C}$ , (B) with  $2.0\text{ Na}^+/\text{dGMP}^{1.5-}$  at  $0.7^{\circ}\text{C}$ , and (C) with  $2.0\text{ Na}^+/\text{dGMP}^{1.5-}$  at  $26.2^{\circ}\text{C}$ . 173
- Figure 54. A temperature study ( $^{\circ}\text{C}$ ) of the H(8) region of  $1.08\text{ M (TMA)}_2\text{dGMP}$  at pH = 5.45 containing  $0.245\text{ M NaTSP}$  to give a ratio of  $4.4\text{ dGMP}^-/\text{Na}^+$ . 176
- Figure 55. A temperature study ( $^{\circ}\text{C}$ ) of the H(8) region of  $0.61\text{ M (TMA)}_2\text{dGMP}$  at pH = 6.2 containing  $0.15\text{ M NaCl}$  to give a ratio of  $4.07\text{ dGMP}^-/\text{Na}^+$ . 178
- Figure 56. A temperature profile ( $^{\circ}\text{C}$ ) of the H(8) region of  $0.70\text{ M (TMA)}_2\text{dGMP}$  at pH = 5.45 containing  $0.16\text{ M KCl}$  to give a ratio of  $4.4\text{ dGMP}^-/\text{K}^+$ . 181
- Figure 57. A temperature study ( $^{\circ}\text{C}$ ) of the H(8) region of  $0.61\text{ M (TMA)}_2\text{dGMP}$  at pH = 6.2 containing  $0.16\text{ M KCl}$  to give a ratio of  $4.4\text{ dGMP}^-/\text{K}^+$ . 183
- Figure 58. A temperature study ( $^{\circ}\text{C}$ ) of the H(8) region of  $0.61\text{ M (TMA)}_2\text{dGMP}$  at pH = 6.3 containing  $0.11\text{ M RbCl}$  to give a ratio of  $5.27\text{ dGMP}^-/\text{Rb}^+$ . 186

- Figure 59. A comparison of the H(8) regions of solutions of 0.61 M (TMA)<sub>2</sub>dGMP at pH = 6.2 and 0.7° C with (A) 0.6 M LiCl, (B) 1.3 M CsCl, (C) 0.2 M KCl, (D) 0.2 M SrCl<sub>2</sub> and (E) 0.2 M NaCl. 188
- Figure 60. A temperature study (° C) of the H(8) region of 0.61 M (TMA)<sub>2</sub>dGMP at pH = 6.2 containing 0.12 M SrCl<sub>2</sub> to give a ratio of 5.01 dGMP<sup>2-</sup>/Sr<sup>2+</sup>. 191
- Figure 61. A representation (schematic) of the various stacking patterns for two tetramers. The double arrow represents the direction of the hydrogen bonds. 197
- Figure 62. Models proposed by Laszlo for the self-structures of 5'-GMP. (A) Shows the "staircase" model where M<sup>+</sup> represents either Na<sup>+</sup> or K<sup>+</sup>. The differences in H(8) environments he rationalizes in terms of (B), showing the overlap of tetramer units, where the open circles represent phosphates pointed "down" and the darkened circles represent phosphates pointed "up". 200
- Figure 63. A schematic diagram of the head-to-tail Na<sup>+</sup> self-structure. Na<sup>+</sup>'s are located above and below the top and bottom plates, respectively, complexed in the principal structure-directing site to the O(6) position. Additional Na<sup>+</sup> binding sites are the phosphates (represented by curved lines) from adjacent tetramers chelating the Na<sup>+</sup>. 205
- Figure 64. A schematic diagram of the sodium tetramer with the phosphate positions blocked by Li<sup>+</sup>. 207
- Figure 65. A schematic diagram of the proposed "simple" K<sup>+</sup> self-structure. 210

F

F

F

F

Fi

Fi

Fi

Fi

Fi

Fi

Figure 66.	A schematic diagram of the proposed "complex" $K^+$ self-structure.	211
Figure 67.	Proposed structure (schematic) of the "complex" $K^+$ structure in the presence of $Li^+$ . The increased phosphate shielding by $Li^+$ allows more plates to be stacked together without excessive build up of negative charge.	213
Figure 68.	A representation (schematic) of the ionic strength effects observed for the "complex" $K^+$ self-structure.	215
Figure 69.	Proposed structure (schematic) of a $Na^+$ self-structure in the presence of $K^+$ . The $Na^+$ occupies the principal structure-directing site at the center of the tetramer and the $K^+$ occupies the phosphate sites, stabilizing the self-structure.	217
Figure 70.	A schematic diagram of the relative stabilities of the $Na^+$ and $K^+$ pure and mixed $GMP^{2-}$ systems.	220
Figure 71.	Proposed structure (schematic) of the $Cs^+$ self-structure in the presence of $Na^+$ .	224
Figure 72.	A possible mixed $Cs^+-K^+$ or $Cs^+-Rb^+$ self-structure (schematic). The $Cs^+$ associates with the outer tetramer plates, while the $K^+$ or $Rb^+$ occupy the sites between the tetramers as well as the phosphate sites.	226
Figure 73.	A comparison of 0.72 $M$ $Na_2GMP$ and 0.72 $M$ $Li_2GMP$ at 2° C.	252
Figure 74.	A temperature profile of 0.72 $M$ $Na_2GMP$ from 2-30° C.	254
Figure 75.	A temperature profile of 0.72 $M$ $Na_2GMP$ from 35-45° C.	256

Figure 76.	A temperature profile of a 0.72 <u>M</u> $\text{GMP}^{2-}$ solution containing 12.5% $\text{Na}^+$ and 87.5% $\text{Li}^+$ .	258
Figure 77.	A temperature profile of a 0.72 <u>M</u> $\text{GMP}^{2-}$ solution containing 25% $\text{Na}^+$ and 75% $\text{Li}^+$ .	260
Figure 78.	A temperature profile from 2-30° C of a 0.72 <u>M</u> $\text{GMP}^{2-}$ solution containing 37.5% $\text{Na}^+$ and 62.5% $\text{Li}^+$ .	262
Figure 79.	A temperature profile from 35-45° C of a 0.72 <u>M</u> $\text{GMP}^{2-}$ solution containing 37.5% $\text{Na}^+$ and 62.5% $\text{Li}^+$ .	264
Figure 80.	A temperature profile of a 0.72 <u>M</u> $\text{GMP}^{2-}$ solution containing 50% $\text{Na}^+$ and 50% $\text{Li}^+$ .	266
Figure 81.	0.72 <u>M</u> $\text{GMP}^{2-}$ solutions containing different ratios of $\text{Na}^+$ to $\text{Li}^+$ at 2° C.	268
Figure 82.	0.72 <u>M</u> $\text{GMP}^{2-}$ solutions containing different ratios of $\text{Na}^+$ to $\text{Li}^+$ at 15° C.	270
Figure 83.	0.72 <u>M</u> $\text{GMP}^{2-}$ solutions containing different ratios of $\text{Na}^+$ to $\text{Li}^+$ at 20° C.	272
Figure 84.	0.72 <u>M</u> $\text{GMP}^{2-}$ solutions containing different ratios of $\text{Na}^+$ to $\text{Li}^+$ at 30° C.	274
Figure 85.	A 0.76 <u>M</u> $\text{Na}_2\text{GMP}$ solution containing 10% $\text{Tl}^+$ at 2° C.	277

STRUCTURE DIRECTING ALKALI  
AND ALKALINE EARTH METAL IONS IN THE SOLUTION ORDERING  
OF GUANOSINE MONOPHOSPHATES

## INTRODUCTION

### I. Statement of General Objective

The discovery of nucleic acids in the 1890's<sup>1</sup> opened a new, extremely vast and important area of research which has come to the forefront in the last thirty years. As the building blocks of life, DNA and RNA are the fundamental units which enable genetic information to be transmitted and preserved. A plethora of literature exists from a wide variety of disciplines relating to nucleic acids due to their multifaceted involvement in vital life processes. The biological functions of nucleic acids have been shown to often involve the participation of metal ions.<sup>2</sup> Due to the existence of multiple naturally occurring coordination sites, great interest has been generated with respect to different metal ion-nucleic acid interactions. Interest has been further spurred by the finding that Pt(II)-nucleic acid complexes have significant antineoplastic activity.<sup>3</sup> Several reviews of the literature on metal binding by nucleic acids and their constituents have appeared over the last decade,<sup>4</sup> but only recently have the alkali and alkaline earth metal ions not been overlooked completely.<sup>4e</sup> Despite the fact that a 70 kg healthy adult human contains  $2.3 \times 10^3$  g  $\text{Na}^+$  and  $1.7 \times 10^3$  g  $\text{K}^+$ ,<sup>5</sup> little is known about the specific interactions of these ions with nucleic acids. Far more is known about the actions of the less abundant transition metal ions.

In general, the role of the alkali metal ion in nucleic acid chemistry has been relegated to one of neutralizing the negative charge

on

den

di

re

re

on

de

so

th

su

se

of



on the phosphate groups. In contrast, Pinnavaia et al.<sup>6</sup> have demonstrated the first example of the ability of alkali metal ions to direct structure formation of a nucleotide through a size-selective mechanism. They found that the 5'-guanosine monophosphate dianion forms regular ordered structures in aqueous solution that are slow to exchange on the  $^1\text{H}$  NMR time scale. This self-assembly phenomenon was found to depend dramatically on the nature of the alkali metal ion present in solution.

The general objective of this research was a more detailed study of the metal ion directed self-assembly of 5'-guanosine monophosphate and a survey of some other guanosine monophosphate derivatives. The following sections give a brief review of guanine chemistry prior to a discussion of the specific goals of this research.



## II. Guanine and It's Derivatives

### A. Guanine

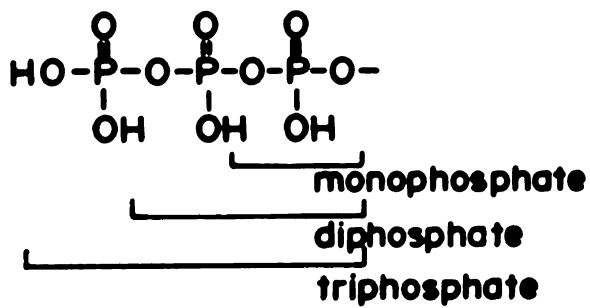
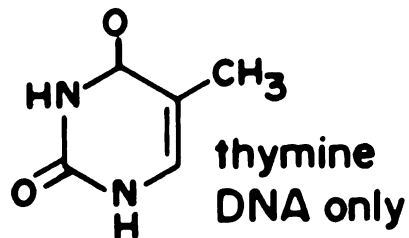
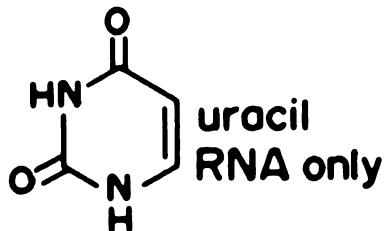
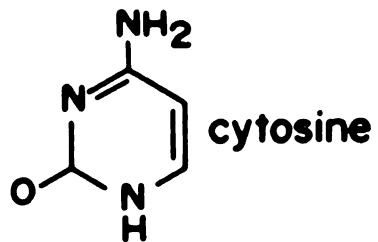
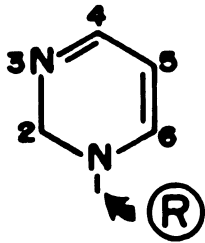
i. The Bases of DNA and RNA. Guanine is one of five aromatic nitrogenous bases that commonly occur in nucleic acids. The names, structures and the adopted heterocyclic numbering schemes of the five bases are shown in Figure 1. The pyrimidines are six membered rings, with thymine (T) found only in DNA and uracil(U) found only in RNA. The purines are pyrimidines with fused imidazole rings. Adenine (A), guanine (G) and cytosine (C) are found in both forms of cellular polynucleotide. A review of the literature of guanine chemistry and its derivatives through 1968 was compiled by Shapiro.<sup>7</sup>

Guanine was first isolated from bird droppings, although it is found throughout nature. For example, guanine crystals, which have a shiny silver appearance, are found in the scales of most bony fish and give rise to the lustrous appearance.<sup>8</sup> When substituted in the 9-position, guanine is found solely in the lactam (keto) form. Extensive tables of pK values and ultraviolet maxima for guanine and various derivatives have been compiled.<sup>7</sup> Although guanine has been studied by x-ray crystallography, it has a limited solution chemistry. This is primarily attributable to the low solubility of the base in water, one part in 200,000 at 20 °C.<sup>9</sup>

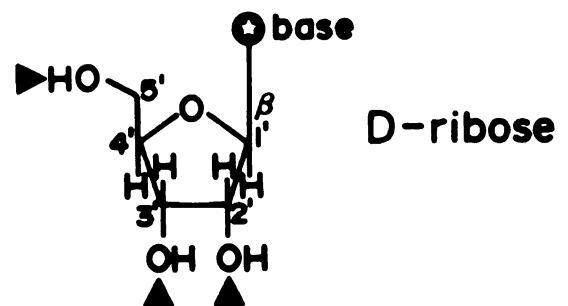
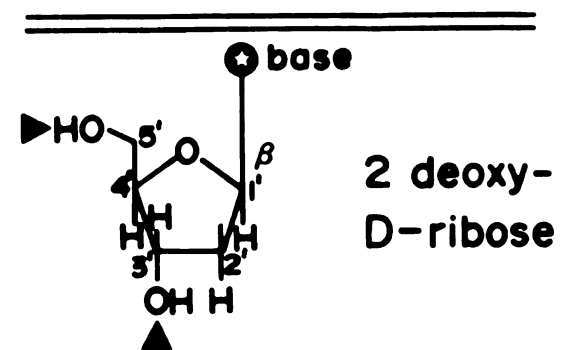
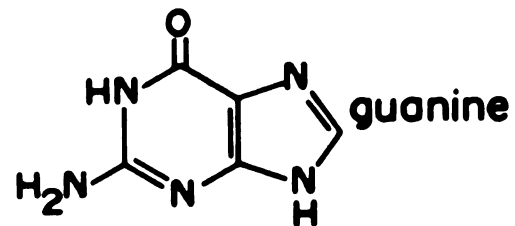
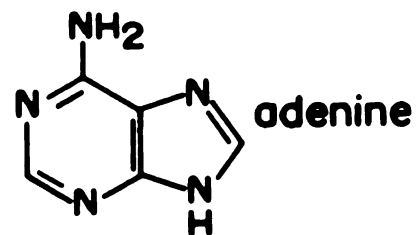
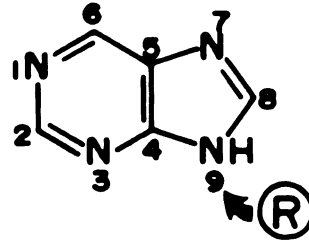
ii. Base Stacking Interactions. C.E. Bugg<sup>10</sup> compiled a review of the most commonly found purine-stacking interaction in crystals of purine derivatives and fibers of polynucleotides. He related these findings to aqueous solution stacking patterns. There are two basic stacking patterns, one with the imidazole moieties pointing in the same direction as found in guanine<sup>11</sup> and 8-azaguanine.<sup>12</sup> The other type of

Figure 1. The purine and pyrimidine parent compounds nucleosides and nucleotides.  denotes a point of ribose attachment.  denotes points of possible phosphate attachment.

## Pyrimidines



## Purines



stacking involves the bases being rotated about  $180^\circ$  with respect to each other, thus the imidazoles of adjacent bases point in opposite directions, although N(9) in both bases is found on the same side. He concluded that purine-stacking patterns involve overlapping the polar regions (carbon-heteroatom bonds) of one base with the polarizable ring system of an adjacent base. Bugg concluded that although purine derivatives<sup>13</sup> are known to stack vertically in aqueous solution, and to a far lesser extent in nonaqueous solvents, stacking is not entirely the result of hydrophobic solvent effects, although they are usually deemed responsible for base stacking. He agreed with Hanlon<sup>14</sup> that polarizable solvents which possess polar substituents, like dimethyl sulphoxide, interact with the polarizable  $\pi$ -electron systems of the purines to account for the absence of stacking interactions.

Gupta and Sasisekharan<sup>15</sup> have done theoretical calculations of base-base stacking interactions in the free base systems. They stated that in the guanine system, minimum energies are encountered for what they define as normal stacking (where the six membered ring of the one base is generally located over the five membered ring of the other and the upper and lower N(9) positions can be superimposed by performing a  $C_2$  rotation perpendicular to the plane of the base on the upper guanine unit) and inverted stacking (where the six membered ring is still over the five membered ring, but the N(9) positions are superimposable only by a  $C_2$  rotation about the C(4)-C(5) double bond of the upper guanine unit). Furthermore, they concluded that the highest geometric overlap between the bases does not necessarily give the most stable stacking pattern. The best base orientations were derived from consideration of monopole-monopole interactions and monopole-induced dipole interactions

in conjunction with the London-dispersion interaction and repulsive interaction. They felt that H-bonding plays an important role and compensated for stacking patterns that appear unfavorable or could have an additive effect.

B. Guanosine. Nucleosides are purine or pyrimidine bases linked to a D-ribose or D-deoxyribose sugar as the R group in the structures shown in Figure 1. The glycoside linkage involves a bond between either N(1) in a pyrimidine or N(9) in a purine and C(1') of the nonpolar furanose sugar ring. All naturally occurring nucleosides exist as the  $\beta$ -epimer; the  $\alpha$ -form has never been observed to date. A detailed discussion of the ribose moiety will be presented later. The nucleosides exhibit a higher solubility than do their parent compounds.

Of all the nucleic acid components, guanosine has the most complex structure, with the widest variety of possible hydrogen-bonding interactions.<sup>16</sup> Guschlbauer<sup>17</sup> noted that physio-chemical properties of the guanosine-containing region of nucleic acids frequently are different from the rest of the molecule. Intercalating dyes often prefer guanosine rich regions. For example, actinomycin<sup>18</sup> or ethidium bromide<sup>19</sup> are known to bind to guanosine residues preferentially. Platinum anticancer drugs,<sup>20</sup> specifically cis-(NH<sub>3</sub>)<sub>2</sub>PtCl<sub>2</sub>, have been shown to selectively associate with guanosine nucleotides as well as guanosine rich regions in DNA. The uniqueness of guanosine has been attributed to the multiple degrees of freedom about the glycosidic bond,<sup>21,22</sup> the different electronic structures of guanine resulting in a completely different orientation of the dipole moment compared to other bases,<sup>23</sup> as well as multiple protonation sites.<sup>16,24</sup>

Guanosine has been studied in aqueous<sup>25</sup> and nonaqueous<sup>26</sup> solution

as well as in the solid state. A crystal structure of guanosine<sup>27</sup> indicates that the purines are stacked in parallel columns, with 3.3 Å between successive purine rings within the stacks. Adjacent bases are hydrogen bonded through the N(1)-N(7) and the N(2)-O(6) positions. Base-base interactions are also present in aqueous solution. Schellman<sup>28</sup> has used thermal osmometry and equilibrium sedimentation techniques to find an association constant of 10-12 molal<sup>-1</sup> and a standard free energy change of -1500 cal for deoxyguanosine self-association in aqueous solution.

### C. Guanosine Monophosphates

i. Acyclic Mononucleotides. Nucleotides are composed of nucleosides plus a monophosphate residue (only the monophosphates will be discussed here, although di-, tri-, etc. phosphates exist) attached to the five membered sugar ring through a phosphate ester linkage. The phosphate group may be bound to the 2'-, 3'- or 5'-positions. All the mononucleotides are strong acids with two dissociable protons on the phosphoric acid group having  $pK_a$  values of about 1.0 and 6.2. At neutral pH, the free nucleotide therefore exists primarily as the dianion. The 5'-isomer is the most abundant in the cell,<sup>29</sup> and the protonated form of 5'-guanosine monophosphate is commonly referred to as guanylic acid. A crystal structure of guanylic acid has shown the guanine bond lengths and angles to be very close to those of guanine bases and their derivatives.<sup>30</sup> The existence of the lactam form is verified, with the C(2)-N(2) bond showing a considerable amount of double bond character. The perpendicular distance between two parallel guanine bases was found to be 3.09 Å. There was no discussion of hydrogen bonding between bases.

ii. Cyclic Mononucleotides. The single phosphate residue may also be joined to the 3'- and 5'-positions or the 2'- and 3'-positions, generating the cyclic nucleotides. 3',5'-Cyclic GMP is a biologically very prevalent molecule. The natural occurrence of cyclic GMP was first noted by Ashman and coworkers.<sup>31</sup> Since then, cyclic GMP has been detected in all phyla of the animal kingdom. The absolute level of cyclic GMP varies from tissue to tissue, over the range  $10^{-8}$  to  $10^{-6}$  moles/Kg. A review of cyclic GMP chemistry through 1973 has been compiled by Goldberg, O'Dea and Haddox.<sup>32</sup> Cyclic GMP has been associated with calcium ion activity in organelles, and it is believed to play a role in immunocytochemistry.<sup>33</sup> It is suggested that due to the large amount of cyclic GMP in nuclear elements, it may be binding to a receptor protein involved in the control of transcription or DNA synthesis. Experiments with EDTA have suggested that the calcium ion can influence the binding of the nucleotide to its receptor.<sup>34</sup> The interaction of calcium metabolism with cyclic GMP has been investigated in a biological context;<sup>35</sup> however, actual coordination was not addressed. Cyclic GMP has also been associated with differences in the metabolism of a normal and proliferating epidermis,<sup>36</sup> the action of opiates,<sup>37</sup> regulation of the cellular metabolism or function of retinal photoreceptor cells,<sup>33b,38</sup> the action of antipsychotic drugs,<sup>39</sup> water and membrane ion transport,<sup>40</sup> the central nervous system,<sup>41</sup> and anaphylactic reactions<sup>42</sup> to name a few. Thus, cyclic 3',5'-GMP is associated with an ever increasing number of physiological processes, many of which are related to or directly invoke alkali or alkaline earth metal ions.

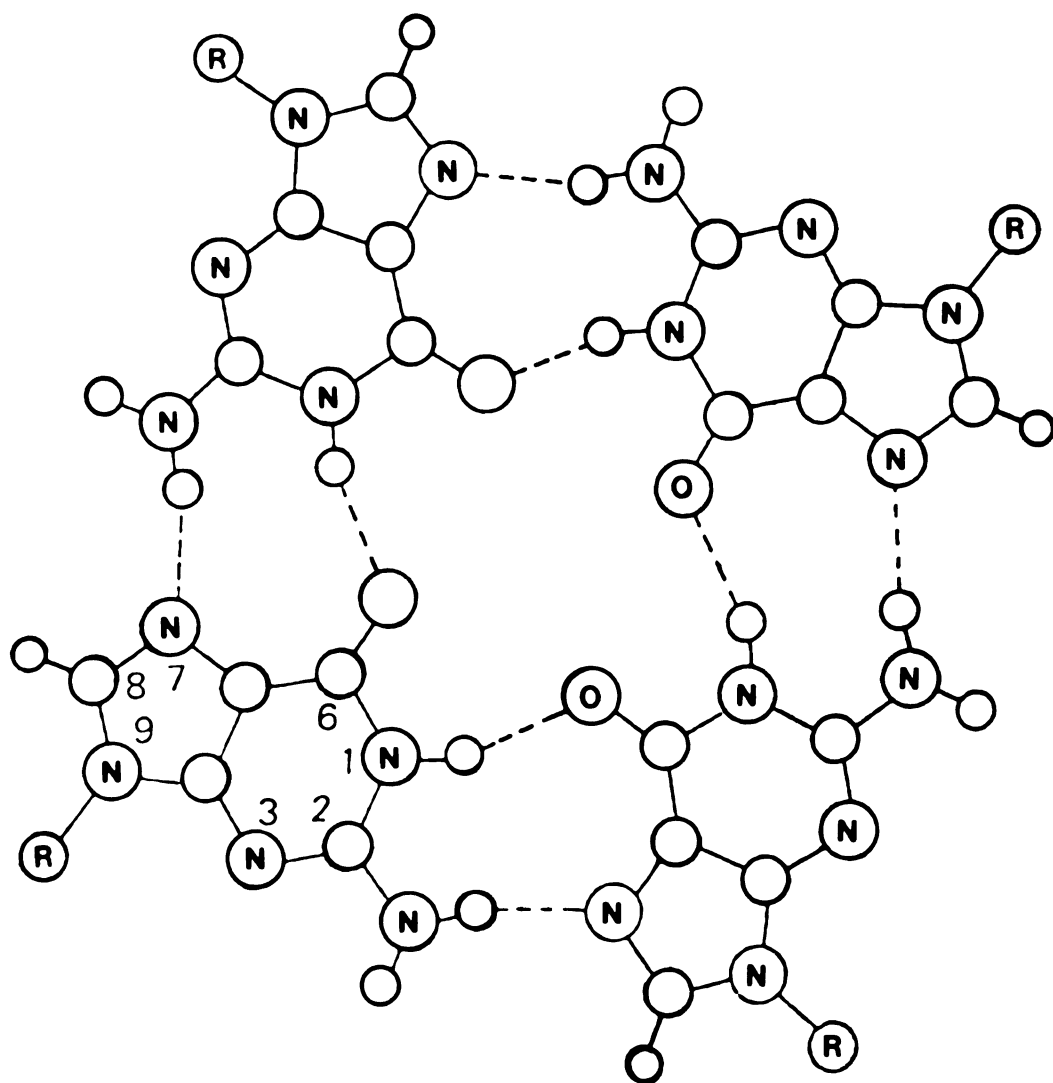


### iii. Complementary Hydrogen Bonding and Self Association.

Mononucleotides, as well as the parent bases and nucleosides, are capable of undergoing hydrogen bonding with its complementary base-pair as defined by Watson and Crick.<sup>43</sup> Hydrogen bonds are the result of an associative interaction between a hydrogen-bearing atom (the donor atom) and an electronegative atom (the acceptor atom) and have a binding energy of a few kilocalories per mole. This highly specific base pairing has been studied for nucleosides in non-aqueous solvents by infrared spectroscopy.<sup>44</sup> Evidence for complementary base hydrogen bonding has also come from crystal structure determination<sup>45</sup> and aqueous proton NMR solution studies.<sup>26</sup> Hydrogen bonded amino protons are shifted downfield from the monomer position in aqueous solution as detected by  $^1\text{H}$  NMR.

Guanylic acid and its derivatives are known to be capable of hydrogen bonding to themselves, resulting in some rather unique properties. In 1910, Bang<sup>46</sup> reported the formation of gels in concentrated, acidic guanylic acid solutions. This phenomenon, which occurs for guanosine and its analogues as well as for 5'-GMP, 3'-GMP and 5'-dGMP between pH 2-5, has been investigated by infrared spectroscopy,<sup>47</sup> optical rotatory dispersion (ORD),<sup>48</sup> raman,<sup>49</sup> calorimetry,<sup>50</sup> and x-ray fiber diffraction.<sup>51</sup> Based on these data, 5'-GMP at acid pH has been proposed to form a continuous helix with 15 nucleotide units in four turns. 3'-GMP at acid pH is proposed to form planar tetramer units, as shown in Figure 2, arranged in a stacked helical array. In both structures, the guanine bases form two hydrogen bonds per nucleotide unit. This self-association involves the N(1) and N(2) positions as proton donors and the O(6) and N(7) positions as

Figure 2. The planar tetramer unit showing hydrogen bonding between N(1) and O(6) as well as N(2) and N(7) by dashed lines. R represents the ribophosphate group. Note the cavity formed in the center of the tetramer by the O(6) positions.



proton acceptors.

In 1972, Miles and Frazier<sup>52</sup> reported I.R. evidence for a regular, ordered structure of 5'-GMP in neutral solution (pH about 8). This structuring was distinguished from that found in acidic 5'-GMP solutions by the lack of gel formation and by different I.R. properties. The dianion also showed a more cooperative melting profile with a lower  $T_m$  than the monoanionic gels. Based on the marked similarities between the I.R. spectra of 3'-GMP in acid solution and 5'-GMP in neutral solution, they were postulated to have the same stacked planar tetramer unit structure.

D. Polynucleotides. Mononucleotide units can be joined by phosphoric acid bridges to create nucleotide chains of varying length. The bridging phosphodiester linkage usually joins the 5'-hydroxyl of one nucleotide sugar to the 3'-hydroxyl of the following pentose moiety. A shorthand notation to indicate base sequence is commonly used where p designates the phosphate group. When p appears to the left of the base it designates a phosphodiester link to the 5'-position; a p to the right of the base designates a linkage through the 3'-position. A d before the base indicates that the sugar is the 2-deoxy-D-ribose. DNA and the three different forms of RNA (messenger RNA, transfer RNA and ribosomal RNA) are linear polymers of mononucleotide units. Thus, nucleic acids are composed of a covalently bonded chain of alternating pentose and phosphoric acid groups, with the purine or pyrimidine bases representing side chains attached to the pentose. These side chains can all be the same heterocyclic base, guanine for example. Such a molecule is known as poly(G).

### III. Conformational Studies

A. Definition. A great deal of interest has been expressed in both theoretical<sup>53</sup> and experimental aspects of the stereochemistry of nucleoside and nucleotide units. There are almost an infinite number of ways the ribose can be oriented with respect to the base, a large variety in the possible relative spatial arrangement of the 5 atoms in the sugar ring, and various angles of attachment between the ribose and the phosphate. Donohue and Trueblood<sup>54</sup> found that essentially two preferred conformations exist about the glycoside bond of purine nucleosides and nucleotides. Rotation about this bond is defined in terms of  $\chi$ ,<sup>55</sup> the angle defined by O(1')-C(1')-N(9)-C(8) as shown in Figure 3. These two common conformations have been termed syn (where the N(9)-C(4) bond is projected onto or near the sugar ring) and anti (where the N(9)-C(8) bond is projected onto or near the sugar ring).

Different conformations in the sugar ring arise from rotation about the O1'-C1', C1'-C2', C2'-C3', C3'-C4' and C4'-O1' bonds and are referred to by Sundaralingam as  $\tau_0$ ,  $\tau_1$ ,  $\tau_2$ ,  $\tau_3$  and  $\tau_4$  respectively.<sup>55</sup> Although Arnott<sup>56</sup> has used a different designation for torsion angles, Sundaralingam's conventions will be used for all conformations. The sugar ring is considered to fall into one of four main classes as shown in Figure 4: C3'-endo, C2'-endo, C3'-exo or C2'-exo puckers.<sup>55</sup> This nomenclature refers to the position of the designated atom with respect to C5'. If C5' is on the same side as the designated atom with respect to the other 4 (presumably close to planar) atoms of the ribose ring, the conformation is termed endo. If the designated atom is displaced toward the opposite side, it is termed exo. Another nomenclature to describe this phenomenon is the envelope (E) or twist (T) form.<sup>57</sup> Twist

Figure 3. Newman projections showing the preferred nucleotide conformations and their nomenclature.

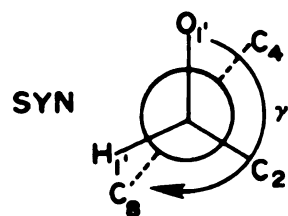
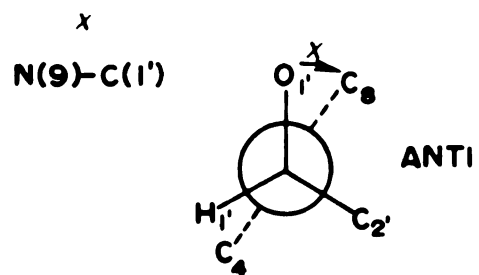
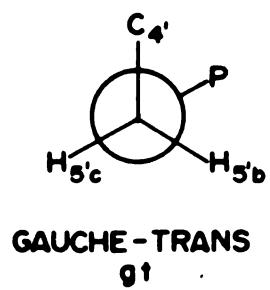
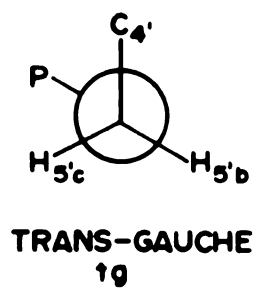
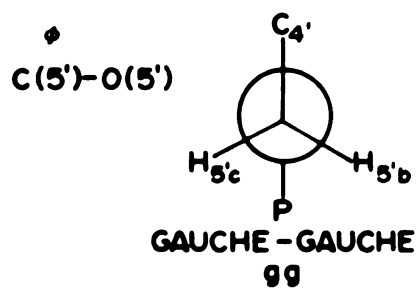
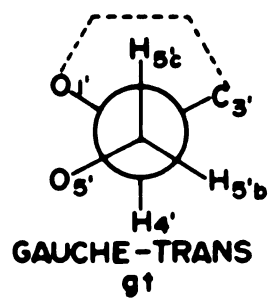
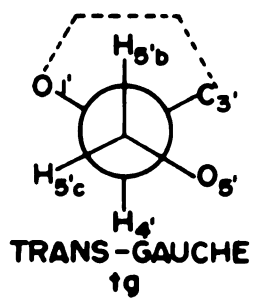
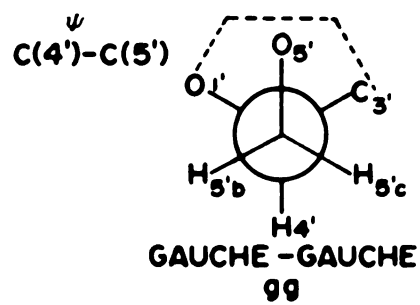
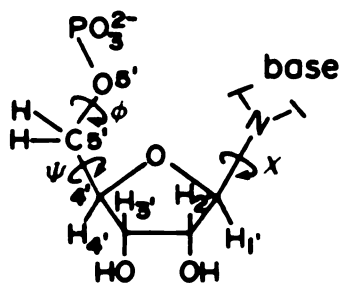
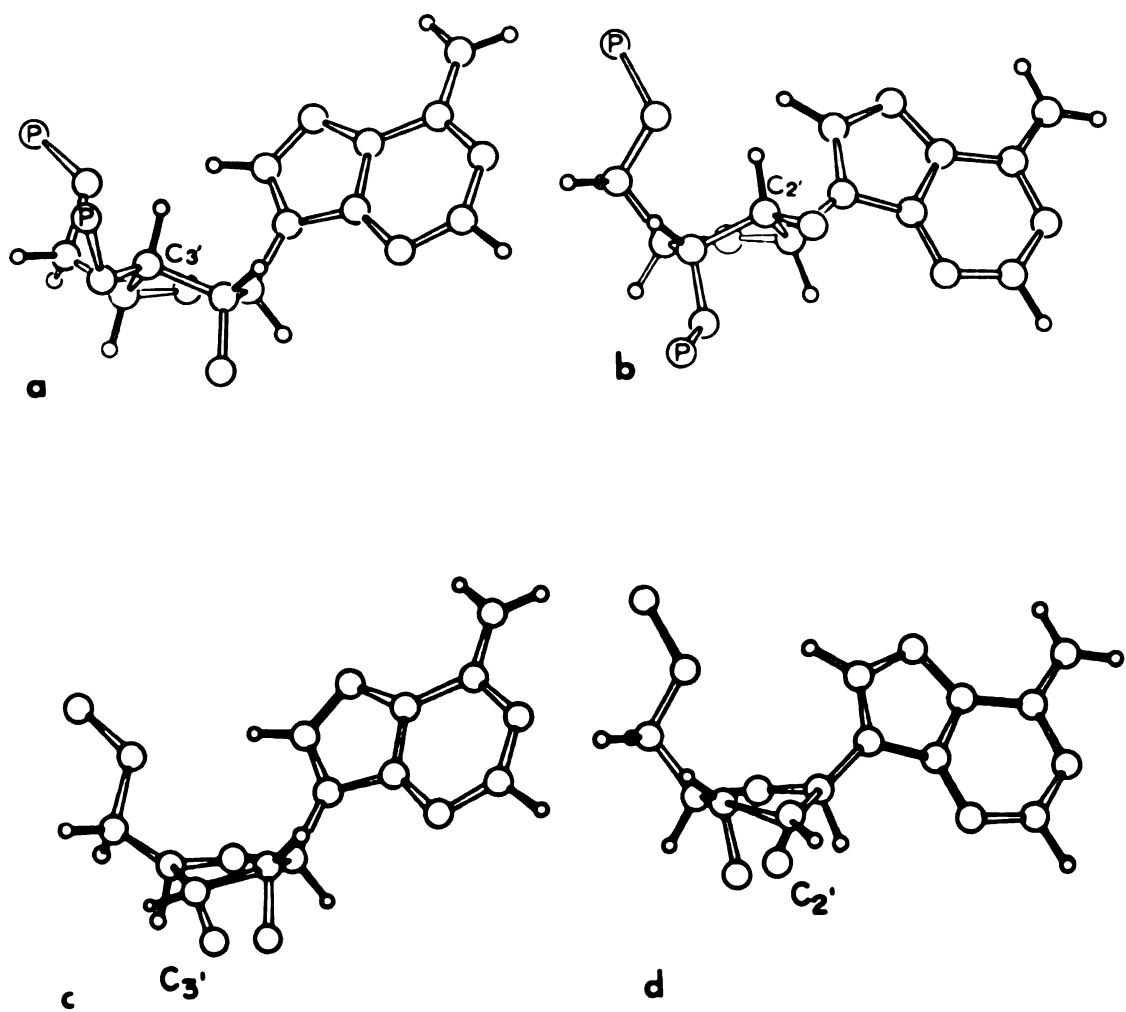


Figure 4. Four preferred conformations for the nucleotides:  
(a) C(3')-endo, anti, *gg*; (b) C(2')-endo, anti, *gg*;  
(c) C(3')-exo, anti, *gg*; (d) C(2')-exo, anti, *gg*.  
Taken from reference 55.





nomenclature assumes two atoms show a maximum pucker, and these two atoms are once again referenced to C5'. The number preceeding the T refers to the atom that shows major puckering, and the number following the letter denotes secondary puckering. A superscript denotes endo, whereas a subscript denotes exo. Envelope nomenclature assumes displacement of only one atom from the ring plane, where the same subscript and superscript conventions apply as in the twist system. Still another nomenclature to describe ring pucker involving the concept of pseudorotation was developed by Kilpatrick<sup>58</sup> and refined by Altona and Sundaralingam.<sup>59</sup> Here, each conformation is defined by the phase angle of pseudorotation, P, and the degree of pucker,  $\tau_M$ . Knowing the torsion angles,  $\tau$  as defined by Sundaralingam,<sup>55</sup> P can be calculated as follows:

$$\tan P = \frac{[(\tau_4 + \tau_1) - (\tau_3 + \tau_0)]}{2\tau_2(\sin 36 + \sin 72)} \quad (1)$$

For negative values of  $\tau_2$ , 180 ° is added to the calculated value for P from equation (1). A standard conformation is chosen for P=0 ° which corresponds to a maximum positive value for  $\tau_2$ . Figure 5 shows the relationship between the various nomenclatures.

In 5'-nucleotides, the conformation about the exocyclic C4'-C5' bond is defined by the orientation of the C5'-O5' bond with respect to the C4'-O1' and C4'-C3' bonds as shown in Figure 3, and is defined as the angle  $\psi$ .<sup>55</sup> The orientation of the phosphate with respect to C4' is defined as the angle  $\phi$ ,<sup>55</sup> also shown in Figure 3.

B. Syn vs. Anti Conformations. Based on crystal structure determination, it is generally believed that the anti conformer is more stable than the syn conformer (Table 1). Nuclear Overhauser studies in

Figure 5. The pseudo rotation circle shows the relationship between the phase angle of pseudo rotation  $P$  and the 10 envelope  $C_s$  and 10 symmetric twist  $C_2$  conformations of the furanose ring. The pseudo mirror symmetry in the envelope conformations is indicated by the dashed lines and the pseudo twofold axis in the symmetric twist conformations is shown by the arrows. The signs of the torsional angles of the sugar ring are indicated within the furanose ring. The preferred regions for the  $P$  values are 0-18 and 144-180 and they are generally referred to as C(3')-endo and C(2')-endo puckerings. Taken from reference 57.

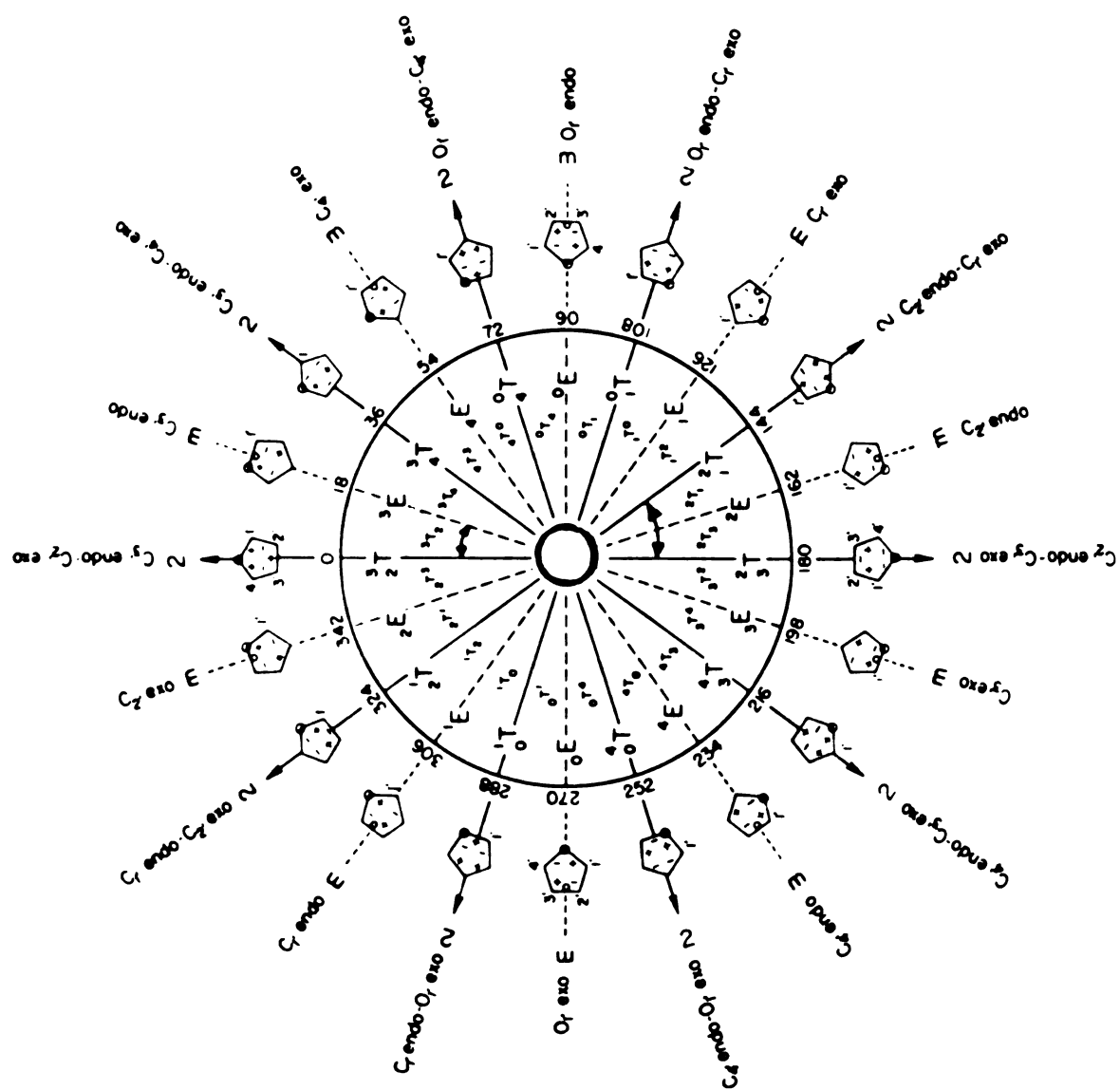


Table 1. Molecular Conformation of Some Nucleotides<sup>a</sup>

	P ~	χ	ψ
1. 5'-AMP·H <sub>2</sub> O	C(3')-endo (11.3°)	anti (25°)	g <sup>+</sup>
2. 5'-ATP·Na <sub>2</sub> ·4H <sub>2</sub> O (molecule 1)	C(3')-endo (13.4°)	anti (69°)	g <sup>+</sup>
3. 5'-GMP·3H <sub>2</sub> O	C(3')-endo (8.0°)	anti (12°)	g <sup>+</sup>
4. 5'-TMP·Ca·6H <sub>2</sub> O	C(3')-endo (25.2°)	anti (44°)	g <sup>+</sup>
5. 5'-IMP·Ni·7H <sub>2</sub> O	C(3')-endo	anti (34°)	g <sup>+</sup>
6. 5'-GMP·Ni	C(3')-endo	anti	g <sup>+</sup>
7. 5'-ADP·Rb·4H <sub>2</sub> O	C(2')-endo (163.8°)	anti (38°)	g <sup>+</sup>
8. 5'-ATP·Na <sub>2</sub> ·4H <sub>2</sub> O (molecule 2)	C(2')-endo (155.6°)	anti (39°)	g <sup>+</sup>
9. 5'-IMP·Na·8H <sub>2</sub> O	C(2')-endo (166.8°)	anti (41°)	g <sup>+</sup>
10. 5'-IMP·Na <sub>2</sub>	C(2')-endo (162.8°)	anti (43°)	g <sup>+</sup>
11. 5'-IMP·Ba (molecule 1)	C(2')-endo (158.9°)	anti (46°)	g <sup>+</sup>
12. (molecule 2)	C(2')-endo (152.5°)	anti (34°)	g <sup>+</sup>
13. 5'-UMP·Ba·7H <sub>2</sub> O	C(2')-endo (170.2°)	anti (43°)	g <sup>+</sup>
14. 5'-dCMP·H <sub>2</sub> O	C(1')-endo (213.6°)	anti (-6°)	g <sup>+</sup>
15. 5'-CMP·Ba·8H <sub>2</sub> O (molecule 1)	C(1')-endo (152.4°)	anti (40°)	g <sup>+</sup>
16. (molecule 2)	C(1')-endo (148.2°)	anti (47°)	g <sup>+</sup>
17. 5'-dAMP·6H <sub>2</sub> O·Na	C(1')-endo (149.4°)	anti (63°)	g <sup>+</sup>
18. 5'-dGMP	C(1')-endo (83.6°)	anti (54°)	t
19. 5'-6aza UMP <sup>b</sup>	C(3')-endo	anti (84.5°)	t

<sup>a</sup>Taken from reference 99

aqueous dimethylsulfoxide (DMSO)<sup>60</sup> have shown that guanosine exists in a ratio of 46:54 syn to anti. 2',3'-Isopropylidene guanosine was shown to exist as 80% syn conformer. Circular dichroism (CD) has been used to investigate the conformation of guanine derivatives.<sup>61</sup> The CD spectrum was observed to invert on protonation of the base and this was interpreted as a change from anti to syn conformation. Independent <sup>1</sup>H NMR studies by P.O.P. Ts'0 and coworkers<sup>62</sup> and Danyluk and Hruska,<sup>63</sup> concluded that all 5'-nucleotides in aqueous solution must be in an anti conformation. Using Nuclear Overhauser techniques, Guschlbauer<sup>64</sup> and coworkers found that at neutral pH at low concentration (0.025 M), the concept of a rigid molecule cannot explain the enhancements observed. Thus, they concluded that the molecule is flexible. They also concluded that at neutral pH, the relative time spent as the syn conformer vs the anti conformer is 1.7 for 2'-GMP, 2.6 for 3'-GMP and 1.1 for 5'-GMP; whereas under acid conditions, pH=1, the portion of the time spent as the syn conformer relative to the anti conformer is 4.0 for 2'-GMP, 3.5 for 3'-GMP and 1.0 for 5'-GMP. Independent investigations by other researchers have shown general agreement with these results.<sup>65-67</sup>

Independently, Sundaralingam<sup>55</sup> as well as Haschemeyer and Rich<sup>21</sup> have correlated the relationship between  $\chi$  and the mode of sugar ring puckering. A recent <sup>1</sup>H NMR study by Jordan and Niv<sup>68</sup> on substituted adenosine and guanosine nucleoside solutions has shown that although the ribose conformations remained about the same in all C(8)-amino nucleosides, the dimethylamino compound was fixed in the syn conformation whereas the amino and monomethylamino substrates were anti. Thus, they concluded that no direct interaction between ribose pucker and glycosyl conformation exists. Correlating theoretical chemical

shift C

Pullman

conform

C

shown

ribonuc

conter

equili

confor

contr

UMP s

as do

shown

favor

the r

[C2'-

nucle

endo,

GMP.

both

shows

agree

conj

favor

3',5'

shift calculations with literature experiments, Giessner-Piettre and Pullman<sup>69</sup> have concluded that C(8) substituted purines favor conformations with  $240^\circ < \chi_{\text{CN}} < 60^\circ$ .

C. Ribose Conformation. Crystal structure determinations have shown either the 2'- or 3'-endo to be the favored conformation in ribonucleotides and nucleosides, whereas the 1'-endo appears to be a contender with the deoxyribonucleotides (Table 1). In solution, an equilibrium is assumed<sup>65,70,71</sup> to exist between two extremes, the conformations [C2'-endo, C3'-exo] and [C3'-endo, C2'-exo], the contributions of which can be determined from coupling constants. <sup>1</sup>H NMR studies have shown that deoxynucleosides favor the same conformation as do nucleotides, the [C2'-endo, C3'-exo].<sup>72</sup> Davies and Danyluk<sup>70</sup> have shown that for ribonucleotides, a [C2'-endo, C3'-exo] conformation is favored 70:30 over a [C3'-endo, C2'-exo] conformation. The ratio for the ribonucleotide systems was found to be 60:40. They also found<sup>71</sup> the [C2'-endo, C3'-exo] conformer to be favored in the case of 2'- and 3'-nucleotides. Guschlbauer<sup>65</sup> generally agreed, noting an increase in [C3'-endo, C2'-exo] conformation on decreasing pH for 5'-GMP, 3'-GMP and 2'-GMP. Dobson<sup>66</sup> and coworkers concluded 30% [C3'-endo, C2'-exo] exist for both 5'-GMP and 5'-dGMP at neutral pH, whereas at pH=2 the 5'-GMP system shows 57% [C3'-endo, C2'-exo].

D. The C(4')-C(5') and C(5')-O(5') Conformations. General agreement between different solution studies<sup>60,63,65,73</sup> and in conjunction with x-ray studies indicate the gauche-gauche conformer is favored for both bonds.

E. Cyclic Nucleotide Conformations. The conformation of cyclic 3',5'-GMP has been studied in the solid state by x-ray



crystallography,<sup>74</sup> and in solution by  $^{13}\text{C}$  NMR<sup>75</sup> and by theoretical calculations.<sup>76</sup> There is good agreement between the different studies. The base exists in a syn conformation with respect to the sugar ring, with the ribose forced into a [C4'-exo, C3'-exo] conformation due to the cyclized phosphate group. The phosphate ring is locked in a chair conformation, being puckered at the C3'-C4' bond and flattened at the phosphate end.

The conformation of 2',3'-cyclic GMP has been studied by  $^{13}\text{C}$  NMR and  $^1\text{H}$  NMR.<sup>77</sup> Based on  $^1\text{H}$ - $^1\text{H}$  and  $^1\text{H}$ - $^{31}\text{P}$  coupling constants, guanosine shows no conformational preference for any of the principle conformers. The conformation about the 5'-CH<sub>2</sub>OH was found to be mainly gauche-gauche (47%), but with an appreciable amount of gauche-trans (34%) for the sodium salt. The pyridinium salt shows a more even distribution between the two rotamers, 48% and 47%, respectively.

#### IV. The Interaction of Metal Ions with Guanine and Its Derivatives

The multiple bonding possibilities, solvation, hydrogen bonding and stacking capabilities of nucleic acid derivatives make them unique ligands to study with a variety of metal ions. Reflecting this, the literature shows a large number of techniques have been used to investigate the effects of metal ions on nucleic acids and their components. Both solution techniques and x-ray crystallography have been applied to help identify the species formed.

A number of different potential sites exist for bonding of metal ions in guanine and its derivatives.<sup>4e</sup> The N(7) position is unprotonated at neutral pH, and has a lone pair which is available for donation to a metal makes this a favored binding position for many transition metal ions. The N(1) site is protonated at neutral pH; however, bonding can be so favored as to lower the effective  $pK_a$ . The deprotonated nitrogens are very strong binding sites. The  $NH_2$  site is not available for bonding normally, since the lone pair is delocalized into the  $\pi$ -ring system. Thus, bonding must be preceded by deprotonation. N(3) shows no evidence for binding, probably due to steric considerations. Evidence for monodentate binding to O(6) is ambiguous. N(7)-O(6) chelation or N(1)-O(6) chelation has been proposed, although no strong evidence exists. Other possible modes of chelation involve N(ring)-O(sugar), O(ribose)-O(ribose), O(ribose)-O(phosphate), N(exocyclic)-O(phosphate), N(ring)-O(phosphate) and O(phosphate)-O(phosphate). X-ray crystallographic results have been used to help interpret solution studies and thus will be considered first.

### A. X-Ray Structure Determination

i. Transition Metal Ions. In neutral guanine, N(1) and N(9) are protonated<sup>11a</sup> in the solid state. Ionization leads to deprotonation at the N(1) position resulting in the anion.<sup>7</sup> The cation is formed by adding a proton at N(7)<sup>78</sup> leaving only N(3) unprotonated. The complex bis(9-methylguanine)triquocopper(II) sulfate trihydrate [Cu(9-MeG)<sub>2</sub>(OH<sub>2</sub>)<sub>3</sub>]SO<sub>4</sub>·3H<sub>2</sub>O,<sup>79</sup> contains two neutral 9-methylguanine ligands coordinated to the copper through N(7). O(6) of both purine ligands act as hydrogen bond acceptors forming hydrogen bonds to the same coordinated water molecule. N(1) and N(2) of one purine act as hydrogen bond donors when they form a hydrogen bond with a sulfate anion. In the complex dichloro(aquo)(9-ethylguanine)zinc(II), N(7) coordination is also observed.<sup>4e</sup> Two cationic complexes of guanine have been investigated and both exhibit coordination through the N(9) position. In trichloroguaninium zinc(II), the nitrogen atoms N(1), N(3) and N(7) are all protonated in order to allow for coordination at N(9).<sup>80</sup> The dimeric complex di- $\mu$ -chloro-bis[dichloroguaninium copper(II)] dihydrate contains a Cu-N(9) bond length of 1.98 Å.<sup>81</sup>

Relatively few crystal structures are available for guanosine complexes. The crystal structure of [Pt(en)(guanosine)<sub>2</sub>]<sup>2+</sup> indicates coordination of the Pt(II) with the N(7) atoms of the two guanosine ligands. The Pt-N bond length is found to be 1.97 Å.<sup>82</sup>

Although far more crystal structure determinations are available for metal ion nucleotide systems, most of those involving transition metal ions have the same general form. Nickel (II),<sup>83</sup> cobalt (II),<sup>84</sup> manganese (II)<sup>85</sup> and cadmium (II)<sup>86</sup> exhibit octahedral coordination with five water molecules and N(7) of the 5'-guanosine monophosphate. One of

the water molecules is also involved in an intramolecular hydrogen bond with O(6), while two other waters are hydrogen bonded to phosphate oxygens. A different type of structure was found for a 1:1 complex of Cu(II) and 5'-GMP.<sup>87</sup> The compound is polymeric with a spiralling sequence,  $(-\text{Cu-phosphate-sugar-base-})_{\infty}$ , where the turns are crosslinked by additional copper-phosphate oxygen bonds as well as by hydrogen bonding between coordinated water molecules and phosphate oxygens. There are three independent square pyramidal Cu atoms, each bound to N(7) of the GMP, but with varying numbers of H<sub>2</sub>O and phosphate oxygens in the other coordination sites.

A summary of transition metal ion coordination to guanine and its derivatives as well as other purines is given in Table 2. A number of reviews describe the interactions of metal ions with nucleic acids; however, frequently no mention is made of alkali or alkaline earth coordination.<sup>2,4</sup>

ii. Alkali and Alkaline Earth Metal Ions. The crystal structure of the disodium salt of deoxyguanosine-5'-phosphate has been solved independently by two different groups.<sup>88</sup> There are two types of sodium coordination. One sodium has an octahedral coordination geometry involving four water molecules, the O(3') of one dGMP and the O(6) of another. The other sodium is five coordinate, showing a distorted square-pyramidal geometry. The second sodium is coordinated to two phosphate oxygens, a water, and the other two coordination sites are the same O(6) and water found in the coordination sphere of the first sodium. Thus, the two sodium coordination polyhedra share a common edge as shown in Figure 6.

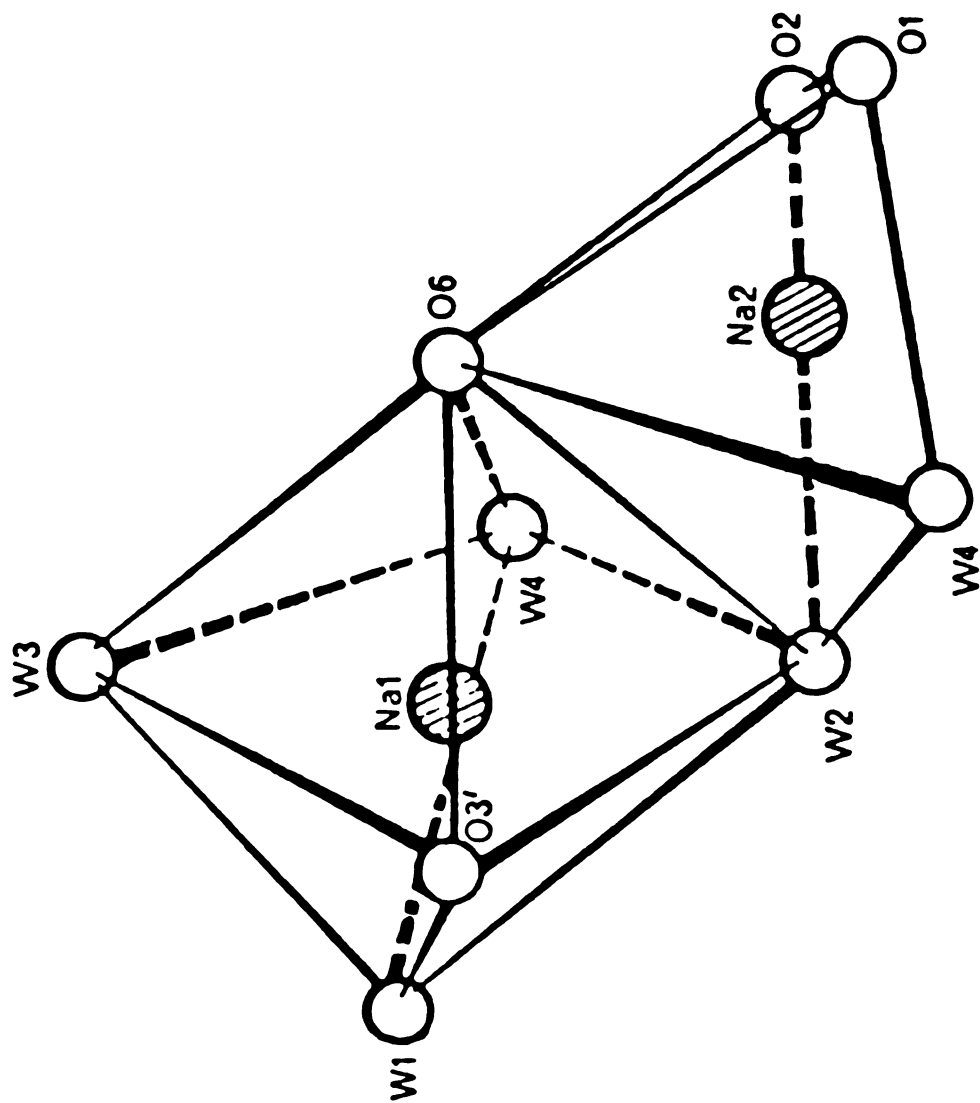
A crystal structure shows that the sodium salt of 3',5'-cyclic

Table 2. Crystallographically Determined Geometries of Metal-Nucleoside and Metal-Nucleotide Complexes<sup>a</sup>

Complex	Coordination Site (s)	M-L, Å
[Cu(glygly)(Cyd)]	N(3)	2.01
	O(2)	2.74
[Cu(ONO)(acac)(dAdO)]	N(7)	1.99
[Pt(en)(GuO) <sub>2</sub> ] <sup>2+</sup>	N(7)	1.967(15)
[Co(5'-IMP)(OH <sub>2</sub> ) <sub>5</sub> ]	N(7)	2.162
[Ni(5'-IMP)(OH <sub>2</sub> ) <sub>5</sub> ]	N(7)	2.105
[Mn(5'-Imp)(OH <sub>2</sub> ) <sub>5</sub> ]	N(7)	
[Ni(5'-GMP)(OH <sub>2</sub> ) <sub>5</sub> ]	N(7)	2.12
[Co(5'-GMP)(OH <sub>2</sub> ) <sub>5</sub> ]	N(7)	
[Mn(5'-GMP)(OH <sub>2</sub> ) <sub>5</sub> ]	N(7)	
[Cd(5'-GMP)(OH <sub>2</sub> ) <sub>5</sub> ]	N(7)	2.37
[Ni(5'-AMP)(OH <sub>2</sub> ) <sub>5</sub> ]	N(7)	2.08
[Cu <sub>3</sub> (5'-GMP) <sub>3</sub> (OH <sub>2</sub> ) <sub>12</sub> ]	N(7)	2.22
	OP <sub>3</sub>	1.94
[Zn(5'-IMP)(OH <sub>2</sub> ) <sub>n</sub> ]	N(7)	
	OP <sub>3</sub>	
[Cd <sub>2</sub> (5'-IMP) <sub>3</sub> (OH <sub>2</sub> ) <sub>6</sub> ]	N(7)	
	OP <sub>3</sub>	
[Cd(5'-CMP)(OH <sub>2</sub> )]	N(3)	2.36
	OP <sub>3</sub>	2.24
[Co(5'-CMP)(OH <sub>2</sub> )]	N(3)	1.96
	OP <sub>3</sub>	1.95
[Pt(NH <sub>3</sub> ) <sub>2</sub> (5'-IMP) <sub>2</sub> ] <sup>2-</sup>	N(7)	2.02

<sup>a</sup>Taken from reference 4f

Figure 6. The sodium ion environments in 5'-Na<sub>2</sub>dGMP. Taken from reference 88.



guanosine monophosphate<sup>74</sup> shows only one type of sodium. In this structure, the sodium is not directly attached to the base or the phosphate oxygens, but is coordinated to six water molecules. Adjacent sodium octahedra share edges to form an infinite column. Thus, the crystal packing consists of alternating layers of stacked nucleotides with the interstitial holes filled by the sodium-water octahedra. The structure of the free acid of 3',5'-cyclic GMP is quite similar to that of the sodium salt, the most noteworthy point being that the compound exists as a zwitterion in the solid state, with N(7) of the base protonated.

The crystal structures of two GpC dinucleotide units have been solved, one as the disodium salt<sup>89</sup> and the other as the calcium salt<sup>90</sup>, and the structures are shown in Figure 7. In the sodium case, the cations exhibit face-sharing octahedral coordination, involving four waters and two phosphate oxygens from different dinucleotide segments. The sodium cations serve to bridge the GpC fragments and organize them into sheets within the crystal. The  $\text{Ca}^{2+}$  also shows octahedral coordination, with the  $\text{Ca}^{+}$  bridging phosphate oxygens from different dimers. Table 3 shows a summary of alkali and alkaline earth metal ion coordination in several nucleotide and dinucleotide systems.

B. Nucleoside-Metal Ion Interactions In DMSO. Wang and Li<sup>92</sup> investigated the interactions of  $\text{ZnCl}_2$  with guanosine in DMSO solution. They concluded that although the solvent allows greater nucleoside solubility and the observation of NH resonances,<sup>26</sup> the base-stacking interactions are diminished in comparison to water. A similar study using  $\text{HgCl}_2$  was reported by Kan and Li.<sup>93</sup> The interactions of  $\text{HgCl}_2$  and  $\text{CH}_3\text{HgCl}$ <sup>94</sup> with 6-thioguanosine and 8-thioguanosine were examined by



Figure 7. (A) The calcium ion environments in GpC. Taken from reference 90. (B) The sodium ion environments in GpC. Taken from reference 89.

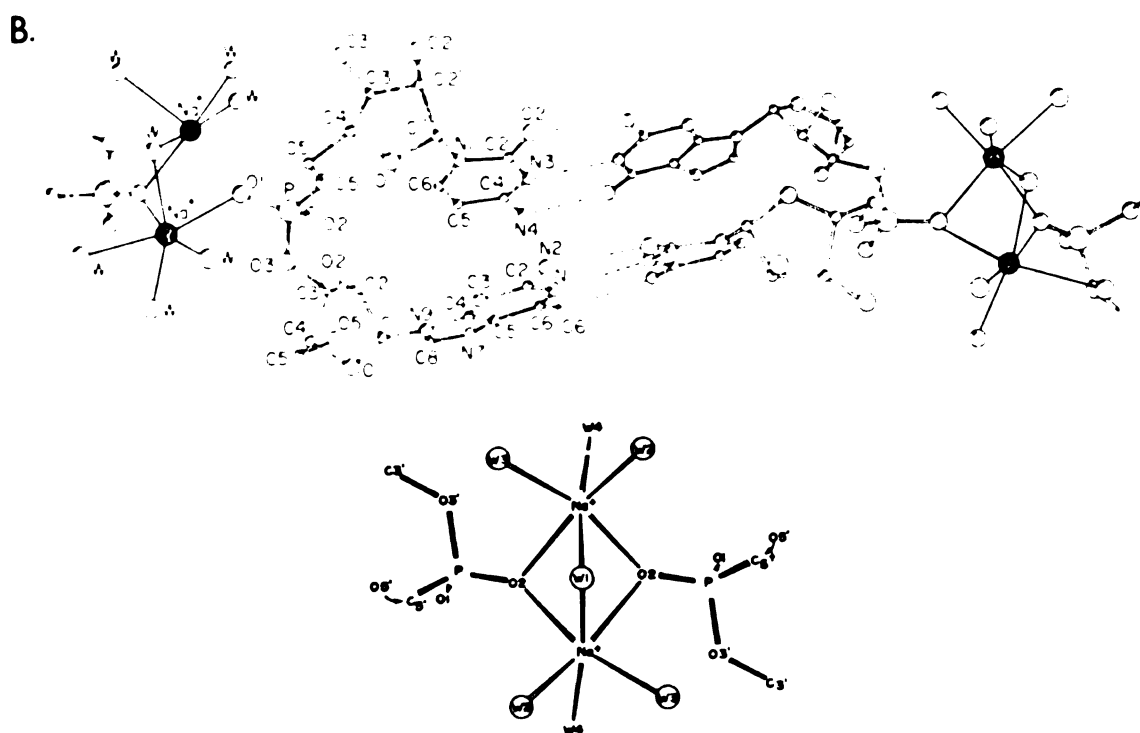
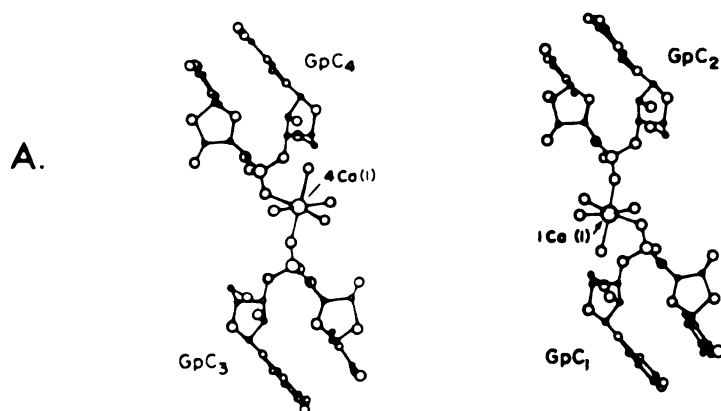


Table 3. Alkali and Alkaline Earth Nucleotide and Dinucleotide Coordination.

Complex	Coordination Site(s)	M-L Å	Reference
Na urate	O(6)	2.53	88d
	O(8)	2.35	
	O(2)	2.38	
$[\text{Na}_2(5'\text{ATP})(\text{H}_2\text{O})_3]$	N(7) OP <sub>3</sub>	2.69 to 2.90	88e
$[\text{Ba}(5'\text{UMP})(\text{H}_2\text{O})_8]$	O(2')	2.80	88f
	O(3')	2.90	
	O(2)	2.78	
pdTpdT- $\text{Na}_2$	O(2)	2.54	88g
	O(2)	2.41	
	OP <sub>3</sub> bridge	2.46	
ApU- $\text{Na}_2$	O(2)	2.37	88h, i
	O(2)	2.34	
GpC- $\text{Na}_2$	OP <sub>3</sub>		89, 88j

proton and  $^{13}\text{C}$  NMR in DMSO. The 6-thio derivative showed the largest shifts resulting in the postulation of an N(7) mercury complex.

Although the interaction of transition metal ions with nucleosides was expected, the interaction found between alkali and alkaline earth metal ions was not. Jordan and McFarquhar<sup>95</sup> observed downfield shifts of about 1 ppm for the  $\text{NH}(1)$  and  $\text{NH}_2$  proton resonances when  $\text{CaCl}_2$  was added to DMSO solutions of guanosine.  $\text{MgCl}_2$ , however, did not induce the same shifts. Shimokawa and coworkers<sup>96</sup> studied the influence of  $\text{HgCl}_2$ ,  $\text{CdCl}_2$ ,  $\text{ZnCl}_2$ ,  $\text{BaCl}_2$ ,  $\text{SrCl}_2$ ,  $\text{CaCl}_2$  and  $\text{MgCl}_2$  on the PMR spectra of guanosine in DMSO. They concluded that the alkaline earth cations formed more stable complexes than the transition metal ions. Chang and Marzilli<sup>97</sup> found that the spectral changes caused by the alkaline earth chlorides were not induced by alkaline earth nitrates. They also found that tetraethylammonium chloride induced large spectral shifts. Thus they concluded that the chloride was responsible for the shifts, not the cation. Sohma<sup>98</sup> and coworkers have concluded that both the cation and anion must be considered in interactions between metal salts and nucleosides. Similar discrepancies exist in the study of alkali and alkaline earth cations with cytidine in DMSO.<sup>93</sup>

C. Guanosine Metal Ion Interactions in  $\text{H}_2\text{O}$ . Gushlbauer and coworkers<sup>100</sup> noted that addition of alkali or alkaline earth metal ions to a guanosine solution in water resulted in gel formation which could be monitored by hypochromic effects in the absorption spectra. They noted that a minimal electrolyte concentration (between 0.010 and 0.016 M salt) was necessary for gel formation. They further concluded that the nature of the cation as well as the ionic strength influenced the formation and thermal stability of the aggregate, whereas anions had

only a minor effect. Potassium salts gave stable gels, whereas sodium salts caused gelation followed by precipitation of the guanosine. Gel formation was also dependent on a minimum nucleoside concentration (about 0.002 M for guanosine). The results of a survey of various guanosine derivatives indicate the importance of the 5' OH on gel formation. They suggest a possible hydrogen bonding interaction between the 5' OH of guanosine units in one tetramer, with the NH<sub>2</sub> groups of guanosine units of upper or lower tetramers, thus acting as vertical connectors. The 2' OH<sup>51d</sup> of one guanosine tetramer has been proposed to hydrogen bond to a 5'-O two levels above.

Double logarithmic plots<sup>101</sup> of hypochromicity vs. concentration for a number of guanine nucleotides have consistently shown graphs with lines of 3 different slopes. The linear regions have been assigned to monomer, tetramer, octamer and finally polymer formation.

A recent Raman study<sup>102</sup> of guanosine monomers, gels and polymers assigned bands based on the idea that there are three kinds of interactions which stabilize a structure: horizontal (base-base hydrogen bonds), vertical (base-sugar hydrogen bonds) and stacking interactions between superimposed heterocycles. They concluded that over the concentration range 0.01 - 0.015 M guanosine, the tetramers are all stacked as octamers and are beginning to polymerize. Infrared studies indicate that two different forms can exist for guanine nucleosides in the solid state, a helical tetrameric form and a "crystalline form".<sup>47c</sup>

Of the guanosine derivatives which have been studied, 8-bromoguanosine and N(2)-methylguanosine are the most interesting. 8-Bromoguanosine is in the syn conformation and is able to form a

gel.<sup>51b,d</sup> The gel is postulated to be composed of head to tail stacked tetramers in the same manner proposed for guanosine (all the sugars are oriented in the same direction and therefore the directional hydrogen bonding is the same between tetrameric plates).<sup>51d</sup> A study<sup>103</sup> of  $T_m$  as a function of cation and anion showed  $I^-$  to be the most stabilizing halide anion, and  $SCN^-$  to be the most stabilizing anion studied.  $B_4O_7^{2-}$  prevented gel formation. Approximately a 10 °C difference in  $T_m$  was observed between the various anions. The cations had a more pronounced effect.  $Sr^{2+}$  showed the largest effect,  $K^+$  showed the largest monovalent cation effect, and  $Mn^{2+}$  showed the largest transition metal ion effect ( $Cd^{2+}$  and  $Zn^{2+}$  were also investigated).  $T_m$  values changed over approximately a 30 °C temperature range, indicating that the cation effect is predominant. Although Guschlbauer could not explain the cation dependence of gel formation, a similar dependence was observed by Pinnavaia et. al.<sup>6</sup> in 5'-GMP neutral solutions, which involves a size selective complexation mechanism in solution ordering. The stabilizing effect of the transition metal ions is somewhat curious in light of their known binding site. The association of the nucleosides to form gels must be greater than the metal ion-N(7) binding constant, otherwise gel formation would be inhibited by blocking a hydrogen bonding site. If the tetramer association constant is greater, then a size selective mechanism similar to the group I and II cations operates for transition metal ions.

N(2)-methylguanosine forms the most stable gel of the guanosine derivatives studied.<sup>101</sup> This strongly suggests the absence of hydrogen bonding to the H of the  $NH_2$  not involved in tetrameric hydrogen bonding. Guschlbauer concludes that the amino group must be involved in gel

formation. He postulates that the increased electronegativity of the nitrogen of the amino group with the added methyl should make it a better hydrogen bond acceptor, and postulates a hydrogen bond formed with a 5' OH group of the upper or lower tetramer layer. A comparison of the crystal structures of guanosine<sup>27</sup> and N(2)-methylguanosine<sup>104</sup> shows very similar bond lengths for the C(2)-N(2) bond, 1.338 or 1.347 Å and 1.329 Å, respectively. The bond lengths indicate that a large degree of double bond character is present in the C(2)-N(2) bond, indicating the lone pair exists in a p orbital. Thus, the lone pair is not available for H-bonding, and Guschlbauer's explanation is somewhat suspect.

D. 5'-GMP Alkali Metal Ion Interactions in Water. The dianion of GMP has been reported to form regular ordered structures in aqueous solution that are slow to exchange on the <sup>1</sup>H NMR time scale.<sup>105</sup> The most compelling evidence for structure formation is provided by the presence of multiple inequivalent H(8) resonances in the limiting spectra of dialkali metal ion salts in D<sub>2</sub>O solution near 0 °C. This self assembly process is dramatically dependent on the nature of the alkali metal ion which is believed to direct structure through a size-selective coordination mechanism. The large chemical shift differences for the H(8) protons and the appearance of nonequivalent amino proton lines indicate that both base stacking and hydrogen bonding are important in the self-structuring process. Based on these observations and consideration of infrared frequency shifts in the carbonyl stretching region, it was concluded that structure formation arises from limited stacking of planar tetramer units formed by hydrogen bonding between positions N(1) and N(2) as donors and O(6) and N(7) as

acceptors.

In dilute solution (about 0.02 M) all salts exhibit a single sharp H(8) resonance near 8.17 ppm downfield from TSP(sodium 3-trimethylsilylpropionate-2,2,3,3-d<sub>4</sub>), characteristic of unassociated 5'-GMP.<sup>6</sup> Li<sub>2</sub>GMP and TMA<sub>2</sub>GMP (TMA= tetramethylammonium) show no evidence for structure formation at low temperatures. Na<sub>2</sub>GMP shows a four line spectrum in the H(8) region, K<sub>2</sub>GMP shows a 6 or 7 line spectrum, Rb<sub>2</sub>GMP shows a 4 or 5 line spectrum, and Cs<sub>2</sub> GMP shows only a small amount of structure with 2 new lines. Although some coincidence occurs, the chemical shifts of these H(8) resonances span more than 1 ppm. The binding constants for complexation of alkali metal ions by phosphate groups in polyphosphates,<sup>106</sup> adenine nucleotides<sup>107</sup> and DNA<sup>108</sup> are known to decrease with increasing metal ion radius. In contrast to the cation stabilization order that would be predicted on electrostatic grounds, the observed qualitative stability order of self-assembled 5'-GMP salts is  $K^+ > Na^+, Rb^+ \gg Cs^+ \gg Li^+$ . This type of metal ion ordering has been observed when a size selective mechanism is operative,<sup>109</sup> although it is unprecedented for other nucleotide systems.

The stacked tetramer model has been used to explain the order of metal ion stability. The center of the planar tetramer unit is about 2.2-2.3 Å from the center of the carbonyl oxygens, a value close to that observed for Na-O bonds. Thus, the Na<sup>+</sup> is proposed to fit in the center of a tetramer with the possibility of a solvent molecule or another GMP<sup>2-</sup> in its fifth position. When two tetramers are stacked, a central cavity is formed that can easily accommodate the K-O bond length of 2.6-2.9 Å. With a 3.4 Å spacing between plates the calculated K-O distance would be 2.8 Å. Since Rb<sup>+</sup> is similar in size to K<sup>+</sup> a similar





coordination mechanism to  $K^+$  was predicted.  $Li^+$  and  $Cs^+$ , however, have ionic radii which do not fit the "hole" hypothesis, and experimentally are found not to be good structure directors.

The multiple H(8) environments for the sodium system have been explained by observing the symmetry of the tetramer unit and building models.<sup>110</sup> Based on the directional character of the hydrogen bonds, stacking can occur one of two ways in an octamer. Either the direction of hydrogen bonding can be the same in the two tetramers (referred to as head-to-tail stacking) or can be in opposite directions (referred to as head-to-head stacking). Model studies were based on Zimmermans<sup>111</sup> results from his fiber diffraction studies of 5'-Na<sub>2</sub>GMP. The plates were set at a twist angle of 30 ° with respect to each other, and the ribose was placed in an anti configuration with respect to the base and in a C(3')-endo conformation. Then the symmetry of the two stacking patterns was considered. In the head-to-tail pattern, four H(8) lines are predicted with the two plates of the octamer being inequivalent. In the head-to-head pattern, the plates are equivalent with four H(8) lines also predicted. Chemical shift values can be predicted using the theoretical calculations of Giessner-Prettre, B. Pullman and coworkers<sup>112</sup>. These calculations are based on the spatial dependence of the ring-current magnetic anisotropy of nucleic acid bases at a vertical stacking distance of 3.4 Å. In classical mechanics, in the absence of an applied field, charges are assumed to circulate in the  $\pi$ -cloud rings of the base. Although the predicted shifts are not as large as those actually observed, they still prove useful in the overall qualitative model. This model system has been invoked to explain <sup>13</sup>C NMR results in a Na<sub>2</sub>GMP system.<sup>113</sup>

Several other groups have investigated the self-assembly of 5'-GMP in aqueous solution. Klump<sup>114</sup> used Raman spectroscopy in conjunction with calorimetry to determine the enthalpy of stacking in a 5'-Na<sub>2</sub>GMP system to be 1.75 Kcal/mole. Laszlo<sup>115</sup> has used <sup>23</sup>Na and <sup>39</sup>K NMR to study 5'-K<sub>2</sub>GMP as well as 5'-Na<sub>2</sub>GMP systems. He has predicted a number of structures based on lineshape analysis.

E. Other Systems. Polyriboguanylic acid is known to self structure in aqueous solution; however, no specific metal ion is necessary for self association to occur.<sup>116</sup> Gels of GpG have been studied by Raman spectroscopy and calorimetry<sup>117</sup> at pH=5, although similar results were obtained over the range 3-7. Peticolas and coworkers found that aggregation of GpG is a multistep process which involves intermediates whose concentration decreases with increasing temperature, thus slowing the process. The slow rate of structure formation of GpG parallels that of GpGpG.<sup>118</sup> The rate of disaggregation of GpG was also found to be slow. The model proposed<sup>119</sup> requires the 3'- and 5'- bound guanosine residues to be engaged in the formation of alternate tetramers related by a 54 ° screw rotation. These pseudo octamers which are formed by 4 GpG molecules are linked together in 4-stranded helical arrangements by hydrogen bonding involving the 3'- and 5'- OH groups of the sugars.

In contrast to poly(G), both poly(X)<sup>120</sup> and poly(I)<sup>121</sup> exhibit size selective alkali metal ion complexation in the central channel of a 4-stranded helical structure. Cooperative melting profiles, as detected by IR, were found for both systems. The qualitative stability order for the interaction of alkali metal ions with poly(I) is  $K^+ > Rb^+ > Cs^+ \gg Na^+$ . The magnitudes of the metal ion effect are smaller for poly(X),

and somewhat different from poly(I). This has been attributed to the additional counterion screening at the non size-specific C(2) oxygens.

A number of theoretical studies have recently appeared that investigate cationic binding to nucleic acid substituents,<sup>122</sup> anion binding to nucleic acids,<sup>123</sup> and cation binding to biomolecules.<sup>124</sup>

## V. Specific Goals of this Research

All work to date on alkali metal ion interactions with 5'-GMP has been done on pure salt systems with a metal ion to  $\text{GMP}^{2-}$  ratio of 2:1.<sup>6</sup> Under these conditions, the structure directing metal ion was present in excess. Therefore, the prime objective of this research was to look at systems with a metal ion to  $\text{GMP}^{2-}$  ratio between 0 and 2, since in this range different self-structures might be formed. In order to attain such conditions, a salt of  $\text{GMP}^{2-}$  was required where the cation is structure inert. A size selective binding mechanism is known to be essential for self-assembly; however, multiple equilibria may be involved that are either size or nonsize specific. Thus, both specific and nonspecific metal ion complexation was investigated. If nonspecific metal ion interactions are important, then  $\text{Li}^+$  is expected to have an effect on self-assembly. An investigation of the effects of  $\text{K}^+$  and  $\text{Na}^+$  was especially of interest since they are biologically active, and also induce self-assembly. Although preliminary investigation of 5'- $\text{M}_2\text{GMP}$  interactions have been done, where M is any of the alkali metal ions, nothing is known about alkaline earth metal ion interactions or other GMP derivatives. Thus, an investigation of 5'-GMP with the alkaline earths was undertaken. Also, a survey of alkali and alkaline earth metal ion interactions with 3'-GMP, 2'-GMP, 5'-dGMP, 2',3'- $\underline{\text{c}}$ GMP and 3',5'- $\underline{\text{c}}$ GMP was undertaken to investigate their metal ion dependence.

## VI. Practical Considerations

The range of structure and composition that might be encountered in metal ion directed self-assembly represents a formidable multi-dimensional puzzle. There are three major components which create the system of interest; they are the metal ion, the nucleotide and the solvent, all of which can be varied. The metal ions of interest are those which do not bind to a base hydrogen bond donor or acceptor, and do not cause a change in pH on binding. They also must be sufficiently soluble to allow adequate quantities into solution to meet the criteria of self-assembly. Thus, most transition metal ions are ruled out since they preferentially bind at the N(7) positions of the 5'GMP,<sup>83-85</sup> and  $\text{Ag}^+$  is ruled out since a proton is released on binding.<sup>125</sup> Another important criterion is that of ion size. The ion should have a radius close to 1.5 Å, 0.7 Å being too small and 1.9 Å being too large.<sup>6</sup> Thus, certain alkali and alkaline earths,  $\text{Tl}^+$  and  $\text{Eu}^{2+}$  are potentially suitable. Of these,  $\text{Li}^+$ ,  $\text{Na}^+$ ,  $\text{K}^+$ ,  $\text{Rb}^+$ ,  $\text{Cs}^+$ ,  $\text{Ca}^{2+}$ ,  $\text{Mg}^{2+}$ ,  $\text{Sr}^{2+}$  and  $\text{Ba}^{2+}$  will be investigated in this study.

The nucleotide that has been most extensively investigated is 5'-GMP. The nucleotide is made up of 3 major parts: the base, the sugar, and the phosphate. In order to have an understanding of the unit as a whole, an understanding of each component and its relationship to the others, as well as with the various metal ions, is important. By slightly altering the nucleotide unit, the role of the metal ion in the self-assembly process can be investigated. The guanine base has the unique property of having hydrogen bond donors (N(1) and N(2)) at right angles to hydrogen bond acceptors (O(6) and N(7)). Since protonation or deprotonation of the base is known to disrupt self-structure formation,

not many modifications of the base can be perpetrated. Substitution of a halide, amino or alkyl group for the H(8) position is possible, but even this will cause some change in the electronic properties of the molecule and was not investigated in this study. Modifications, however, can be made in the sugar region with little effect on the base. The most similar molecule to 5'-GMP is that which has been modified in the 2'-hydroxy position. Structural differences exist between DNA and RNA, so there is reason to believe that the presence or absence of the 2'-oxygen and the resulting conformational change might have an impact on the self-assembly process. This was the only ribose modification studied in this research. Other possible modifications could involve changing the ribose to a different sugar, either a larger ring or the other epimer, for example. The ribophosphate could also be forced to either the syn or anti configuration with respect to the base, changing the overall shape of the molecule. However, the phosphate can be changed most of all. The phosphate can be situated between the 2'- or 3'- position, can be cyclic between the 2'- and 3'- positions or the 3'- and 5'- positions, or can be removed altogether. Thus, the nucleotide can be redesigned in a wide variety of ways to help assess the role played by each component. All phosphate modified nucleotides mentioned above were studied in this investigation.

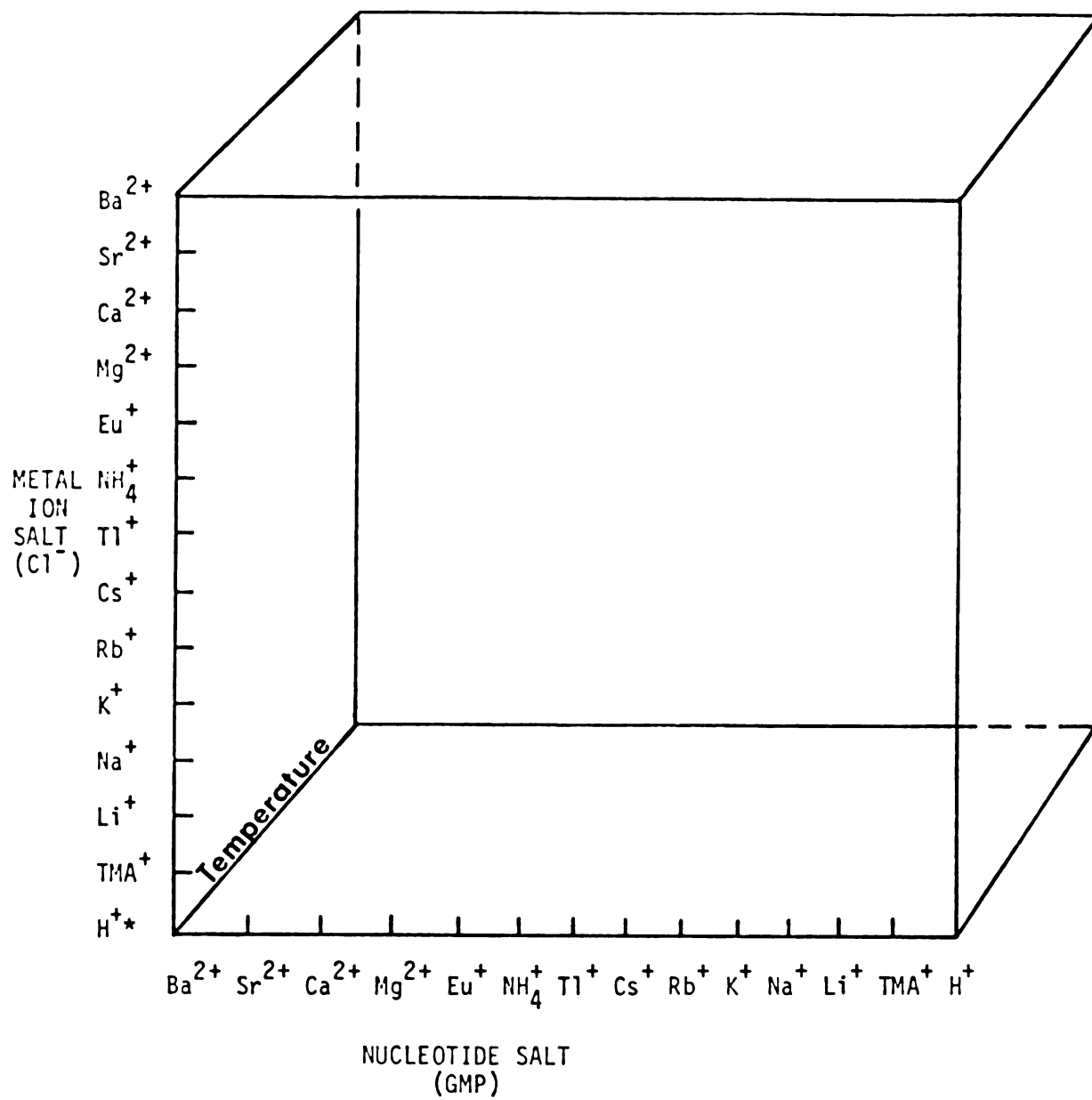
The solvent must be either H<sub>2</sub>O or D<sub>2</sub>O since the nucleotide has not been found to be sufficiently soluble in other solvents. The solution pH, temperature and nucleotide concentration are important factors in the self-assembly of guanine nucleotides. 5'-GMP is known to gel at pH values less than 6 or greater than 2, the range where the phosphate is monoprotonated. No self-assembly is observed at pH values less than 2

or greater than about 9 in the range where the base is protonated or deprotonated, respectively. The question exists as to whether or not these same properties are observed when the nucleotide is modified. Structure formation is favored at low temperatures ( $\Delta H < 0$ ), but structure formation has been observed at temperatures as high as 70 °C. Thus, investigation of all systems over a range of temperatures was necessary. Self-assembly is favored at high concentrations, but it has been found to occur over a broad range of concentrations, from about 0.2 M to the limits of solubility, about 1.2 M. Since the ordered structure is slow to exchange on the NMR time scale, and since  $^1\text{H}$  NMR is the only technique where the individual structures can be observed, it appears to be the technique best suited for preliminary investigation of this phenomenon. Secondary investigation by metal ion NMR,  $^{31}\text{P}$  NMR,  $^{13}\text{C}$  NMR, IR, Raman, UV, CD and ion selective electrode techniques may prove useful once a clear overview exists; however, these techniques were not applied in this investigation.  $^1\text{H}$  NMR in  $\text{H}_2\text{O}$  has the advantage of enabling observation of hydrogen bonded NH and OH protons not observable in  $\text{D}_2\text{O}$ . Thus, spectra in  $\text{H}_2\text{O}$  are of interest in investigating hydrogen bonding schemes, but spectra in  $\text{D}_2\text{O}$  are also necessary in order to distinguish between H(8) and N-H or O-H protons which often occur in similar chemical shift regions.

An idealized complete investigation of the metal ion and mixed metal ion dependence of the GMP systems can be represented schematically as shown in Figure 8. Each metal ion GMP system has other metal ions added to it in increasing concentration until precipitation occurs. Each system would be investigated over a temperature range from 0 °C until melting out of structure is complete; a concentration range from



Figure 8. A schematic representation of an idealized complete set of experiments to study each nucleotide system. The x-axis indicates all dimetal nucleotide systems of interest. For each set of divisions, concentration increases from left to right. The z-axis represents all metal ions of interest to be added to the dimetal nucleotide systems. A single anion should be used in all metal salts. Concentration within each division increased from bottom to top. The y-axis represents temperature from 0-100° C.



\*Between pH = 2-9.

dilute solutions exhibiting only monomer until concentrations are reached which induce precipitation should be considered. Other dimensions are those of time and pH. A "cube" of experiments would ideally be performed on each guanine nucleotide with both  $\text{H}_2\text{O}$  and  $\text{D}_2\text{O}$  as the solvent. Since time did not permit such an extensive investigation, selected experiments were performed to maximize information gained about the number of unique structures which can be formed for a given metal ion in a given nucleotide system. In addition, experiments were designed to investigate the relationship between the structures and the role of the metal ion in those structures with respect to specific and nonspecific binding.

## EXPERIMENTAL

### I. Materials, Techniques and Preparation

5'-Guanosine monophosphate was purchased as the disodium salt monohydrate from Calbiochem, Inc., and as the free acid from Sigma Chemical Co. All other nucleotides were purchased from Sigma Chemical Co. 5'-Inosine monophosphate, 2'-deoxyguanosine-5'-monophosphate, and cyclic 3',5'-guanosine monophosphate were purchased as the free acids. The desired metal ion forms of these nucleotides were obtained by titrating the free acid with the appropriate metal hydroxide. Dilute solutions ( $\sim 0.01M$ ) were titrated to a pH of  $\sim 7.8$  (unless otherwise specified) with the use of a Fisher model 370 pH meter with a Markson combination pH electrode. Guanosine-3'-monophosphoric acid and guanosine-2'-monophosphoric acid were purchased as the disodium salts, while guanosine-2',3'-cyclic monophosphoric acid was acquired as the monosodium salt. Exchange of metal ions was accomplished using a Dowex 50W-X8 (100-200 mesh) cation exchange resin obtained from Dow Chemical Company. The resin had a cation exchange capacity of 1.7 meq/mL. The resin was prepared by the following wash procedure: (1) 10% HCl, (2) H<sub>2</sub>O and EDTA, (3) 10% NaOH, (4) H<sub>2</sub>O, (5) 1:1 H<sub>2</sub>O-CH<sub>3</sub>OH, (6) CH<sub>3</sub>OH, (7) 1:1 CH<sub>3</sub>OH-CH<sub>2</sub>Cl<sub>2</sub>, (8) CH<sub>2</sub>Cl<sub>2</sub>, (9) 1:1 CH<sub>3</sub>OH-CH<sub>2</sub>Cl<sub>2</sub>, (10) CH<sub>3</sub>OH, (11) 1:1 H<sub>2</sub>O-CH<sub>3</sub>OH, (12) H<sub>2</sub>O, (13) 10% HCl, (14) H<sub>2</sub>O and EDTA, (15) 1N solution of the desired metal ion hydroxide and (16) washed back to neutrality with water. Water purification was accomplished by passing

distilled water through an Illinois Water Treatment Company purification system to remove paramagnetic ion impurities and organic residues. All nucleotide solutions not prepared in  $\text{H}_2\text{O}$  were lyophilized three times from 99.8%  $\text{D}_2\text{O}$  (Stohler Isotope Chemicals). The  $\text{D}_2\text{O}$  solutions were usually prepared under nitrogen to minimize  $\text{H}_2\text{O}$  contamination. NMR spectra were obtained from samples in 5mm tubes stoppered with rubber serum caps, then placed in 10 mm tubes positioned by Teflon O-ring spacers.

The metal hydroxides were used without further purification.  $\text{RbOH}$  and  $\text{CsOH}$  were purchased from Apache Chemical, Inc. Tetramethylammonium hydroxide solution was purchased from Matheson, Coleman and Bell,  $\text{LiOH}$  from Alfa-Ventron, and  $\text{KOH}$  from Mallinckrodt. The metal chlorides were also used without further purification.  $\text{LiCl}$ ,  $\text{NaCl}$ ,  $\text{KCl}$  and  $\text{BaCl}_2$  were purchased from Mallinckrodt,  $\text{RbCl}$  and  $\text{CsCl}$  were ultrapure quality from Alfa-Ventron.  $\text{MgCl}_2$  and  $\text{CaCl}_2$  were obtained from Matheson, Coleman and Bell and tetramethylammonium chloride was purchased from Aldrich Chemical Company.  $\text{SrCl}_2$  was purchased from J.T. Baker Chemical Co. Sodium 2,2,3,3- $\text{d}_4$ -3-trimethylsilylpropionate (TSP), purchased from Merck and Company, was used either as an internal reference (0.1 wt%) or as an external reference in the 10 mm tube while the sample was in the 5 mm tube.

## II. Instrumentation

A. Nuclear Magnetic Resonance Spectroscopy. NMR spectra were obtained on a Bruker WH-180 interfaced to a Nicolet 1180 with 32 K of memory. Probe temperatures were maintained by a Bruker temperature control unit, and monitored by means of a thermocouple mounted in the

probe and attached to a Doric trendicator that gave a constant visual temperature display. Temperatures were measured to within  $\pm 1$  °C.

Due to the dynamic range problems created by the solvent peak of samples run in H<sub>2</sub>O, some of the spectra were run on other instruments, and this is indicated in the captions. These spectra were run courtesy of Bruker (250 MHz and 200 MHz), Varian (200 MHz), Nicolet (200 MHz), and Jeol (200 MHz).

NOE experiments at two different field strengths necessitated the use of a lower field frequency instrument. Dr. R. Newmark of 3M kindly provided Varian XL-100 spectra for this purpose. Probe temperature was determined by measuring the chemical shift differences between methanol proton resonances and applying the Van Geet equations.

B. Ultraviolet Absorption Spectroscopy Concentrations of all guanosine monophosphate solutions were determined by UV absorption using a Beckman DU spectrophotometer updated with a Gilford photometer 252. Solution concentrations were determined using Beer's Law. The molar absorptivity ( $\epsilon$ ) at the absorption maximum is listed below for the nucleotides studied and was assumed to be independent of metal ion.

<u>nucleotide</u>	<u><math>\epsilon</math> (M<sup>-1</sup>cm<sup>-1</sup>)</u>	<u><math>\lambda_{\text{max}}</math> (nm)</u>
5'-GMP	13,700	252
2'-GMP	13,300	253
3'-GMP	13,300	253
3',5'-GMP	12,900	254
2',3'-GMP	12,900	254
5'-IMP	12,700	249
5'-dGMP	13,800	253

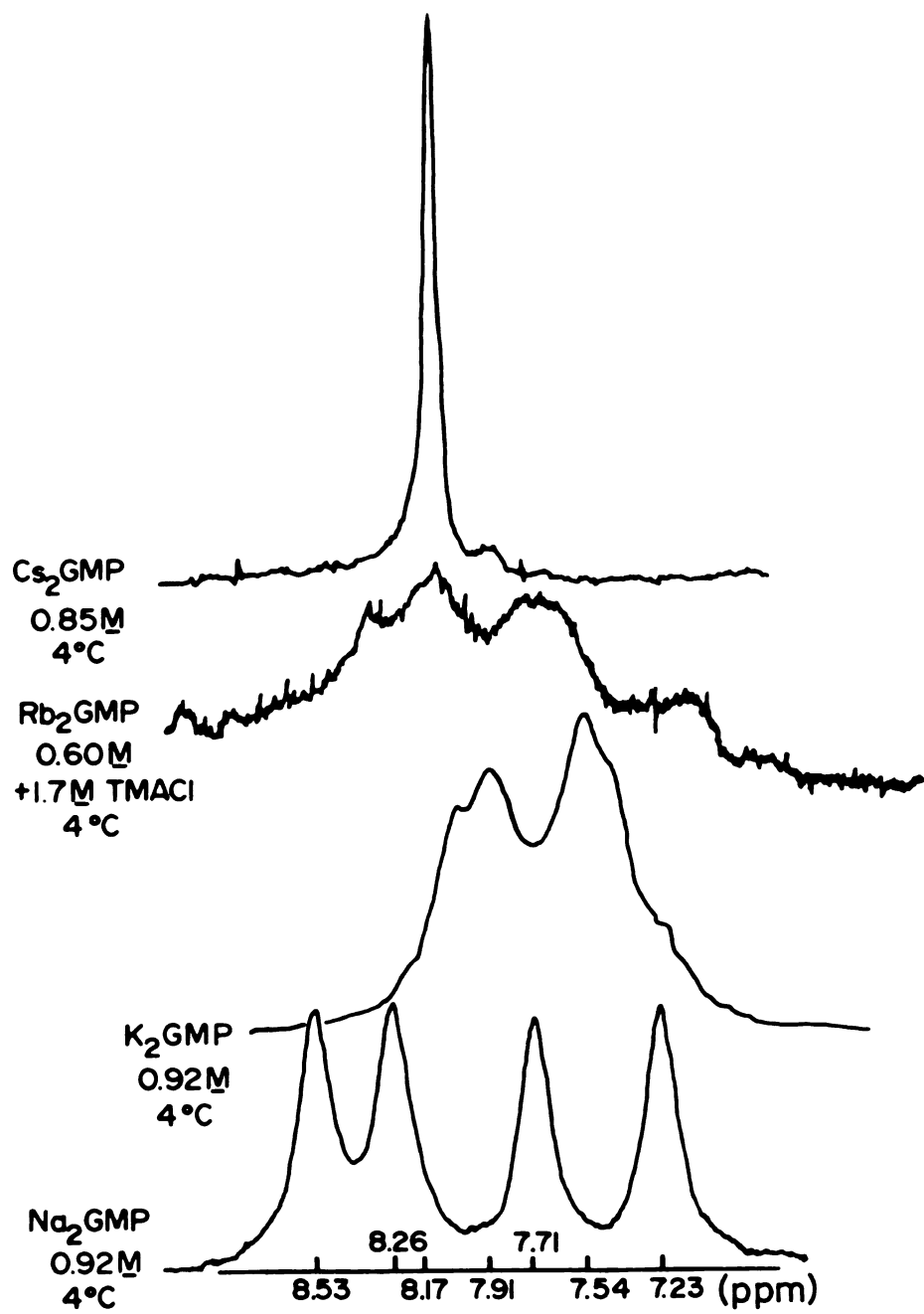
## RESULTS

### I. Structure Forming Homoionic Salts of 5'-GMP.

Structure formation of  $\text{GMP}^{2-}$  in aqueous solution is indicated by the appearance of new lines in the  $^1\text{H}$  NMR spectrum. Although spectral changes occur throughout the spectrum, structure formation is most clearly evident from the appearance of new well-resolved lines in the H(8) region from about 6.5 to 9 ppm downfield from TSP. Figure 9 shows spectra of the H(8) regions of the ordered forms of the structure directing homoionic alkali metal salts. The top spectrum is of 0.85 M  $\text{Cs}_2\text{GMP}$  at 4 °C. The large peak at 8.17 ppm represents unstructured monomer. The smaller upfield peak represents the  $\text{Cs}^+$  self-structure. The maximum extent of structure formation that has been observed for a pure  $\text{Cs}^+$  system corresponds to about 5% of the total nucleotide concentration. The next spectrum is that of 0.6 M  $\text{Rb}_2\text{GMP}$  at 4 °C. Four broad lines are present indicating that more than one large complex exists in this self-assembled form. Tetramethylammonium chloride (TMACl) is present in the solution to increase the solubility of the nucleotide as will be discussed later. The following spectrum is for 0.92 M  $\text{K}_2\text{GMP}$  at 4 °C. The  $\text{K}^+$  structure consists of two main peaks, one at 7.91 ppm and one at 7.54 ppm. The chemical shifts of the ordered  $\text{K}^+$  structures are all quite similar, making quantitative structure evaluations difficult. A low field shoulder is clearly present on the 7.91 ppm peak. A low field shoulder is detectable in addition to at least two high field shoulders on the 7.54 ppm peak, to yield a total of

Figure 9. The H(8) regions of the self-assembled alkali metal  
5'-GMP<sup>2-</sup> salts at low temperature.





at least five structure lines. The monomer concentration is too low to give a distinct and separate resonance; the system is thus estimated to be more than 90% self-assembled. The bottom spectrum is for 0.92 M Na<sub>2</sub>GMP at 4 °C. Three structure lines are present at 8.55, 8.26 and 7.25 ppm. The 7.71 ppm peak has been assigned to the monomer line. Integration of the H(8) lines reveals that the solution is about 75% structured.

## II. The Sodium-GMP Self-Structure

A. Tetramethylammonium as a Structure-Inert Cation. Studies of the tetramethylammonium ( $\text{TMA}^+$ ) salt of  $\text{GMP}^{2-}$  over wide ranges of concentration and temperature have shown that  $\text{TMA}_2\text{GMP}$  does not form an ordered structure. Under nonstructure forming conditions (i.e., at elevated temperatures and/or low concentrations) all  $\text{GMP}^{2-}$  salts exhibit only a single sharp monomer resonance at about 8.17 ppm. This same chemical shift value is observed for  $\text{TMA}_2\text{GMP}$  even at concentrations greater than 1.0 M and temperatures of 0.1 °C; neither additional H(8) lines nor any shift or broadening in the monomer line ( $\nu_{1/2} \approx 6.2$  Hz) are observed. Thus  $\text{TMA}^+$  is not a structure directing cation.

Comparison of spectra before and after addition of 0.5 M  $\text{TMACl}$  to 0.78 M  $\text{Na}_2\text{GMP}$  shows that at 0.3 °C, within experimental error, there is no change in the fraction of structured nucleotide. Thus,  $\text{TMA}^+$  does not inhibit the formation of sodium self-structure. The structure inertness of  $\text{TMA}^+$  is further verified by the spectra in Figure 10 in which aliquots of 4.0 M  $\text{NaCl}$  are added to a solution of 0.76 M  $(\text{TMA})_2\text{GMP}$  at 2.8 °C. The three new H(8) structure lines, which appear at the expense of the monomer line, grow in at the same rate and are identical to those observed for a self-assembled solution of pure  $\text{Na}_2\text{GMP}$ . Analogous results are obtained when solid  $\text{NaCl}$  is added to a  $(\text{TMA})_2\text{GMP}$  solution to maintain constant GMP concentration and when  $(\text{TMA})_2\text{GMP}$  and  $\text{Na}_2\text{GMP}$  solutions are mixed in the presence of  $(\text{TMA})\text{Cl}$  to maintain constant GMP concentration and ionic strength as shown in Table 4. Thus, the structure formation observed is not a consequence of ionic strength changes or dilution effects, but is the result of increasing  $\text{Na}^+/\text{GMP}^{2-}$  ratio. Figure 11 shows the behavior of the sodium self-structure lines

Figure 10. Effect of adding aliquots of 4.0 M NaCl on the H(8) region of 0.76 M (TMA)<sub>2</sub>GMP at 2.8° C. Initial GMP<sup>2-</sup> concentration (upper spectrum) is 0.76 M. Final GMP<sup>2-</sup> concentration (lower spectrum) is 0.64 M.

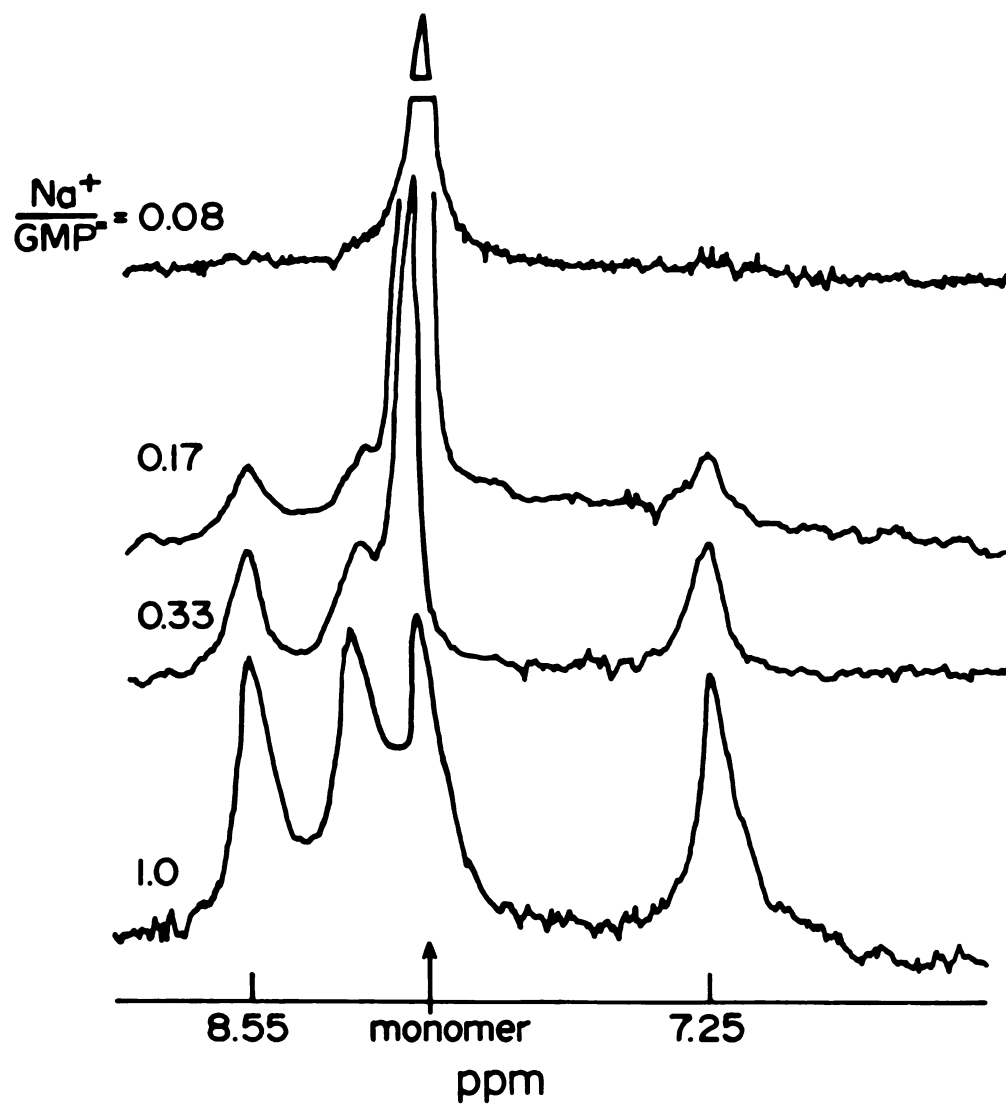


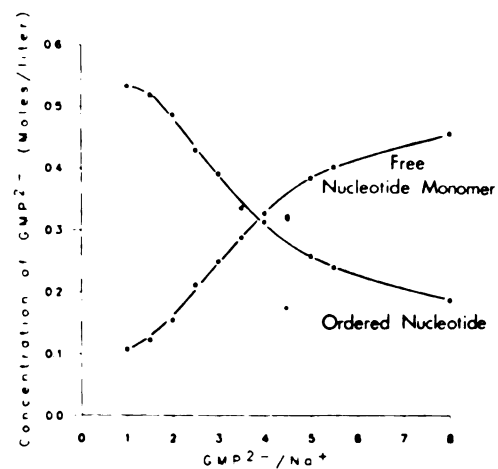
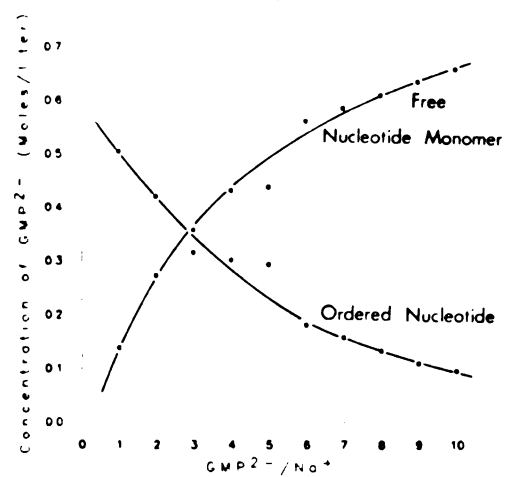
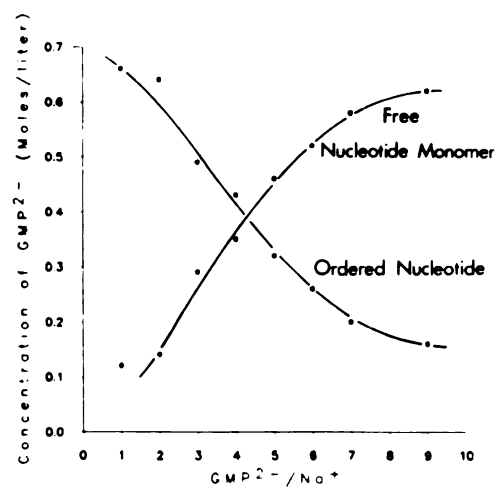


Table 4. Dependence of Na<sup>+</sup>-Structure Formation on Na<sup>+</sup>/GMP Concentration for Three Different TMA<sup>+</sup>/Na<sup>+</sup>-GMP<sup>=</sup> Solutions.

GMP <sup>2-</sup> /Na <sup>+</sup>	Mole % Ordered Forms of GMP <sup>2-</sup>		
	0.76M TMA <sub>2</sub> GMP 4M NaCl 2.8° C	0.64M TMA <sub>2</sub> GMP solid NaCl constant [GMP <sup>2-</sup> ] 2.0° C	0.78M TMA <sub>2</sub> GMP 0.78M Na <sub>2</sub> GMP 0.5 M TMACl constant [GMP <sup>2-</sup> ] and ionic .3° C strength
1.0	78.6	83.2	85.0
2.0	60.7	75.9	81.6
3.0	50.4	61.1	62.5
4.0	41.2	51.0	54.9
5.0	40.2	40.1	41.2
6.0	24.2	--	33.6
7.0	21.2	--	26.2
8.0	17.8	29.1	--
9.0	14.5	--	20.6
10.0	12.7	--	--

Figure 11. Graphical representations showing the results of three different experiments. The results of integrating the H(8) resonances to determine the concentration of structured nucleotide in solution when: (a) solid NaCl is added to 0.64 M (TMA)<sub>2</sub>GMP at 1.0° C; (b) solution NaCl is added to 0.78 M (TMA)<sub>2</sub>GMP at 2.8° C; (c) ratios of 0.76 M (TMA)<sub>2</sub>GMP and 0.76 M 11a<sub>2</sub>GMP are mixed maintaining constant volume in the presence of 0.5 M TMACl at 0.3° C.



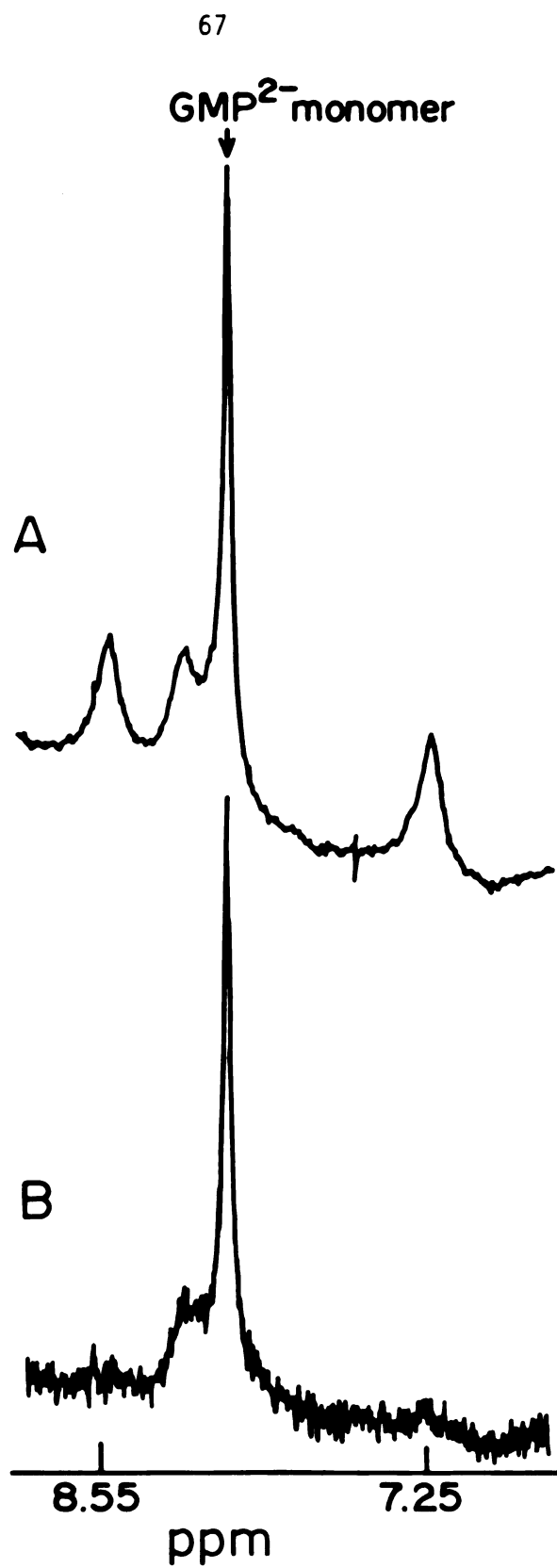
a) Self-assembly:  $\text{Na}^+$  Saltb) Self-assembly:  $\text{Na}^+$  Saltc) Self-assembly:  $\text{Na}^+$  Salt

as a function of increasing  $\text{GMP}^{2-}$  to metal ion ratio. Clearly no sharp end point exists, although a definite change in slope occurs between  $\text{GMP}^{2-}/\text{Na}^+ = 3$  and  $\text{GMP}^{2-}/\text{Na}^+ = 6$ .

The only difference observed between a mixed  $\text{Na}^+/\text{TMA}^+ - \text{GMP}^{2-}$  solution and a pure  $\text{Na}_2\text{GMP}$  solution is the chemical shift of the monomer line,  $\Delta\delta \sim 0.3$  ppm. Studies of the concentration dependence of  $\text{Na}_2\text{GMP}$  ordering have shown an upfield chemical shift of the monomer line to be associated with increasing solution structure. In the  $\text{Na}^+/\text{TMA}^+$  system, the monomer line appears to experience this shift to a far lesser extent. The upfield shift in the monomer line is presumably the result of diamagnetic ring current effects that result from non-specific base stacking interactions between monomeric and ordered  $\text{GMP}^{2-}$  species. The suppression of the base stacking interactions in the presence of  $\text{TMA}^+$  may arise from differences in the ability of  $\text{Na}^+$  and  $\text{TMA}^+$  to form ion pairs with monomeric and ordered forms of  $\text{GMP}^{2-}$ .

B.  $\text{TMA}^+/\text{GMP}^{2-}$  Ion Pairing. In an attempt to minimize the dynamic range of the  $\text{TMA}^+$  resonance in the  $^1\text{H}$  NMR spectra of  $\text{TMA}_2\text{GMP}$  solutions and facilitate data collection, a gated decoupling experiment was undertaken. Figure 12 shows a 0.55 M  $\text{TMA}_2\text{GMP}$  solution with 0.31 M NaCl at 4 °C, both with and without peak suppression. Clearly, in the spectrum where the  $\text{TMA}^+$  line was irradiated, the two outer sodium H(8) structure lines at 8.55 and 7.25 ppm are selectively reduced drastically in intensity, whereas little change in intensity is observed in the ribose region or the remaining H(8) lines. This reduction in intensity of one peak when another is irradiated is a negative intermolecular nuclear Overhauser effect (NOE) and can arise from one of two mechanisms. It can either originate from exchange modulation of scalar

Figure 12. The H(8) resonances of 0.55 M (TMA)<sub>2</sub>GMP with 0.31 M NaCl at 4° C (A) without peak supression and (B) irradiating the methyl resonance of TMA<sup>+</sup> at 3.2 ppm.



coupling or it can be the result of dipole-dipole interactions.<sup>126</sup>

Since neither TMA protons nor H(8) protons are capable of rapid exchange, a dipole-dipole mechanism must be invoked. NOE can be correlated to internuclear distance  $d$  by equation (2).<sup>127</sup>

$$\text{NOE} = 100 / A d^6 \quad (2)$$

where the magnitude of the NOE is measured in percent and  $A = 1.8 \times 10^{-2}$  Å for H-H interactions. Using NOE = 90, a distance of about 2 Å is calculated for  $d$ . Glickson et al.<sup>126</sup> have shown the relationship between homonuclear NOE and correlation time ( $\tau_c$ ). They have found that when tumbling is slower, the NOE is reduced and "negative enhancements" of the type observed here are possible. The slow tumbling region is defined when  $\omega_0 \tau_c \gg 1$ , where  $\omega_0$  is the precession frequency and  $\tau_c$  is the tumbling correlation time. Independent measurements of  $T_1$  and  $T_2$  for the outer two sodium structure H(8) lines ( $T_1=2.17$  and  $T_2=0.016$  sec at 1 °C and 0.59 M Na<sub>2</sub>GMP) confirm that the spectra are in fact for the slow tumbling region.<sup>134</sup>

The observed NOE is proportional to the concentration of TMA<sup>+</sup> in solution and to the frequency of the NMR, as expected. Figure 13 shows the results of irradiating the methyl resonance at 3.2 ppm on a 100 MHz spectrometer. Table 5 shows the difference in the effect observed at 180 MHz and 100 MHz. The solution contained 0.56 M Na<sub>2</sub>GMP and 0.36 M TMACl at 0° C. Clearly, when the TMA<sup>+</sup> is present in smaller amounts, the observed NOE is less as can be seen by comparison of Figures 12 and 13.

Figure 13. The H(8) resonances of 0.56 M Na<sub>2</sub>GMP with 0.36 M TMACl. The dashed line represents the spectrum without peak suppression. The solid line represents the spectrum when the methyl resonance of TMA<sup>+</sup> is irradiated at 3.2 ppm. These spectra were recorded at 100 MHz on a Varian instrument, and were provided courtesy of 3M.

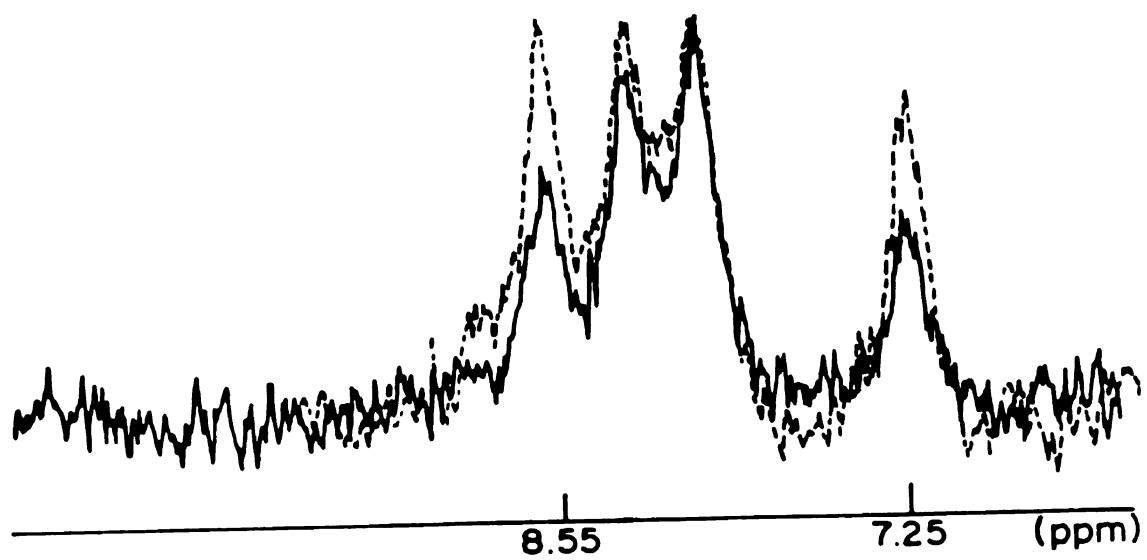


Table 5. The difference in the percent species present represented by a peak as determined by integration at two different field strengths, both with and without TMA<sup>+</sup> peak suppression (0.56 M Na<sub>2</sub>GMP with 0.32 M TMAcI at 0° C).

	8.55	8.26	Monomer	7.25
	(ppm)			
<hr/>				
<u>100 MHz Varian</u>				
1. No Peak Suppression	26%	26%	29%	19%
2. Peak Suppression	22%	29%	32%	17%
 <u>180 MHz Bruker</u>				
1. No Peak Suppression	27%	23%	24%	26%
2. Peak Suppression	15%	32%	38%	15%



C. HDO/GMP<sup>2-</sup> Association. Irradiation of the ribose peaks in a Na<sub>2</sub>GMP spectrum results in only a slight drop in intensity of the lines in the H(8) region as well as the rest of the ribose region. Irradiation of the HDO peak, however, results in the asymmetric reduction in peak intensity of the outer two H(8) lines. The ordered structure line at 8.55 ppm is affected more than the line at 7.25 ppm as shown in Figure 14. Thus, H<sub>2</sub>O is in close proximity to H(8) in the structure giving rise to the outer lines. Although these lines are believed to arise from the same structure, the H(8) environment giving rise to the downfield line either has more H<sub>2</sub>O in its immediate surroundings or is closer to the H<sub>2</sub>O molecules than the environment corresponding to the upfield H(8) line. This is in direct contrast to the results of irradiating the TMA<sup>+</sup> peak, where the NOE is equal for the outer lines.

D. Destabilization of the Na<sup>+</sup> Self-Structure by Excess Na<sup>+</sup> and K<sup>+</sup>. The addition of excess Na<sup>+</sup> to a structured solution of Na<sub>2</sub>GMP leads to a reduction in the extent of the Na<sup>+</sup> self-structure. This observation is illustrated by the H(8) resonances in Figure 15, where the relative intensity of the monomer line for 0.78 M Na<sub>2</sub>GMP is markedly increased in the presence of added NaCl. The addition of aliquots of NaCl to Na<sub>2</sub>GMP showed the same effect as shown in Figure 16. As shown in Figure 17, a similar decrease in the fraction of structured nucleotide is observed for a mixed Na<sup>+</sup>/TMA<sup>+</sup> - GMP<sup>2-</sup> solution when the GMP<sup>2-</sup>/Na<sup>+</sup> ratio is < 1.0. The decrease in the fraction of structured GMP<sup>2-</sup> with increasing Na<sup>+</sup> concentration beyond optimum concentration suggests that multiple equilibria are probably involved in the complexation of the metal ion by the ordered nucleotide.

Figure 14. The H(8) resonances of 0.36 M Na<sub>2</sub>GMP at 1.5° C where the solid line represents the spectrum without peak supression and the dashed line represents the spectrum when the HDO resonance is irradiated.

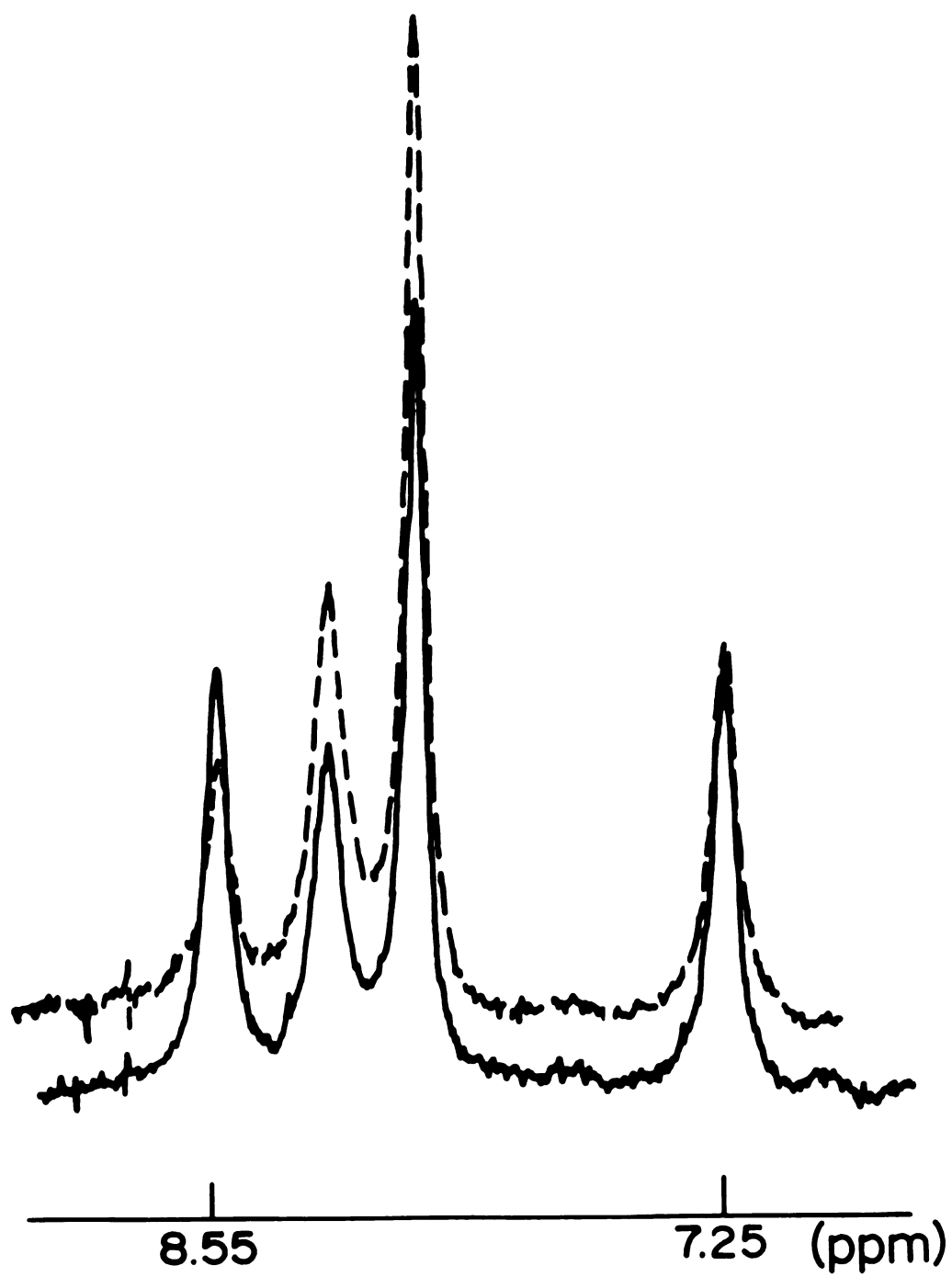


Figure 15. Comparison of the H(8) region of 0.78 M Na<sub>2</sub>GMP (lower spectrum) with 0.78 M Na<sub>2</sub>GMP containing 0.38 M NaCl (upper spectrum). Note the relative intensities of the monomer line and the structure lines.

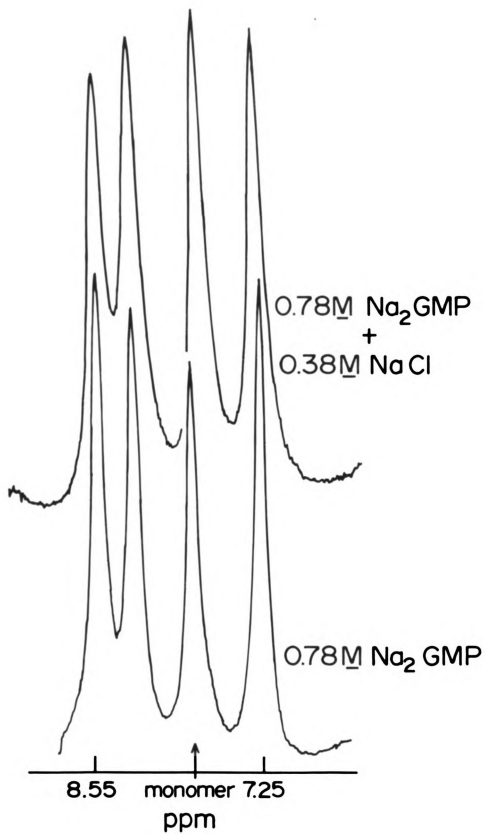


Figure 16. Effect of adding aliquots of 4.0 M NaCl on the H(8) resonances of 0.91 M Na<sub>2</sub>GMP at 4° C. The initial GMP<sup>2-</sup> concentration (lower spectrum) is 0.91 M. The final GMP<sup>2-</sup> concentration (upper spectrum) is 0.84 M. Note that the intensity of the monomer resonance increases slightly with increasing Na<sup>+</sup>/GMP<sup>2-</sup> ratio.

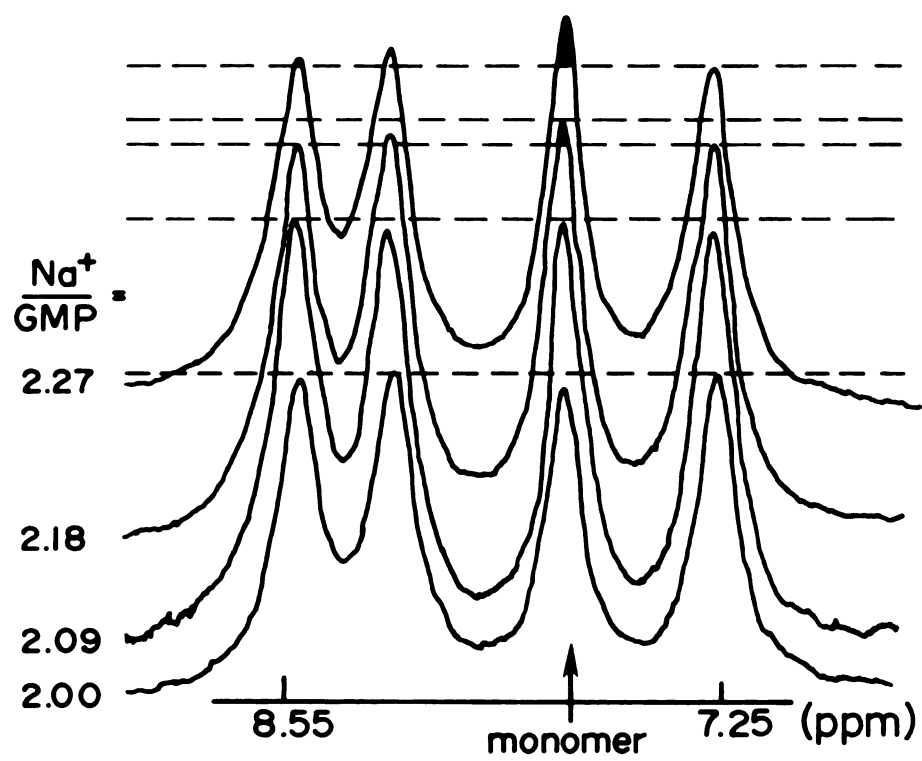
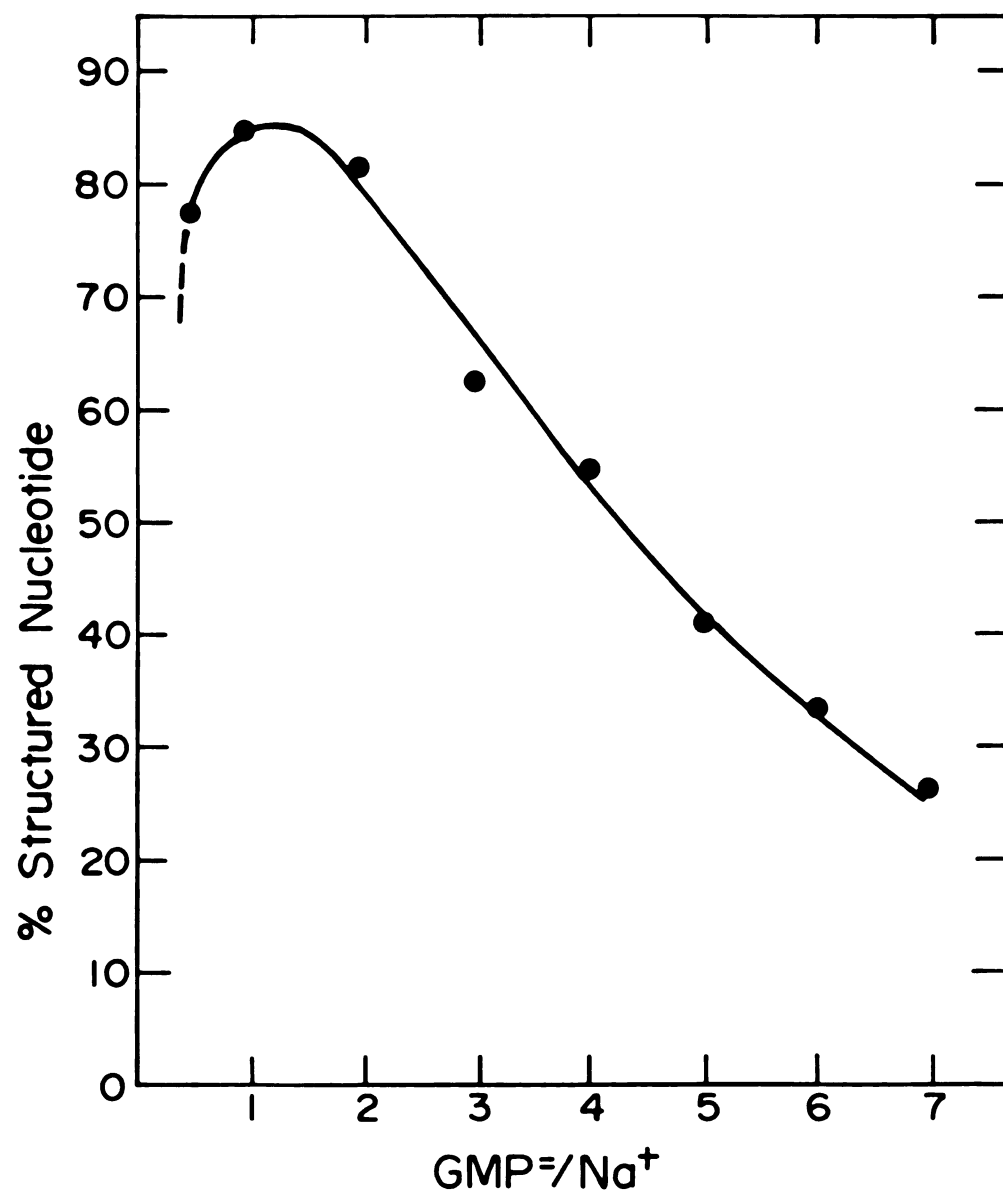


Figure 17. Effect of varying the  $\text{GMP}^{2-}/\text{Na}^+$  ratios on the fraction of structured  $\text{GMP}^{2-}$  in 0.78 M  $(\text{TMA})_2\text{GMP}$  at 0.3° C;  $[(\text{TMA})\text{Cl}] = 0.5$  M.





The addition of excess  $K^+$  to a solution of structured  $Na_2GMP$  also leads to a decrease in the fraction of structured nucleotide, as shown in Figure 18. Upon addition of sufficient excess  $K^+$ , the  $Na^+$  self-structure is replaced eventually by a  $K^+$  self-structure, which will be discussed in more detail later.

E. Stabilization of the  $Na^+$  Self-Structure by  $K^+$ . Although the extent of  $Na^+$  self-structure in solution is decreased on addition of  $Na^+$  or  $K^+$  at  $M^+/GMP^{2-}$  ratios greater than about 1.0, the  $Na^+$  self-structure is actually stabilized by  $K^+$  at  $Na^+/GMP^{2-}$  ratios below 1.0. As shown in Figure 19, the addition of KCl to a 0.63 M  $GMP^{2-}$  solution containing 0.5  $Na^+/GMP^{2-}$  leads initially to a dramatic increase in the intensity of the  $Na^+$  self-structure lines and a concomitant decrease in the intensity of the monomer resonance. The increase in percent sodium self-structure in solution is accompanied by the disappearance of the highest field structure line and a new line growing in just downfield of it. The line position exchange is clearly shown in the spectrum with a  $K^+/Na^+$  ratio of 0.51. The changes in equilibrium concentrations caused by the added  $K^+$  are much greater than would be observed by the addition of an equivalent amount of  $Na^+$ .

The further addition of KCl beyond a  $K^+/Na^+$  ratio of 1.0 leads to the appearance of new H(8) lines which can be assigned to a  $K^+$  self-structure (cf., Figure 19). However, even at a  $K^+/Na^+$  ratio of 2.2, the  $Na^+$  self-structure dominates. This means that the species represented by the  $Na^+$  self-structure lines are more favored than those represented by the  $K^+$  self-structure lines. Since the  $Na^+$  and  $K^+$  self-structures involve specific complexation of  $Na^+$  and  $K^+$ , respectively, it is apparent that  $Na^+$  is a stronger structure directing cation than  $K^+$ .

Figure 18. Effect of adding aliquots of 4.0 M KCl on the H(8) region of 0.9 M Na<sub>2</sub>GMP at 3.4° C. Note the increase in monomer line intensity and the increase in K<sup>+</sup> structure lines with the decrease in Na<sup>+</sup> structure lines.

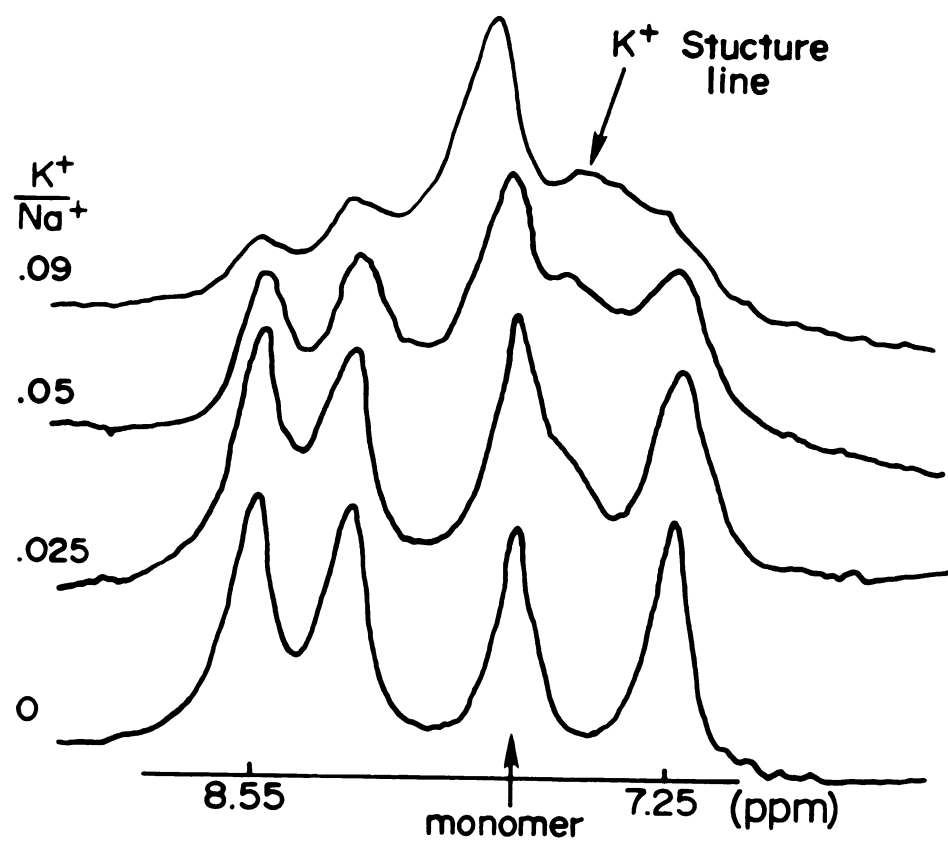
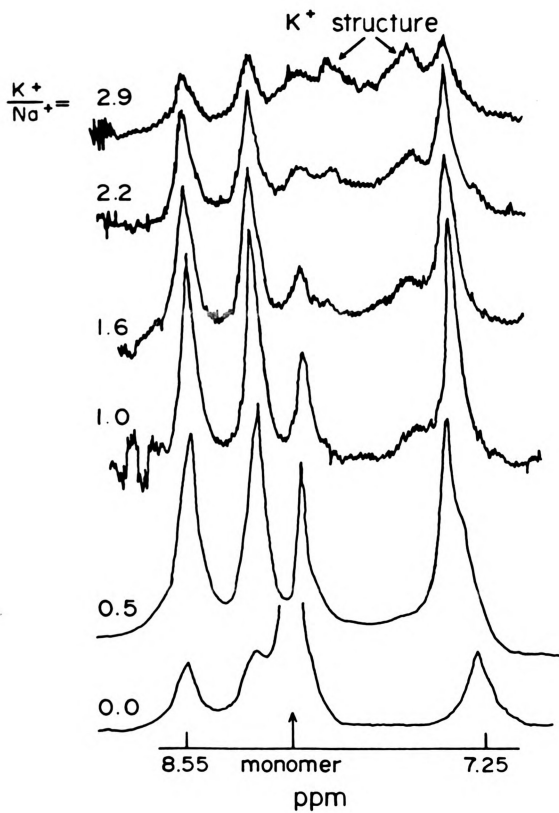


Figure 19. Effect of adding aliquots of 4.0 M KCl on the H(8) lines of a solution containing the Na<sup>+</sup> self-structure at a Na<sup>+</sup>/GMP<sup>2-</sup> ratio of 0.5. Note the dramatic increase in the IIa self-structure lines that appear at the expense of the monomer line at low K<sup>+</sup>/Na<sup>+</sup> ratios. [(TMA)<sub>2</sub>GMP] = 0.63 M, [NaCl] = 0.32 M. Temperature is 2.9° C.



However, non-specific metal ion complexation reactions also appear to be operating in the self-assembly process. Relative to  $\text{Na}^+$ , the binding of  $\text{K}^+$  at the non-specific sites is more effective in stabilizing the  $\text{Na}^+$  self-structure.

The stabilization of the  $\text{Na}^+$  self-structure by  $\text{K}^+$  at low  $\text{Na}^+/\text{GMP}^{2-}$  ratios is also illustrated by the melting experiments shown in Figure 20. The mixed metal ion solution containing 0.50  $\text{K}^+/\text{GMP}^{2-}$  and 0.16  $\text{Na}^+/\text{GMP}^{2-}$  (total  $\text{M}^+:\text{GMP}^{2-} = 0.66:1$ ) is not entirely melted out to monomer at 41 °C, whereas an analogous solution containing only  $\text{Na}^+$  metal ions at 0.66  $\text{Na}^+/\text{GMP}^{2-}$  is completely melted out by 26.5 °C.

F. The Structure Directing Influence of  $\text{Li}^+$ . Unlike  $\text{TMA}^+$ ,  $\text{Li}^+$  cannot be used as a structure-inert ion in  $\text{GMP}^{2-}$  systems. Pure  $\text{Li}_2\text{GMP}$  shows no evidence for structure formation at high concentrations and low temperatures. Figure 21 shows the result of mixing  $\text{Li}_2\text{GMP}$  and  $\text{Na}_2\text{GMP}$  at 2 °C. Clearly, the spectrum corresponding to  $4\text{GMP}^{2-}/\text{Na}^+$  is quite different from that of an equivalent solution where  $\text{Li}^+$  is replaced by  $\text{TMA}^+$ . Also, the addition of  $\text{Li}^+$  to a solution often induces precipitation whereas the addition of  $\text{TMA}^+$  often has a solubilizing effect. Thus, although  $\text{Li}^+$  is not a structure directing ion, it does not play a passive structural role in the presence of a strong structure director such as  $\text{Na}^+$ . The complete results of the  $\text{Na}_2\text{GMP}-\text{Li}_2\text{GMP}$  experiment are contained in Appendix A.

Figure 20. The melting out of H(8) lines for two solutions containing the  $\text{Na}^+$  self-structure at a total alkali metal ion to  $\text{GMP}^{2-}$  ratio of 0.66:1. Solution A contains a mixture of  $\text{K}^+$  and  $\text{Na}^+$  ( $\text{K}^+/\text{GMP}^{2-} = 0.50$ ,  $\text{Na}^+/\text{GMP}^{2-} = 0.16$ ); solution B contains only  $\text{Na}^+$  ( $\text{Na}^+/\text{GMP}^{2-} = 0.66$ ).  $[(\text{TMA})_2\text{GMP}] = 0.57 \text{ M}$ .



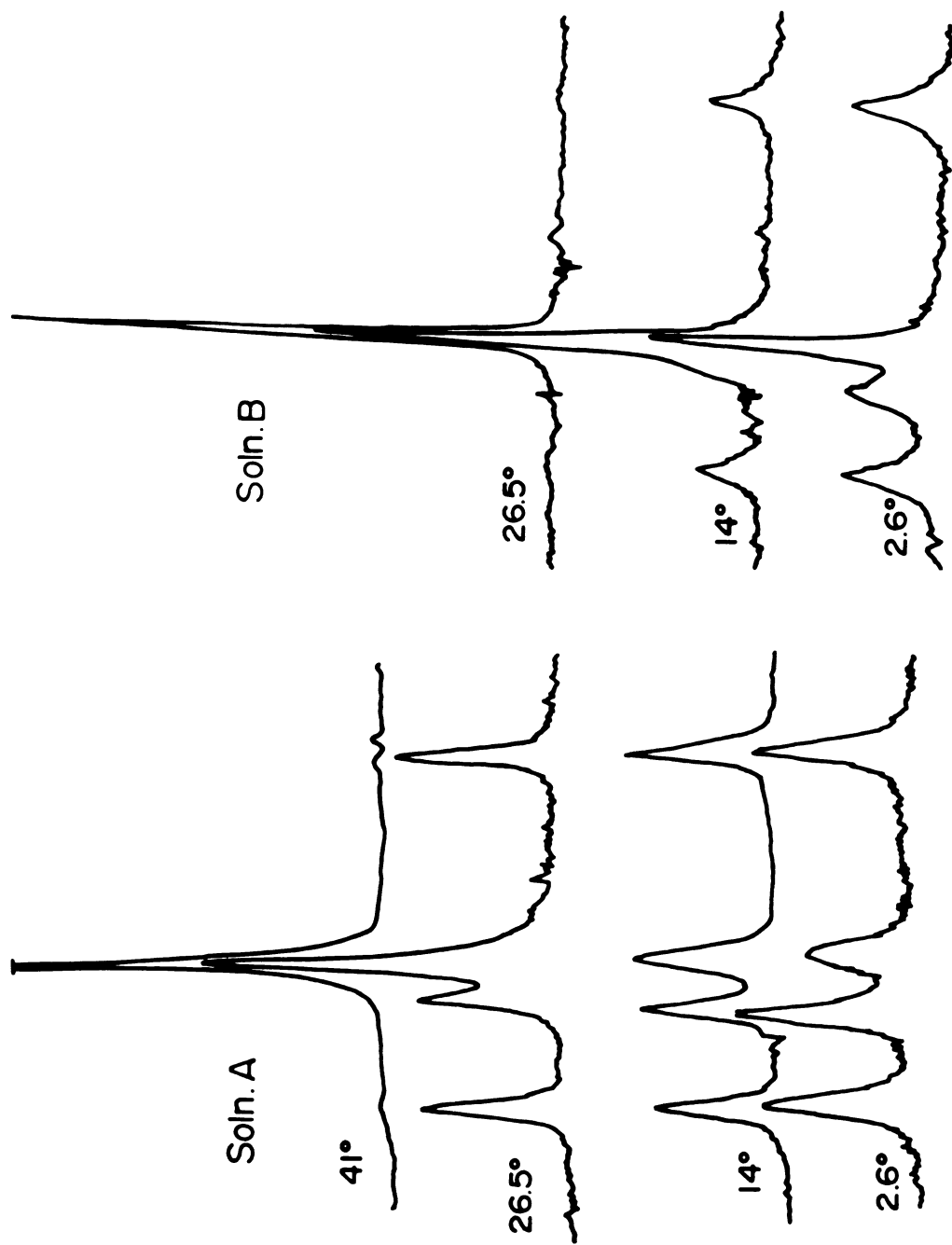
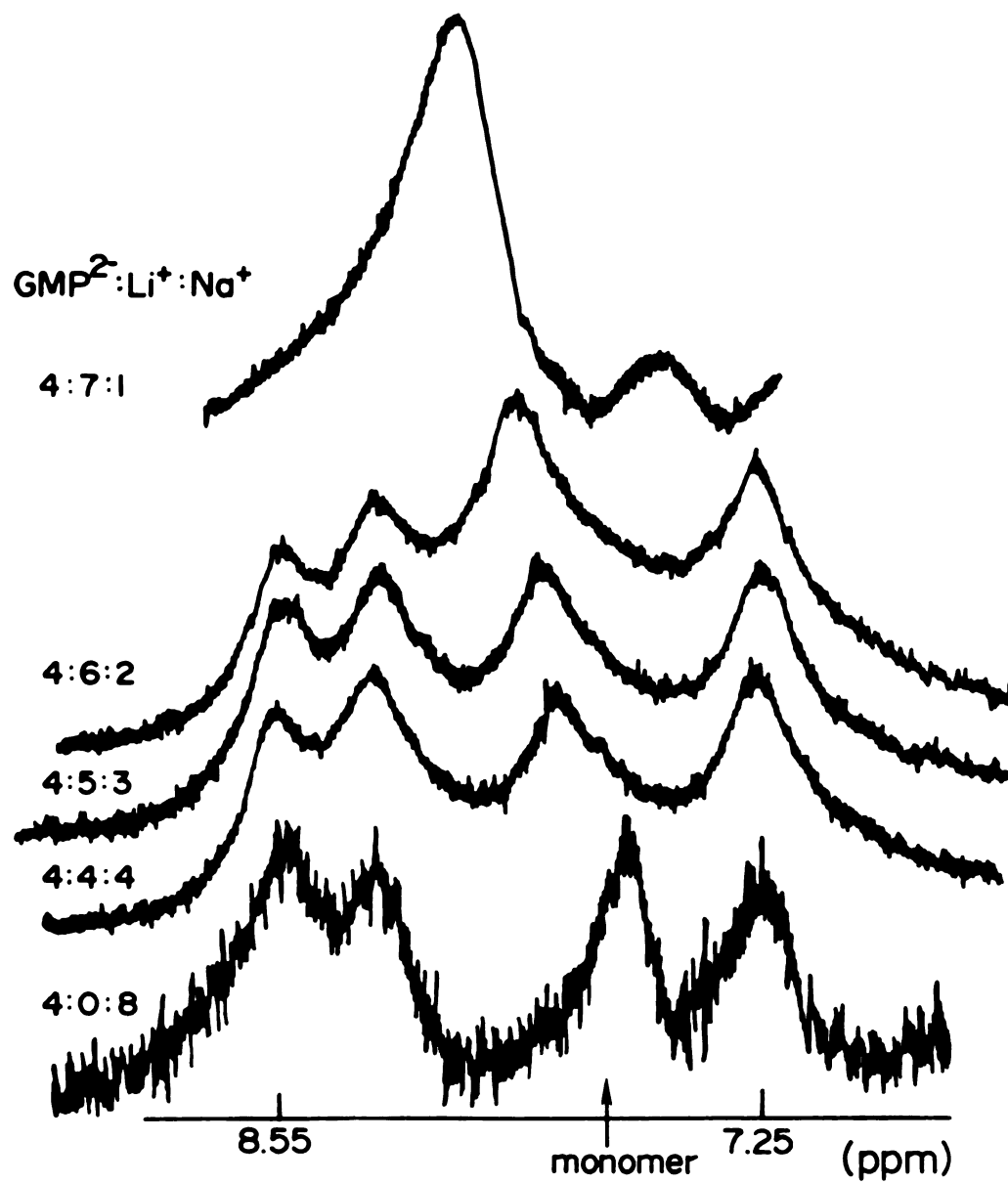


Figure 21. Effect on the H(8) region of mixing different volumes of 0.72 M  $\text{Li}_2\text{GMP}$  and 0.72 M  $\text{Na}_2\text{GMP}$  at 2° C and constant overall volume. Note that at high  $\text{Li}^+$  concentration (upper spectrum) the lines arising from a normal sodium self-structure are no longer present.



### III. The Potassium GMP Self-Structure

A. "Simple" and "Complex"  $K^+/GMP^{2-}$  Structure. Figure 22 shows the results of addition of KCl to a 0.85 M TMA<sub>2</sub>GMP solution at 3.2 °C. Structure formation begins with a marked broadening of the monomer line and the appearance of two new high field lines. Further addition of KCl promotes an increase in intensity of the new lines until at  $GMP^{2-}/K^+ = 2$ , all of the monomer is converted into a self-assembled form. Spectra of solutions whose ratio of  $GMP^{2-}$  to  $K^+$  was greater than or equal to two showed no similarity to a pure K<sub>2</sub>GMP spectrum at corresponding concentrations and temperatures. There is a marked difference between the spectrum at  $GMP^{2-}/K^+ = 2$  and  $GMP^{2-}/K^+ = 1$ , although over this range the change is gradual. Spectra showing structure up to and including  $GMP^{2-}/K^+ = 2$  represent the "simple" structure. The "complex" structure is represented by  $GMP^{2-}/K^+ \leq 1$ .

Figure 23 shows a melting profile of a 0.70 M TMA<sub>2</sub>GMP solution with  $GMP^{2-}/K^+ = 1$ . The "complex" structure is never converted to the "simple" even as the "complex" structure is melted out. The existence of two types of K<sub>2</sub>GMP structures is quite different from what is observed for ordered Na<sub>2</sub>GMP, which exhibits only one pattern of structure lines regardless of  $GMP^{2-}/Na^+$  ratio.

#### B. Effect of Excess $K^+$ on the "Complex" K<sub>2</sub>GMP Self-Structure.

Addition of KCl to K<sub>2</sub>GMP results in a marked shift in the equilibrium concentrations of the self-assembled species as a function of time and temperature. Two solutions of 0.5 M K<sub>2</sub>GMP made up at room temperature, one stored at 0 °C and the other at 20 °C, gave identical spectra at 3.6 °C. These solutions showed no change in the H(8) resonances with time as shown in Figure 24. In contrast, two different solutions containing



Figure 22. H(8) resonances observed upon addition of aliquots of 4.19 M KCl to 0.85 M (TMA)<sub>2</sub>GMP at 3.2° C. The "simple" structure (and monomer) is seen at  $\text{GMP}^{2-}/\text{K}^+ = 12, 6$  and 2. The "complex" structure is represented  $\text{GMP}^{2-}/\text{K}^+ = 1$  and 0.5. The initial  $\text{GMP}^{2-}$  concentration (lower spectrum) is 0.85 M. The final  $\text{GMP}^{2-}$  concentration (upper spectrum) is 0.60 M.

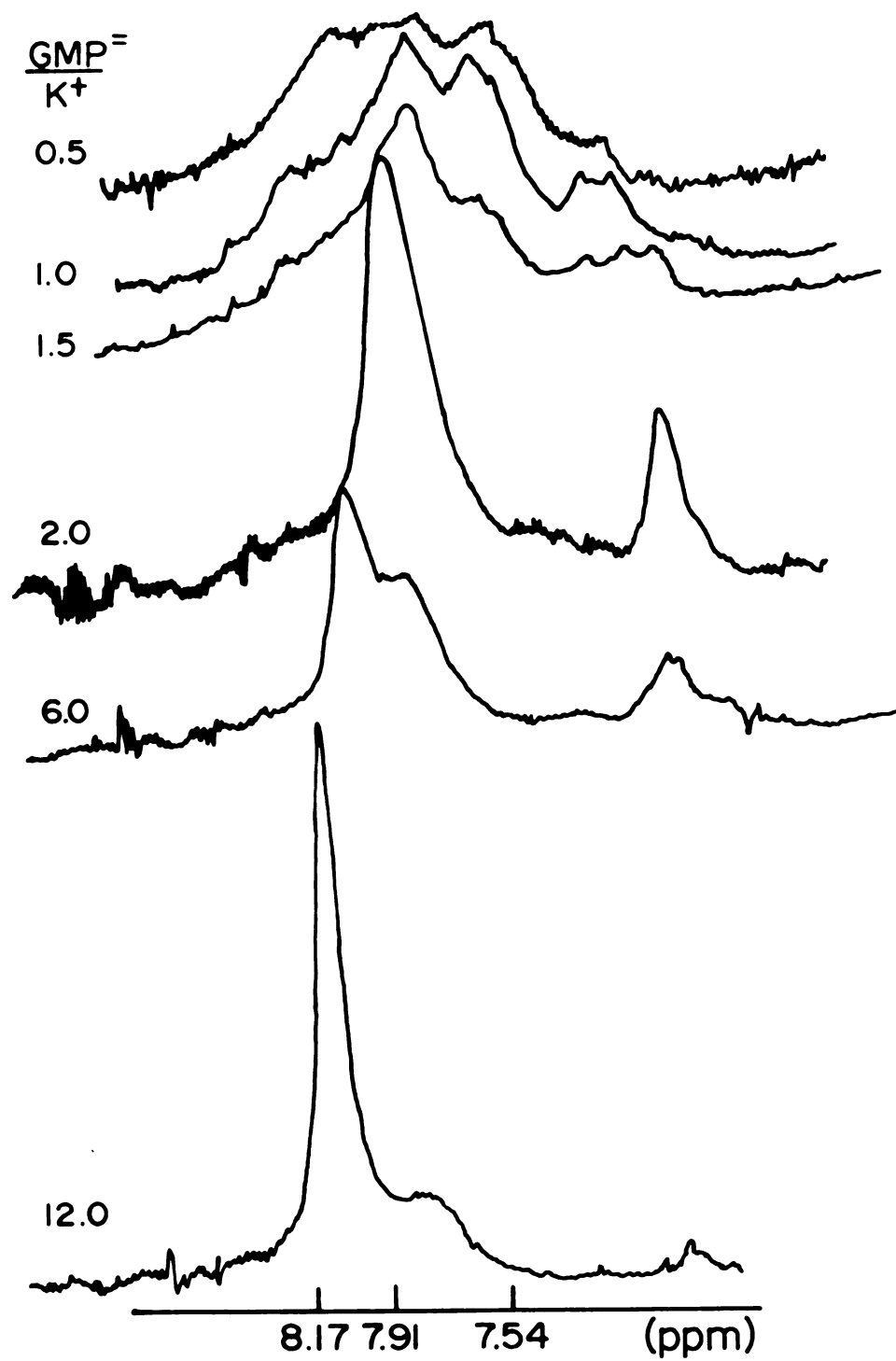


Figure 23. The melting out of H(8) resonances of the "complex"  $K^+$ - $GMP^{2-}$  self-structure at  $GMP^{2-}/K^+ = 1.0$ .  $[(TMA)_2GMP] = 0.70$  M.  $[KCl] = 0.70$  M.



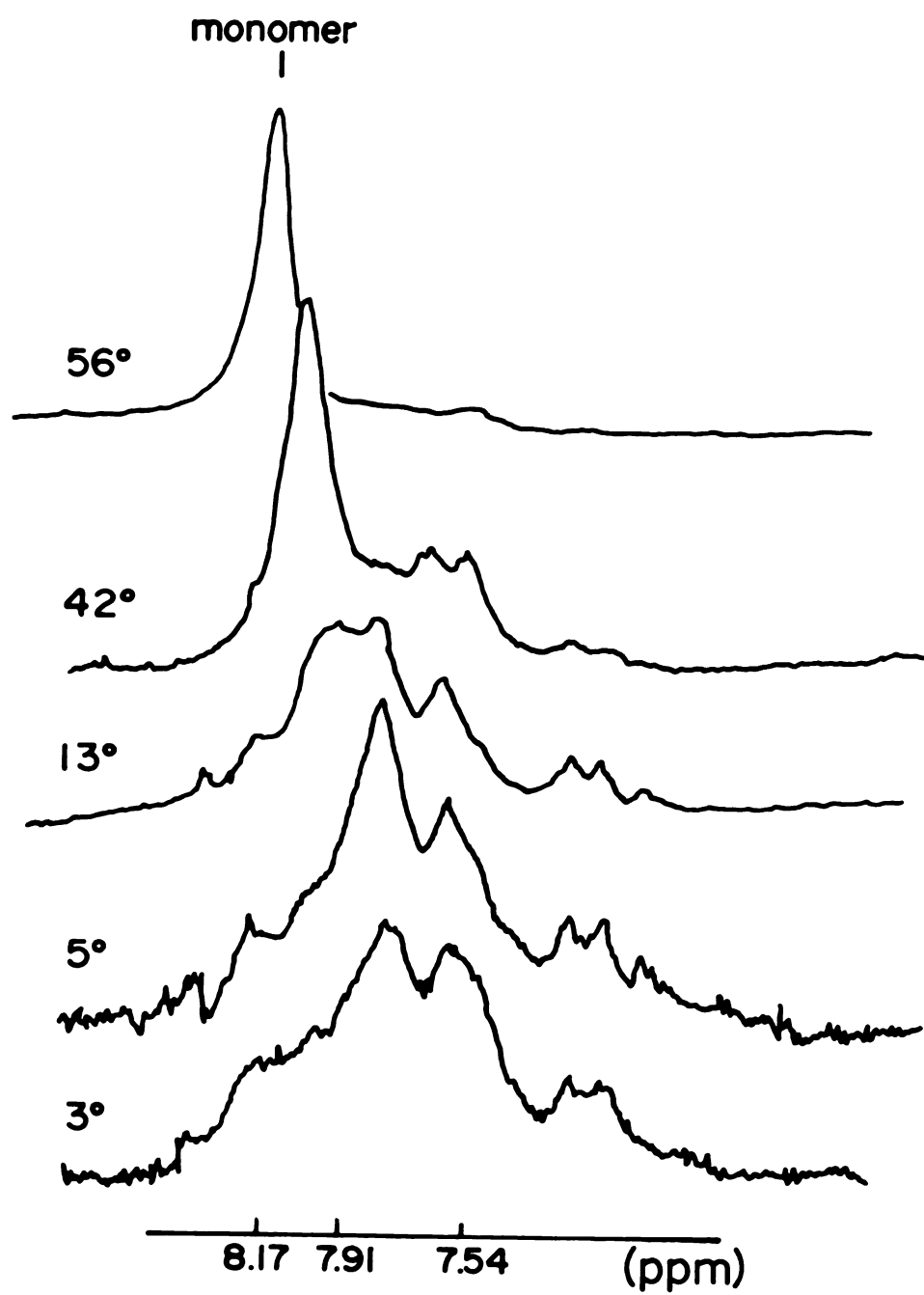
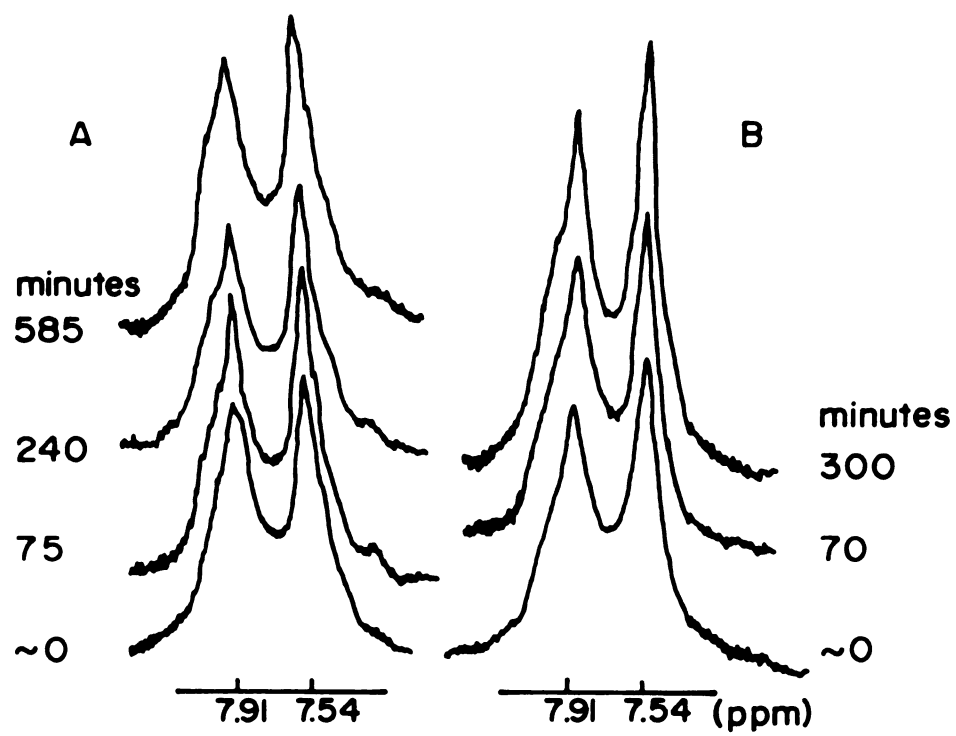


Figure 24. The H(8) region of (A) 0.5 M K<sub>2</sub>GMP prepared at room temperature and stored at 0° C as a function of time expressed in minutes, and (B) 0.5 M K<sub>2</sub>GMP prepared and stored at room temperature as a function of time in minutes. Spectra obtained at 3.6° C.



0.5 M  $K_2GMP$  and 0.38 M KCl made up and stored under conditions identical to those discussed above showed "new" structure formation as a function of time. These "new" structure lines are present to some extent in more concentrated  $K_2GMP$  solutions, but are "new" at the concentrations discussed. Thus, they actually represent a change in the relative concentrations of the different ordered structures in a given solution. Figure 25 shows that the shoulders at 8.04 and 7.44 ppm increase in intensity until they are larger than the 7.91 and 7.54 ppm  $K^+$ -structure peaks. The peak at 7.23 ppm also increases in intensity. The peaks sharpen with this increase, suggesting the presence of smaller, more discrete structural units. It is clear from comparison of the 300 minute spectra for the solutions containing KCl, that the equilibrium shift to "new" structures is more dramatic for the solution stored at 0 °C than at 20 °C. Thus, it appears that the "new" structures are formed from self-structures normally present in an ordered  $K_2GMP$  solution. Melting profiles of solutions with and without KCl indicate that the "new" structures melt out to the structures corresponding to the inner peaks as shown in Figure 26. Although about 10 hours are necessary to reach an equilibrium state in the KCl- $K_2GMP$  system at 3.6 °C, rapid equilibrium (several minutes) occurs on melting at elevated temperatures. Heating a KCl- $K_2GMP$  solution until only monomer is present and then rapidly cooling and recording the spectrum resulted in broad lines, and the absence of an upfield shoulder on the highest field peak (Figure 27.E).

The effect observed on addition of KCl to a  $K_2GMP$  solution appears to be a nonspecific cation effect. Similar, although not identical effects are observed on addition of TMAcI (Figure 27). If an anion

Figure 25. The time dependence of the H(8) region of (A) 0.5 M  $K_2GMP$  containing 0.38 M  $KCl$  prepared at room temperature and stored at 0° C, and (B) 0.5 M  $K_2GMP$  containing 0.38 M  $KCl$  prepared and stored at room temperature. Time is measured in minutes from the time the solution was prepared as zero minutes. Spectra measured at 3.6° C.

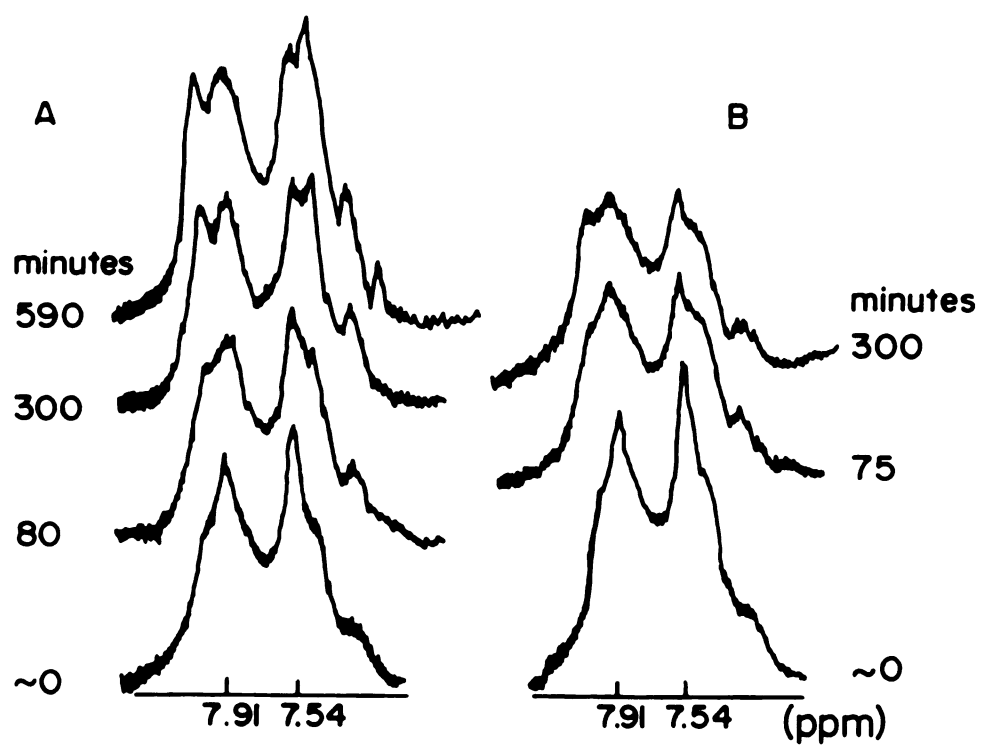


Figure 26. The melting out of the H(8) region of (A) 0.5 M  $K_2GMP$  prepared and stored at room temperature, and (B) 0.5 M  $K_2GMP$  containing 0.38 M  $KCl$  prepared and stored at room temperature.

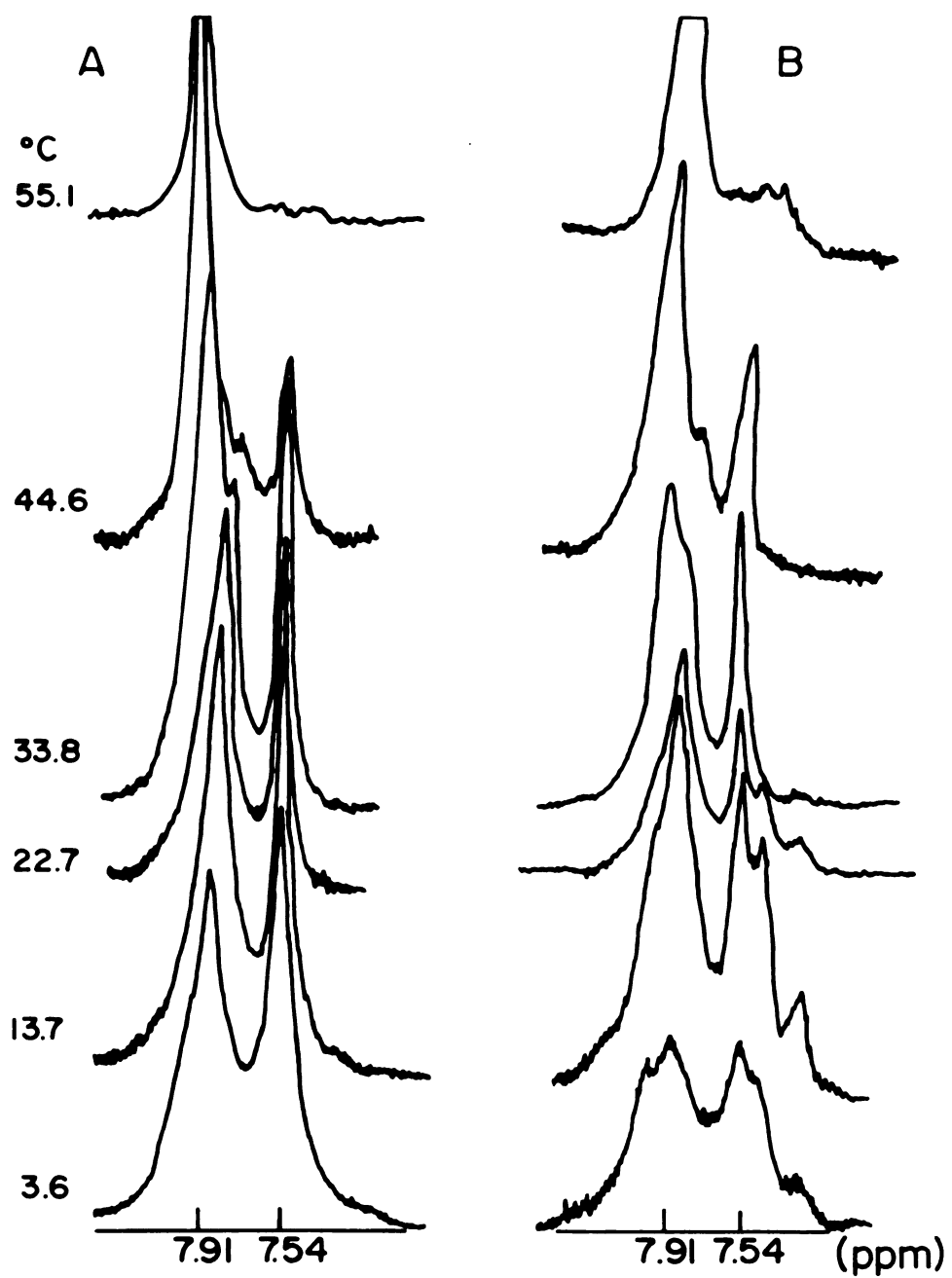
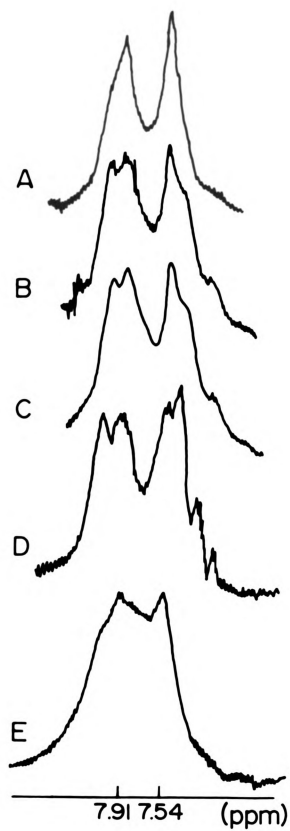




Figure 27. The H(8) region of (A) 0.5 M K<sub>2</sub>GMP stored for 10 hours at 0° C and recorded at 3.6° C, (B) 0.5 M K<sub>2</sub>GMP containing 0.38 M KNO<sub>3</sub> stored for more than 10 hours at 0° C and recorded at 3.6° C, (C) 0.5 M K<sub>2</sub>GMP containing 0.38 M TMACl stored for more than 10 hours at 0° C and recorded at 3.6° C, (D) 0.5 M K<sub>2</sub>GMP containing 0.38 M KCl stored for 10 hours at 0° C and recorded at 3.6° C, and (E) 0.5 M K<sub>2</sub>GMP heated to boiling and then cooled in ice to 0° C with the spectrum immediately recorded at 3.6° C.



effect were operative, these "new" structures would not be present in the more concentrated solutions of  $K_2GMP$  which contain no other anion. Also, addition of  $KNO_3$  has virtually the same effect as  $KCl$ , as shown in Figure 27. In effect, the cation appears to be causing a shift in the equilibrium which normally occurs with increasing  $K_2GMP$  concentration, except without the increase in  $GMP^{2-}$  concentration. Addition to  $NaCl$  to  $K_2GMP$  resulted in similar time dependent changes in the spectra (Figure 28). Figure 29 shows NMR spectra of a  $K_2GMP/KCl$  system with conditions comparable to those for an analogous  $K_2GMP/NaCl$  system. When aliquots of  $NaCl$  were added to the  $K_2GMP$  system, the equilibrium shifts were not observed unless the system was allowed to remain undisturbed for a period of time (days). In contrast, the addition of aliquots of  $KCl$  induced more immediate perturbations. This is quite different from  $Na_2GMP$  self-assembly, which shows no spectral changes as a function of time to date, with or without excess cations present. It is evident from the  $TMACl/K_2GMP$  system (Figure 27), that the 8.04 and 7.44 ppm peaks do not arise from the same structure. Clearly, they are more different in intensity in the  $KCl/K_2GMP$  system than they are in the  $TMACl/K_2GMP$  system. Thus, different cations favor different structures, and cause "new" structure formation to varying degrees. However, if one discounts details in spectral intensities, the same general effect is observed for three cations with markedly differing size and solvation properties.

C. Stability of the "Simple"  $K^+$  Structure in the Presence of  $Na^+$ . Figure 30 shows how a sodium like structure grows in when  $NaCl$  solution is added to a "simple"  $K^+$  structure, 0.63 M  $TMA_2GMP$  with  $GMP^{2-}/K^+ = 2$  at 2.3 °C. Addition of only a small amount of  $Na^+$  is necessary

Figure 28. Effect on the H(8) resonances of 0.92 M K<sub>2</sub>GMP on addition of aliquots of 4.01 M NaCl at 4° C. The initial concentration of GMP<sup>2-</sup> (lower spectrum) is 0.92 M and the final concentration of GMP<sup>2-</sup> (upper spectrum) is 0.83 M. Note the ratio 1:2:0.17, (A) was recorded 96 hours after (B). The sample was stored at room temperature. A definite change in the relative intensities of the inner and outer lines is apparent.

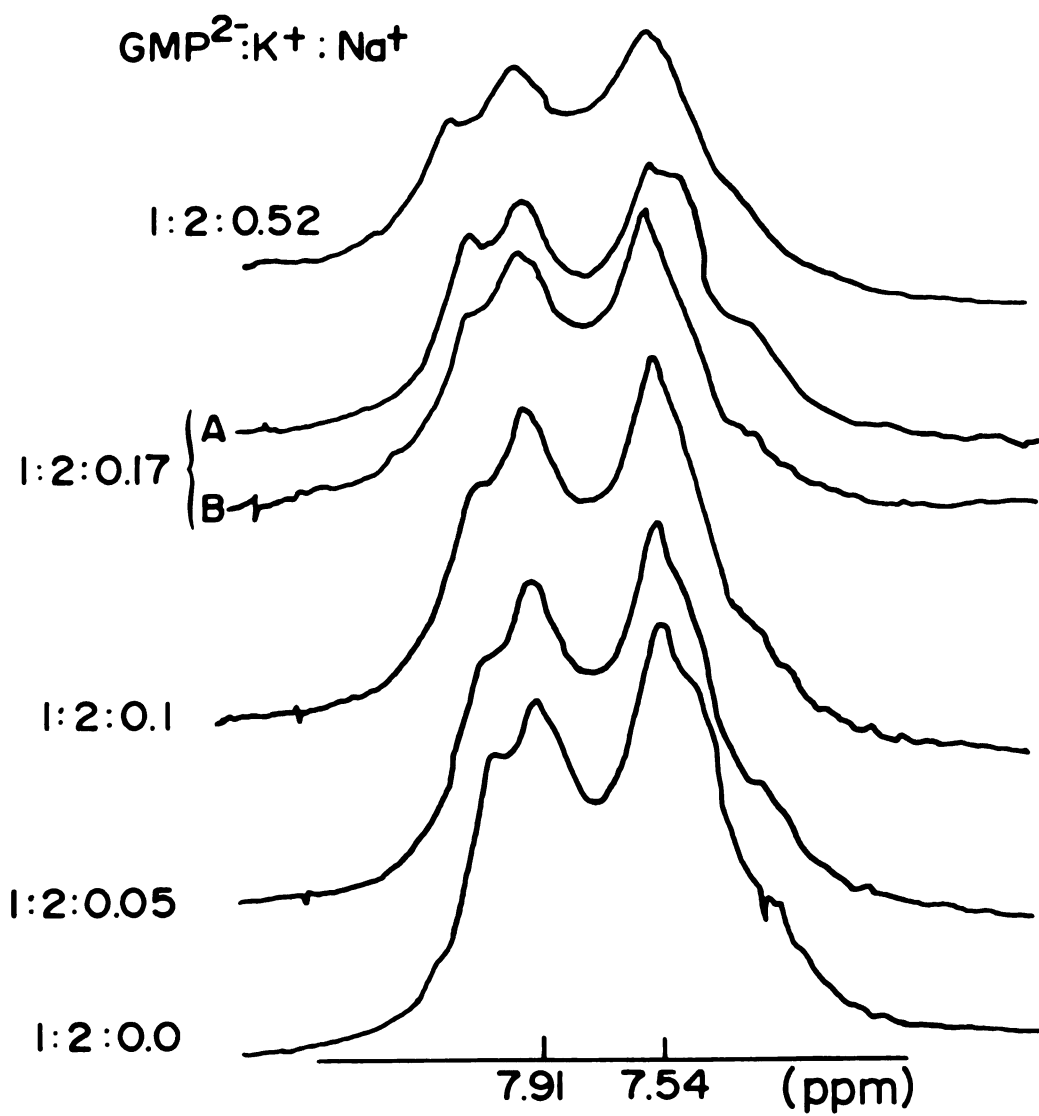


Figure 29. Effect on the H(8) resonances of 0.92 M  $K_2GMP$  on addition of aliquots of 4.03 M  $KCl$  at 4° C. The initial concentration of  $GMP^{2-}$  (lower spectrum) is 0.92 M and the final concentration of  $GMP^{2-}$  (upper spectrum) is 0.59 M.

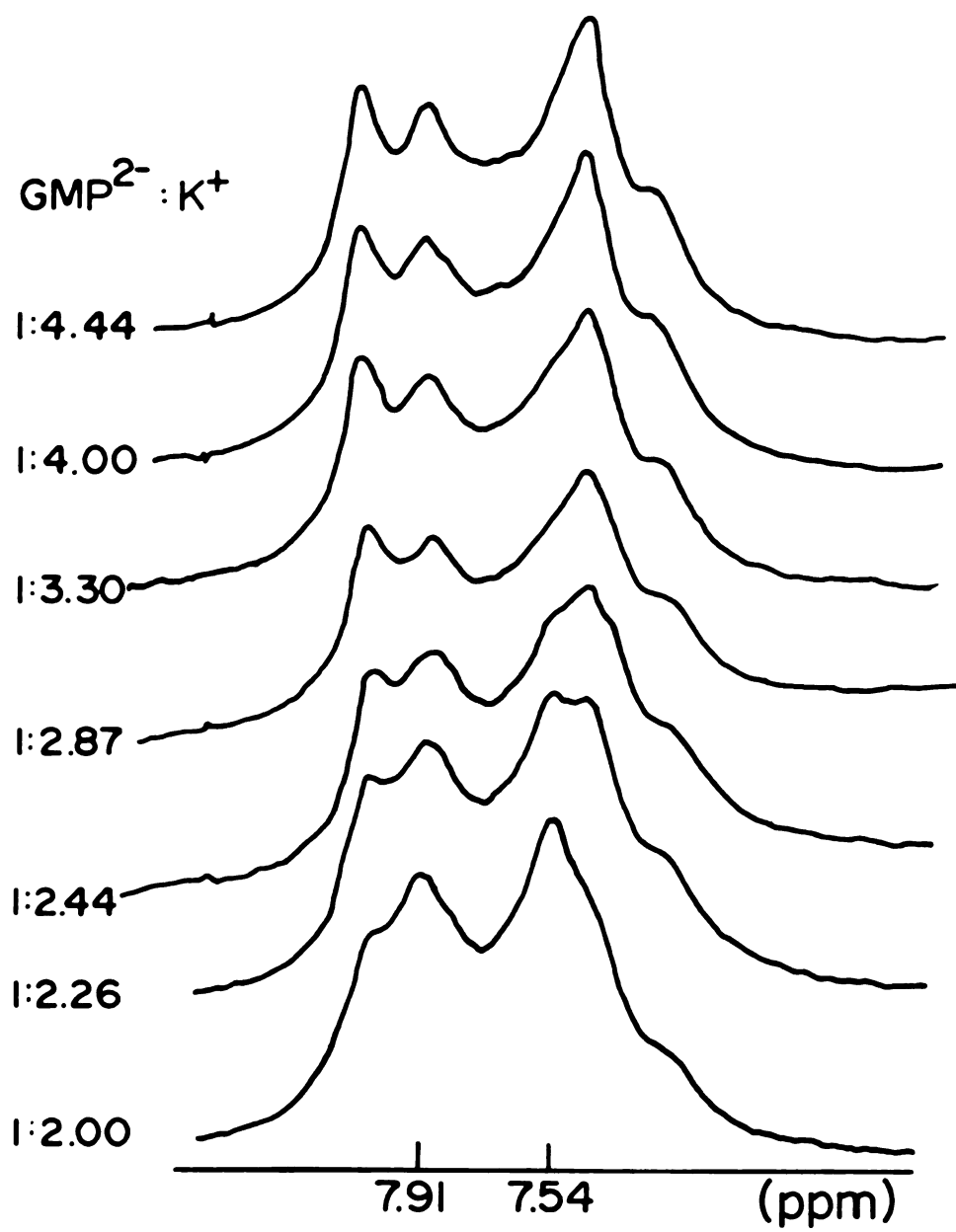
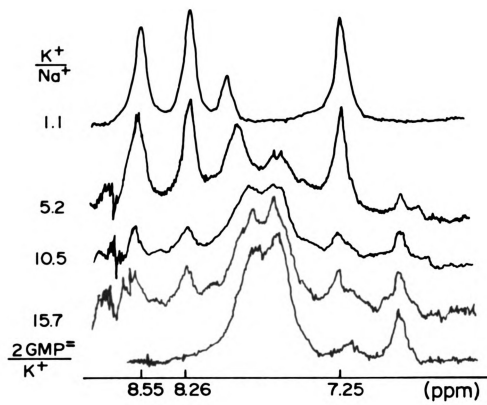


Figure 30. Effect on the H(8) resonance of adding aliquots of 4.0 M NaCl to the "simple" potassium self-structure at 2.3° C. [(TMA)<sub>2</sub>GMP] = 0.63 M. [KCl] = 0.32 M.

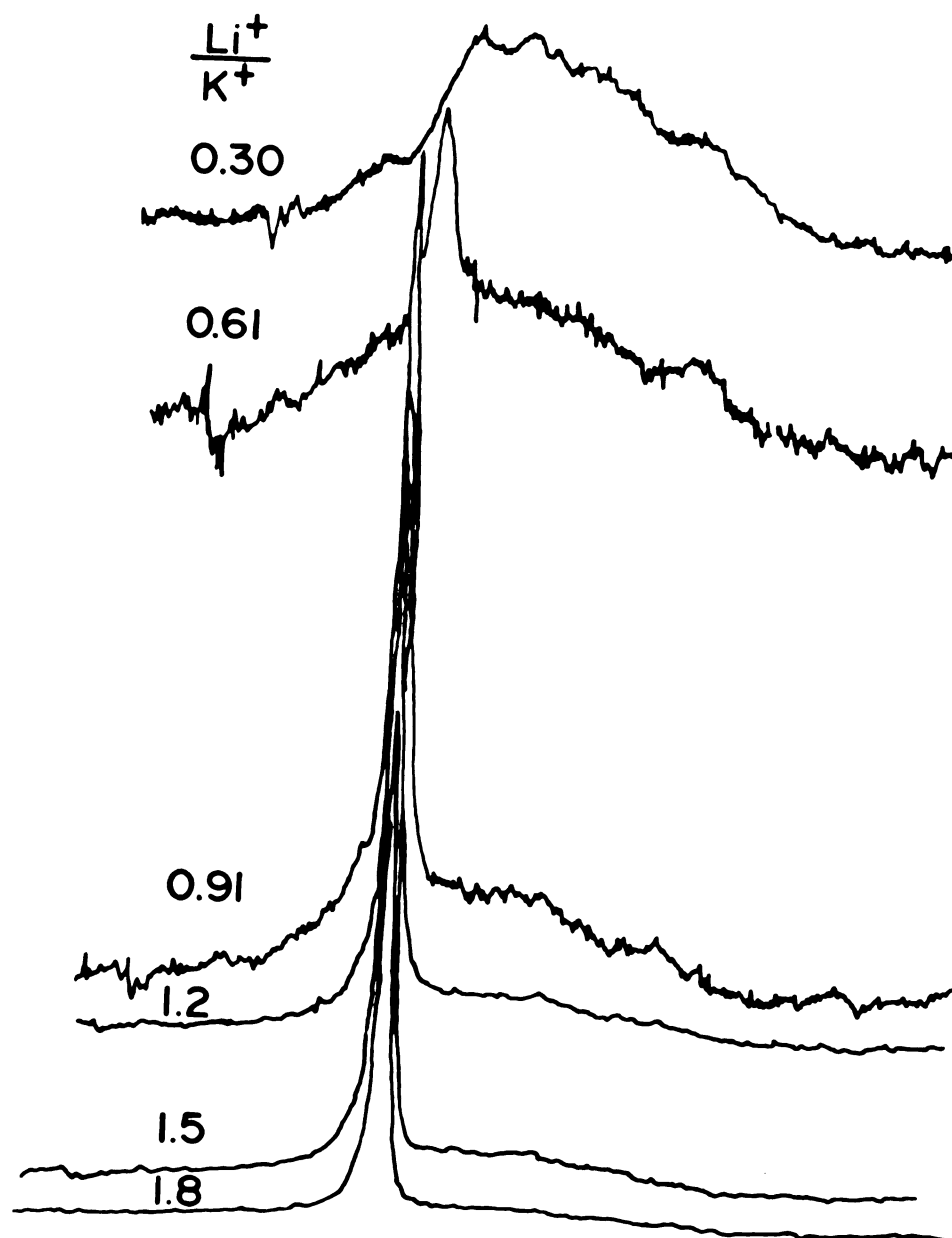




to induce formation of a sodium-type self-assembled structures. Eventually all the "simple"  $K^+$  structure had disappeared and only  $Na^+$  self-structure was present in solution. Further addition of  $K^+$  resulted in a "complex"  $K^+$  self-structure beginning to grow in. The "simple" and "complex"  $K^+$  structures are most easily distinguished by the presence of a structure line upfield of the highest field sodium self-structure line in the "simple"  $K^+$  case. In the presence of  $K^+$ , there is a marked decrease in the intensity of the monomer line in the  $Na^+$  self-structure, indicating that the  $K^+$  is stabilizing the  $Na^+$  self-structure as discussed earlier. Thus, by varying the relative amounts of  $K^+$  and  $Na^+$  in a  $TMA_2GMP$  solution, the two  $K^+$  self-structures and the one  $Na^+$  self-structure can be interconverted with the following order of increasing stability: "simple"  $K^+$  <  $Na^+$  (in the presence of  $K^+$ ) < "complex"  $K^+$ .

D. Effects of  $Li^+$  on the  $K^+$  Self-Structures. Addition of KCl to a concentrated  $Li_2GMP$  solution results in precipitation. In order to avoid this problem, KCl was added to 0.72 M  $GMP^{2-}$  with  $GMP^{2-}/TMA^+ = 4.2$  and  $GMP^{2-}/Li^+ = 6.6$  as shown in Figure 31. The ordered species which grew in were different from either the "simple" or "complex"  $K^+$  self-structures. Although  $Li^+$  is not a structure directing ion itself, it has structure perturbing ability when present with a stronger structure director. The lines were extremely broad, and it was difficult to distinguish any structural features other than the presence of a peak with a chemical shift equal to that of the second highest field line in the "simple"  $K^+$  structure. The other peaks characteristic of the "simple"  $K^+$  structure were clearly absent however. It is also noteworthy that in the presence of  $Li^+$ , the onset of observable self-assembly occurred at much lower  $GMP^{2-}/metal$  ion ratio than in the pure

Figure 31. Effect on the H(8) region of adding aliquots of 4.0 M KCl to 0.72 M  $\text{GMP}^{2-}$  containing 0.56 M  $\text{TMA}^+$  and 0.88 M  $\text{Li}^+$  at 2.3° C.

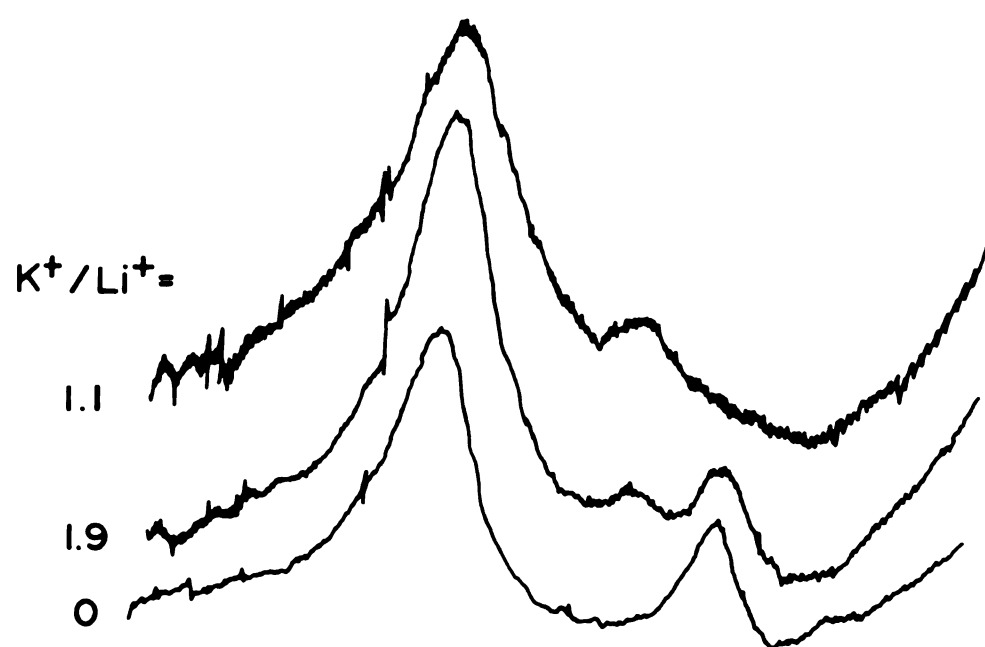


TMA<sup>+</sup> system.

In order to investigate the effect of Li<sup>+</sup> on the "simple" K<sup>+</sup> structure, LiCl was added to 0.78 M TMA<sub>2</sub>GMP with  $\text{GMP}^{2-}/\text{K}^+ = 2$  at 0.3 °C as shown in Figure 32. As the amount of Li<sup>+</sup> in solution increased, a new line grew in between the two structure lines, and the highest field line began to melt out. Eventually the highest field line melted out completely and only the new line remained.

Thus it is clear that Li<sup>+</sup> does not play a passive role in the presence of structure directing ions, although it is not a structure director in itself. Based on the marked increase of line widths in the presence of Li<sup>+</sup>, it appears that the extent of aggregation is increased.

Figure 32. Effect on the H(8) resonance of adding LiCl to a  
"simple"  $K^+$ -GMP self-structure at 0.3° C.  $[(TMA)_2GMP]$   
= 0.775 M.  $[KCl] = 0.36$  M.



#### IV. The Rubidium GMP Self-Structure

A. Similarity of  $K^+$  and  $Rb^+$  Structuring Patterns. Figure 33 shows the addition of  $RbCl$  to  $0.85 \text{ M TMA}_2\text{GMP}$  at  $3.2^\circ\text{C}$ . Comparison of Figure 33 and Figure 22, which shows the effect of the addition of  $KCl$  to  $\text{TMA}_2\text{GMP}$ , shows that self-assembly follows virtually identical patterns in the two systems. Self-structure formation begins with a broadening of the monomer line and the appearance of two new upfield lines. At any  $\text{GMP}^{2-}$  to metal ion ratio the extent of structure formation is greater in the  $K^+$  system than in the  $Rb^+$  system. The  $Rb^+$  case appears to initially form the same "simple" structure as the  $K^+$  system, which is then transformed into a "complex" structure on addition of more  $RbCl$ . The "complex" structure for the  $Rb^+$  system, in much the same way as the  $K^+$  system, shows a unique melting out of structure lines which does not invoke the "simple"  $Rb^+$  structure, as shown in Figure 34. The presence of the highest field line in the  $0.5 \text{ GMP}^{2-}/\text{Rb}^+$  spectrum, however, suggests that the conversion from "simple" to "complex" structure in the  $Rb^+$  case is incomplete. Thus, it appears that the  $Rb^+$  and the  $K^+$  structures in solution in the presence of  $\text{TMA}^+$  form the same structures; however, the  $K^+$  structure has a higher ratio of "complex" to "simple" structure at low  $\text{GMP}^{2-}/\text{metal}$  ion ratios.

Similar spectral changes are observed on adding  $RbCl$  and  $KCl$  to  $\text{Cs}_2\text{GMP}$ , as shown in Figures 35 and 11, respectively. Figure 35 shows the effect of addition of  $RbCl$  to  $0.72 \text{ M Cs}_2\text{GMP}$  at  $3.6^\circ\text{C}$ . An increase in self-structure formation begins with a broadening of the monomer line, due in part to the presence of a downfield shoulder. As the monomer line broadens and decreases in intensity, the upfield structure line increases in intensity. On further addition of  $RbCl$ , two



Figure 33. The H(8) resonances observed upon addition of aliquots of 4.15 M RbCl to 0.85 M (TMA)<sub>2</sub>GMP at 3.2° C. The final GMP<sup>2-</sup> concentration was 0.60 M.

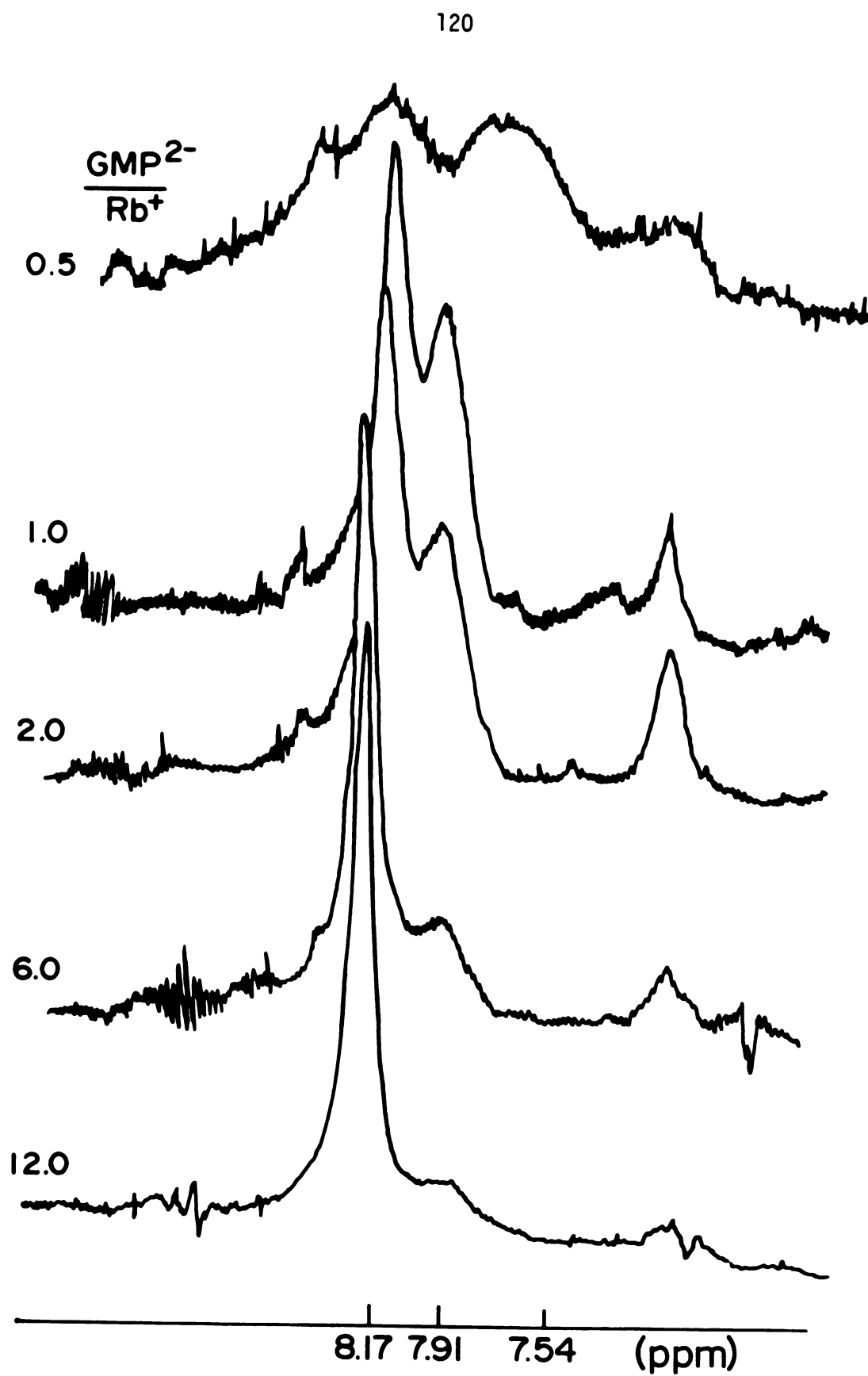


Figure 34. Melting out of the structure lines in the H(8) region of 0.60 M  $\text{Rb}_2\text{GMP}$  containing 1.70 M (TMA)Cl.

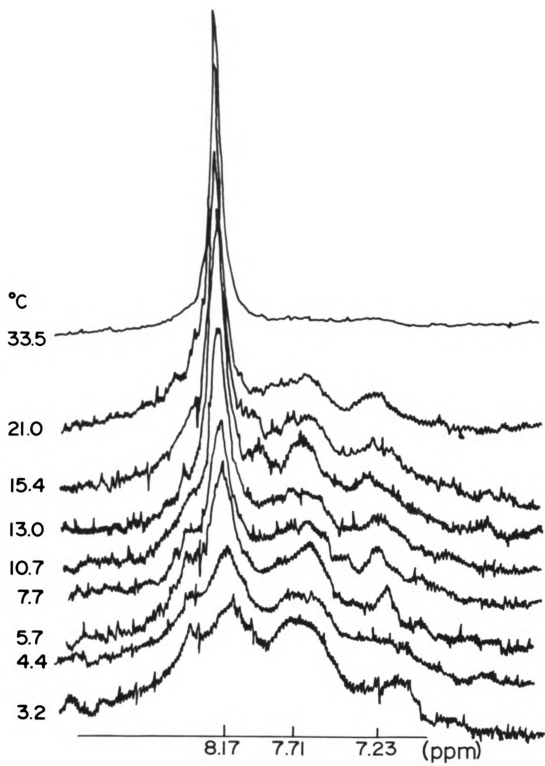
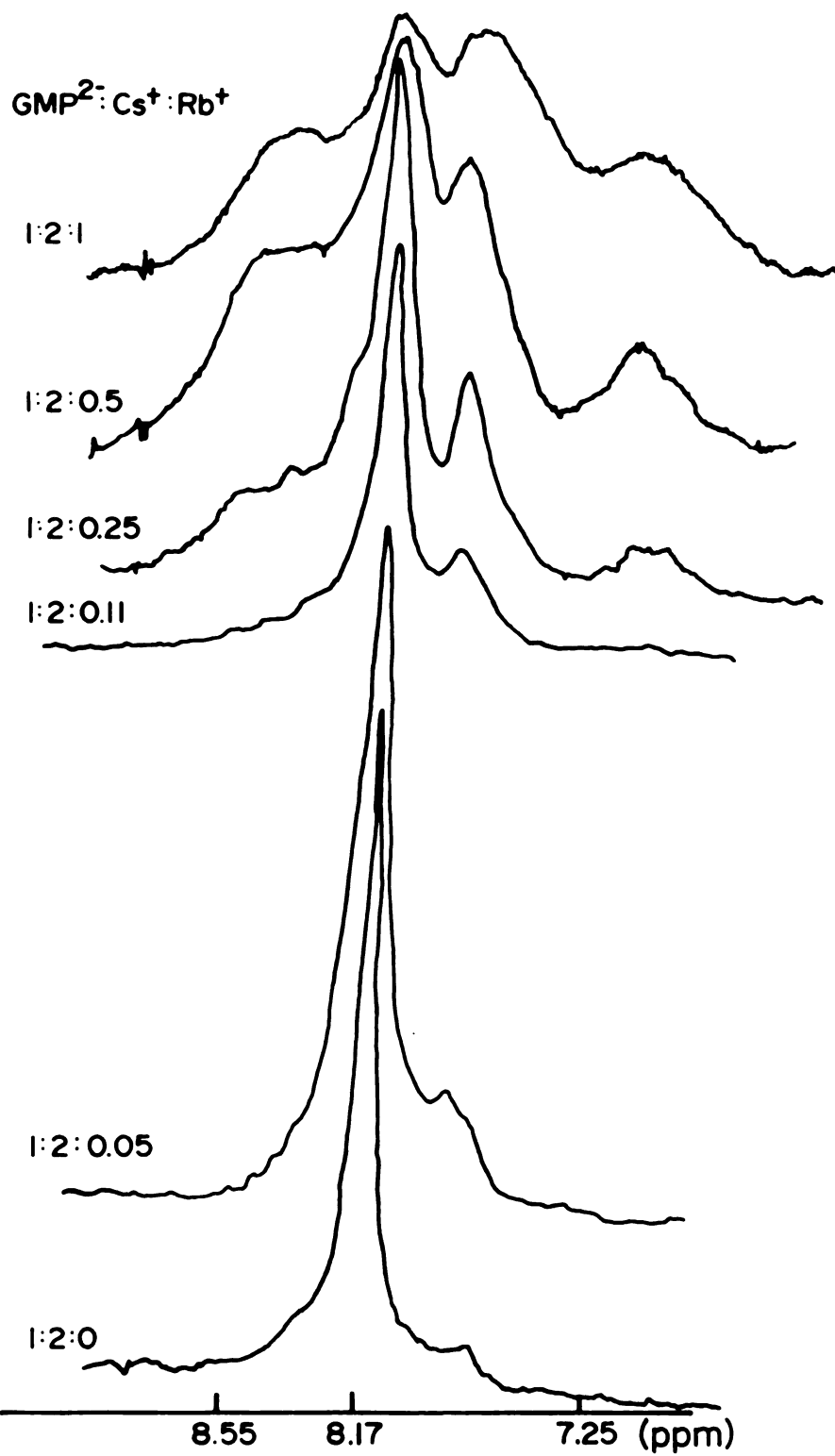


Figure 35. Effect on the H(8) resonance of 0.72 M Cs<sub>2</sub>GMP upon addition of aliquots of 4.15 M RbCl at 3.6° C.



additional structural lines grow in, one upfield and one downfield of the already existing lines. Although these "outer" lines grow in at a higher  $\text{GMP}^{2-}$  to metal ion ratio in the  $\text{K}^+$ - $\text{Cs}^+$  system, the chemical shifts of the lines in the  $\text{Cs}^+$ - $\text{Rb}^+$  and  $\text{Cs}^+$ - $\text{K}^+$  systems are identical. The difference in structure onset is probably attributable to the difference in structure directing ability of the two ions. Based on comparison of the results of addition of  $\text{RbCl}$  and  $\text{KCl}$  to  $\text{TMA}_2\text{GMP}$  and  $\text{Cs}_2\text{GMP}$ , it is clear that  $\text{Rb}^+$  and  $\text{K}^+$  are similar in their mode of self-structure directing, and markedly different from  $\text{Na}^+$ .

B.  $\text{Li}^+$ - $\text{Rb}^+$ / $\text{GMP}^{2-}$  Gel Formation. An attempt to investigate the effect of  $\text{Li}^+$  on the  $\text{Rb}^+$ -system resulted in gel formation. Combinations of different volumes of 0.5 M  $\text{Rb}_2\text{GMP}$  and 0.5 M  $\text{Li}_2\text{GMP}$  resulted in gel formation on contact of the two solutions. The gel could be melted out by heating, but many of the solutions gelled again upon cooling. It appeared qualitatively that the gel formation occurred most readily from a 1:1 ratio of  $\text{Li}_2\text{GMP}$  and  $\text{Rb}_2\text{GMP}$ . No further investigation of the effects of  $\text{Rb}^+$  in conjunction with  $\text{Li}^+$  on  $\text{GMP}^{2-}$  were undertaken.

## V. The Cesium-GMP Self-Structure

### A. Effect of Addition of $\text{Li}^+$ on the Extent of the $\text{Cs}^+$ -GMP $^{2-}$

Self-Structure. Figure 36 shows the addition of aliquots of CsCl to 0.85 M TMA<sub>2</sub>GMP at 4.2 °C. There is no evidence for structure formation until the solution contains 1GMP $^{2-}$ /2Cs $^+$ . Since less than 5% of pure Cs<sub>2</sub>GMP forms a self-structure, this result is expected.

Figure 37 shows the effect of the addition of LiCl to 0.72 M Cs<sub>2</sub>GMP. The solution showed no change in percent structure up to the point where precipitation occurred. Similarly, addition of CsCl to 0.96 M Li<sub>2</sub>GMP showed no structure formation at 3.6 °C prior to precipitation at a ratio of 1GMP $^{2-}$ /Cs $^+$ . Thus, Li $^+$  induces no changes in the stability of the Cs $^+$  structure, nor changes in the type(s) of structure(s) formed.

### B. Effect of Addition of Na $^+$ and K $^+$ to the Cs $^+$ Self-Structure.

Figure 38 shows the addition of aliquot of NaCl to 0.72 M Cs<sub>2</sub>GMP at 3.3 °C. Only a very small amount of Na $^+$  need be present to create a dramatic increase in the amount of structure present. Initially, the upfield and downfield lines closest to the monomer line are cesium structure lines whereas at 7.6 ppm there is a new structure line. Chemical shifts are calculated based on the lowfield sodium self-structure line consistently appearing at 8.55 ppm downfield from an internal TSP reference. Increasing the Na $^+$  concentration resulted in an increase in the intensity of all structure lines and the appearance of two new structure lines. These new lines are on either side of the monomer line at 8.4 and 7.4 ppm. Further addition of Na $^+$  resulted in a shoulder on the monomer peak. As this peak grew in with increasing Na $^+$ , a new lowfield peak grew in at 8.6 ppm. The highest and lowest field structure lines at 8.6 and 7.4 ppm, together with a structure line



Figure 36. Effect on the H(8) resonance of 0.85 M (TMA)<sub>2</sub>GMP upon addition of 3.2 M CsCl at 3° C. The final GMP<sup>2-</sup> concentration was 0.57 M.

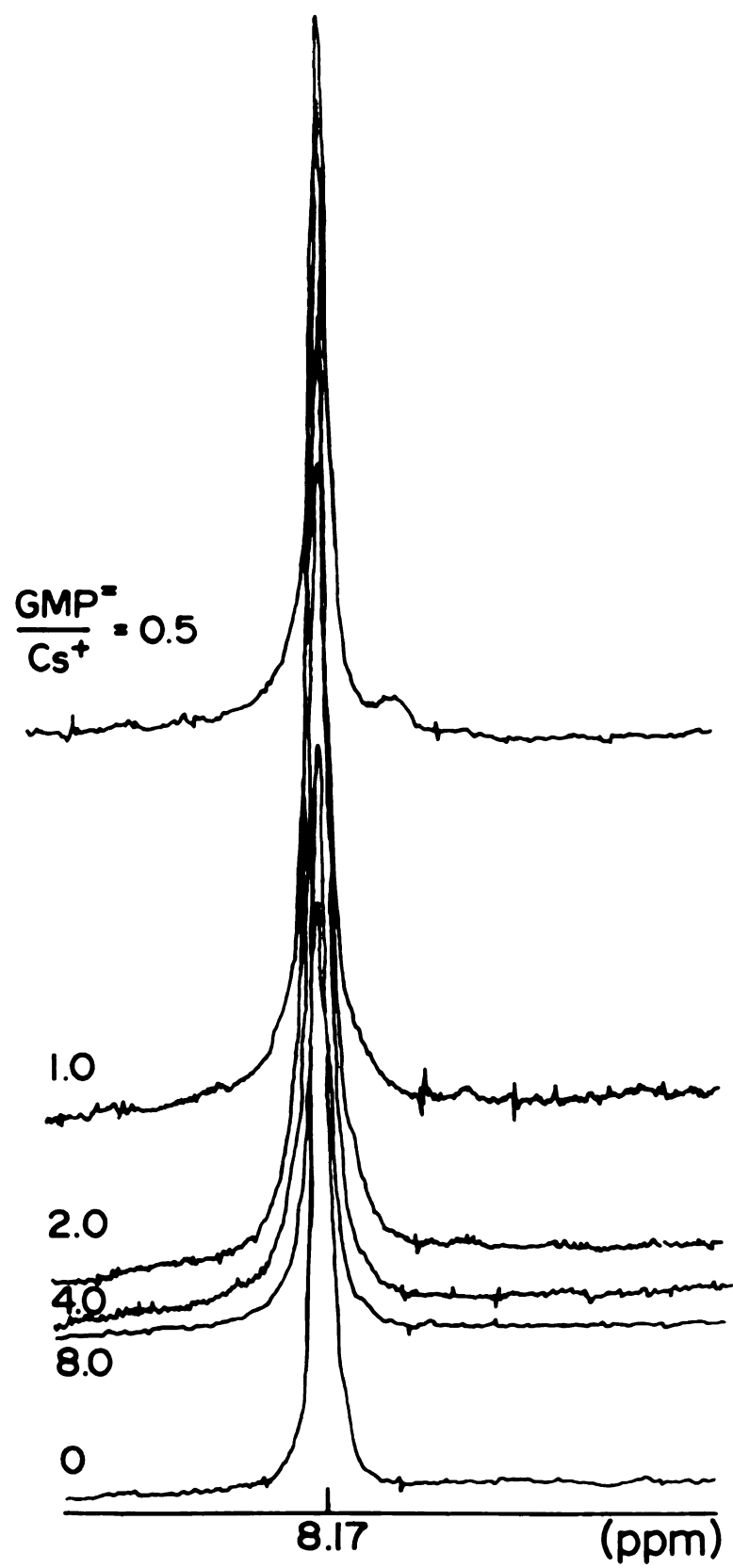


Figure 37. Effect on the H(8) region of adding 4.0 M LiCl to 0.72 M Cs<sub>2</sub>GMP at 3.6° C. The final GMP<sup>2-</sup> concentration was 0.61 M.

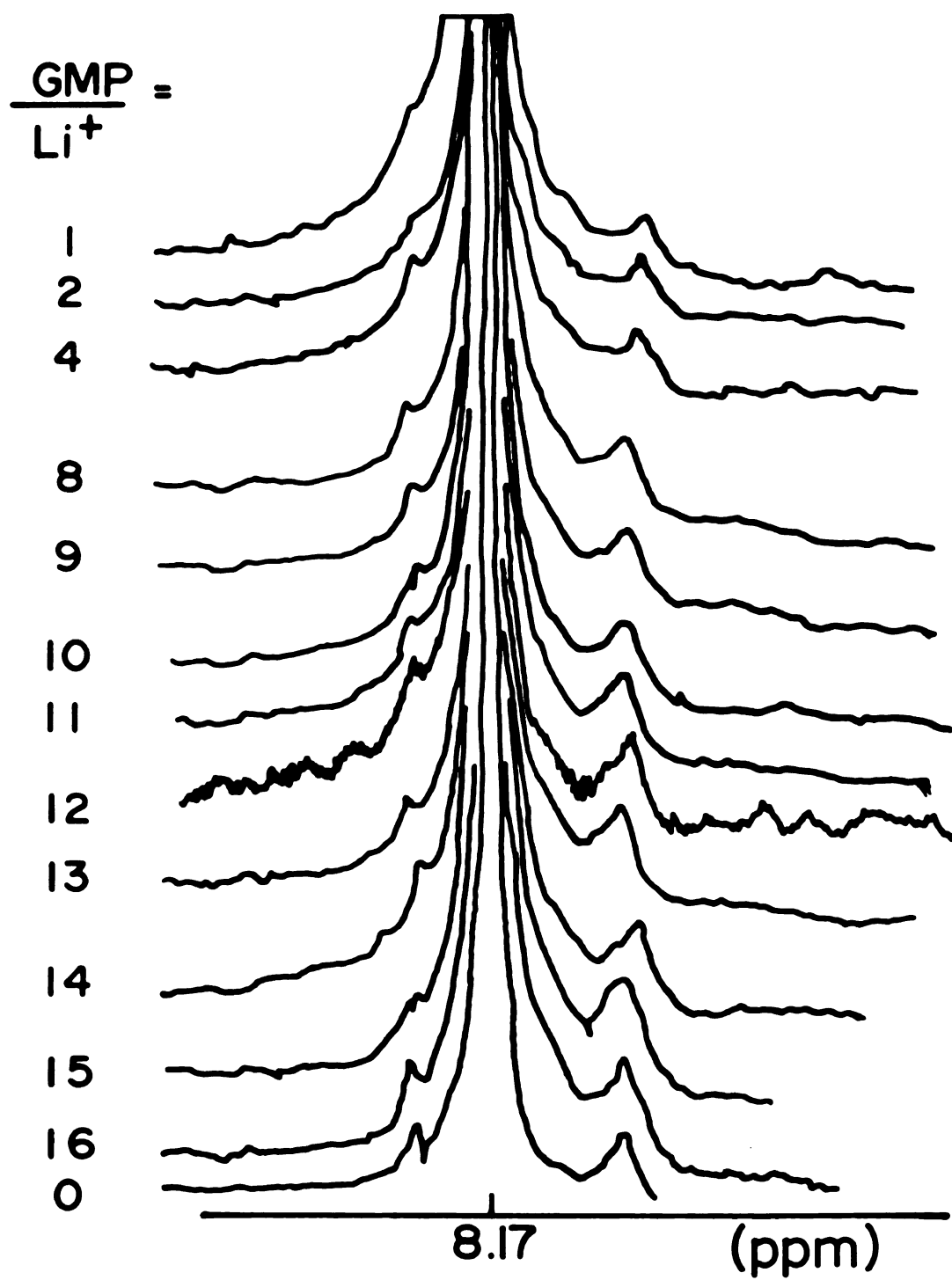
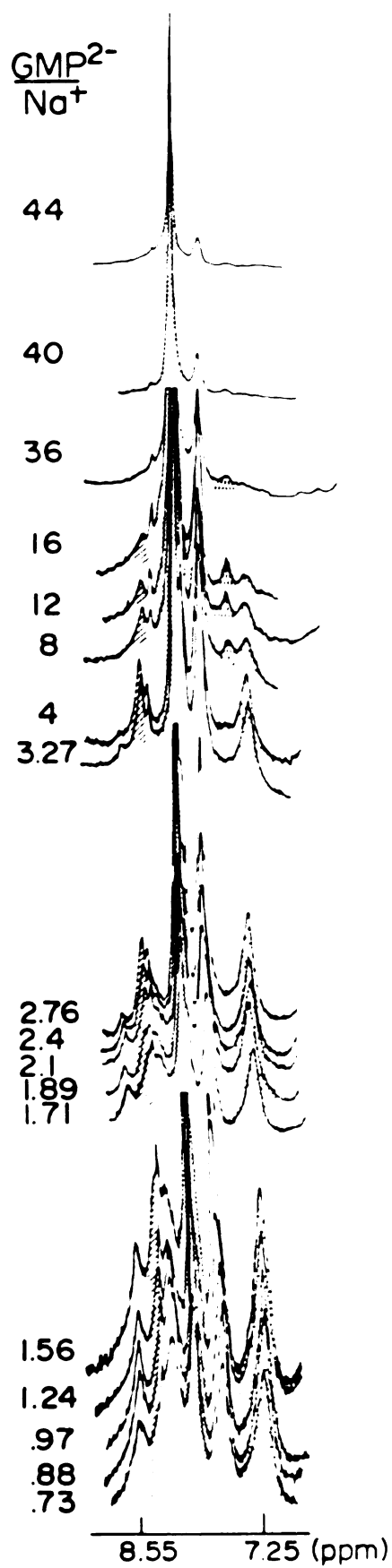


Figure 38. Effect on the H(8) resonances of 0.72 M Cs<sub>2</sub>GMP upon addition of 4.0 M NaCl at 3.3° C. The final GMP<sup>2-</sup> concentration was 0.58 M.



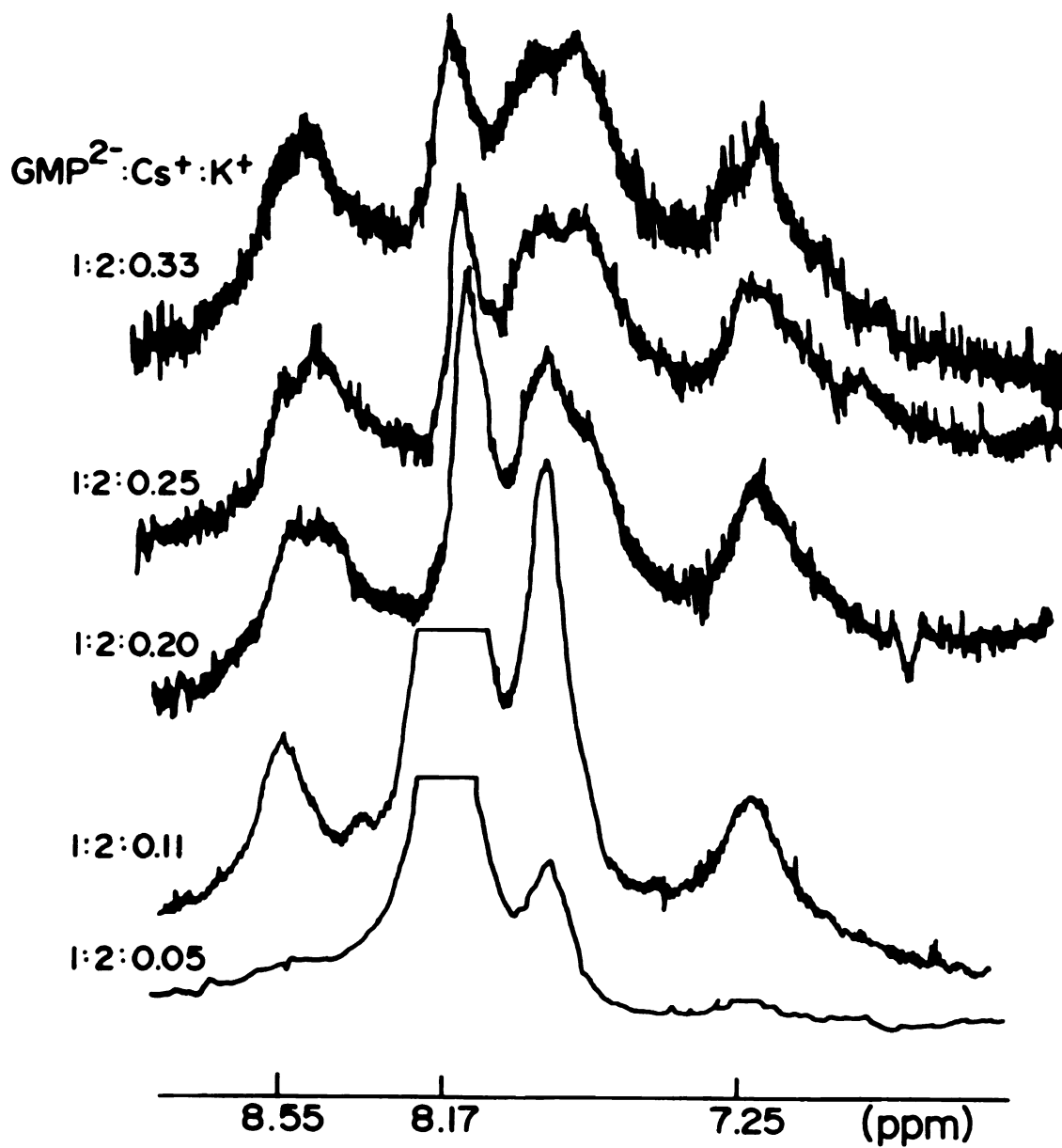
downfield of the monomer line at 8.3 ppm have chemical shifts virtually identical to the three structure lines of a pure  $\text{Na}_2\text{GMP}$  system of comparable temperature and  $\text{GMP}^{2-}$  concentration. Concurrent with the increase in the intensity and number of self-structure lines was a decrease in the intensity of the monomer line. The structure lines corresponding to the  $\text{Na}^+$  system and the  $\text{Cs}^+$  lines were initially present at low  $\text{GMP}^{2-}$  to metal ion ratios. It is interesting to note that the  $\text{Cs}^+$  structure lines remained present. In an analogous experiment adding  $\text{CsCl}$  to  $\text{Na}_2\text{GMP}$ , the  $\text{Na}^+$  self-structure remained unperturbed except for a new line growing in at about 7.7 ppm. This structure line corresponds to the structure line present in the pure  $\text{Cs}_2\text{GMP}$  system.

Figure 39 shows the effects of the addition of aliquots of  $\text{KCl}$  to  $1.19 \text{ M } \text{Cs}_2\text{GMP}$  at  $5.0^\circ\text{C}$ . Two new structure lines grow in at the same rate with increasing  $\text{K}^+$  concentration, one upfield and one downfield of the  $\text{Cs}^+$  structure lines. These new structure lines and the  $\text{Cs}^+$  structure line just upfield of the monomer line increase in intensity with increasing  $\text{K}^+$  concentration, whereas the monomer line decreases in intensity. At low  $\text{GMP}^{2-}/\text{K}^+$  ratios, shoulders or new peaks grew in upfield of the originally present structure lines. The increase in new peaks was accompanied by line broadening until precipitation occurred.

Many of the structures formed for  $\text{Cs}_2\text{GMP}$  in the presence of  $\text{Na}^+$  are unique to that system of cations. The ordered forms in the presence of  $\text{K}^+$  appear to be different than those formed in the presence of  $\text{Na}^+$ . Thus, although  $\text{Cs}^+$  is a very weak structure directing ion by itself, in the presence of strong structure directors,  $\text{Cs}^+$  actively participates in the self-assembly process.

Figure 39. Effect on the H(8) resonances of 1.19 M Cs<sub>2</sub>GMP upon addition of aliquots of 1.1 M KCl at 5° C. The final GMP<sup>2-</sup> concentration was 0.87 M.





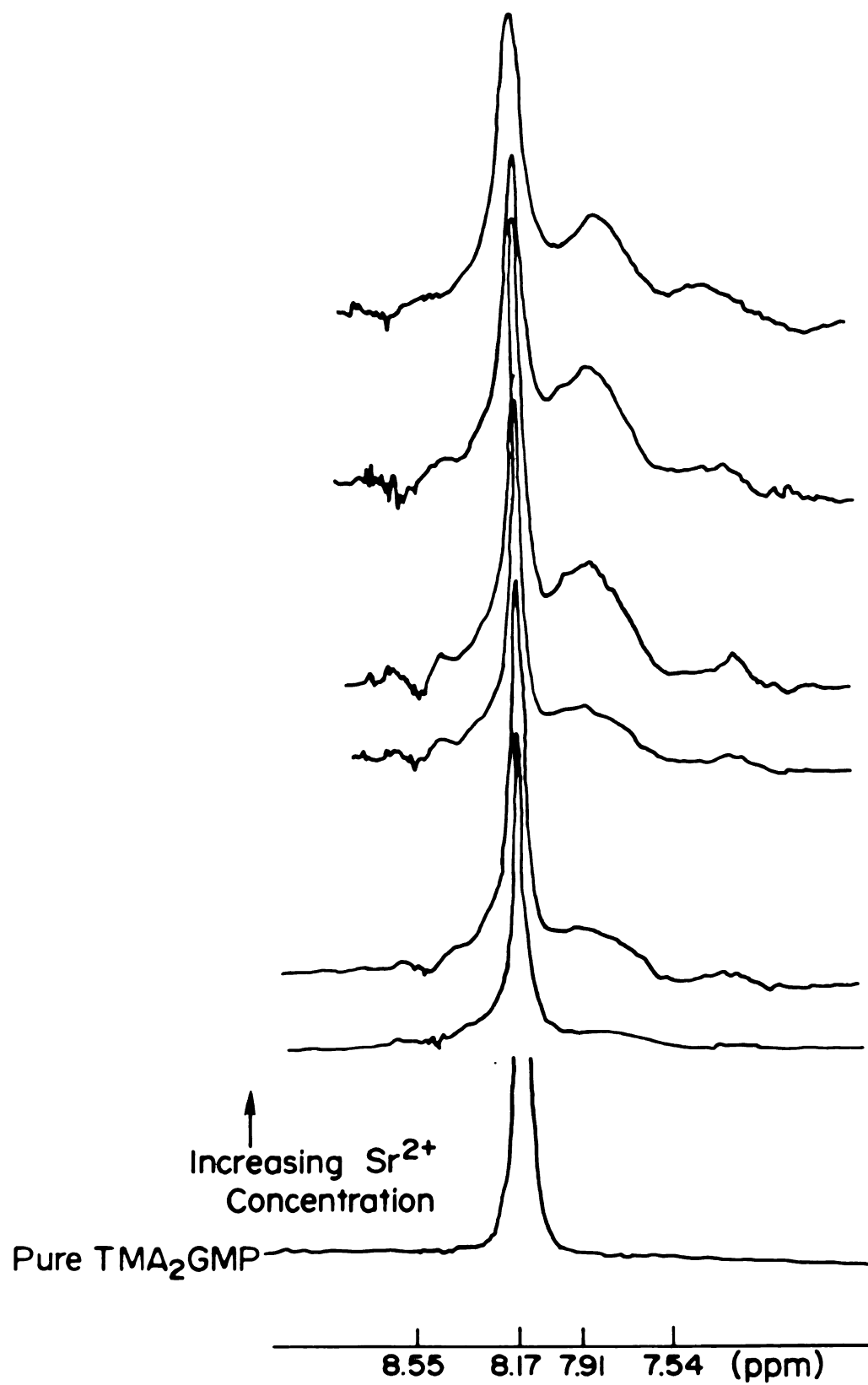
## VI. Alkaline Earth Salts of 5'-GMP

The homoionic alkaline earth salts are too insoluble to allow proton NMR investigation of structure formation. Thus, an alternative approach was taken. Alkaline earth chlorides were added to  $\text{TMA}_2\text{GMP}$  systems. The increased solubility induced by the  $\text{TMA}^+$  was sufficient to allow enough salt into solution to qualitatively investigate the structure directing ability of the +2 ions, although limiting spectra were still unattainable.

The addition of  $\text{MgCl}_2$  or  $\text{CaCl}_2$  to 0.73 M  $\text{TMA}_2\text{GMP}$  solutions, respectively, resulted in precipitation prior to structure formation at 3.2 °C. Addition of  $\text{CaCl}_2$  to a  $\text{Na}_2\text{GMP}$  solution in a ratio of  $4\text{GMP}^{2-}/\text{Ca}^{2+}$  resulted in precipitation. The solution was stored at room temperature for a month at which time the formation of white spherical particles of solid material was noted, while the solution was clear. Scanning electron micrographs revealed that the spheres were made up of small, flat sheets. No further investigations with  $\text{Mg}^{2+}$  or  $\text{Ca}^{2+}$  were undertaken in a 5'-GMP system.

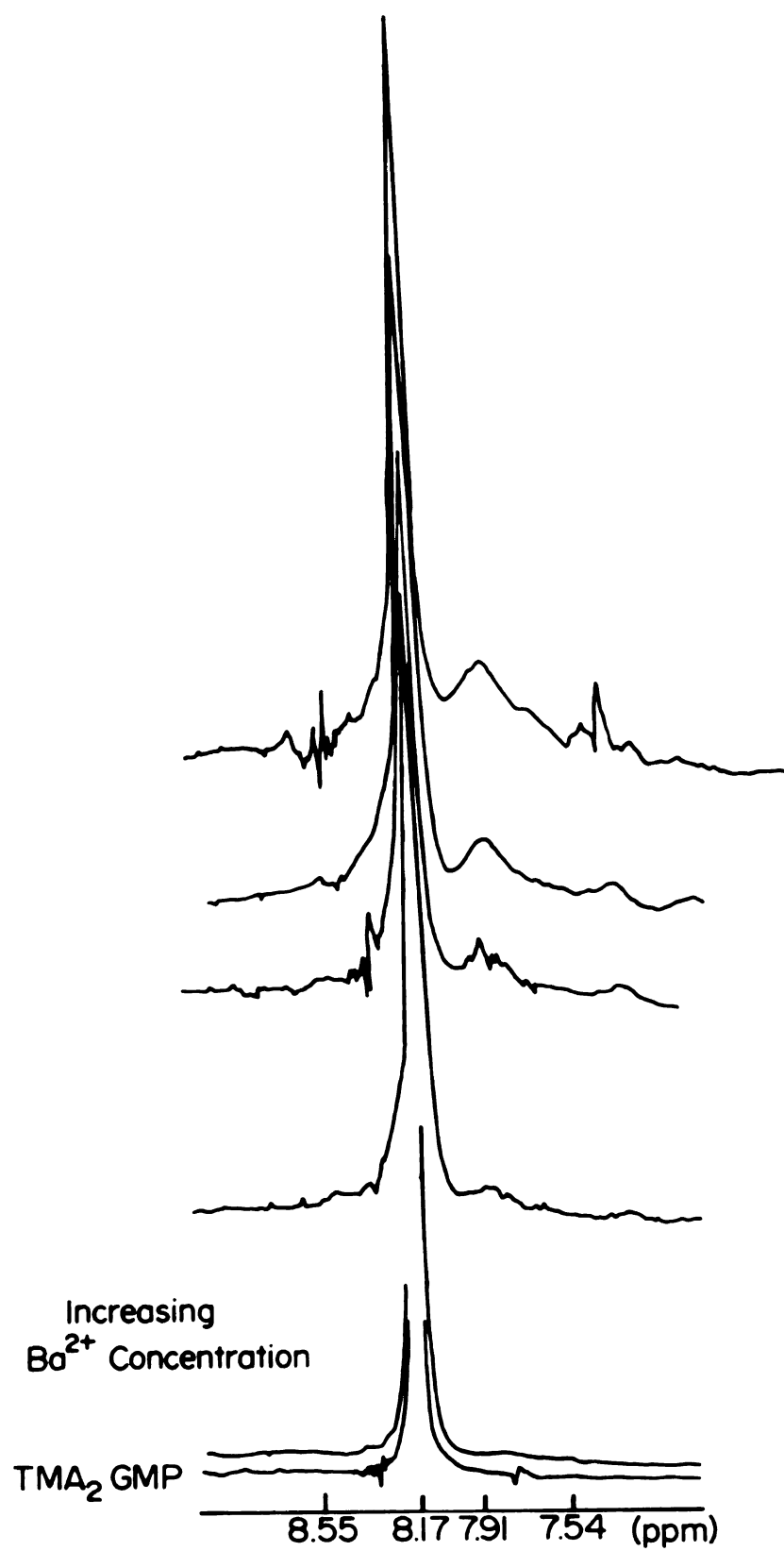
The addition of both  $\text{SrCl}_2$  and  $\text{BaCl}_2$  to 0.73 M  $\text{TMA}_2\text{GMP}$ , resulted in self-association of the nucleotide. Since a certain amount of precipitate was always present, quantitative studies were not feasible. Figure 40 shows the effect of the addition of microliter quantities of 4.74 M  $\text{SrCl}_2$  to a  $\text{TMA}_2\text{GMP}$  solution. After addition of each aliquot, the solution was heated to boiling and then cooled to 3.6 °C. Structure formation is evident. The monomer line decreases in intensity with increasing  $\text{Sr}^{+2}$  concentration, and two new lines are present upfield of the monomer peak. The solution represented by the uppermost spectrum gelled on aging at room temperature for two hours.

Figure 40. Effect on the H(8) resonance of 0.73 M (TMA)<sub>2</sub>GMP upon addition of aliquots of 4.74 M SrCl<sub>2</sub> at 3.2° C. Due to the presence of precipitate, exact solution ratios were unattainable.



$\text{Ba}^{2+}$  is also a structure director as shown in Figure 41. The scheme of ordering for  $\text{Ba}^{2+}$  is quite similar to that for  $\text{Sr}^{2+}$ , although less structure is observed for the  $\text{Ba}^{2+}$  system. Both  $\text{Sr}^{2+}$  and  $\text{Ba}^{2+}$  showed H(8) line patterns more similar to  $\text{K}^{+}$  than  $\text{Na}^{+}$ , as expected from comparison of ionic radii. An interesting phenomenon observed for the +2 ions was the formation of gels on heating, and increased solubility on cooling. The gelling phenomenon was totally reversible. Although the  $\text{Ba}^{2+}$  and  $\text{Sr}^{2+}$  ions appear to form identical structures, this is not necessarily the case since limiting spectra were not obtained.  $\text{Rb}^{+}$  and  $\text{K}^{+}$  also appear to form identical self-assembled units prior to total ordering of the solution, at which time it is quite clear that they are different. The  $\text{Ba}^{2+}$  solution represented by the uppermost spectrum of Figure 41 yielded small fibers over a 24 hour period. The use of mixed ion systems allowed an investigation of the interaction of the alkaline earth cations with 5'-GMP by increasing the solubilities, and thus allowed  $\text{Sr}^{2+}$  and  $\text{Ba}^{2+}$  to be identified as structure directing ions.

Figure 41. Effect on the H(8) resonance of 0.73 M (TMA)<sub>2</sub>GMP upon addition of aliquots of 2.0 M BaCl<sub>2</sub> at 3.2° C. Due to the presence of precipitate, exact solution ratios were unattainable.



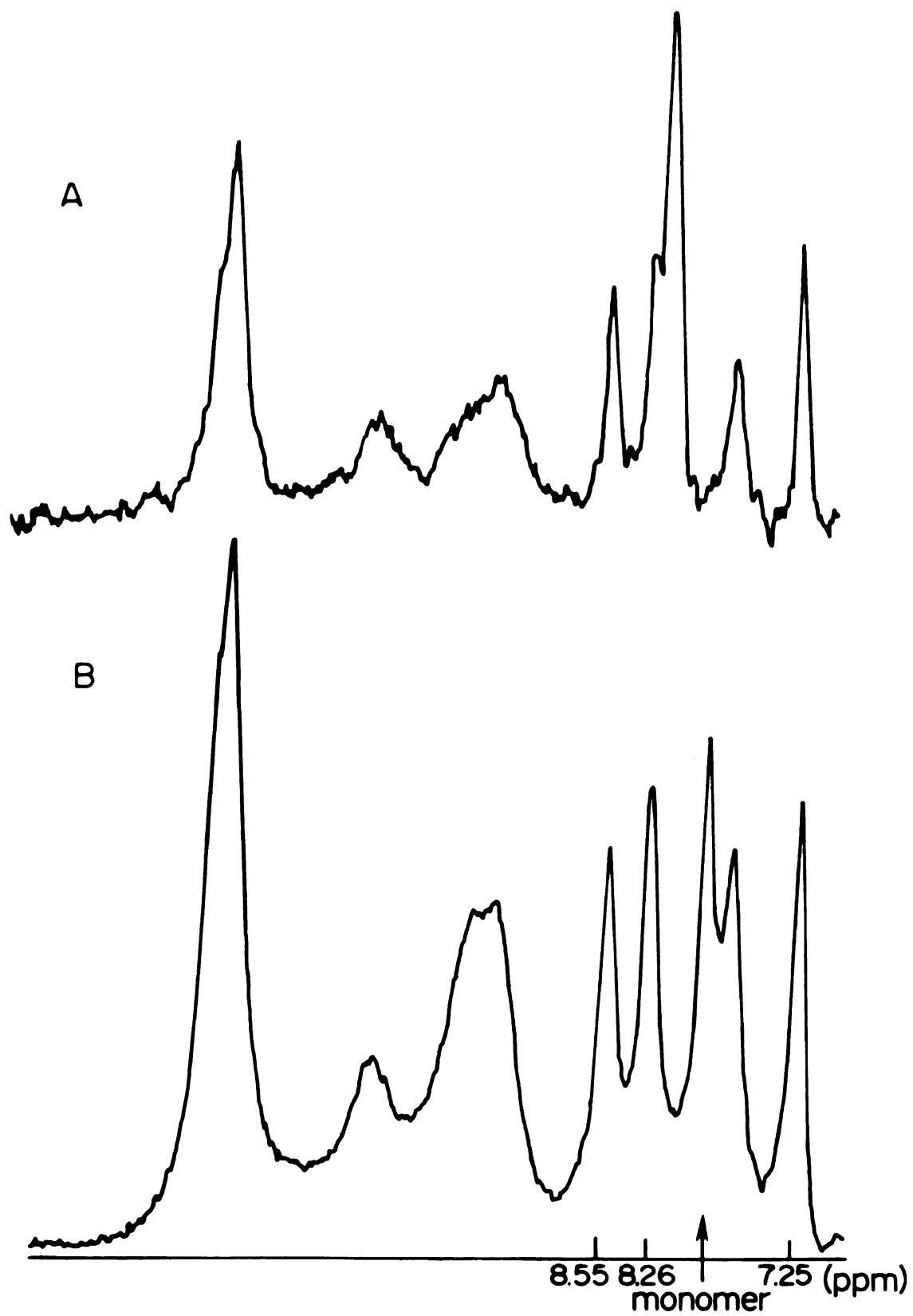
## VII. NH Proton Resonances of GMP Self-Structures in Water

A wealth of information on ordered forms of  $\text{GMP}^{2-}$  is available from the NH region of the NMR spectra, which ranges from about 6 to 12 ppm downfield from TSP. The NH region shows unique multiline patterns which can be used in conjunction with the H(8) lines to create a picture of the self-structures formed. In order for the NH protons to be observable, spectra must be recorded in  $\text{H}_2\text{O}$  at low temperatures to prevent rapid exchange. By comparing the number of hydrogen bonded NH protons with the number of structured H(8) protons, insight into the number of hydrogen bonds per structured nucleotide should be attainable. At about 6.3 ppm in  $\text{H}_2\text{O}$  at 0 °C the  $\text{GMP}^{2-}$  monomer is known to exhibit an amino proton signal, which shifts to about 6.5 ppm on hydrogen bonding with 5'-CMP.<sup>128</sup> Thus, information with respect to monomer can also be acquired. Difficulties, however, arise when using  $\text{H}_2\text{O}$  solutions due to the extremely large intensity of the water peak. As discussed earlier, peak suppression of the  $\text{H}_2\text{O}$  peak perturbs the H(8) region and therefore cannot be employed with routine spectra. Another problem occurs in distinguishing between N-H and O-H protons. O-H protons usually exhibit chemical shifts of less than 6 ppm downfield from TSP; they have, however, been reported to have chemical shifts as large as about 7.2 ppm in cyclic nucleotide systems.<sup>129</sup>

Figure 42 shows spectra of several different concentrations of  $\text{Na}_2\text{GMP}$  in  $\text{H}_2\text{O}$  at low temperature. In the concentrated solution spectrum, the presence of the three H(8) sodium self-structure lines at 8.55, 8.26 and 7.25 ppm is quite clear. The monomer line is at 8.00 ppm. In addition, concentration dependent lines are clearly present at about 11.14, 10.16, 9.35, and 7.69 ppm. All these peaks have been



Figure 42. The NH and H(8) regions of (A) 0.3 M Na<sub>2</sub>GMP in H<sub>2</sub>O at 2° C, and (B) 0.7 M Na<sub>2</sub>GMP in H<sub>2</sub>O at 2° C. These spectra were provided courtesy of Jeol. Co.



assigned as originating from NH protons.<sup>105</sup> Since the 7.69 ppm peak is similar in chemical shift to the 2'-OH peaks which have been observed hydrogen bonded to H<sub>2</sub>O in cyclic nucleotides,<sup>129</sup> further investigation of this peak seemed warranted. Based on the probable difference in relaxation rates between an amino and a hydroxyl proton, a relaxation experiment was done. Inversion recovery T<sub>1</sub> experiments revealed very small differences existed between T<sub>1</sub> values for all peaks in this region, and thus were inconclusive.

Figure 43 shows the behavior of the 6.3 ppm NH<sub>2</sub> resonance of monomeric GMP<sup>2-</sup> as a function of concentration. At intermediate concentration, the NH<sub>2</sub> peak has broadened. In the concentrated spectrum, where the self-assembled unit is the predominant species in solution, the NH<sub>2</sub> appears to be present as two peaks, one at 6.3 ppm and the other at 6.1 ppm. These lines may correspond to the unassociated monomer (6.3 ppm), and GMP<sup>2-</sup> involved in disordered base stacking (6.1 ppm). If tetramers existed in solution to a significant extent, a downfield shift to 6.5 ppm would be expected based on the results of G-C pairing experiments.<sup>128</sup> Thus, although the lines are broadened, and obscured by the intensity of the water peak, these results provide further evidence for the presence of a "fully" self-structured Na<sub>2</sub>GMP solution. Thus, assignment of the third highest field line as monomer is justified.

A spectrum of self-assembled K<sub>2</sub>GMP in H<sub>2</sub>O at low temperature showed a different NH pattern from the sodium system as shown in Figure 44. The chemical shifts of the NH lines are 11.25, 10.48, 9.54 and 8.64 ppm downfield from TSP. A TMA<sub>2</sub>GMP system containing 6GMP<sup>2-</sup>/Na<sup>+</sup> and 2GMP<sup>2-</sup>/K<sup>+</sup>, which exhibits a Na<sup>+</sup> type of self-structure, shows neither a

Figure 43. The H(8) and unstructured NH<sub>2</sub> resonances for (A) 0.7 M Na<sub>2</sub>GMP at 2° C in H<sub>2</sub>O, (B) 0.3 M Na<sub>2</sub>GMP at 2° C in H<sub>2</sub>O, and (C) 0.1 M Na<sub>2</sub>GMP at 2° C in H<sub>2</sub>O. These spectra were provided courtesy of Jeol. Co.

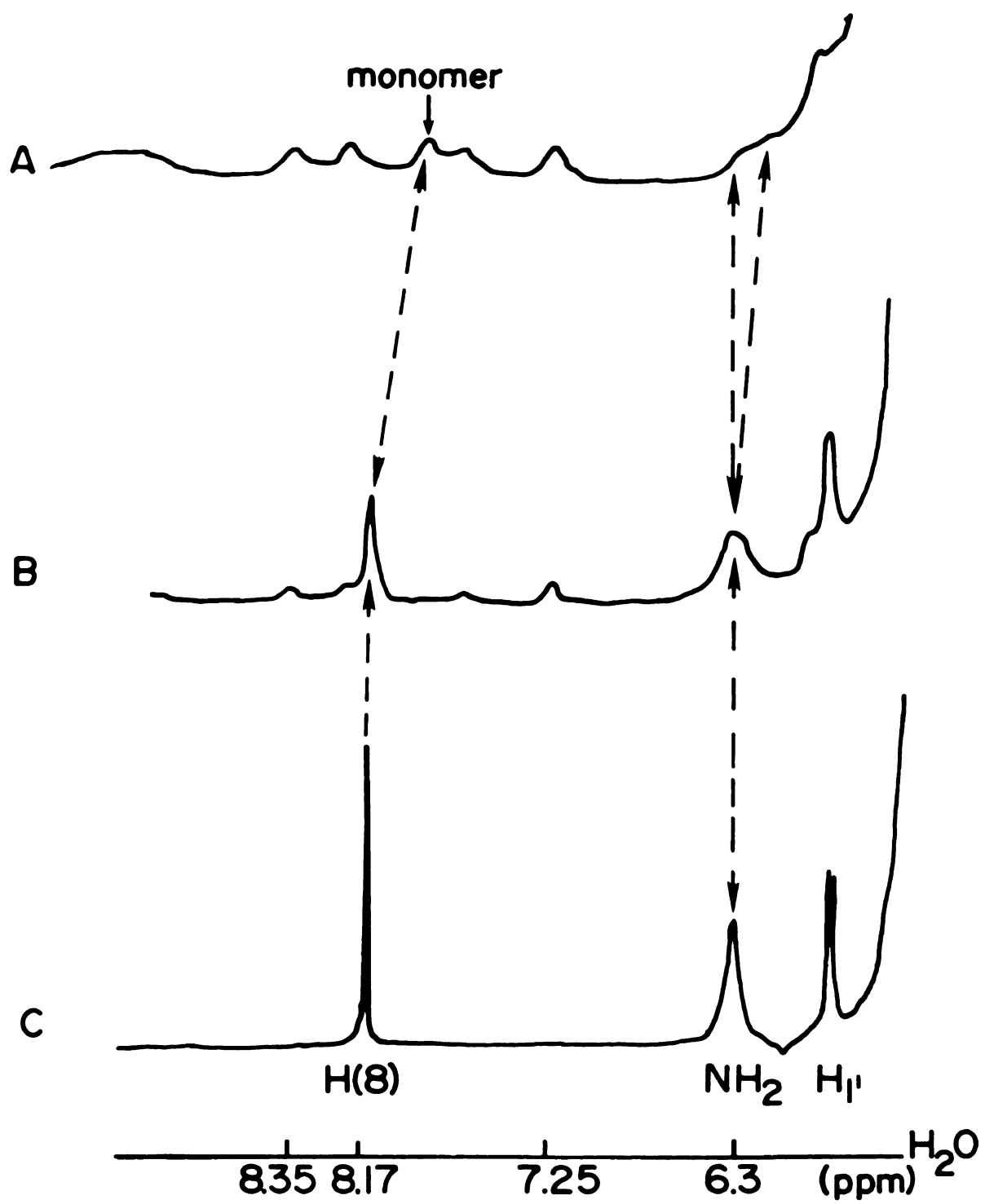
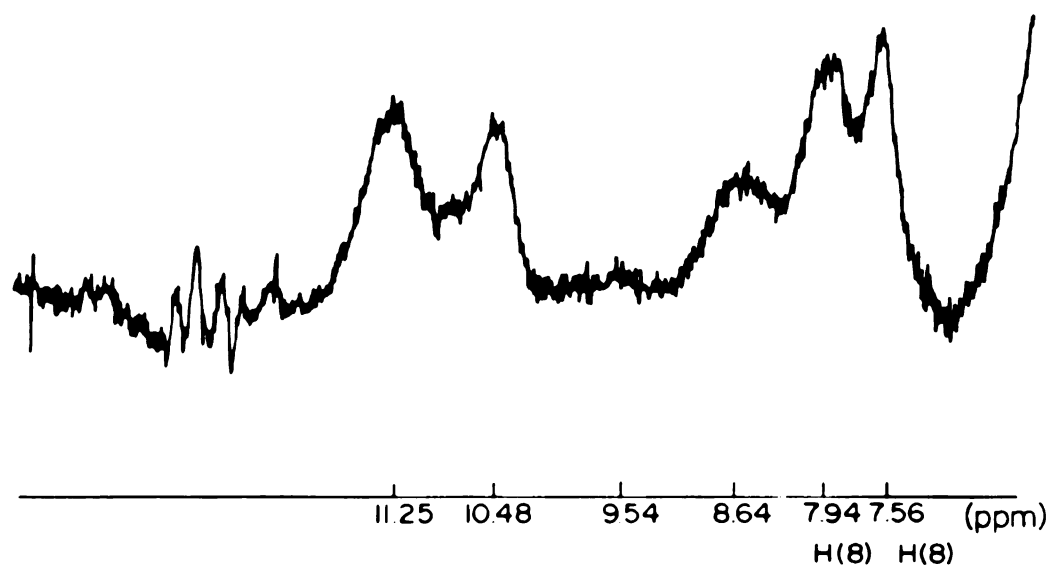


Figure 44. The H(8) and NH resonances of 0.91 M K<sub>2</sub>GMP at 2° C in H<sub>2</sub>O containing NaTSP (1 wt%).



sodium nor a potassium N-H hydrogen bond pattern as shown by the upper spectrum in Figure 45. This spectrum was obtained on the Bruker WH-180 and is typical of the quality of spectra observed from water solutions. The lower spectrum was obtained on a Bruker WP-200 and shows markedly better signal to noise. Unfortunately, the two spectra were recorded at different scales so comparison is somewhat difficult. The lower spectrum shows the result of H<sub>2</sub>O peak suppression in this system. Note the marked decrease in the intensity of the 7.69 ppm line relative to the highest field sodium structure line when peak suppression is applied.

Table 6 shows the ratio of the concentration of NH protons to structured CH protons. Due to the problem of the origin of the 7.69 ppm peak which may be either a NH or ribose proton line, ratios were calculated both including and not including protons giving rise to this peak. In addition to the hydrogen bonds between O(6), N(7) and N(1), N(2), respectively, additional hydrogen bonding could be envisioned between the phosphate groups and NH<sub>2</sub>, 2'-OH, 3'-OH or some type of water interaction with an NH<sub>2</sub> or ribose. Thus, in addition to the two known hydrogen bonding sites, others could exist giving rise to NH to CH ratios greater than two. At low temperatures, the ratio was about 3 for a 0.7 M Na<sub>2</sub>GMP solution. This value may, however, be artificially high since at low temperature monomer NH peaks could be present in addition to structured NH peaks. At slightly higher temperatures these NH peaks from the monomer would not be present due to exchange. At higher temperatures, it appears a value of about 2 predominates. Thus, this suggests that extensive hydrogen bonding beyond tetramer formation is unlikely.



Figure 45. A comparison of the NH and H(8) regions of two spectra of 0.79 M (TMA)<sub>2</sub>GMP in H<sub>2</sub>O with 0.13 M NaCl and 0.40 M KCl at 1° C. (A) was recorded on a Bruker WH-180 without H<sub>2</sub>O peak suppression. (B) was provided courtesy of Bruker and represents the same system with H<sub>2</sub>O peak suppression. Note the intensity of the 7.57 ppm peak relative to the 7.25 ppm peak in both cases.

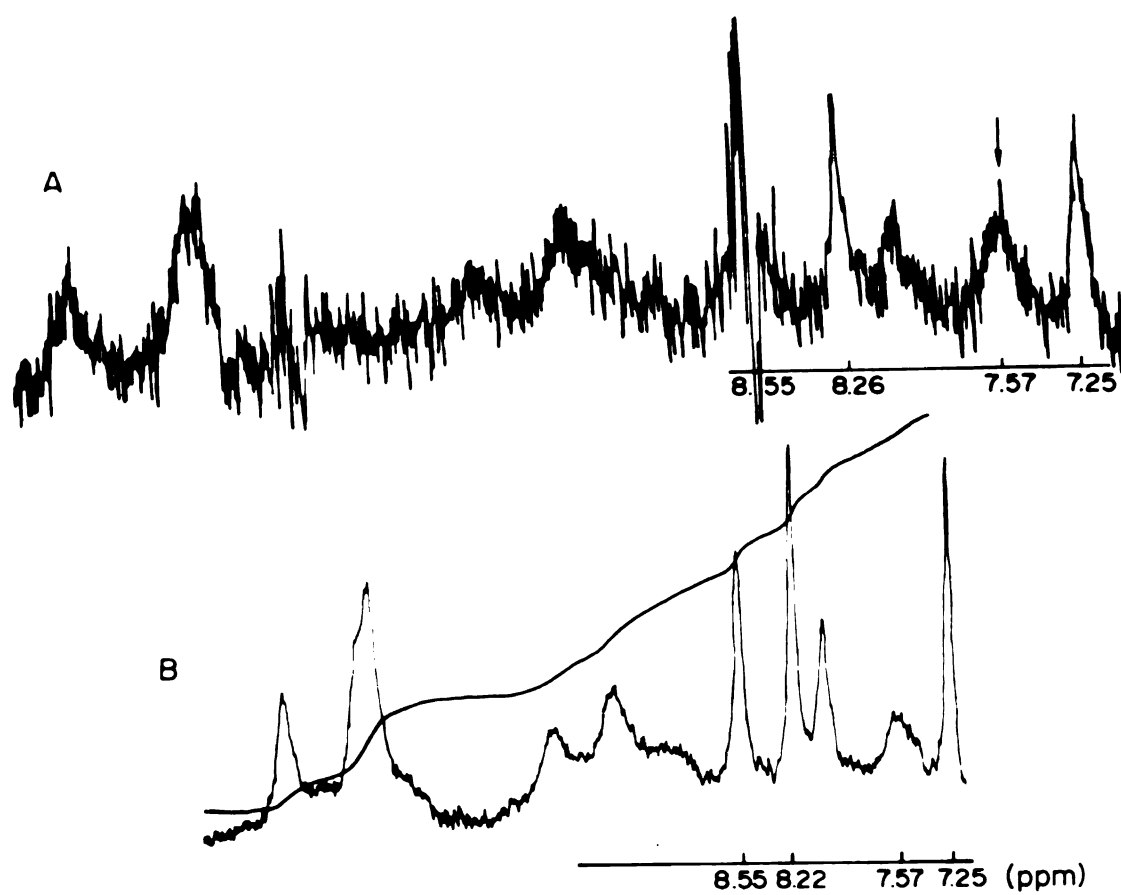


Table 6. Effective NH/H(8) Ratios for Various Temperatures and Concentrations of Solutions Exhibiting a "Sodium" Self-Structure.

<u>Solution</u>	<u>Temperature</u>	<u>NH/H(8)</u>
0.7 <u>M</u> Na <sub>2</sub> GMP	2.0° C	3.08 (2.69) <sup>a</sup>
0.45 <u>M</u> Na <sub>2</sub> GMP	4.2° C	2.77 (2.40) <sup>a</sup>
0.77 <u>M</u> Na <sub>2</sub> GMP	8.0° C	2.04 (1.67) <sup>a</sup>
0.77 <u>M</u> Na <sub>2</sub> GMP	21.0° C	1.78 (1.54) <sup>a</sup>
0.79 <u>M</u> (TMA) <sub>2</sub> GMP	2.7° C	2.33
0.13 <u>M</u> NaCl		(1.92) <sup>a</sup>
0.53 <u>M</u> KCl		

---

<sup>a</sup>The values in parenthesis were obtained by excluding the resonance at 7.69, which could be a ribose OH line rather than NH line.

### VIII. A Survey of GMP Derivatives

A. 2'-M<sub>2</sub>GMP (M = Na<sup>+</sup>, K<sup>+</sup>). Figure 46 shows the extent of structure formation of 2'-Na<sub>2</sub>GMP. Comparison of the spectra at 1.3 °C (lower spectrum) and 26 °C (upper spectrum) reveals an upfield shift of the monomer line as well as two new lines growing in, one at 7.23 ppm and one at 8.51 ppm relative to TSP, indicative of structure formation. From examination of the spectra, it is clear that at 1.3 °C, a 0.64 M 2'-Na<sub>2</sub>GMP solution shows less than 10% structure formation. Thus, although the chemical shifts are similar to those for 5'-Na<sub>2</sub>GMP, the extent of structure formation is considerably less.

In contrast to the sodium case, 2'-K<sub>2</sub>GMP exhibits far more extensive self-structure formation as shown by the melting profile in Figure 47. The 0.85 M 2'-K<sub>2</sub>GMP solution at 1.3 °C shows seven distinct structure lines which span 1.2 ppm. On heating, the monomer line shifts to lower field as the intensity of the structure lines decreases. Structure is totally melted out by 44 °C. The concentration study shown in Figure 48, together with Figure 47, indicates the similarity in H(8) behavior with concentration and temperature dependence. At 1.3 °C, a 0.20 M solution shows only a monomer line. The 2'-K<sub>2</sub>GMP structure appears quite different from that of 5'-K<sub>2</sub>GMP. The extent of structure formation is greater for K<sup>+</sup> than Na<sup>+</sup> in the 2'-GMP case, which is consistent with observations for 5'-GMP. The degree of structure formation, however, is much more extensive for 5'-GMP than 2'-GMP.

B. 3'-M<sub>2</sub>GMP (M = TMA<sup>+</sup>, Na<sup>+</sup>, K<sup>+</sup>). In neutral solution, 3'-Na<sub>2</sub>GMP was too insoluble to ever attain concentrations where structure would be expected to be observable. Solutions of 3'-TMA<sub>2</sub>GMP were very viscous, but saturated solutions showed no observable structure at 0.7 °C. In

Figure 46. H(8) resonances of 0.64 M 2'<sup>1</sup>Na<sub>2</sub>GMP.

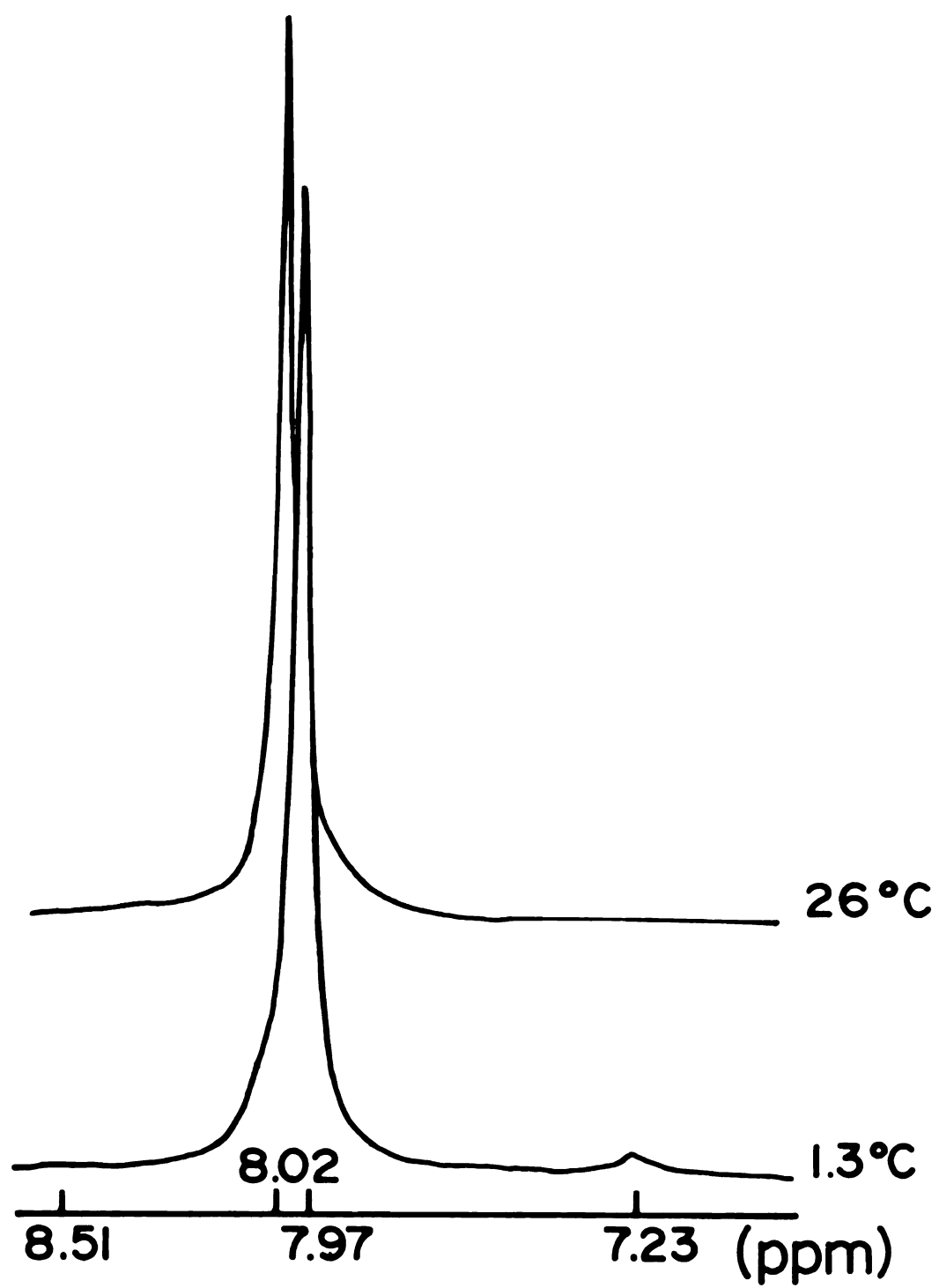


Figure 47. A temperature dependence study ( $^{\circ}\text{C}$ ) of the H(8) resonances of  $0.85\text{ M } 2'\text{K}_2\text{GMP}$ .

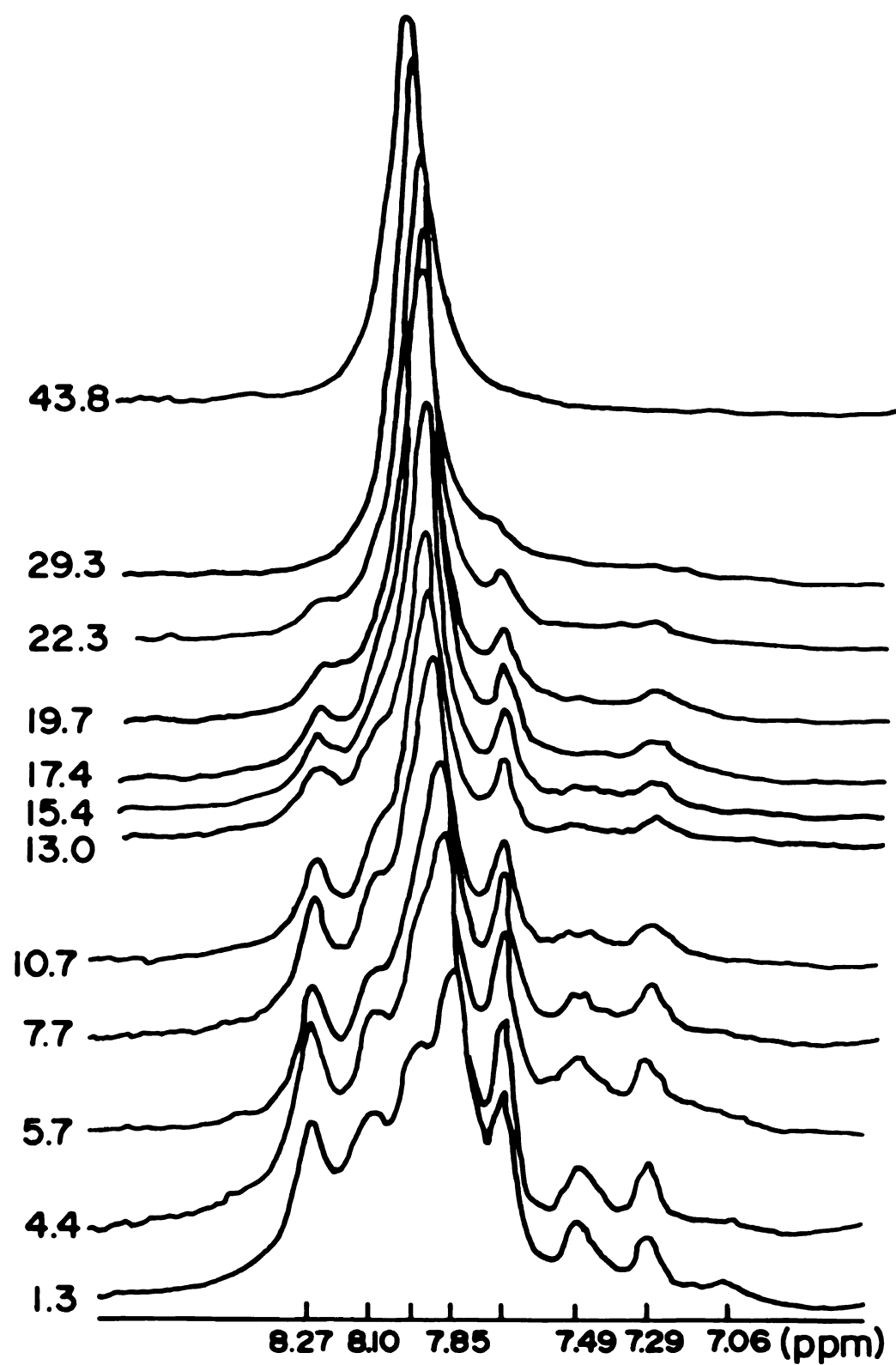
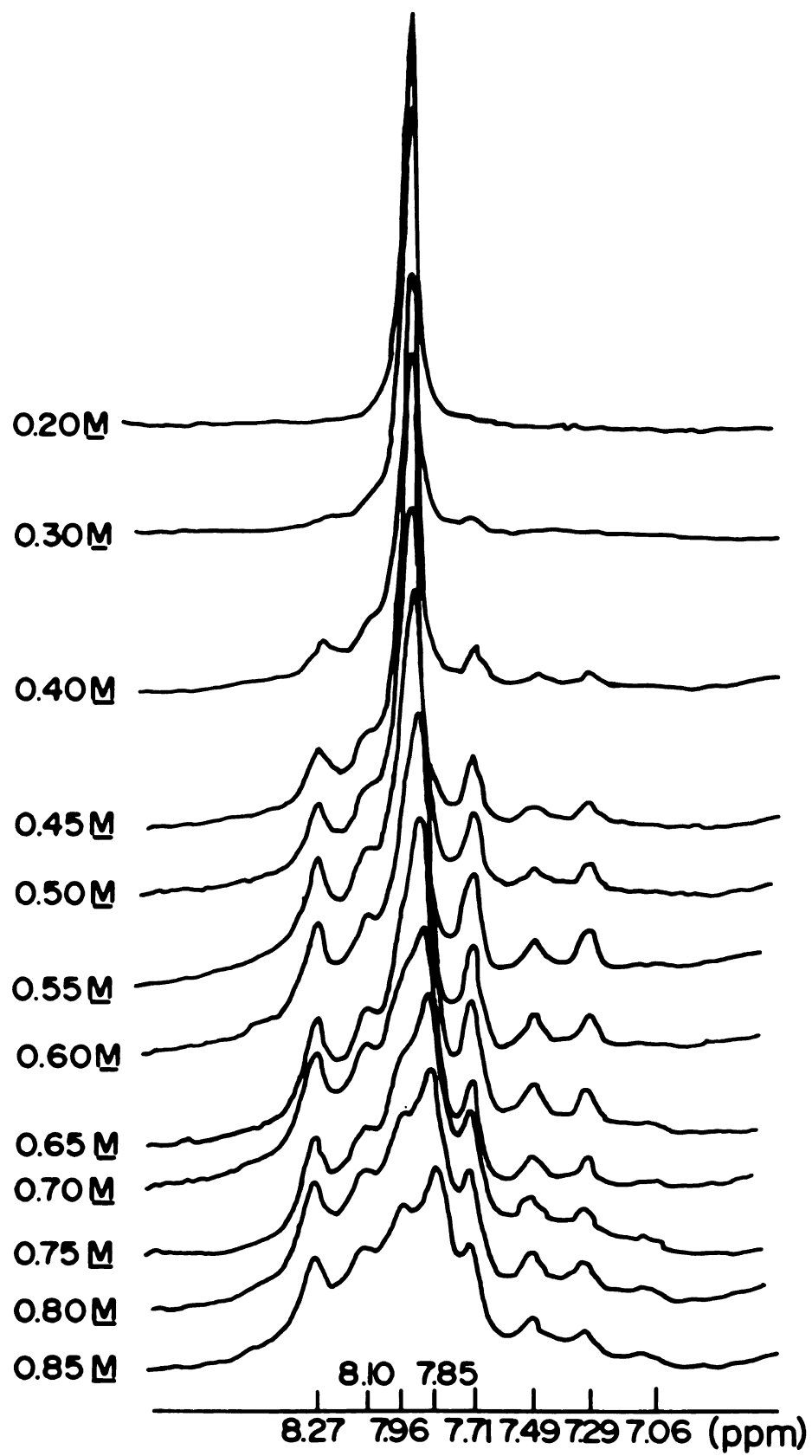




Figure 48. A concentration study of the H(8) resonances of  $2'\text{K}_2\text{GMP}$  at  $1.3^\circ\text{C}$ .



the presence of 0.19 M KCl precipitation occurred.

A spectrum of the solution and precipitate revealed structure was present as indicated by the line upfield of the monomer as shown in Figure 49. Addition of NaCl to 3'-TMA<sub>2</sub>GMP resulted in partial gelling at low temperature. A spectrum of the partially gelled solution showed very broad lines and a small broad structure peak 0.8 ppm upfield of the monomer line. Thus, although it is qualitatively clear that the sodium and potassium salts of 3'-GMP form ordered self-structures, due to the various solubility problems, no quantitative studies have been undertaken.

C. 2',3'-Cyclic GMP. The Li<sup>+</sup> salt of 2',3'-cGMP does not form an ordered structure. Addition of KCl to create a Li<sup>+</sup>/K<sup>+</sup> ratio equal to one resulted in the formation of a clear gel. The sodium salt of 2',3'-cGMP gelled on attempting to make a concentrated solution. Neither spectra of the gel nor spectra taken of the viscous solution which resulted from heating the gel gave any indication of structure formation. No further studies were attempted.

D. 3',5'-Cyclic GMP. The TMA<sup>+</sup> salt of 3',5'-cGMP showed no structure at high concentrations and low temperatures. Addition of KCl to attain a ratio of 4cGMP<sup>-</sup>/K<sup>+</sup> resulted in gelation at room temperature and no NMR detectable structure. Attempts to form a concentrated solution of the K<sup>+</sup> salt of 3',5'-cGMP resulted in gelation. Diluting the sample until a viscous solution remained, or heating the gel in an attempt to observe NMR detectable structure were to no avail. Addition of K<sup>+</sup> to the Na<sup>+</sup> salt also resulted in gel formation. In all cases the gels were clear and colorless. The Na<sup>+</sup> salt of 3',5'-cGMP, however, did exhibit NMR detectable structure.

Figure 49. The H(8) region of (A)  $0.5 \text{ M } 3'(\text{TMA})_2\text{GMP}$  containing  $0.19 \text{ M KCl}$  and (B)  $0.5 \text{ M } 3'(\text{TMA})_2\text{GMP}$  both at  $0.7^\circ \text{ C}$ . Some precipitate is present in solution (A).

The  $\text{Na}^+$  salt of 3',5'- $\underline{\text{cGMP}}$  crystallizes quite readily. In order to attain super saturated solutions of sufficient concentration for structure to be observed, solutions were heated and then cooled rapidly; spectra were then recorded as quickly as possible. A 0.74  $\underline{\text{M}}$  3',5'- $\underline{\text{cGMP}}$  solution at 5 °C showed a marked broadening of the monomer line, in addition to the presence of an upfield shoulder as shown in Figure 50. In this system, indications of structure formation are more dramatic in the ribose region than in the H(8) region. In the ribose region, extreme line broadening and a total change in peak pattern occur as shown in Figure 51.

Since 3',5'-cyclic  $\text{Na}_2\text{GMP}$  was capable of self-structure formation, an investigation was undertaken to see if it could be incorporated into the 5'- $\text{Na}_2\text{GMP}$  self-structure. Figure 52 shows the addition of 0.74  $\underline{\text{M}}$  cyclic-3',5'- $\text{NaGMP}$  to an initially 0.58  $\underline{\text{M}}$  5'- $\text{Na}_2\text{GMP}$  solution at 5 °C. Increasing the  $\underline{\text{cGMP}}^-$  concentration resulted in a line growing in just downfield of the 7.25 ppm sodium self-structure line. This new line increased in intensity and shifted downfield with increasing cyclic nucleotide concentration. This new peak, however, never reached the normal chemical shift for the cyclic  $\text{GMP}^-$  monomer. Thus, it is clear that although  $\underline{\text{cGMP}}^-$  did not incorporate into the 5'- $\text{GMP}^{2-}$  structure, some sort of interaction did occur between the two nucleotides.

It is likely that a simple stacking interaction took place between 3',5'- $\underline{\text{cGMP}}^-$  and the ordered 5'- $\text{GMP}^{2-}$ . It is obvious that incorporation into the 5'- $\text{GMP}^{2-}$  self structure did not occur since the simple sodium type of H(8) pattern is retained. If incorporation had occurred, the symmetry of the self-assembled units would be expected to be drastically decreased and subsequently new H(8) environments would be expected,

Figure 50. A temperature study ( $^{\circ}$  C) of the H(8) region of 0.74 M 3',5'-cyclic NaGMP. As the temperature increases the concentration decreases due to crystallization of the salt.

Figure 51. A temperature study ( $^{\circ}$  C) of the ribose region of 0.74 M 3',5'-cyclic GMP as the sodium salt. As the temperature increases the concentration decreases due to crystallization of the salt.

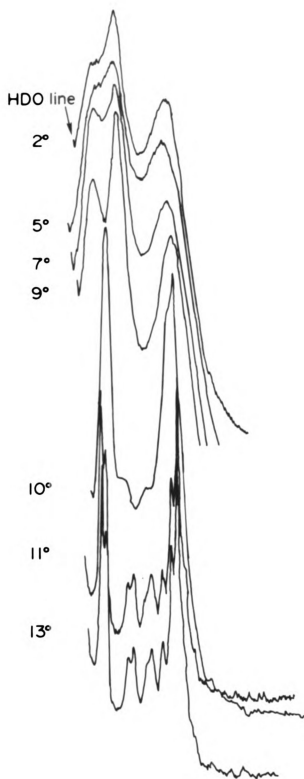
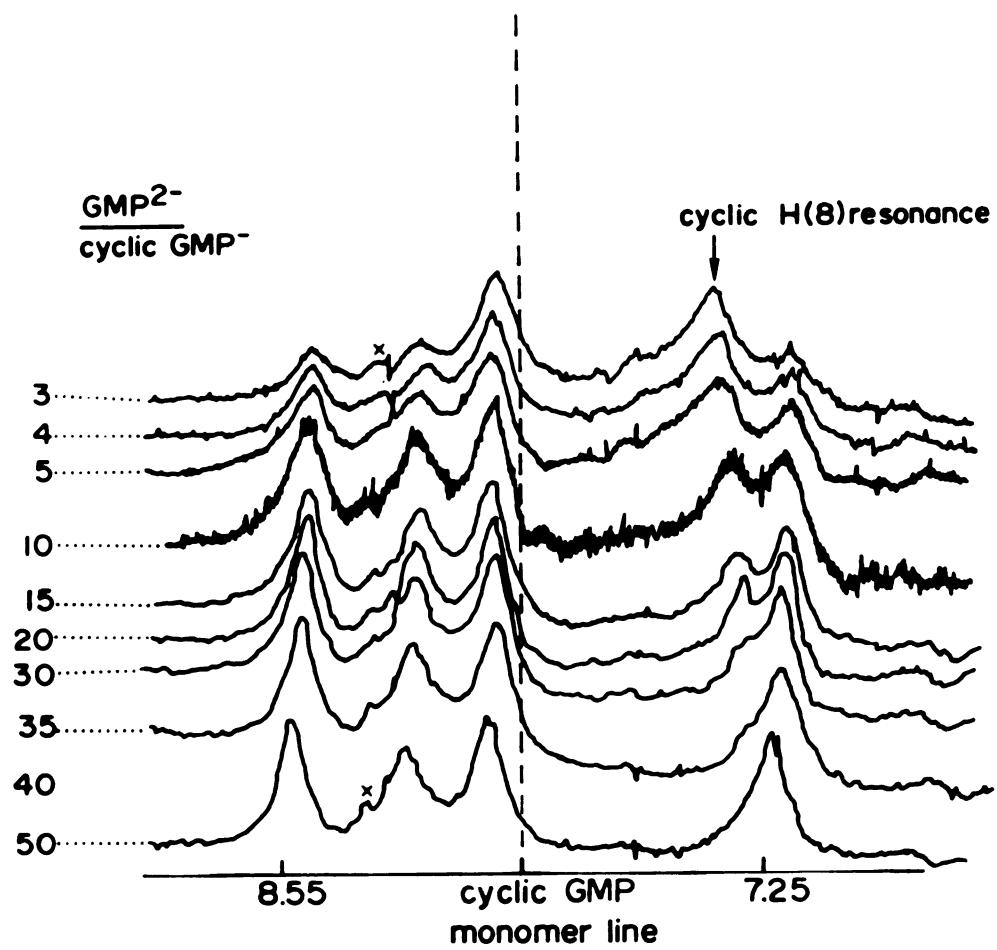




Figure 52. Effect on the H(8) resonance of 0.58 M Na<sub>2</sub>GMP upon addition of aliquots of 0.74 M Na-3',5'-cGMP at 5° C. An impurity in the system is marked with an X.



manifesting themselves as new H(8) resonances. Since the cyclic nucleotide resonance was the only line that was shifted, it is likely that the cyclic nucleotide merely associated with the outside of the octamer unit.

E. Inosine-5'-monophosphate. Although all of the salts investigated were quite soluble, none of the  $\text{IMP}^{2-}$  systems studied showed any evidence for structure formation. The salts investigated include  $\text{TMA}^+$ ,  $\text{Li}^+$ ,  $\text{Na}^+$ ,  $\text{K}^+$ ,  $\text{Rb}^+$  and  $\text{Cs}^+$ .  $\text{IMP}^{2-}$  differs from  $\text{GMP}^{2-}$  in the 2 position. Whereas  $\text{GMP}^{2-}$  has an amino group in this position capable of hydrogen bond formation,  $\text{IMP}^{2-}$  has only a hydrogen. Combinations of  $5'\text{-K}_2\text{GMP}$  and  $\text{K}_2\text{IMP}$  showed no perturbation of the H(8) or H(2) resonances, indicating that the structured  $5'\text{-K}_2\text{GMP}$  neither incorporated the  $\text{IMP}^{2-}$  into the self-assembled units nor associated with it to any great extent.

F.  $\text{M}_2\text{dGMP}$  ( $\text{M} = \text{TMA}^+$ ,  $\text{Li}^+$ ,  $\text{Na}^+$ ,  $\text{K}^+$ ,  $\text{Rb}^+$ ,  $\text{Cs}^+$ ,  $\text{Sr}^{2+}$ ).

i. Sodium. Figure 53 shows a 1.0 M  $\text{dGMP}^{2-}$  solution at 0.7 °C with  $\text{dGMP}^{2-}/\text{Na}^+ = 0.67$  (lowest spectrum) and  $\text{dGMP}^{2-}/\text{Na}^+ = 0.5$  (middle spectrum). The H(8) region shows no change between 26 °C (top spectrum) and 0.7 °C; however, the entire ribose region showed a marked broadening of lines and a change in intensities as well as changes in chemical shifts of the lines. Thus, structure formation is reflected in the ribose region although it is not necessarily indicated by the H(8) region. Since the  $\text{Na}^+$  salt showed the ability for self-assembly, an attempt was made to titrate deoxyguanylic acid to make  $\text{K}_2\text{dGMP}$  and  $(\text{TMA})_2\text{dGMP}$ . Unexpectedly, the titrations both resulted in precipitation of the very dilute solutions (1.0 g of  $\text{H}_2\text{dGMP}$  in > 100 mL  $\text{H}_2\text{O}$ ) at  $\text{pH} \geq 6$ . Apparently, the neutral  $\text{K}^+$  and  $\text{TMA}^+$  salts must be prepared by ion

Figure 53. The H(8) and H(1)' regions of a 0.9 M solution of 2'deoxy-5'-GMP at neutral pH (A) with 1.5 Na<sup>+</sup>/dGMP<sup>1.5-</sup> at 0.7° C, (B) with 2.0 Na<sup>+</sup>/dGMP<sup>1.5-</sup> at 0.7° C, and (C) with 2.0 Na<sup>+</sup>/dGMP<sup>1.5-</sup> at 26.2° C.

exchange, although this was not undertaken. Instead, a number of studies were performed at  $\text{pH} \leq 6$  rather than the usual  $\text{pH} = 8.3$  of 5'-GMP solutions investigated. Although the solutions did not gel, they were quite viscous and often turbid.

Figure 54 shows a melting profile for a  $1.08 \text{ M}$   $\text{dGMP}^{2-}$  solution with  $\text{dGMP}^{2-}/\text{Na}^+ = 4.4$ , prepared by titrating to a  $\text{pH} = 4.75$  with TMAOH. In the absence of  $\text{Na}^+$ , the  $1.08 \text{ M}$  TMA $\text{dGMP}$  solution (which had a  $\text{pH} = 5.45$  due to the concentration change) showed no structure at less than  $1^\circ\text{C}$ . Addition of  $\text{Na}^+$  resulted in new lines at 8.08, 7.64 and 7.09 ppm, while the monomer always remained at 8.02 ppm. Further addition of NaCl to the solution creating a ratio of  $\text{dGMP}^-/\text{Na}^+ = 1$  resulted in precipitation. A spectrum of the  $\text{dGMP}^-$  remaining in solution showed only a monomer line in the H(8) region at  $0.7^\circ\text{C}$ .

Figure 55 shows a "melting profile" for a  $0.61 \text{ M}$   $\text{dGMP}^-$  solution with  $\text{dGMP}^-/\text{Na}^+ = 4.07$ . The  $\text{TMA}^+$  salt was prepared by titrating  $\text{H}_2\text{dGMP}$  to a  $\text{pH} = 5.5$  with TMAOH. The  $\text{TMA}^+-\text{dGMP}^-$  solution showed no evidence for structure formation at low temperature prior to additions of  $\text{Na}^+$ . The  $\text{pH}$  of the concentrated solution was 6.2. The addition of  $\text{Na}^+$  resulted in a four line spectrum at  $1.0^\circ\text{C}$ . The highest field line at 6.95 ppm appears to correspond to the 7.09 ppm line of Figure 54, based on comparison of the  $\text{TMA}^+$  peaks and the ribose regions of the two sets of spectra. The difference is attributable to placing the TSP reference in the outer tube for the spectra shown in Figure 55 and in the inner tube with the sample for the spectra shown in Figure 54. Although the same lines appear to be present at both  $\text{pH}$  values, at the higher  $\text{pH}$  the lines appear to be shifted slightly upfield. At both  $\text{pH}$  values investigated, it appears that heating of the  $0.7^\circ\text{C}$  solutions results in a decrease in

Figure 54. A temperature study ( $^{\circ}\text{C}$ ) of the H(8) region of 1.08 M  $(\text{TMA})_2\text{dGMP}$  at  $\text{pH} = 5.45$  containing 0.245 M  $\text{NaTSP}$  to give a ratio of 4.4  $\text{dGMP}^-/\text{Na}^+$ .

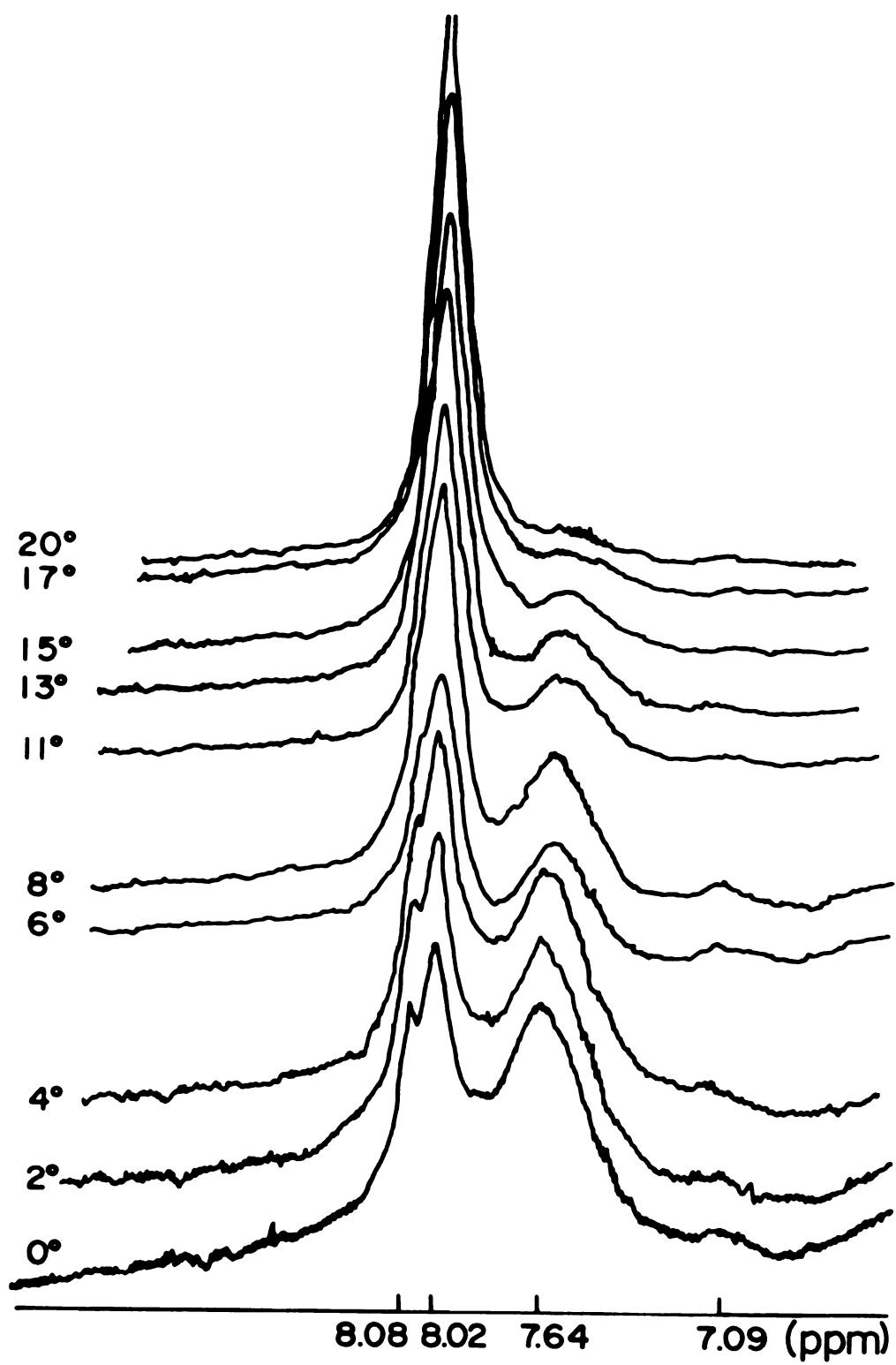
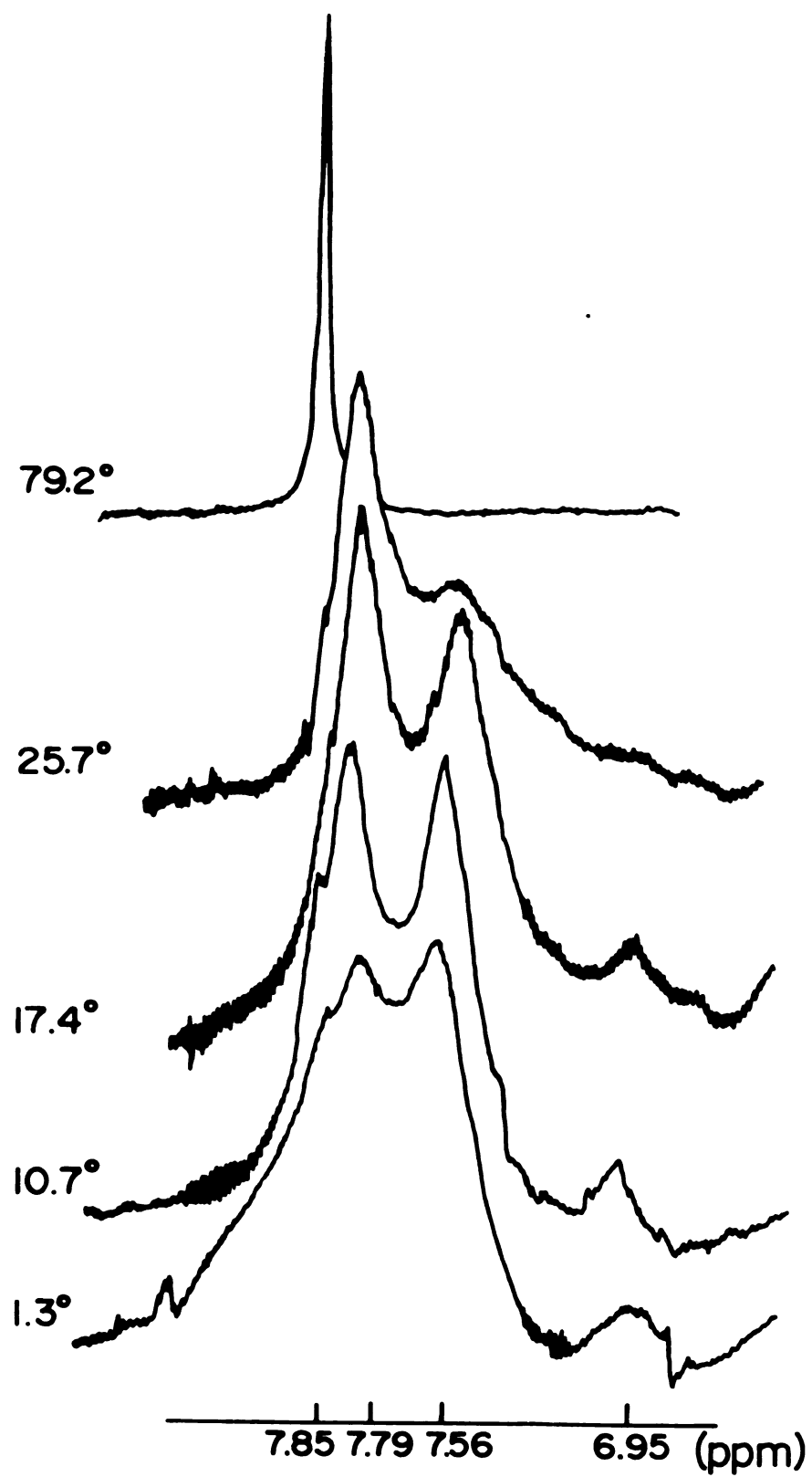


Figure 55. A temperature study ( $^{\circ}\text{C}$ ) of the H(8) region of 0.61 M  $(\text{TMA})_2\text{dGMP}$  at  $\text{pH} = 6.2$  containing 0.15 M  $\text{NaCl}$  to give a ratio of 4.07  $\text{dGMP}^-/\text{Na}^+$ .





the intensity of the two highest field lines, concurrent with the merging and subsequent increase in intensity of the two lowfield lines. Although the solution with pH=5.45 has a considerably higher concentration than the solution with pH=6.2, both contain roughly equal sodium concentrations. Comparison of the 17 °C spectra in both cases reveals that the solution with the higher pH and lower dGMP<sup>2-</sup> concentration exhibits a greater degree of structure formation.

ii. Potassium. Figure 56 shows a melting profile for a 0.70 M dGMP<sup>2-</sup> solution with 4.4 dGMP<sup>2-</sup>/K<sup>+</sup> at pH = 5.45. Figure 57 shows a melting profile for a 0.61 M dGMP<sup>2-</sup> solution with 4.4 dGMP<sup>2-</sup>/K<sup>+</sup> at pH=6.2. The melting profiles are quite similar to each other; both have the smaller highfield line which melts out around 70 °C, the lowfield peak which is made up of at least two structure lines and monomer, and the middle peak composed of at least three structure lines which change in relative intensity as a function of temperature. The highest field structure line has a chemical shift of 6.96 from an external TSP reference, which is the same as the highest field sodium structure line. The lowest field sodium structure lines are also identical to the K<sup>+</sup> lowest field structure line with a chemical shift of 7.85 ppm. The chemical shifts of the middle peaks, however, are different in the sodium and potassium cases. The middle peaks in the K<sup>+</sup> system have lines at 7.64 and 7.44 ppm in addition to other lines which are less well defined. Although the Na<sup>+</sup> and K<sup>+</sup> systems may appear quite similar at low temperature, they follow quite different melting patterns. In the K<sup>+</sup> system the monomer line grows in at 7.85 ppm, without any interaction with the central peak whereas the sodium monomer results from the merging of a central peak and the 7.85 ppm line. The

Figure 56. A temperature profile ( $^{\circ}$  C) of the H(8) region of 0.70 M (TMA)<sub>2</sub>dGMP at pH = 5.45 containing 0.16 M KCl to give a ratio of 4.4 dGMP<sup>-</sup>/K<sup>+</sup>.

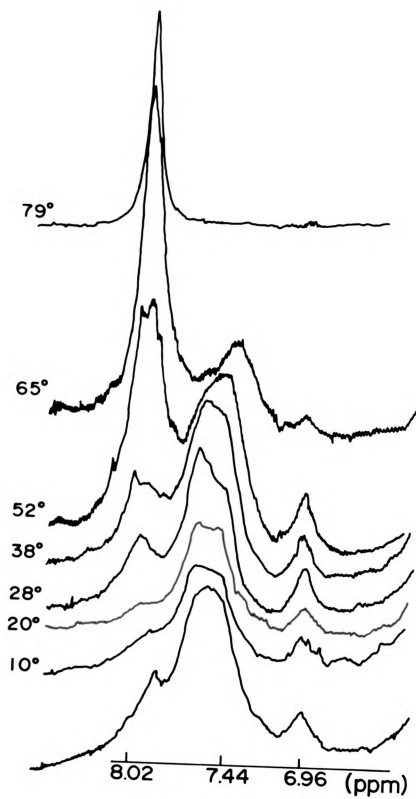
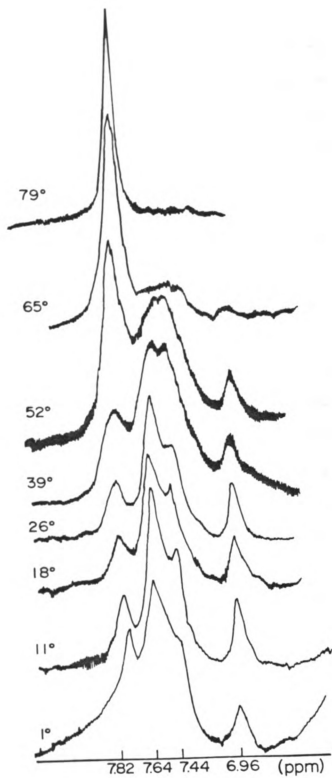


Figure 57. A temperature study ( $^{\circ}$  C) of the H(8) region of 0.61 M (TMA)<sub>2</sub>dGMP at pH = 6.2 containing 0.16 M KCl to give a ratio of 4.4 dGMP<sup>-</sup>/K<sup>+</sup>.



relative stabilities of the  $\text{Na}^+$  and  $\text{K}^+$  systems are not as markedly different as would be expected based on observations of the  $\text{Na}^+$  and  $\text{K}^+$  5'-GMP systems.

iii. Rubidium. Figure 58 shows a melting profile for a 0.61 M  $\text{dGMP}^{2-}$  solution with 5.27  $\text{dGMP}^{2-}/\text{Rb}^+$  at pH = 6.2. The greatest amount of structure is observed at 0.7 °C as portrayed by the two overlapping lines at 6.99 ppm, a large peak consisting of several lines at 7.54 ppm and a broad shoulder on the 7.54 ppm peak ending at about 7.91 ppm arising from the overlap of several lines including the monomer. All chemical shifts are referenced from an external TSP solution. Melting out of the structure on heating can be followed by an increase in the monomer line, while the peaks at 7.54 ppm and 6.99 ppm decrease in intensity. Comparison of the 0.7 °C 4.07 $\text{dGMP}^{2-}/\text{Na}^+$  spectrum in Figure 55 and the 17.4 °C 5.27 $\text{dGMP}^{2-}/\text{Na}^+$  spectrum in figure 58 clearly shows the definite similarities between the two systems. It appears as if the  $\text{Rb}^+$  system is more extensively structured at the lower temperature, if the systems are assumed to follow similar structuring patterns. This is in fact shown by the fact that the  $\text{Rb}^+$  system still shows some structure at 38.5 °C, whereas the  $\text{Na}^+$  system shows no structure. Increasing the extent of structure in the sodium system would be expected to result in a spectrum similar to that of the  $\text{Rb}^+$  system at lower temperatures. The bottom spectrum in Figure 59 shows a 0.61 M solution with  $\text{dGMP}^-/\text{Na}^+ = 3.0$  at 0.7 °C with pH = 6.2, which is in fact very similar to the bottom spectrum of Figure 58, 0.61 M and  $\text{dGMP}^-/\text{Rb}^+ = 5.3$  at 0.7 °C with pH=6.2. Thus,  $\text{Rb}^+$  is clearly a better structure director than  $\text{Na}^+$ , although it is not as good a structure director as  $\text{K}^+$ .

Figure 58. A temperature study ( $^{\circ}\text{C}$ ) of the H(8) region of 0.61 M (TMA)<sub>2</sub>dGMP at pH = 6.3 containing 0.11 M RbCl to give a ratio of 5.27 dGMP<sup>-</sup>/Rb<sup>+</sup>.



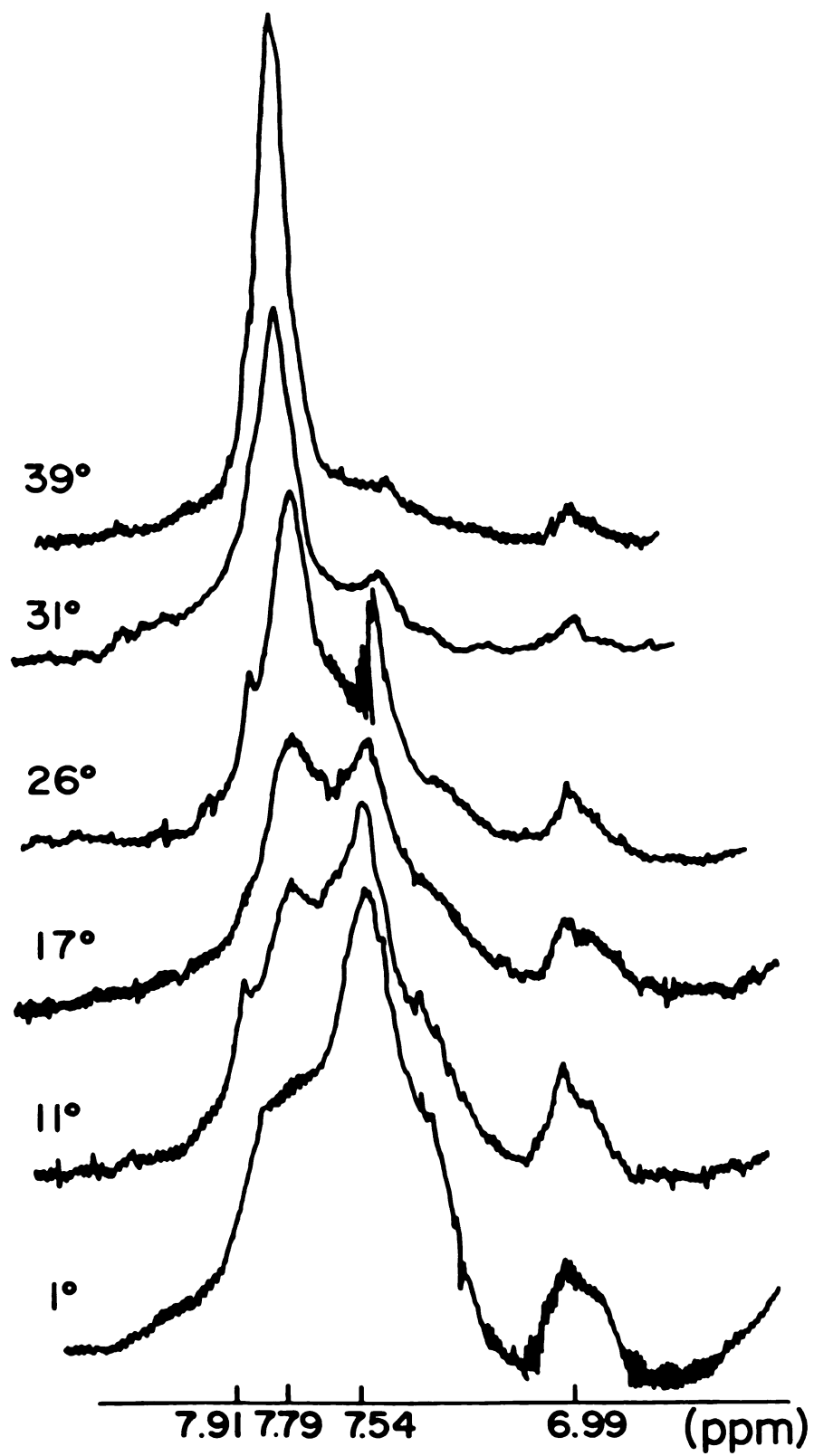
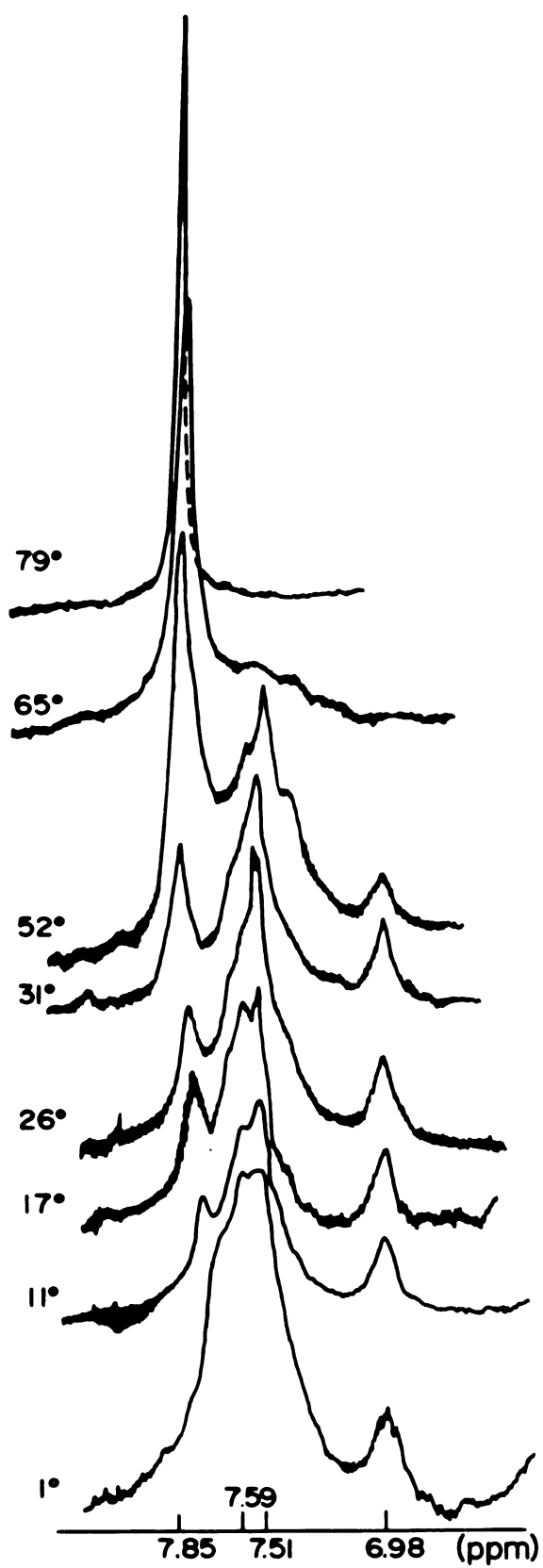


Figure 59. A comparison of the H(8) regions of solutions of 0.61 M (TMA)<sub>2</sub>dGMP at pH = 6.2 and 0.7° C with (A) 0.6 M LiCl, (B) 1.3 M CsCl, (C) 0.2 M KCl, (D) 0.2 M SrCl<sub>2</sub> and (E) 0.2 M NaCl.

iv. Strontium. Figure 60 shows the melting profile for a 0.61 M  $\text{dGMP}^{2-}$  solution with 5.01  $\text{dGMP}^{2-}/\text{Sr}^{2+}$  at pH = 6.2. Structure lines for the most ordered solution appear at 6.98, 7.51, 7.59 and 7.85 ppm as referenced from external TSP. Melting out of the structure is clearly denoted by the increase in monomer line at 7.85 ppm, and a decrease in the remaining structure line. The overlapping peaks at 7.59 and 7.51 ppm become better resolved on heating, and it becomes clear that there is at least one definite line between the 7.85 and 7.59 lines, as well as a shoulder upfield of the 7.51 line. The melting pattern for  $\text{Sr}^{2+}$  is far more similar to that of  $\text{K}^+$  than to that of the  $\text{Na}^+$  or  $\text{Rb}^+$  systems. This is the expected result based on the similarity between the ionic radius of  $\text{K}^+$  and  $\text{Sr}^{2+}$ . Figure 59 shows in Spectrum D a  $4\text{dGMP}^{2-}/\text{Sr}^{2+}$  solution, and in Spectrum C a  $3\text{dGMP}^{2-}/\text{K}^+$  solution, both 0.61 M at 0.7 °C with pH = 6.2. Comparison of these two spectra show the similarities between the two systems. Further similarities are observed in the melting patterns in that there is a central broad peak made up of several overlapping peaks, a small upfield peak, and an independent downfield monomer peak which grows in "separately" from structure line decrease. In the  $\text{Rb}^+$  and  $\text{Na}^+$  systems, the increase in monomer line intensity and the decrease in structure line intensity appear concomitantly.

The top two spectra of Figure 59 show  $1\text{dGMP}^{2-}/\text{Li}^+$  and  $0.48\text{dGMP}^{2-}/\text{Cs}^+$ , both 0.61 M at 0.7 °C with pH = 6.2. The  $\text{Li}^+$  system shows no structure, but only the monomer at 7.9 ppm. Further addition of  $\text{LiCl}$  resulted in precipitation and gelling. The  $\text{Cs}^+$  system shows some structure, but it is less than 10%. Structure formation is indicated by the upfield shift of the monomer line to 7.65 ppm and the

Figure 60. A temperature study ( $^{\circ}$  C) of the H(8) region of 0.61 M (TMA)<sub>2</sub>dGMP at pH = 6.2 containing 0.12 M SrCl<sub>2</sub> to give a ratio of 5.01 dGMP<sup>2-</sup>/Sr<sup>2+</sup>.



small broad peak at 7.29 ppm from external TSP. This is similar to the 5'-GMP system.

v. Summary. Thus, in the 5'-deoxyguanosine monophosphate system the order of structure directing ability is found to be  $\text{Sr}^{2+} > \text{K}^+ \gg \text{Rb}^+ > \text{Na}^+ \gg \text{Cs}^+ > \text{Li}^+, \text{TMA}^+$ . The four principal structure directors all exhibit a similar peak at about 6.95 ppm and one at about 7.85 ppm from an external TSP reference. They also all give parallel melting patterns, although  $\text{Sr}^{2+}$  and  $\text{K}^+$  are most similar to each other and  $\text{Na}^+$  and  $\text{Rb}^+$  are quite similar. This is quite different from what is found in the 5'-GMP system, where sodium displays a very unique structure line pattern as well as melting profile. It must be noted, however, with regard to  $\text{Sr}^{2+}$ ,  $\text{K}^+$  and  $\text{Rb}^+$  that in the 5'-GMP system, their individual characteristics did not appear until a  $\text{GMP}^{2-}$  to metal ion ratio of 1:1 was reached. This may be the case for all four structure directing ions for the 5'-dGMP system discussed here. Unfortunately, ratios of 1dGMP/metal ion were unattainable due to precipitation of the nucleotide. Although the 5'-GMP and 5'-dGMP systems were studied at different pH's, qualitative comparison of trends seems valid in attempting to evaluate the different possible mechanisms for structure formation.

## DISCUSSION

### I. The Advantages of $\text{TMA}^+$ as a Counter-Ion.

We have seen that the addition of  $\text{TMA}^+$  to a  $\text{Na}_2\text{GMP}$  solution induces an upfield shift of the monomer H(8) line, although it causes no change in the percent nucleotide self structure in solution. We have also seen that the presence of  $\text{TMA}^+$  in solution allows one to add metal chlorides that would otherwise induce precipitation of the nucleotide.

With the information that  $\text{TMA}^+$  is a structure inert ion and that it also enhances the solubility of the  $\text{GMP}^{2-}$  unit, we were able to investigate structure formation as a function of metal ion concentration. The H(8) NMR results shown in Section II A. of Results showed that the types of self-structures formed with  $\text{Na}^+$  as structure director are independent of  $\text{GMP}^{2-}/\text{Na}^+$  ratio. In contrast,  $\text{K}^+$  and  $\text{Rb}^+$  show structural properties that depend on metal ion concentration.

The structure inertness and high solubility of  $\text{TMA}_2\text{GMP}$  also allowed the investigation of  $\text{Sr}^{2+}$  and  $\text{Ba}^{2+}$  as structure directors. The pure GMP salts of these alkaline earth metals are very sparingly soluble in water and do not lend themselves to structural investigation by NMR.

## II. Specific and Non-Specific $\text{Na}^+$ and $\text{K}^+$ Ion Complexation Reactions.

A. The Best Structural Model and Evidence for Specific Metal Ion Binding. Previous results of fiber diffraction studies<sup>111</sup> on neutral fibers of  $\text{Na}_2\text{GMP}$  indicated the presence of stacked planar tetramer units. In addition, infrared studies of the carbonyl region of structured  $\text{Na}_2\text{GMP}$  and  $\text{K}_2\text{GMP}$  showed features which are indicative of structures involving hydrogen bonding and base stacking. It is likely, therefore, that the forces operating between the nucleotide units are quite similar in both the  $\text{Na}^+$  and  $\text{K}^+$  ordered forms.<sup>110</sup> The fact that the order of stability of the metal ion complexed self-assembled units,  $\text{K}^+ > \text{Na}^+, \text{Rb}^+ \gg \text{Cs}^+, \text{Li}^+$ , is unrelated to the expected electrostatic ordering<sup>106-108</sup> suggests that a size selective mechanism is operative. An analogous stability order has been observed for alkali metal ion complexes of macrocyclic antibiotics and cyclic ether systems.<sup>109</sup> Thus, the proposed model for self assembled alkali metal ion complexes of GMP involves complexation of the metal ion through a size specific binding cavity. The center of the tetramer was proposed as the sodium binding site and the center of the octamer was proposed as the potassium binding site,<sup>6</sup> based on size considerations.

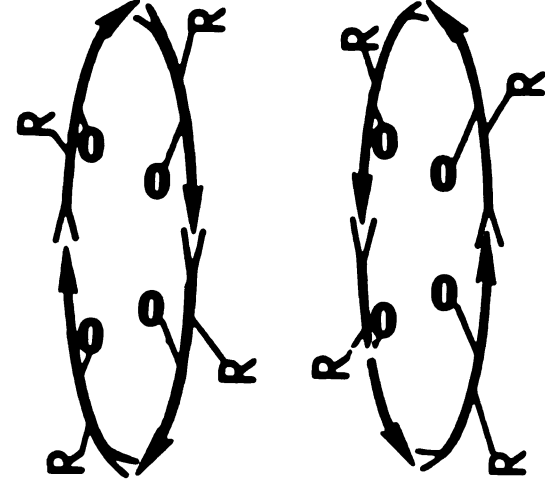
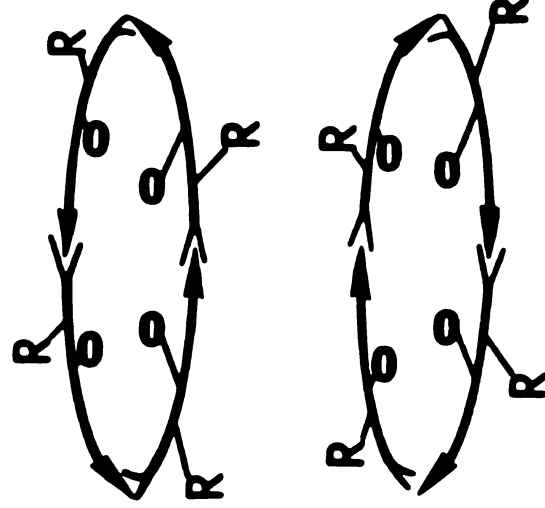
Based on the symmetry of the stacked tetramers, several geometrical isomers are possible, giving rise to multiple H(8) environments.<sup>113</sup> Without considering the chiral ribophosphate, the symmetry of the eclipsed or staggered head-to-head stack of two



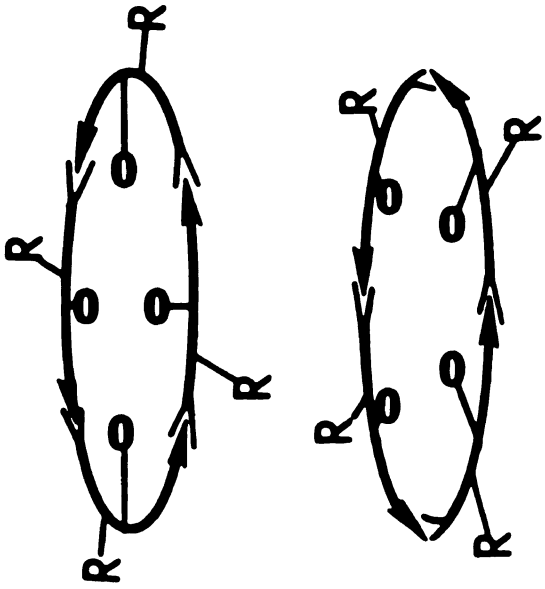
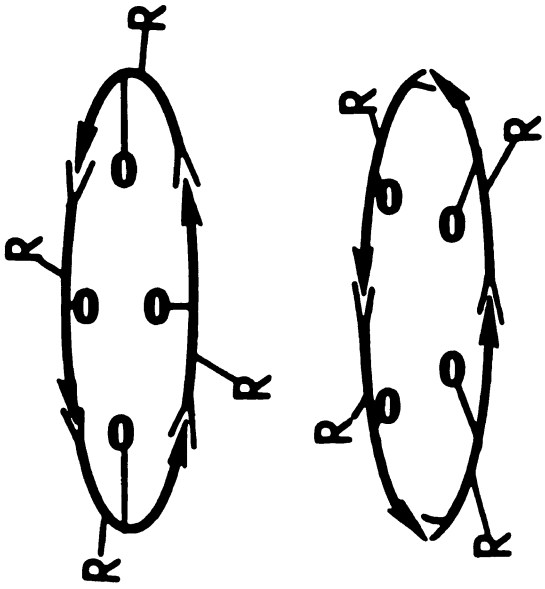
tetramer units is  $D_4$ . Thus, the octamer is chiral and the plates are equivalent; by considering the ribophosphate, two diastereomers can be envisioned. Since the plates are equivalent, each diastereomer should give rise to a single H(8) environment. Thus, with a  $+30^\circ$  twist angle between the two tetramer plates, two H(8) resonance lines are expected, one from each diastereomer. Similarly, for a  $-30^\circ$  twist angle, two lines are expected since the two twist angles are inequivalent. The likelihood of a  $\pm 30^\circ$  twist angle is indicated by the fiber diffraction studies of Zimmerman.<sup>111</sup> If restricted rotation is assumed about the glycosidic bond, then tail-to-tail stacking becomes distinguishable from head-to-head stacking and four additional isomers are possible. Schematics of the various stacking patterns are shown in Figure 61. In head-to-tail stacking, the symmetry is  $C_4$  for staggered tetramers without considering the ribophosphate. Thus, the octamer is chiral, and in the presence of the chiral ribophosphate two diastereomers result. The point group of the total octamer is  $C_4$ , thus the plates are inequivalent. For a twist angle of  $+30^\circ$ , two H(8) environments are expected and for a  $-30^\circ$  twist angle, two H(8) environments are expected. Thus, twelve distinct H(8) environments are possible through stacking of two tetramer units, if all eight isomers are present. The twist angles, head-to-head, tail-to-tail or head-to-tail stacking patterns may be influenced by the metal ion(s) in solution.

Figure 61. A representation (schematic) of the various stacking patterns for two tetramers. The double arrow represents the direction of the hydrogen bonds.

# Head to Head



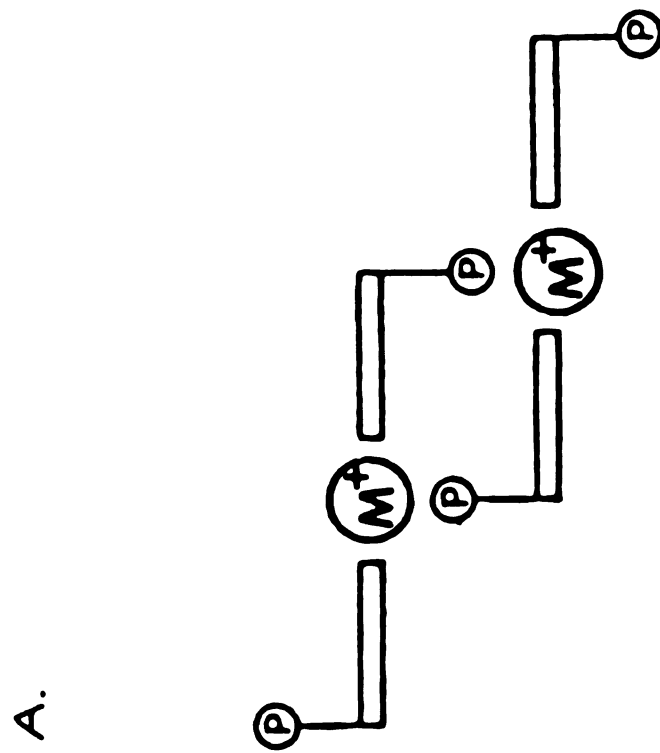
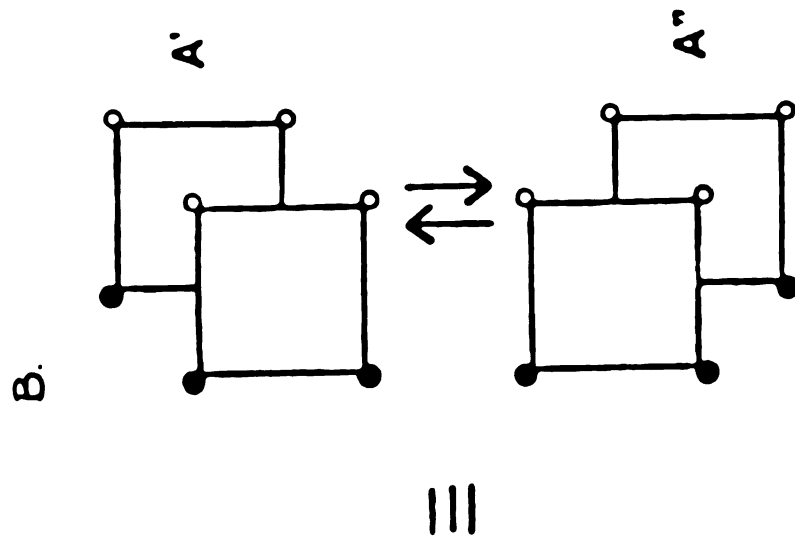
# Head to Tail



B. Other Models Which Have Been Proposed. Laszlo<sup>115</sup> has proposed several different structures for self-assembled Na<sub>2</sub>GMP and K<sub>2</sub>GMP. Based on <sup>31</sup>P, <sup>23</sup>Na and <sup>39</sup>K NMR results. One structure is the staircase model shown in Figure 62a. The tetramer is indicated by the rectangle. The metal ion is situated in the center of the tetramer, and is also coordinated to a phosphate of an adjacent plate. He suggests that the multiple H(8) lines result from different degrees of stacking of this structure. He indicates that two of the adjacent phosphates of a tetramer unit point in the opposite direction of the other two phosphates. From this he concludes that a rapid exchange occurs as shown in Figure 62. In the same paper he proposed a stacked tetramer type of structure where Na<sup>+</sup> is found either at the center of the tetramer plate or the center of two stacked tetramers.

There appears to be some basic discrepancies in Laszlo's model. He proposes the same coordination sites and identical structural arrangements to account for sodium self-structure<sup>115d</sup> and potassium self-structure.<sup>115a</sup> Clearly, if identical structures existed, the H(8) regions of both systems would be identical. Since this is not the case, it appears inconsistent to invoke the same model in both instances. In both cases, he assigns the staircase structure to have C<sub>2h</sub> symmetry neglecting the chiral ribophosphate. In the staircase he indicates only a partial overlap of tetramer units. This would result in only minimal hydrophobic interactions, whereas direct overlap would be expected to be energetically favored. This model is unable to explain the differences observed between "simple" and

Figure 62. Models proposed by Laszlo for the self-structures of 5'-GMP. (A) Shows the "staircase" model where  $M^+$  represents either  $Na^+$  or  $K^+$ . The differences in H(8) environments he rationalizes in terms of (B), showing the overlap of tetramer units, where the open circles represent phosphates pointed "down" and the darkened circles represent phosphates pointed "up".



"complex"  $K^+$  spectra. Another attempt by Laszlo at rationalizing the multi-line H(8) environment in the  $K^+$  system was to change the number of phosphates pointing "up" and "down" in an octamer staircase unit.<sup>115a</sup> In order to achieve these "up" or "down" orientations of the ribose, a conformation other than anti must be generated about the glycosidic bond. If Sundarlingam is correct in his proposed rigid nucleotide concept where there are definite preferred conformations, it is unlikely that the nucleotide would be found in both syn and anti conformations at fixed ratios, which Laszlo seems to imply change, depending on the alkali metal ion in solution. Although there is no direct experimental evidence to support or rule out Laszlo's staircase model, it ignores the precedent for the tetramer stacking pattern observed by fiber diffraction studies. More importantly, his model is almost completely lacking in interpretive power and it should be abandoned in favor of the stacking model proposed above.

C. Evidence for Non-Specific Metal Binding Sites and a Suggested Model. If a simple association occurs between  $Na^+$  and  $GMP^{2-}$  with only one metal ion site involved in the self-assembly process, increasing the sodium to  $GMP^{2-}$  ratio should increase the degree of structure formation. As shown in Figure 17, however, the degree of structuring decreases with increasing sodium ion concentration beyond a ratio of about 1.0-1.5  $GMP^{2-}/Na^+$ . This strongly suggests that multiple binding sites exist and excess sodium in the system blocks a site which favors structure formation. The sites available for metal ion coordination other than O(6) or positions involved in

hydrogen bonding are the ribose and the phosphate. In addition to binding of  $\text{Na}^+$  at the principal structure directing O(6) positions of a tetramer unit, a second binding site involving a sodium - phosphate interaction is proposed to play a part in structure formation. Support for phosphate participation is given by the  $\text{Li}^+$  -  $\text{Na}^+$  system. Addition of  $\text{Na}^+$  to  $\text{Li}_2\text{GMP}$  results in precipitation; however, the spectrum of the  $\text{GMP}^{2-}$  remaining in solution is different from that of a  $\text{Na}^+$ -GMP system. Instead of the usual  $\text{Na}^+$  four line pattern in the H(8) region, the  $\text{Li}^+$ - $\text{Na}^+$  system shows only monomer and a smaller upfield line (cf., Figure 21). Thus, although  $\text{Li}^+$  is not a structure directing ion, it is not a structure "inert" ion either. The spectrum of a system containing  $4\text{GMP}^{2-}/7\text{Li}^+$  and  $1\text{Na}^+$  shows the same "nonsodium" type of structure as addition of  $\text{Na}^+$  to  $\text{Li}_2\text{GMP}$ . The binding constant for  $\text{Li}^+$ -phosphate association in  $\text{AMP}^{2-}$  is 4.1, 1.6 times that of  $\text{Na}^+$ . Since similar relative association constants are expected for  $\text{GMP}^{2-}$  and  $\text{AMP}^{2-}$ ,  $\text{Li}^+$  should be more strongly ion paired to the phosphate than  $\text{Na}^+$ , and not allow the  $\text{Na}^+$  to associate. The proposed association between  $\text{Na}^+$  and  $\text{GMP}^{2-}$  involves sodium chelation of interplate phosphates. The binding of more than one phosphate oxygen to  $\text{Na}^+$  is not uncommon. For example, in the crystal structure of NaGpC, the sodium ions are bound by the phosphate groups of two different double-helical fragments with O-Na distances of  $\sim 2.3 - 2.4$  Å.<sup>89</sup> In the crystal structure of NaApU, one sodium coordination site involves two oxygens of one phosphate from different fragments.<sup>130</sup> In  $\text{Na}_2\text{ATP}$ , one of the purposes of the sodium is to link the ATP dimers together by bridging phosphate oxygens. The Na-O distances are  $\sim 2.3$

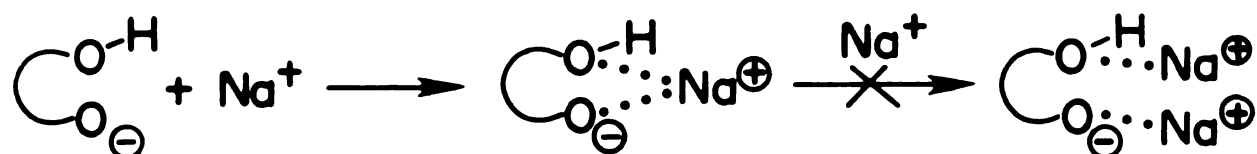


Å.<sup>131</sup> Thus, in the  $\text{GMP}^{2-}$  system, interplate phosphate oxygen distances should theoretically be  $4.6 \text{ Å}$  or less in order to consider chelation as feasible. Model studies,<sup>113</sup> compatible with Zimmermans x-ray results,<sup>111</sup> have shown that interplate phosphate distances can range from 2 to  $12 \text{ Å}$  depending on the stacking pattern,  $[01'-C1'-N9-C8]$  twist angle, and the  $[05'-C5'-C4'-C3']$  twist angle. Thus chelation of  $\text{Na}^+$  can occur within the constraints of the proposed models.

Sodium ion chelation is also supported by the dependence of structure formation on  $\text{Na}^+/\text{GMP}^{2-}$  ratio in the  $\text{Na}^+ \text{-TMA}^+$  systems (cf., Figure 10). The addition of NaCl to the  $\text{TMA}^+$  system resulted in a constant ratio of two structured  $\text{GMP}^{2-}$  units per  $\text{Na}^+$ , until a ratio of two total  $\text{GMP}^{2-}/\text{Na}^+$  was reached. This value of two was determined by using the concentration of self assembled  $\text{GMP}^{2-}$  for a given  $\text{GMP}^{2-}/\text{Na}^+$  ratio as calculated from the percent solution structure shown in Table 4. This concentration was then divided by the concentration of sodium in solution for the particular  $\text{GMP}^{2-}/\text{Na}^+$  ratio. 2:1 is an overall ratio, including a fraction at size-specific structure directing positions and the remainder at non-specific positions. At  $\text{GMP}^{2-}/\text{Na}^+$  ratios greater than about 1.0, the amount of self-structure decreases while the concentration of monomer increases. The equilibrium constant for self assembly of  $\text{Na}_2\text{GMP}$  at  $0^\circ\text{C}$  has been estimated to be about 15,<sup>132</sup> and the phosphate association constant for  $\text{Na}^+$  and  $\text{AMP}^{2-}$  is 2.6.<sup>107b</sup> A comparable value is expected for the  $\text{Na}^+ \text{-GMP}^{2-}$  system.

Based on the  $\text{GMP}^{2-}/\text{Na}^+$  ratio and these equilibrium constants, a structure is proposed that has sodiums at the center of each tetramer,

and in addition, sodiums at opposing edges of the octamer as shown schematically in Figure 63. Thus, the tetrameric plates are proposed to be held together by interplate phosphate chelation of the sodium ions, in addition to the stacking interactions. There are three types of interplate interactions which will be considered: (1) a phosphate-phosphate sodium chelation interaction, (2) a phosphate-ribose sodium chelation interaction and (3) hydrogen bonding between a phosphate and a hydrogen bond donor not involving a metal ion. A phosphate-phosphate sodium chelate is proposed instead of a phosphate-ribose sodium chelate based on two observations. First, in the absence of a size-specific coordination site the sodium would have a greater affinity for a charged oxygen than an uncharged one. Second, excess sodium should enhance the ribose chelation. If a sodium were necessary for a ribose-phosphate interaction, addition of sodiums should lead to additional chelation and thus greater stability. This is shown below schematically.



The last step is probably unlikely, since the ribose hydroxyl has a limited affinity for the sodium ion. If a ribose-phosphate interaction occurred, and addition of too much sodium blocked the phosphate site for H-bonding, this could explain the sodium results, but it cannot explain the effects observed upon the addition of  $\text{K}^+$ ,

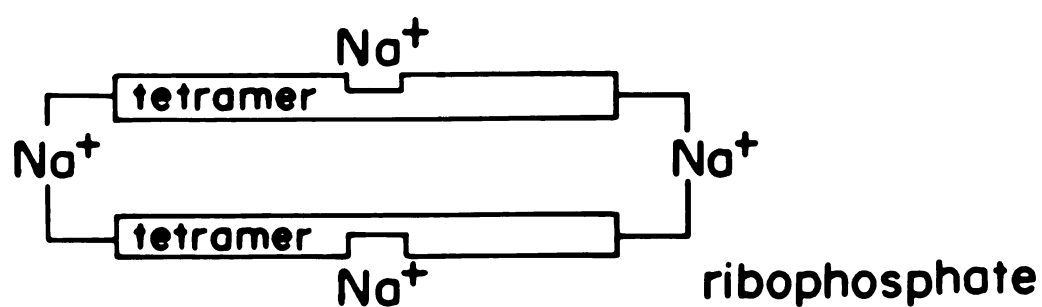


Figure 63. A schematic diagram of the head-to-tail  $\text{Na}^+$  self-structure.  $\text{Na}^+$ 's are located above and below the top and bottom plates, respectively, complexed in the principal structure-directing site to the 0(6) position. Additional  $\text{Na}^+$  binding sites are the phosphates (represented by curved lines) from adjacent tetramers chelating the  $\text{Na}^+$ .

as will be seen later. In a phosphate-phosphate sodium chelation, with a small amount of sodium in the system, the phosphates on adjacent plates are forced to "share" a sodium in common in order to effectively shield the phosphate charge. As more sodium is added and all the phosphates become partially coordinated, maximum stability is achieved. If still more  $\text{Na}^+$  is added, this "sharing" is no longer necessary since there are enough  $\text{Na}^+$  ions to complex each phosphate individually, and this results in a decrease in stability since the plates are no longer tied together by the phosphate shared sodiums, i.e., the equilibrium shifts from chelation to monodentate binding.

In pure  $\text{Na}_2\text{GMP}$ , at  $0^\circ\text{C}$  and a concentration of  $0.41 \text{ M}$ , a fifth structure line has been observed at 7.6 ppm downfield from TSP.<sup>132</sup> This is the same chemical shift as the fifth line observed in the  $\text{Li}_2\text{GMP}$  system, or the only structure line observed when precipitation occurs in the  $\text{Na}^+ - \text{Li}_2\text{GMP}$  system. It is proposed that these lines arise from the same basic structure in both cases, a tetramer with sodiums directing from the center and either sodium or lithium ions blocking phosphate chelation sites as shown in Figure 64. Indirect support for the existence of a tetramer is given by  $T_1$  studies. The  $T_1$  of the 5<sup>th</sup> line is shorter than the other structured H(8) resonances in the pure  $\text{Na}_2\text{GMP}$ , which suggests it is a smaller species than those giving rise to the other H(8) resonances.<sup>132</sup>

Unlike the sodium self structure, where the same complexes are present at both high and low  $\text{GMP}^{2-}/\text{Na}^+$  ratio, potassium exhibits different types of self structures depending on the metal ion to

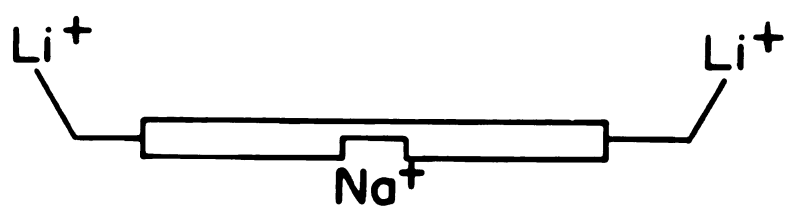


Figure 64. A schematic diagram of the sodium tetramer with the phosphate positions blocked by  $\text{Li}^+$ .

nucleotide ratio. At high  $\text{GMP}^{2-}/\text{K}^+$  ratios, self-association leads to the appearance of three lines upfield from the monomer line. The complex(es) giving rise to these lines are referred to as the "simple" structure(s). As the  $\text{GMP}^{2-}/\text{K}^+$  ratio is lowered, the highest field line melts out and several broad lines grow in from about 7.9 to 7.4 ppm. The complexes represented by these lines are referred to as the "complex" structure.

Phosphate participation in structure formation is readily apparent in the potassium case. At high  $\text{GMP}^{2-}$  to  $\text{K}^+$  ratios, the ratio of the concentration of metal ion in solution relative to the concentration of self-structure is constant at 1:4. This ratio was established by integrating the spectra from the experiment shown in Figure 22, determining the concentration of self-structured species, and then taking the ratio of self-assembled  $\text{GMP}^{2-}$  to  $\text{K}^+$  in solution. This suggests a higher coordination number for the  $\text{K}^+$  ion than the  $\text{Na}^+$  ion, as well as a lower extent of phosphate-metal ion binding in the "simple" potassium structure than the sodium self-structures. This is expected since  $\text{K}^+$  has a phosphate association constant of 1.7 with  $\text{AMP}^{2-}$ , a value which is 0.65 times smaller than that for sodium.<sup>107b</sup> The binding of  $\text{K}^+$  to phosphate oxygens is also consistent with the finding that addition of  $\text{LiCl}$  to the "simple"  $\text{K}^+$  structure causes a new H(8) line to grow in at the expense of the highest field H(8) line (cf., Figure 32); and these two lines are within 0.23 ppm of each other. There is, however, no dramatic change in the spectrum. Thus, the "simple"  $\text{K}^+$  structure has minimal phosphate participation.

As more  $K^+$  is added to the "simple" system, the  $K^+$  complexes change their structures, as indicated by the appearance of new H(8) lines (cf., Figure 24). This change is attributable to  $K^+$ -phosphate interactions, since heating the "complex" structure does not cause it to revert to the "simple" structure; only lowering the  $K^+$  to  $GMP^{2-}$  ratio can accomplish this. Addition of  $K^+$  to a  $Li^+$ - $GMP^{2-}$  system results in structure formation occurring at much lower  $GMP^{2-}/K^+$  ratio than in a  $TMA^+$ - $GMP^{2-}$  system (cf., Figures 31 and 22). The lines appear very broad. The increased phosphate coordination by the lithium ion appears to result in a different mechanism of self-association, eliminating a pathway for "simple" structure formation. Whether or not a "complex"  $K^+$  structure is formed in the mixed  $Li^+$ - $K^+$  system is not clear due to the extensive peak overlap resulting in broad lines.

Based on model building studies and consideration of metal ion radii,<sup>6</sup> the  $K^+$  has been proposed to fill the hole in the center of the octamer. Thus, the "simple" structure is proposed to be an octamer unit as shown in Figure 65. The "complex" structure is proposed to be stacked octamer units with chelating  $K^+$  ions as shown in Figure 66. The presence of  $Li^+$  may result in more effective shielding of charge and thus allow further stacking, resulting in even broader lines. This type of extensive stacking is not possible in the  $Na^+$  case since the central  $Na^+$  is probably positioned just outside the plane of the tetramer with a water molecule in its fifth coordination site. Thus, stacking of octamers would result in unfavorable  $Na^+$  contacts. Furthermore, in the sodium system, if the phosphate sites are blocked

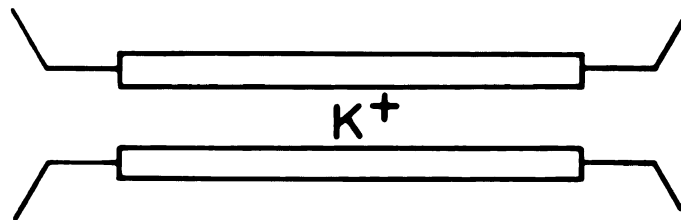


Figure 65. A schematic diagram of the proposed "simple"  $K^+$  self-structure.



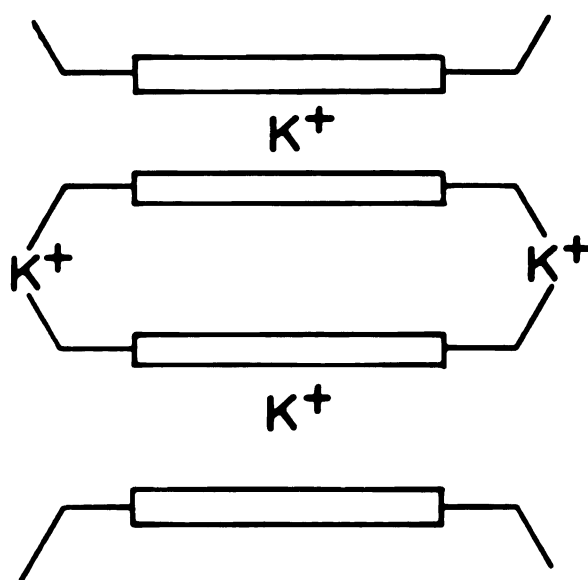


Figure 66. A schematic diagram of the proposed "complex"  $K^+$  self-structure.

to interplatelet phosphate interactions, no hydrogen bonding or metal ion coordination would be available to hold the plates together. Thus, only stacking interaction would remain. Thus, the model would predict that an ion that binds strongly to phosphate could dramatically disrupt  $\text{Na}^+$  directed self structures; this is in fact observed when  $\text{Li}^+$  is added to the  $\text{Na}^+$  self-structure.

In the  $\text{K}^+$  case, metal ion coordination holds the plates together regardless of phosphate interaction; thus,  $\text{Li}^+$  would be predicted to have minimal effects on the complexed units. Lithium would be expected to influence the extent of stacking, however, based on a balance between the blocking of chelation sites and the increased shielding of phosphate charge as shown in Figure 67. Since the  $\text{K}^+$  is proposed to be in the center of the octamer, extensive stacking should be able to occur without unfavorable metal ion contacts. The limiting factor in the extent of stacking would be the unfavorable build up of too much negative phosphate charge in the aggregated units. Thus,  $\text{Li}^+$  would be expected to effectively shield the phosphates and allow more extensive stacking, resulting in a broader H(8) resonance than in the absence of  $\text{Li}^+$ . This is in fact observed (cf., Figure 31). The extent of nucleotide stacking may explain why  $\text{K}_2\text{GMP}$  gels far more readily than  $\text{Na}_2\text{GMP}$ , and why addition of  $\text{Li}^+$  appears to promote gel formation in  $\text{K}_2\text{GMP}$ .

Addition of  $\text{K}^+$ , as either the chloride or nitrate salt, to the "complex"  $\text{K}^+$ - structure results in a decrease in line widths as well as a dramatic shift in the equilibrium concentrations of the structured species present (cf., Figure 27). Decreases in line width seem to

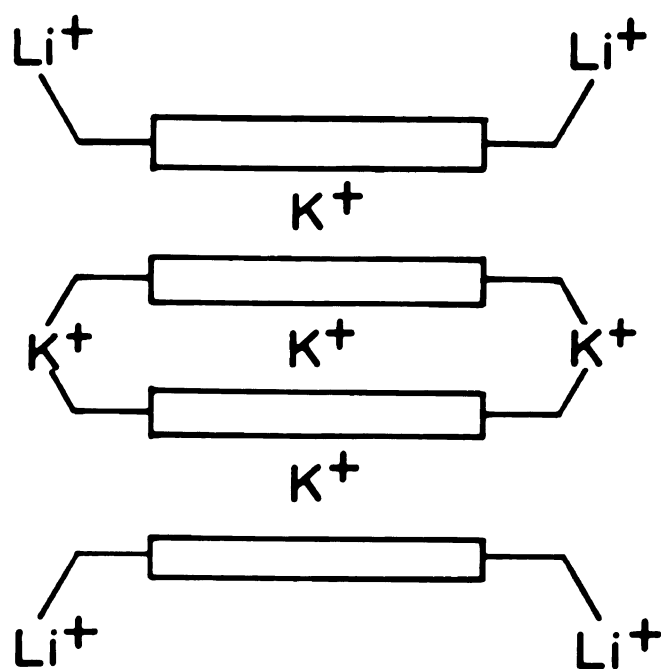


Figure 67. Proposed structure (schematic) of the "complex"  $K^+$  structure in the presence of  $Li^+$ . The increased phosphate shielding by  $Li^+$  allows more plates to be stacked together without excessive build up of negative charge.

suggest a decrease in viscosity, which can be related to a decrease in complex size, as shown diagrammatically in Figure 68. This idea is consistent with the model presented, since an increase in  $K^+$  concentration should decrease the fraction of chelated phosphates without acting like  $Li^+$  to markedly decrease the effective phosphate charge. This would thus diminish the extensive stacking that is presumably present in the "complex"  $K^+$  system. This explanation of the effects of excess  $K^+$  on the "complex"  $K^+$  structure contains both long and short patterns of stacked tetramers. The short stacks are slow to form by cleaving long stacks at low temperatures, and the long stacks appear to be thermodynamically favored on heating as shown in Figure 26.

The question arises as to whether the observations are the effect of metal ion chelation involving the phosphate, or hydrogen bonding between the plates involving the phosphate which can be blocked by metal ion interaction. These two cases are not easily distinguished. The question also arises as to whether  $K^+$  can fill the center of the sodium octamer and thus stabilize the sodium structure, or whether sodium can block or inhibit stacking in a potassium structure. These questions will be addressed here. Potassium does not fill the structure-directing position at the center of the octamer in a sodium self-structure. Figure 18 shows that the addition of KCl to a  $Na_2GMP$  system results in a "potassium-type" structure growing in at the expense of the sodium structure. Thus, a completely new set of structures replace the less stable  $Na^+$  structures. This result is not surprising, since in the pure salt systems,  $K^+$  is clearly a better structure director than  $Na^+$ . For a given nucleotide concentration, the  $K^+$  structures have higher melting

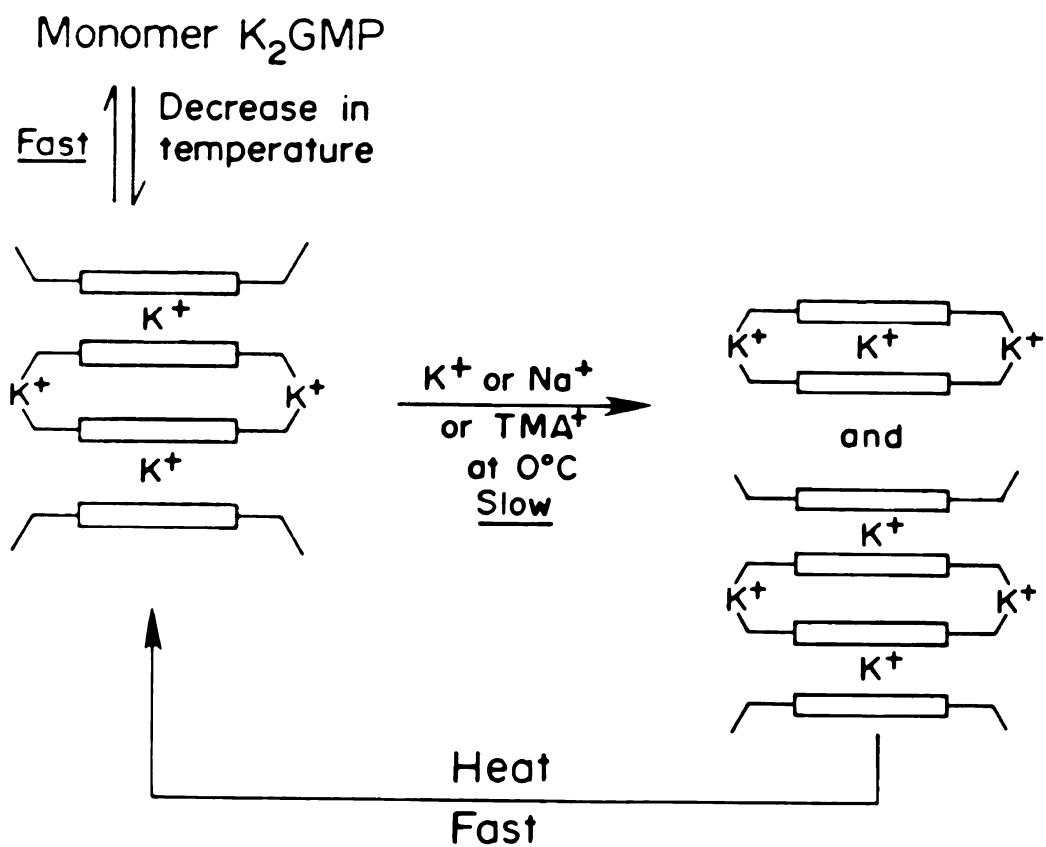


Figure 68. A representation (schematic) of the ionic strength effects observed for the "complex"  $K^+$  self-structure.

temperatures for a given concentration, as well as having a greater percent structure for any given temperature and concentration. Thus,  $K^+$  does not coordinate at the center of the octamer or displace the  $Na^+$  from its central structure directing position.

The addition of KCl to a  $2GMP^{2-}/Na^+$  system, however, clearly stabilizes the  $Na^+$  self-structure (cf., Figure 19). Thus, the addition of  $K^+$  causes an increase in sodium structure and a decrease in monomer intensity. Melting profiles for two solutions of equal  $GMP^{2-}$  concentration and equal metal ion to  $GMP^{2-}$  ratio, one containing exclusively  $Na^+$  and the other containing a mixture of  $Na^+-K^+$ , clearly shows that the solution containing  $K^+$  exhibits a higher  $T_m$  (Figure 20). The  $K^+$  is stabilizing the sodium structure, and this stabilization can not be the result of the  $K^+$  inserting into the center of the octamer, since if this were possible, stabilization of the pure  $Na_2GMP$  system by  $K^+$  would have been observed. Thus,  $K^+$  must be stabilizing the system through phosphate chelation. This is shown schematically in Figure 69. Furthermore, hydrogen bonding schemes between the plates can not be used to explain this phenomenon. The  $K^+$  is actively participating in the sodium structure stabilization.

In the pure  $Na_2GMP$  system, under structure-forming conditions, only one out of eight  $Na^+$  ions is needed for occupying the central cavity of a tetramer unit. The seven "excess"  $Na^+$  ions per tetramer unit are in ion pair equilibrium with the phosphate oxygens. Chelation of  $K^+$  by phosphate is favored over  $Na^+$  when both ions are present at  $GMP^{2-}/metal$  ion ratios greater than or equal to one (cf., Figures 19 and 30). Once

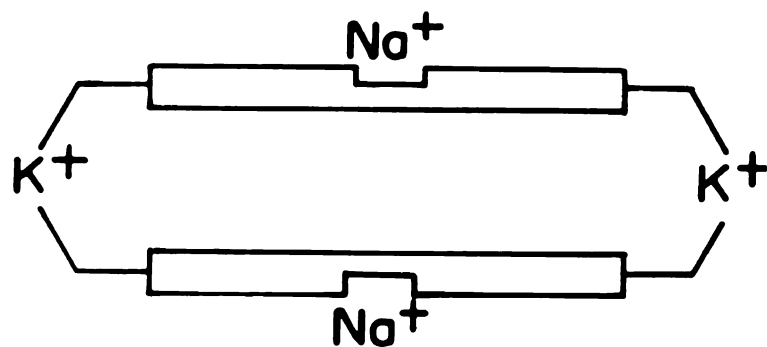


Figure 69. Proposed structure (schematic) of a  $Na^+$  self-structure in the presence of  $K^+$ . The  $Na^+$  occupies the principal structure-directing site at the center of the tetramer and the  $K^+$  occupies the phosphate sites, stabilizing the self-structure.

enough cations are present in solution, chelation sites are saturated by  $\text{Na}^+$  and  $\text{K}^+$  starts to direct a self-association on its own.

Unlike the  $\text{Na}_2\text{GMP}$  system where addition of  $\text{KCl}$ ,  $\text{TMAcI}$  and  $\text{NaCl}$ , produce different results, comparable effects are observed on addition of  $\text{TMAcI}$ ,  $\text{NaCl}$ ,  $\text{KNO}_3$  and  $\text{KCl}$  to a  $\text{K}_2\text{GMP}$  system (cf., Figure 27). The observed effect is thus attributable to nonspecific cation binding to the structural nucleotide. The metal ion complexation is proposed to involve a phosphate interaction. The effect of adding any of the aforementioned salts to a solution containing "complex"  $\text{K}^+$  structures is a time dependent shift in the  $\text{K}^+$  self-structure equilibrium as shown in Figure 27. This excess salt- $\text{K}_2\text{GMP}$  system is the only self-associating system investigated in this study which exhibits a slow ordering. The presence of excess salt induces a slow shift in the species present at equilibrium. At higher ionic strength, the favored species appears to be smaller based on line widths of the structured solution. The slow forming species favored at high ionic strength appears to form from the species favored at lower ionic strength.

In summary, the addition of  $\text{Na}^+$ ,  $\text{K}^+$  and  $\text{TMA}^+$  to  $\text{K}_2\text{GMP}$  causes a shift in the concentration of ordered species present in the "complex" solution structure, a non specific ion effect. The addition of  $\text{Na}^+$  to a "simple" potassium structure results in formation of a sodium-type structure. The addition of  $\text{KCl}$  to  $\text{Na}_2\text{GMP}$  results in a potassium self-structure growing in, and the addition of  $\text{KCl}$  to a  $2\text{GMP}^{2-}/\text{Na}^+$  solution results in a stabilization of the sodium self-structure. Thus, sodium is the better structure director in the presence of  $\text{K}^+$  and potassium is the better at binding at chelating sites. The relative energies of



the different structures are shown in Figure 70. It appears that the structure, however, is also determined by the ability of the metal ion to tie the plates together by binding the phosphate oxygens at the "outer sites."

#### D. Features of the Outer Lines in a Sodium 5'-GMP Self Structure.

From Figure 19 which illustrates the effect of  $K^+$  on the  $Na^+$  self-structure, it is clear that the highest field sodium structure line is being replaced by a new field line just downfield with almost the same chemical shift. This change is not observed for the lowest field line even though the outer lines are proposed to arise from the same structure. The fact that changes can occur in one H(8) environment while leaving the other H(8) environment arising from the same structure unchanged is postulated to result from favored binding of  $K^+$  to one tetrameric plate of the octamer unit over the other. For example, if the outer lines arise from a head-to-tail type of tetramer association, then the two plates of the octamer are inequivalent. Then, the association of the  $K^+$  by the phosphates may result in the  $K^+$  being in closer proximity to the H(8) regions of one tetramer than the other. The presence of  $K^+$  instead of  $Na^+$  would then induce a slight change in the effective shielding of the H(8) region and a change in chemical shift of the H(8) resonance arising from that tetramer would be expected; the H(8) resonance of the other tetramer in the octamer unit would be unaffected. Thus, the tetramers can behave differently from one another to selectively favor binding.

In the experiment involving irradiation of the HDO peak in a 5'- $Na_2GMP$  system shown in Figure 63, the outer H(8) lines are not affected

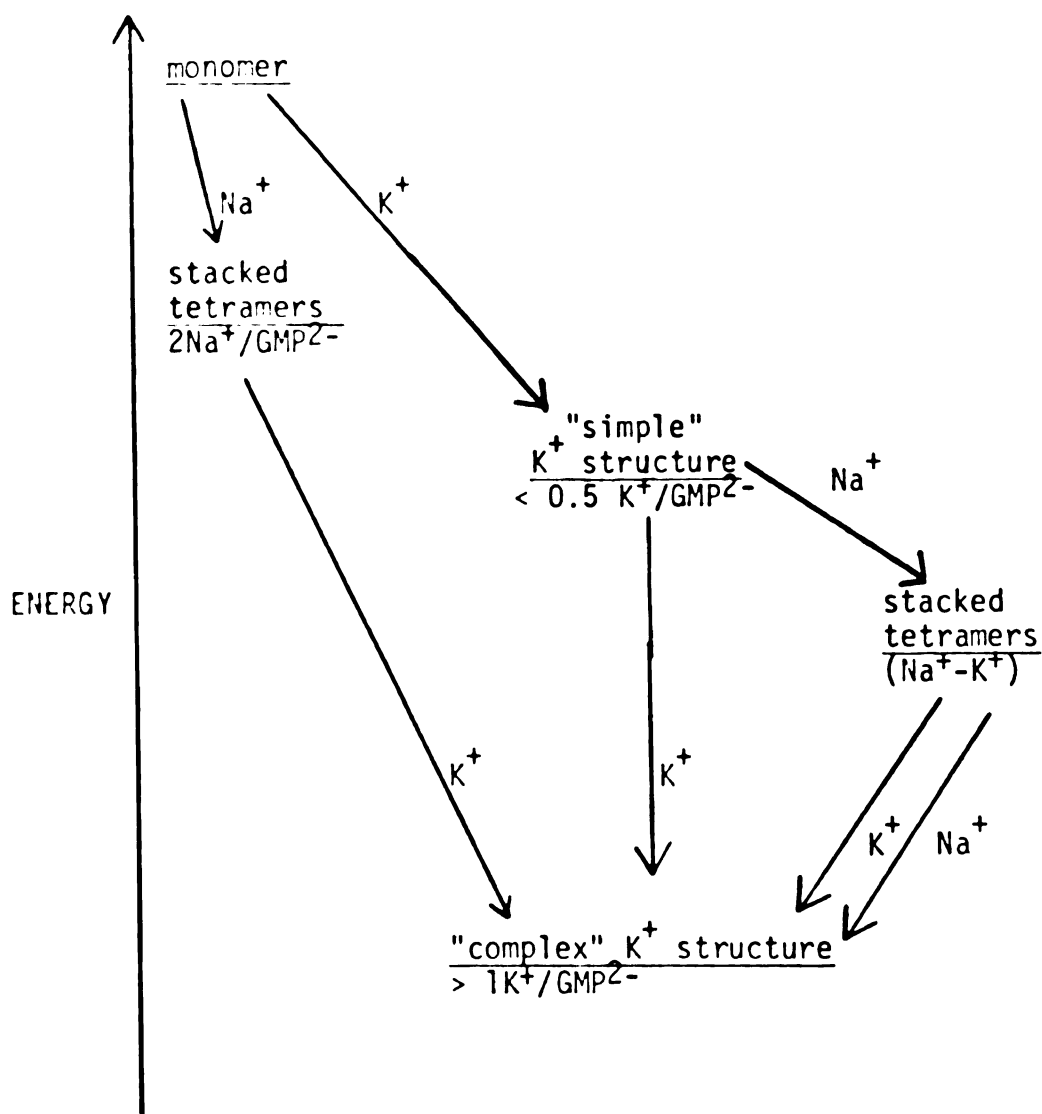
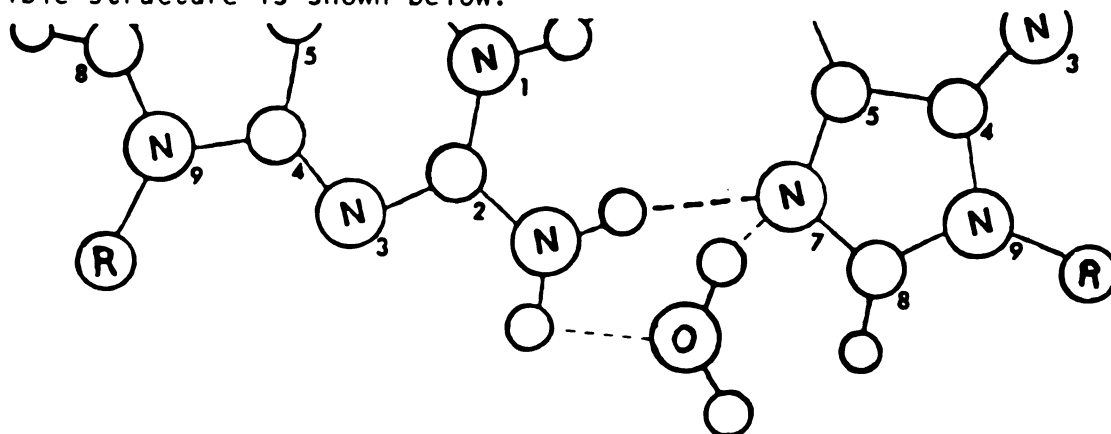


Figure 70. A schematic diagram of the relative stabilities of the  $\text{Na}^+$  and  $\text{K}^+$  pure and mixed  $\text{GMP}^{2-}$  systems.

equally. The low field line shows a larger effect. This observation together with the observation that irradiation of the  $\text{H}_2\text{O}$  peak in a water  $\text{Na}_2$ -5'-GMP system results in a marked decrease in the 7.69 ppm resonance (cf., Figure 45), has led to the postulation of a  $\text{NH}_2$ - $\text{H}_2\text{O}$  association which puts an  $\text{H}_2\text{O}$  molecule in close proximity to H(8). A possible structure is shown below.



The water is in rapid exchange with the bulk water and therefore is saturated by the decoupling experiment. The H(8) of the adjacent resonance is in close proximity and the saturation is transferred to this proton. This type of water association is favored by the opposite tetramer from the one that is affected by  $\text{K}^+$  complexation. This is consistent since steric interactions may interfere with a water molecule associating with the  $\text{NH}_2$  of a guanine unit that is in close proximity to phosphates. The water molecule could be further hydrogen bonded to the ribose or phosphate of an adjacent nucleotide unit, possibly from a different tetramer unit.

Thus, even though the outer lines exhibit different behavior from one another in these two situations, it is still believed that they result from the same structure. This is based on their similar behavior in the presence of  $\text{Mn}^{2+}$ ,<sup>105</sup> the similar  $T_1$  and  $T_2$  values,<sup>105</sup> their

coincidental appearance on addition of NaCl to  $\text{TMA}_2\text{GMP}$ , and the similar behavior on irradiation of one of the outer peaks, followed by the subsequent drop in intensity of the outer peak.

E. Comparison to Polynucleotide and Nucleoside Systems. The finding that  $\text{Na}^+$  is the better director for  $\text{GMP}^{2-}$  than  $\text{K}^+$  is not inconsistent with previously reported results on the effects of alkali metal ions on ordering of nucleosides or polynucleotide systems. The nucleosides<sup>100-103</sup> have no phosphates and therefore, have no considerations as to charge build up and shielding. Similarly in the polynucleotide<sup>120-121</sup> systems, there are no "inner" sodium type of directing positions since all the nucleotides are linked together through phosphodiester bonds. Thus there are only "octamer" type sites which favor  $\text{K}^+$  over  $\text{Na}^+$  binding, except at the ends of the chains. Thus, the fact that  $\text{K}^+$  in either of these systems, nucleosides or polynucleotides, shows a higher  $T_m$  than  $\text{Na}^+$  is not surprising.

### III. Cesium "Structure Director" Systems

$\text{Cs}^+$  is capable of ordering only about 5% of the nucleotides in  $\text{Cs}_2\text{GMP}$ . However, a large number of structures grow in and melt out on increasing  $\text{NaCl}$  concentration (cf., Figure 38). The  $\text{Cs}^+$  ion is too large to fit in the hole of a tetramer, or the center of an octamer without loss of stacking interactions. It seems likely, however, that  $\text{Cs}^+$  could associate with phosphate oxygens on the outside of a tetramer. In a pure  $\text{Cs}_2\text{GMP}$  system, even if tetramer formation were possible, association into vertical stacks would be limited since the  $\text{Cs}^+$  would not be likely to chelate. Thus, rapid exchange would be likely to occur between associated  $\text{GMP}^{2-}$  and monomer. The addition of  $\text{Na}^+$ , however, could help stabilize the  $\text{Cs}^+$  system by chelation or by added tetramer formation. The structures formed on addition of  $\text{Na}^+$  are not  $\text{Na}_2\text{GMP}$  type structures, thus the  $\text{Na}^+$  is merely enhancing the action of the  $\text{Cs}^+$ . The outer structure lines which are present at high  $\text{Na}^+$  concentrations have chemical shifts which correspond to " $\text{Na}^+$  structure" lines. These lines, however, do not grow in together. Since in the sodium system these lines are proposed to arise from the same structure, there must be a coincidence of chemical shifts for the 7.23 ppm peak. Thus, the proposed structures are shown in Figure 71.

A similar mechanism of action appears to be operative for  $\text{Rb}^+$  and  $\text{K}^+$ .  $\text{Rb}^+$  appears to be less effective in aiding  $\text{Cs}^+$  structure formation than  $\text{K}^+$ , although both of these structure directors influence the  $\text{Cs}^+$  system towards formation of species that give broad lines.

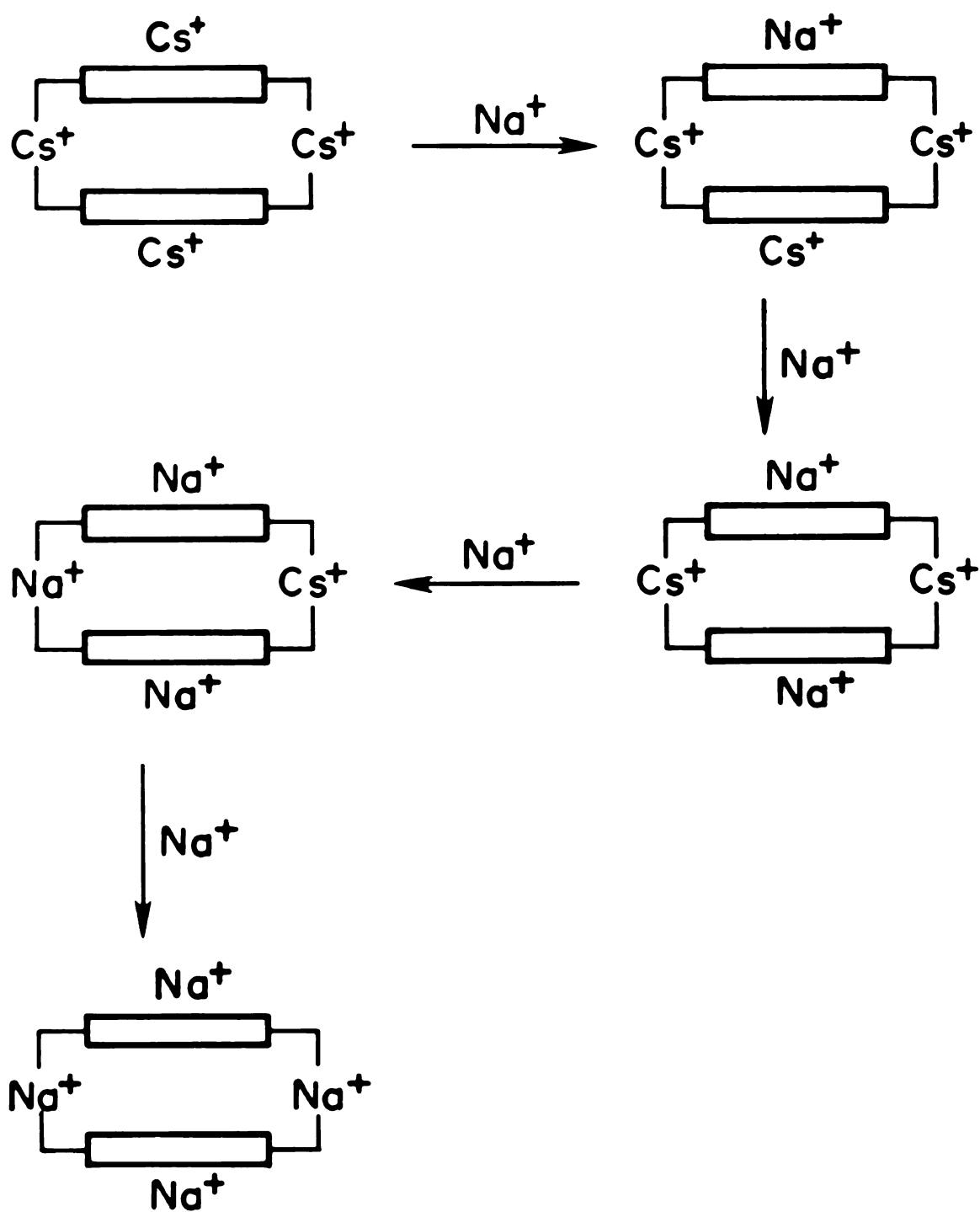
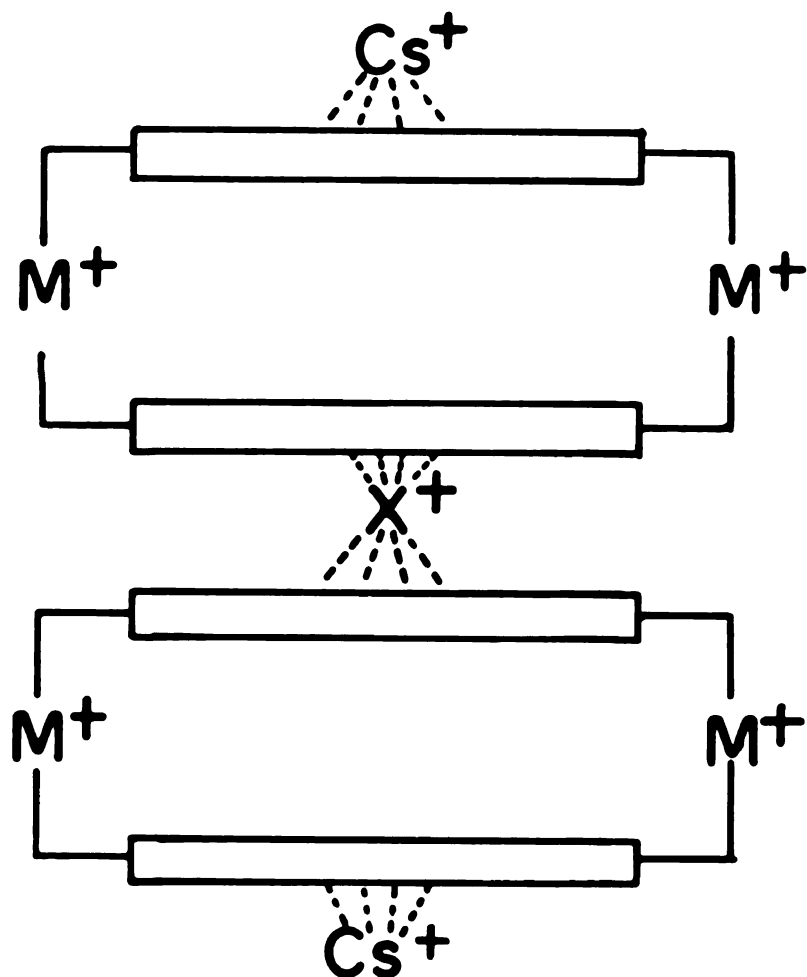


Figure 71. Proposed structure (schematic) of the  $\text{Cs}^+$  self-structure in the presence of  $\text{Na}^+$ .

This is in contrast to the  $\text{Na}^+$  case, where the lines remain narrow. Since the  $\text{K}^+$  or  $\text{Rb}^+$  ions are proposed to direct structure from the center of the octamer, whereas sodium is proposed to direct from the center of a tetramer, it follows that  $\text{K}^+$  and  $\text{Rb}^+$  would not do as well as  $\text{Na}^+$  when forced to direct self-assembly from a tetramer site. The broad lines suggest a further association of the octamer units, as shown in Figure 72, is probably taking place in the  $\text{K}^+$  and  $\text{Rb}^+$  systems. This would be favored since the  $\text{K}^+$  or  $\text{Rb}^+$  could occupy an octacoordinate site, but it would not be favored for  $\text{Na}^+$ .



$\text{M}^+ = \text{K}^+ \text{ or } \text{Rb}^+ \text{ or } \text{Cs}^+$

$\text{X}^+ = \text{K}^+ \text{ or } \text{Rb}^+$

Figure 72. A possible mixed  $\text{Cs}^+ - \text{K}^+$  or  $\text{Cs}^+ - \text{Rb}^+$  self-structure (schematic). The  $\text{Cs}^+$  associates with the outer tetramer plates, while the  $\text{K}^+$  or  $\text{Rb}^+$  occupy the sites between the tetramers as well as the phosphates sites.



#### IV. The $\text{Sr}^{2+}$ and $\text{Ba}^{2+}$ Systems

Due to the limited solubility, a ratio of one metal ion per nucleotide unit was unattainable. Thus, only small amounts of structured nucleotides were observed. Both of these systems exhibit the unusual property of reversibly forming gels on heating. This has led to the postulation of the possibility of helix formation in these systems. If a tight helical system were formed on addition of  $\text{M}^{2+}$ , heating could lead to an unwinding of the helix and formation of a gel in a manner similar to that of protein denaturation.

## V. Derivatives

The derivative survey gave some insight into the important features of the nucleotide which must be present for self-assembly to occur. In gel studies it has been noted that an N,N-dimethylamino group in the 2-position inhibits gel formation.<sup>100</sup> It is clear that in gel systems both hydrogen bonds are necessary for self-assembly. This also appears to be the case in solution. The lack of self-assembly in  $\text{IMP}^{2-}$  systems has shown that the amino group in the 2 position of  $\text{GMP}^{2-}$  is necessary for self-structure formation. Clearly, one hydrogen bond is not sufficient. Furthermore, an attempt to incorporate  $\text{IMP}^{2-}$  into a  $\text{GMP}^{2-}$  structure, using the  $\text{K}^+$  salts in both systems proved unsuccessful. This indicates that guanine nucleotide systems with only single hydrogen bond forming capabilities cannot replace even single  $\text{GMP}^{2-}$  units in a structured system. Thus, the two hydrogen bonding donor-acceptor positions are necessary to form self-assembled units, or to incorporate into an ordered complex.

The ribophosphate is also important to solution structure. If solution ordering were solely dependent on the ability of the guanine base to hydrogen bond, then all guanine nucleotides should form the same self structure, depending only on the metal ion present in the system. Clearly, this is not the case (cf., Figures 56, 47, and 22). For example, the simple modification of removing the 2'-hydroxyl, and replacing it with a hydrogen to form 2'-deoxyguanosine-5'monophosphate drastically changes the extent of solution ordering as well as the types of structures formed. This suggests that either the ribose conformation or the 2'-hydroxyl functionality is crucial to

structure formation. Moving the phosphate to the 2' position also results in changes in the type of structures formed and the extent of structure. In the 2', 3'-cGMP system, the sodium salt as well as combinations of  $K^+$  and  $Li^+$  salts formed gels, where the ordering was too cooperative and the structures too extensive to be NMR detectable. 3', 5'-cGMP also formed gels in pure  $K^+$  systems, or mixed  $K^+/Na^+$  and  $K^+/TMA^+$  systems, showing no NMR evidence for structure on the melting of the gel.

Attempts to incorporate the Na salt of 3', 5'-cGMP into a structured 5'-Na<sub>2</sub>GMP system resulted in the cGMP monomer associating with the 5'-GMP but cGMP did not incorporate into a GMP structured unit. Incorporation of cGMP would be expected to result in additional H(8) resonances for the 5'-GMP system due to the reduced symmetry of the system. This was not observed. Instead, only a downfield shift of the cGMP H(8) resonance on increasing cGMP concentration was observed (cf., Figure 52). Although the  $Na^+$  salt of cGMP was able to form an ordered solution as detected by the appearance of new lines in the H(8) and ribose regions of the NMR spectrum (cf., Figures 50 and 51), it was unable to incorporate into the 5'-Na<sub>2</sub>GMP self-assembled unit. Thus, some sort of interaction, probably involving the phosphate, must be able to occur in order for 5'-GMP units to self-assemble.

It is interesting to note that all guanosine monophosphates are capable of self-association. It also appears that all the systems show a metal ion dependence. Thus, the ability to form self-structures appears to be dependent on the guanine part of the unit, whereas the

type of structure formed appears to be dependent on the metal ion radius and the ribophosphate unit of the nucleotide.

## CONCLUSIONS

All studies of the alkali metal ion dependent self assembly of 5'-guanosine monophosphate in neutral aqueous solution prior to this study have been performed on pure salt systems where the nucleotide to metal ion ratio is 1:2. Under these conditions the metal ion is in excess. The prime objective of this research was to evaluate by proton NMR spectroscopy the self-assembly phenomenon with a metal ion to nucleotide ratio between 0 and 2. This required the presence of a cation which is not a structure director by itself, and does not inhibit the activity of cations capable of directing self-assembly. Tetramethylammonium was found to be such an ion. Although  $\text{TMA}^+$  ion pairs with the structured  $\text{GMP}^{2-}$  units, as indicated by double irradiation experiments as well as by increased nucleotide solubility in its presence,  $\text{TMA}^+$  had no effect on the percent structure in the ordered  $\text{Na}^+$ - $\text{GMP}^{2-}$  system.

Studies of  $\text{Na}^+$  as the structure directing ion in the  $\text{TMA}_2\text{GMP}$  system have shown only one set of sodium self-structures to be generated, regardless of the metal ion to nucleotide ratio. In contrast, the addition of  $\text{K}^+$  or  $\text{Rb}^+$  to  $\text{TMA}_2\text{GMP}$  produces two sets of distinctly different NMR detectable self-structures, depending on the metal ion to  $\text{GMP}^{2-}$  ratio. At high  $\text{GMP}^{2-}/\text{M}^+$  ratio, a "simple" structure is formed. At low  $\text{GMP}^{2-}/\text{M}^+$  ratio, the self-structure formed is that found for the homoionic  $\text{K}_2\text{GMP}$  system, and has been termed a "complex" structure. Thus the sodium self-structures are the simplest of the metal ion self-assembled  $\text{GMP}^{2-}$  complexes.

Primary structure-directing site studies reported are not inconsistent with structure arising from stacking of tetramer units with  $M^+$  and the center of tetramers ( $Na^+$ ) or at the center of two stacked tetramer plates ( $K^+$ ,  $Rb^+$ ). However, evidence was found for multiple equilibria resulting from the existence of more than one type of metal ion binding site per structured nucleotide unit. The fraction of structure present in solution as a function of  $GMP^{2-}$  to  $Na^+$  ration shows a maximum at about one  $GMP^{2-}/Na^+$ . Furthermore, the addition of  $Na^+$  to  $Na_2GMP$  results in a decrease in the extent of self-assembly in solution, suggesting the blocking of sites that are necessary for self-assembly. These sites are concluded to be phosphates on adjacent stacked tetramers which chelate the metal ion. The addition of  $K^+$ , to  $Na^+$  or  $TMA^+$  to  $K_2GMP$  results in a shift in the equilibrium concentrations of the self-assembled structures present in solution to favor those structures present normally only at very high  $K_2GMP$  concentrations. This is a nonspecific ion effect which is time dependent and has been attributed to a phosphate interaction.

Although potassium is the better stabilizing ion, sodium was found to be the better structure director. This conclusion is based on the observation that the addition of  $K^+$  to a high ration of  $GMP^{2-}/Na^+$  results in stabilization of the  $Na^+$  self-structure and that the addition of  $Na^+$  to a high ration of  $GMP^{2-}/K^+$  results in the "simple"  $K^+$  self-structure being replaced by a  $Na^+$ -type structure growing in, suggesting that once the phosphates are blocked by excess  $Na^+$ , the  $K^+$  is forced to compete for the structure directing position. It is clear that  $K^+$  can not stabilize the  $Na^+$  structure by complexing to the

eight O(6) positions formed on stacking of the tetrameric plates. Instead,  $K^+$  forms its own unique structure when it binds to these eight O(6) positions. It is also evident that interplate hydrogen bonding cannot account for the stabilization of the  $Na^+$  self-structure by  $K^+$ , because the  $K^+$  would either be expected to block the phosphate sites and reduce the stability, or have no effect on the stability at all since metal ions are not involved in hydrogen bonding. Thus in no case would a stabilization be observed.

$Li^+$  is not a structure inert cation. Although it does not direct self-association of  $GMP^{2-}$ ,  $Li^+$  in solution can induce changes in the  $Na^+$  and  $K^+$  (but not  $Cs^+$ ) self-structured forms of the nucleotide. This is consistent with the phosphate being involved in structure formation, since  $Li^+$  is expected to closely associate with the phosphate.

$Cs^+$ , on the other hand, can induce about 5% NMR detectable self-structure. Addition of small amounts of a strong structure directing ion such as  $Na^+$ ,  $K^+$  or  $Rb^+$  to  $Cs_2GMP$  dramatically increases the degree of self-structure formation. The self-assembled units are no longer those characteristic of the strong structure director, in the presence of  $Cs^+$ , but are unique. Thus,  $Cs^+$  is an active self-assembly director when in conjunction with a strong self-assembling ion.

The use of the  $TMA^+$  ion facilitated an investigation of the alkaline earth cations.  $Sr^{2+}$  and  $Ba^{2+}$  were found to be capable of directing self-assembly. This is consistent with considerations of

ionic radii applied to the alkali metal ions for the size selective mechanism.

A survey of the structure-forming properties of five other GMP derivatives (2'-GMP, 3'-GMP, 2', 3'-cGMP, 3', 5'-cGMP and 5'-dGMP) has shown that structure formation can occur in all cases in the presence of an appropriate structure directing alkali or alkaline earth metal ion. From studies with IMP it was concluded that both hydrogen bond donor positions as well as both hydrogen bond acceptor positions are necessary for self-structure formation. The inability of 3', 5'-cGMP to incorporate into self-assembled  $\text{Na}_2\text{GMP}$  further indicated the importance of the ribophosphate in sodium directed self-assembly. The differences in the H(8) line patterns formed by the different nucleotides gives further credence to the importance of the ribophosphate group.



## RECOMMENDATIONS

A. General Directions. This research has attempted to qualitatively investigate the relationships between  $\text{GMP}^{2-}$  and mixed metal ion systems, as well as to survey the relative importance of the different nucleotide components. Further research should be directed towards a more quantitative investigation in both these areas. An attempt should be made to determine the number of metal ions necessary to induce self-assembly in each nucleotide system. This would allow determination of equilibrium constants and other thermodynamic data. A detailed investigation of the nonbase sites potentially involved in self-assembly might help to understand the mechanism of guanine nucleotide self-association. Attempts at incorporating dissimilar nucleotides into one self-structure should also help in understanding which features of the nucleotide are necessary for compatible solution ordering. Interactions of structured units with other nucleotides or related molecules may give insight into the relative stability of the self-assembled unit or may possibly be a method of investigating ring current effects.

B. Suggested Experiments. Modifications of the sugar may be helpful in understanding its role in self-assembly. Such changes could involve methylation or acetylation of the ribose, or even changes in sugar ring size.

Since the  $\text{NH}_4^+$  ion has approximately the same ionic radius as  $\text{K}^+$ , IR,  $^1\text{H}$  NMR and  $^{13}\text{C}$  NMR investigations of  $(\text{NH}_4)_2\text{GMP}$  and  $(\text{TMA})_2\text{GMP}$  as a function of  $\text{NH}_4^+$  concentration would be of interest.

Furthermore, the effects of  $\text{Na}^+$ ,  $\text{K}^+$  and  $\text{Rb}^+$  at different  $\text{GMP}^{2-}/\text{NH}_4^+$  ratios could prove to be interesting if  $\text{NH}_4^+$  acts in a manner similar to  $\text{K}^+$  as expected.

A fiber diffraction study of the  $\text{K}_2\text{GMP}$  salt would be quite informative. Low concentrations of  $\text{K}_2\text{GMP}$  gel quite readily; the addition of  $\text{LiCl}$  to higher  $\text{GMP}^{2-}$  concentrations quite often induces gelation with time. A fiber diffraction study could help distinguish between a continuous helix vs. a helix of stacked tetramers, or a different structure altogether. Fibers can be readily drawn with the use of a wooden clothes pin.

Addition of  $\text{KCl}$  to  $\text{TMA}_2\text{GMP}$  should be monitored by IR to see if the "simple" structure produces the same shifts in the  $\text{C=O}$  and ring stretch regions as the homoionic  $\text{K}^+$  system. Although  $\text{K}_2\text{GMP}$  has been investigated by IR, none of the other  $\text{K}^+$ -systems have been studied. Similar studies should be undertaken on higher ratios of  $\text{GMP}^{2-}/\text{Rb}^+$  and  $\text{GMP}^{2-}/\text{Na}^+$ . Similarly, proton  $T_1$  measurements should be performed on the "simple" and "complex" structures as well as the structures formed on addition of  $\text{KCl}$  to  $\text{K}_2\text{GMP}$  to determine their relative sizes.

The addition of  $\text{NaCl}$  to a "simple"  $\text{Rb}^+$  self-structure would be of interest to investigate by  $^1\text{H}$  NMR to see if  $\text{Rb}^+$  behaves in a manner similar to that of  $\text{K}^+$ .

Double irradiation experiments of the outer lines in the sodium self-structure in the presence of  $\text{K}^+$  and  $\text{Cs}^+$  would be of interest, to investigate their behavior in the presence of these ions. In other words, these experiments might determine whether or not there is a coincidence of lines arising from different structured units.

The addition of  $\text{Tl}^+$  to  $\text{K}_2\text{GMP}$  and  $\text{TMA}_2\text{GMP}$  is definitely worthy of investigation. Appendix B shows a spectrum of 10%  $\text{TlCl}$  in  $\text{Na}_2\text{GMP}$  under self-assembling conditions. The  $\text{Tl}^+$  disrupts the  $\text{Na}^+$  self-structure. Further investigation of this phenomenon appears worthwhile.

Based on size considerations, an investigation of  $\text{Eu}^{2+}$  as a self-structure director, as well as in conjunction with other structure directors, would be of interest.

The use of long chain ammonium ions has some interesting possibilities.<sup>133</sup> If the phosphate is in fact involved in the self-assembly process, a long chain amine might help to tie the plates together and increase stability by reducing the exchange rate, enabling isolation of a structured unit. They may also help to induce crystallization. Preliminary studies with  $(\text{CH}_3)_3\text{N}^+(\text{CH}_2)_2^+\text{N}(\text{CH}_3)_3$  indicate that precipitation occurs in a concentrated  $\text{Na}_2\text{GMP}$  system on addition of this ion. However, crystals were present in the solution after several days. No investigation of the crystals was attempted.

A lot of research remains to be done on the derivatives. Investigation of different salts of neutral 5'-dGMP is of prime interest. Incorporation studies, to determine which nucleotides are compatible with the self-assembled forms of different nucleotides, should give some structural insight. Since most available information is for the 5'-GMP system, these studies should begin with an attempt to incorporate 5'-dGMP as either the  $\text{Na}^+$  or  $\text{K}^+$  salt into 5'-GMP as either the  $\text{Na}^+$  or  $\text{K}^+$  salt, respectively. This is most easily

accomplished by means of  $^1\text{H}$  NMR, deuterium exchanging the H(8) of the 5'-dGMP and looking for changes in the 5'-GMP H(8) region. Then, the experiment should be repeated exchanging the 5'-GMP H(8) and observing the 5'-dGMP H(8) resonances.

A systematic approach to all the derivatives should be taken, investigating all the homoionic salts and then investigating self-structure formation as a function of nucleotide to metal ion ratios using the  $\text{TMA}^+$  salt. These derivatives should also be investigated by IR or Raman. Furthermore, some of the derivatives that do not form gels readily at lower pH should be investigated as a function of pH as well as time, concentration and temperature by  $^1\text{H}$  NMR and  $^{13}\text{C}$  NMR for all the alkali and alkaline earth metal ions as well as  $\text{NH}_4^+$ ,  $\text{Eu}^{2+}$  and  $\text{Tl}^+$ . This is shown schematically in Figure 8 of the introduction.

## List of References

### List of References

1. "Die histochemischen und physiologischen Arbeiten von Fridrich Miescher," 2 vols. F. C. W. Vogel, Leipzig, 1897.
2. G. L. Eichorn, Advances in Chemistry Series, 100, 135 (1971).
3. a) B. Rosenberg, Naturwiss., 60, 399 (1973).  
b) B. Rosenberg, L. Van Camp, J.E. Trosko and V.H. Mansour, Nature, 222, 385 (1969).  
c) J.P. Davidson, P.J. Faber, P.G. Fischer, S. Mansy, H.J. Peresie, B. Rosenberg and L. Van Camp, Cancer Chemother. Repr., Part 1, 59, 287 (1975).  
d) J.A. Howle and G.R. Gale, Biochem. Pharmacol, 19, 2757 (1970).  
e) J.A. Howle, G.R. Gale and A.B. Smith, Biochem. Pharmacol., 21, 1465 (1972).
4. a) G.L. Eichorn, Inorganic Biochemistry, 2, 1210 (1973).  
b) R.M. Izatt, J.J. Christensen, and J.H. Rytting, Chem. Rev., 71, 439 (1971).  
c) A.T.T.U and M.J.Heller, Metal Ions in Biological Systems, 1, 1 (1974).  
d) M. Daune, Metal Ions in Biological Systems, 3, 1 (1974).  
e) L.G. Marzilli, Progress in Inorganic Chemistry, 23, 255 (1977).  
f) D.J. Hodgson, Progress in Inorganic Chemistry, 23, 211 (1977).
5. E.-I.Ochiai. "Bioinorganic Chemistry An Introduction," pg. 9, Allyn and Bacon, Inc., Boston 1977.
6. T.J. Pinnavaia, C.L. Marshall, C.M. Mettler, C.L. Fisk, H.T. Miles and E.D. Becker, J.Amer. Chem.Soc., 100, 3625 (1978).
7. R. Shapiro, Progress in Nucleic Acid Research and Molecular Biology, 8, 73 (1968).

8. a) R. Barreswill, Compt. Rend. Acad. Sci., 53, 246 (1861).  
 b) A. Bethe, Z. Physiol. Chem., 20, 472 (1895)  
 c) G.H. Hitchings and E.A. Falco, Proc. Natl. Acad. Sci. U.S.A., 30, 294 (1944)
9. A. Albert and D.J. Brown, J. Chem. Soc., 400 (1954)
10. C.E. Bugg, Proceeding of the Jerusalem Symposia on Quantum Chemistry and Biochemistry, 4, 178 (1972).
11. a) U. Thewalt, C.E. Bugg and R.E. Marsh, Acta Cryst., B27, 2358 (1971).  
 b) C.E. Bugg, U. Thewalt and R.E. Marsh, Biochem. Biophys. Res. Comm., 33, 486 (1968).
12. a) W.M. Macintyre, P. Singh and M.S. Werkema, Biophys. J., 5, 697 (1965).  
 b) J. Sletten, E. Sletten and L.H. Jensen, Acta Cryst., B24 (1962).
13. a) P.O.P. Ts'O, M.P. Schweizer and D.P. Hollis, Ann. N.Y. Acad. Sci., 158, 256 (1969).  
 b) G. Felsenfeld and H.T. Miles, Ann. Rev. Biochem., 36, 407 (1967).  
 c) M.P. Schweizer, A.D. Broom, P.O.P. Ts'O and D.P. Hollis, J. Amer. Chem. Soc., 90, 1042 (1968).  
 d) S.J. Gill, M. Downing and G.F. Sheats, Biochemistry, 6, 272 (1967).
14. S. Hanlon, Biochem. Biophys. Res. Commun., 23, 861 (1966).
15. G. Gupta and V. Sasiskharan, Nucleic Acid Research, 5, 1639 (1978).
16. H.T. Miles, F.B. Howard and J. Frazier, Science, 142, 1458 (1963).
17. W. Guschlbauer, Proceedings of the Jerusalem Symposia on Quantum Chemistry and Biochemistry, 4, 297 (1972).
18. a) W. Kersten, Biochem. Biophys. Acta, 47, 610 (1961).  
 b) Y. Courtois, W. Guschlbauer and P. Fromageot, Eur. J. Biochem., 6, 107 (1968).
19. C. G. Reinhardt and T.R. Krugh, Biochemistry, 17, 4845 (1978) and references therein.
20. a) G.Y.H. Chu, S. Mansy, R.E. Duncan and R.S. Tobias, J. Amer. Chem. Soc., 100, 593 (1978).

- b) S. Mansy, G.Y.J. Chu, R.E. Duncan and R.S. Tobias, J. Amer. Chem Soc., 100, 607 (1978).
- c) S. Mansy, Ph.D. Thesis, Michigan State University, East Lansing, Mich., 1972.
- d) P.J. Stone, A.D. Kelman, F.M. Sinex, M.M. Bhargara and H.O. Halvorson, J. Molec. Biol., 104, 193 (1976).
- e) L.L Munchausen and R.O. Rahn, Biochim. Biophys Acta., 414, 242 (1975).
- 21. A.E.V. Haschemeyer and A. Rich, J. Mol. Biol., 27, 369 (1967).
- 22. F. Jordan and A. Pullman, Theor. Chim. Acta, 9, 242 (1968).
- 23. E.D. Bergman and H. Weiler-Feilchenfeld, Proceedings of the Jerusalem Symposia on Quantum Chemistry and Biochemistry, 4, 21 (1972).
- 24. R.B. Martin and Y.H. Mariam, Metal Ions in Biological Systems, 8, 57 (1979).
- 25. P.O.P. Ts'O, I.S. Melvin and A.C. Olson, J. Amer Chem. Soc., 85, 1289 (1963).
- 26. L. Katz and S. Penmen, J. Mol. Biol., 15, 220 (1966).
- 27. U. Thewall, C.E. Bugg and P.E. Marsh, Acta Cryst, B26, 1089 (1970).
- 28. T.N. Solie and J.A. Schellman, J. Mol. Biol., 33, 61 (1968).
- 29. A.L. Lehninger, "Biochemistry," Worth, New York, 1970, pg. 245.
- 30. W. Murayama, N. Nagashima and Y. Shimizu, Acta Cryst., B25, 2236 (1969).
- 31. D.F. Ashman, R. Lipton, M.M. Melicow and T.D. Price, Biochem and Biophy Res. Comm., 11, 330 (1963).
- 32. N.D. Goldberg, R.F. O'Dea and M.K. Haddox, Advances in Cyclic Nucleotide Research, 3, 155 (1973).
- 33. a) H. Rasmussen, Science, 170, 404 (1970).  
b) M.J. Berridge, Advances in Cyclic Nucleotide Research, 6, (1975).
- 34. A.L. Steiner, Shu-hui Ong and H. James Wedner, Advances in Cyclic Nucleotide Research, 7, 115 (1976).
- 35 a) H. Rasmussen, P. Jensen, W. Lake, N. Friedmann and D.B.P. Goodman, Advances in Cyclic Nucleotide Research, 5, 375 (1975).



- b) D.M. Biddulph and R.W. Wrenn, Journal of Cyclic Nucleotide Research, 3, 129 (1977).
36. a) J.J. Voorhees, E.A. Duell, M. Stawiski and E.R. Harrell, Advances in Cyclic Nucleotide Research, 4, 118 (1974).  
 b) J.J. Voorhees and E.A. Duell, Advances in Cyclic Nucleotide Research, 5, 735 (1975).
37. a) R.Gullis, J. Traber and B. Hemprecht, Science, 256, 57 (1975).  
 b) K.P. Minneman and L.L. Iverson, Nature, 262, 313 (1976).  
 c) M.L. Kohn, M. Kohn and F.H. Taylor, Science, 199, 319 (1978).
38. a) D.B. Farber and R.N. Lolley, Journal of Cyclic Nucleotide Research, 2, 139 (1976).  
 b) R.N. Lolley, D.B. Farber, M.E. Raybory and S.G. Hollyfield, Science, 196, 664 (1977).
39. a) E. Richelson, Nature, 266, 371 (1977).  
 b) G. Biggio and A. Guiditti, Nature, 265, 240 (1977).
40. a) R. Cumming, D. Eccleston and A. Steiner, Journal of Cyclic Nucleotide Research, 3, 275 (197 ).  
 b) G.J. Stewler and J. Orloff, Advances in Cyclic Nucleotide Research, 8, 311 (1977).  
 c) J. Bourgoignie, S. Guggenheim, M. Kipnes and S. Klahr, Science, 165, 1362 (1969).
41. a) P. Greengard, Nature, 260, 101 (1976).  
 b) J.W. Kebabian, Advances in Cyclic Nucleotide Research, 8, 421 (1977).  
 c) M. Katz and R.E. O'Dea, Science, 197, 174 (1977).
42. C.J. Coulson, R.E. Ford, S. Marshall, J.L. Walker, K.R.H. Woolridge, K. Bowder and T.J. Coombs, Nature, 265, 545 (1977).
43. J.D. Watson and F.H.C. Crick, Nature, 171, 737 (1953).
44. a) J. Pitha, R.N. Jones and P. Pithova, Can. J. Chem., 44, 1045 (1966).  
 b) Y. Kyogoku, R. Lord and A. Rich, Science, 154, 518 (1966).

- c) E. Kuchler and J. Derkosch, Z. Naturforsch., 21, 209 (1966).
- d) R.M. Hamlin Jr., R.C. Lord and A. Rich, Science, 148, 1734 (1965).
- 45. A.E.V. Haschemeyer and H.M. Sobell, Acta Cryst., 19, 125 (1965).
- 46. I. Bang, Bioch. Ztschr., 26, 293 (1910).
- 47. a) H.T. Miles and J. Frazier, Biochim Biophys. Acta, 79, 216 (1964).
- b) F.B. Howard and H.T. Miles, J. Biol. Chem., 240, 801 (1965).
- c) J.P.-Leicknam, C. Chauvelier, J.F. Chantot and W. Guschlbauer, Biophysical Chemistry, 134 (1973).
- 48. P.K. Sarkar and J.T. Yang, Biochem. Biophys. Res. Commun., 20, 346 (1965).
- 49. a) V. Gramlich, H. Klump, R. Herbeck and E.D. Schmid, FEBS Letters, 69, 15 (1976).
- b) E.W. Small and W.L. Peticolas, Biopolymers, 10, 1377 (1971).
- 50. C. Becker and T. Ackermann, Ber. Bunsenges. Phys. Chem., 77, 230 (1973).
- 51. a) S.B. Zimmerman, G.H. Cohen and D.R. Davies, J. Mol. Biol., 92,
- b) M. Gellert, M.N. Lipsett and D.R. Davies, Proc. Nat. Acad. Sci. U.S.A., 48, 2013 (1962).
- c) J. Iball, C.H. Morgan and H.R. Wilson, Nature, 199, 688 (1969).
- d) P. Tougard, J.F. Chantot and W. Guschlbauer, Biochim. Biophys. Acta, 308, 9 (1973).
- 52. H.T. Miles and J. Frazier, Biochem. Biophys. Res. Commun., 49, 199 (1972).
- 53. a) B. Pullman and A. Saran, Progress in Nucleic Acid Research and Molecular Biology, 18, 215 (1976).
- b) C. Giessner-Prettre and B. Pullman, J. Theor. Biol., 65, 189 (1977).
- c) C. Giessner-Prettre and B. Pullman, J. Theor. Biol., 65, 171 (1977).
- d) H. Berthod and A. Pullman, Theoret. Chim. Acta (Berl.), 47, 59 (1978).

54. J. Donohue and K. Trueblood, J. Mol. Biol., 2, 363 (1960)
55. M. Sundaralingam, Biopolymers, 1, 821 (1969).
56. S. Arnott, Progr. Biophys. Mol. Biol., 21, 256 (1970).
57. M. Sundaralingam, Proceeding of the Jerusalem Symposia on Quantum Chemistry and Biochemistry, 4, 44 (1972).
58. J.E. Kilpatrick, K.S. Pitzer and R. Spitzer, J. Amer. Chem. Soc., 69, 2483 (1947).
59. C. Altona and M. Sundaralingam, J. Amer. Chem. Soc., 94, 8205 (1972).
60. P.A. Hart and V.P. Davis, Proceedings of the Jerusalem Symposia on Quantum Chemistry and Biochemistry, 4, 297 (1973).
61. W. Guschlbauer and Y. Courtois, Fed. Eur. Biochem. Soc. Lett., 1, 183 (1968).
62. M.P. Schweizer, A.D. Broom, P.O.P. Ts'O and D.P. Hollis, J. Amer. Chem. Soc., 90, 1042 (1968).
63. S.S. Danluk and F.E. Hruska, Biochemistry, 7, 1038 (1968).
64. T.-D. Son, W. Guschlbauer and M. Gueron, J. Amer. Chem. Soc., 94, 7903 (1972).
65. T.-D Son and W. Guschlbauer, Nucleic Acid Research, 2, 873 (1975).
66. C.M. Dobson, C.F.G.C. Geraldles, G. Ratcliffe and P.J.P. Williams, Eur. J. Biochem., 88, 259 (1978).
67. T.-D Son, J. Thiery, W. Guschlbauer and J.-J. Dunand, Biochim. Biophys. Acta, 281, 289 (1972).
68. F. Jordan and H. Niv, Biochim. Biophys. Acta, 476, 265 (1977).
69. C. Giessner-Prettre and B. Pullman, Biochim. Biophys. Res. Commun., 70, 578 (1976).
70. D.B. Davies and S.S. Danyluk, Biochemistry, 13, 4417 (1974).
71. D.B. Davies and S.S. Danyluk, Biochemistry, 14, 543, (1975).
72. K.N. Slessor and A.S. Tracey, Carbohydrate Research, 27, 407 (1973).
73. D.J. Wood, R.J. Mynott, F.G. Hruska and R.H. Sarma, Fed. Eur. Biochem. Soc. Lett., 34, 323 (1973).

74. A.K. Chwang and M. Sundaralingam, Acta Cryst., B30, 1233 (1974).
75. R.D. Lapper, H.H. Mantsch and I.C.P. Smith, J. Amer. Chem. Soc., 95, 2878 (1973).
76. R. Tewari and S.S. Danyluk, Biopolymers, 17, 118 (1978).
77. R.D. Lapper and I.C.P. Smith, J. Amer. Chem. Soc., 95, 2880 (1973).
78. a) J. Iball and H.R. Wilson, Proc. Roy. Soc., Ser. A, 288, 418 (1965).  
       b) L.G. Purnell and D.J. Hodgson, J. Amer. Chem. Soc., 98, 4759 (1976)
79. E. Sletten and N. Flogstad, Acta Cryst., B32, 461 (1976).
80. L. Srinivasan and M. Taylor, Chem. Commun., 1668 (1970).
81. a) M. Sundaralingam and J.A. Carrabine, J. Molec. Biol., 61, 287 (1971).  
       b) J.A. Carrabine and M. Sundaralingam, J. Amer. Chem. Soc., 92, 369 (1970).  
       c) J.P. DeClerq, M. Debbaudt and M. Van Meersche, Bull. Soc. Chim. Belges, 80, 527 (1971).
82. R.W. Gellert and R. Bau, J. Amer. Chem. Soc., 97, 7379 (1975).
83. P. deMeester, D.M.L. Goodgame, A.C. Skapski and B.T. Smith, Biochim. Biophys. Acta, 340, 113 (1974).
84. P. deMeester, D.M.L. Goodgame, T.J. Jones and A.C. Skapski, C.R. Acad. Sci. Paris, Series C, 279, 667 (1974).
85. P. deMeester, D.M.L. Goodgame, T.J. Jones and A.C. Scapski, Biochem. J., 139, 791 (1974).
86. K. Aoki, Acta Cryst., B32, 1454 (1976).
87. a) G.C. Clark, J.D. Orbell and K. Aoki, Acta Cryst., B34, 2119 (1978).  
       b) B.S. Reddy and M.A. Viswamitra, Cryst Struct. Commun., 2, 9 (1976).
88. a) D.W. Young, P. Tollins and H. R. Wilson, Acta Cryst., B30, 2012 (1974).

- b) B.S. Reddy and M.A. Viswamitra, Cryst. Struct. Commun., 2, 9 (1973).
- c) T.P. Seshadri and M.A. Viswamitra, Pramana, 4, 218 (1974).
- d) N.S. Mandel and G.S. Mandel, J. Amer. Chem. Soc., 98, 2319 (1976).
- e) O. Kennard, N.W. Isaacs, W.D.S. Motherwell, J.C. Coppola, D.L. Wampler, A.C. Larson and D.G. Watson, Proc. R. Soc. Lond., A325, 401 (1971).
- f) K.N. Trueblood and E. Shefter, Acta Cryst., 18, 1067 (1965).
- g) N. Camerman, A. Camerman and U.K. Fawcett, J. Mol. Biol., 107, 601 (1976).
- h) A. Rich, J.J.P. Kim, E.L. Suddath, J.M. Rosenberg and N.C. Seeman, J. Mol. Biol., 104, 109 (1976).
- i) A. Rich, H.B. Nicholas, F.L. Suddath, J.J.P. Kim, N.C. Seeman and J.M. Rosenberg, Nature, 243, 150 (1973).
- j) A. Rich, J.M. Rosenberg, N.C. Seeman, R.O. Day, Proc. Nat. Acad. Sci., 70, 849 (1973).
- 89. J.M. Rosenberg, N.C. Seeman, R.O. Day and A. Rich, J. Mol. Biol., 104, 145 (1976).
- 90. T. Sato, S.B. Broyde and R. Landridge, Acta Cryst. B32, 2998 (1976).
- 91. S.M. Wang and N.C. Li, J. Amer. Chem. Soc., 88, 4592 (1966).
- 92. S.M. Wang and N.C. Li, J. Amer. Chem. Soc., 90, 5069 (1968).
- 93. L.S. Kan and N.C. Li, J. Amer. Chem. Soc., 92, 4823 (1970).
- 94. K.W. Jennette, S.J. Lippard and D.A. Ucko, Biochem. Biophys. Acta, 402, 403 (1975).
- 95. R.B. Jordan and B.F. McFarquhar, J. Amer. Chem. Soc., 94, 6557 (1972).
- 96. S. Shimokawa, H. Fukui, J. Sohma and K. Hotta, J. Amer. Chem. Soc., 95, 1777 (1973).
- 97. C.H. Chang and L. G. Marzilli, J. Amer. Chem. Soc., 96, 3656 (1974).
- 98. T. Yokono, S. Shimokawa and J. Sohma, J. Amer. Chem. Soc., 97, 3827 (1975).

99. M. Sundaralingam, Proceeding of the Jerusalem Symposia on Quantum Chemistry and Biology, 5, 417 (1973).
100. J.-F. Chantot, M.T. Sarocchi and W. Guschlbauer, Biochimie, 53, 347 (1971).
101. J.-F. Chantot and W. Guschlbauer, Proceedings of the Jerusalem Symposia on Quantum Chemistry and Biochemistry, 4, 205 (1972).
102. J.-M. Delabar and W. Guschlbauer, Biopolymers, 18, 2073 (1979).
103. J.-F. Chanton and W. Guschlbauer, FEBS. Letters, 4, 183 (1969).
104. R.A.G. deGraaff, F.B. Martens and C. Romers, Acta Cryst, B34, 3012 (1978).
105. T.J. Pinnavaia, H.T. Miles and E.D. Becker, J. Amer. Chem. Soc., 97, 7198 (1975).
106. V.P. Strauss and D.P. Ross, J. Amer. Chem. Soc., 81, 5295 (1959).
107. a) J. Botts, A. Chasin and H.L. Young, Biochemistry, 4, 1788(1965).  
b) R.M. Smith and R.A. Alberty, J. Phys. Chem., 60, 180 (1956).
108. P.D. Ross and R.L. Scruggs, Biopolymers, 2, 79 (1964).
109. a) M.R. Truter, Struct. Bonding (Berlin), 16, 71 (1973).  
b) J.-M. Lehn, Struct. Bonding (Berlin), 16, 1 (1973).
110. C.L. Marshall, M.S. Thesis, Michigan State Univ., E.L., Mich., 1977.
111. S.B. Zimmerman, J. Mol. Biol., 106, 663 (1976).
112. C. Giessner-Prettre, B. Pullman, P.N. Borer, L.-S. Kan and P.O.P. Ts'0, Biopolymers, 15, 2277 (1976).
113. C.L. Fisk, E.D. Becker, H.T. Miles, T.J. Pinnavaia and C.L. Marshall, in preparation.
114. H. Klump, Ber. Bunsenges. Phys. Chem., 80, 121 (1976).
115. a) A. Delville, C. Detellier and P. Laszlo, Journal of Magnetic Resonance, 34, 301 (1979).  
b) C. Detellier, A. Paris and P. Laszlo, Compt. Rend. Ac. Sci. Paris, Series D., 286, 781 (1978).  
c) A. Paris and P. Laszlo, Compt. Rend. Ac. Sci. Paris, Series D, 286, 717 (1978).

- d) M. Borzo and P. Laszlo, Compt. Rend. Ac. Sci. Paris, Series C, 287, 475 (1978).
- e) C. Detellier and P. Laszlo, Helvetica Chimica Acta, 62, 1559 (1979).
- 116. a) A. Yamada, K. Akasaka and H. Hatano, Biopolymers, 17, 749 (1978).
- b) D.M. Gray and F.J. Bollum, Biopolymers, 13, 2087 (1974).
- c) M. Hattri, J. Frasier and H.T. Miles, Biochemistry, 14, 5033 (1975).
- d) F.B. Howard, J. Fraiser and H.T. Miles, Biopolymers, 16, 791 (1977).
- 117. R. Savoie, H. Klump and W.L. Peticolas, Biopolymers, 17, 1335 (1978).
- 118. M.N. Lipsett, J. Biol. Chem., 239, 1250 (1964).
- 119. J.F. Chantot, T. Haertle and W. Guschlbauer, Biochimie, 56, 501 (1974).
- 120. K.B. Roy, J. Frazier and H.T. Miles, in press.
- 121. J. Frazier and H.T. Miles, J. Amer. Chem. Soc., 100, 8037 (1978).
- 122. B. Pullman and A. Pullman, "Metal-Ligand Interactions in Organic Chemistry and Biochemistry," Part 1, pg. 65, Reidel Publishing, Dordrecht-Holland, 1977.
- 123. B. Pullman, A. Goldblum and H. Berthod, Biochem. Biophys. Res. Commun., 77, 1166 (1977).
- 124. B. Pullman, N. Gresh, H. Berthod and A. Pullman, Theoret. Chim. Acta (Berl.), 44, 151 (1977).
- 125. A.T. Tu and J.A. Reinos, Biochem., 5, 3375 (1966).
- 126. J.D. Glickson, S.L. Gordon, T.P. Pitner, D.G. Agresti and R. Walter, Biochemistry, 15, 5721 (1976).
- 127. S.J. Leach, G. Nemethy and H.A. Scheraga, Biochem. and Biophys. Res. Commun., 75, 207 (1977).
- 128. M. Rastka and N.O. Kaplan, Proc. Nat. Acad. Sci. U.S.A., 69, 2025 (1972).

129. P.H. Bolton and D.R. Kearns, J. Amer. Chem. Soc., 101, 479 (1979).
130. N.C. Seeman, J.M. Rosenberg, F.L. Suddath, J.J.P. Kim, A. Rich, J. Mol. Biol., 104, 109 (1976).
131. O. Kennard, N.W. Isaacs, W.D.S. Motherwell, J.C. Coppola, D.L. Wampler, A.C. Larson and D.G. Watson, Proc. R. Soc. London. A, 325, 401 (1971).
132. Personal communication with H.T. Miles, E.D. Becker, C. Fisk and D. Raiford.
133. A.H.-J. Wang, G.J. Quigley, F.J. Kolpak, J.L. Crawford, J.H. vanBoom, G. Vander Merel and A. Rich, Nature, 282, 680 (1979).



## APPENDIX A

Figure 73. A comparison of 0.72 M Na<sub>2</sub>GMP and 0.72 M Li<sub>2</sub>GMP at 2° C.

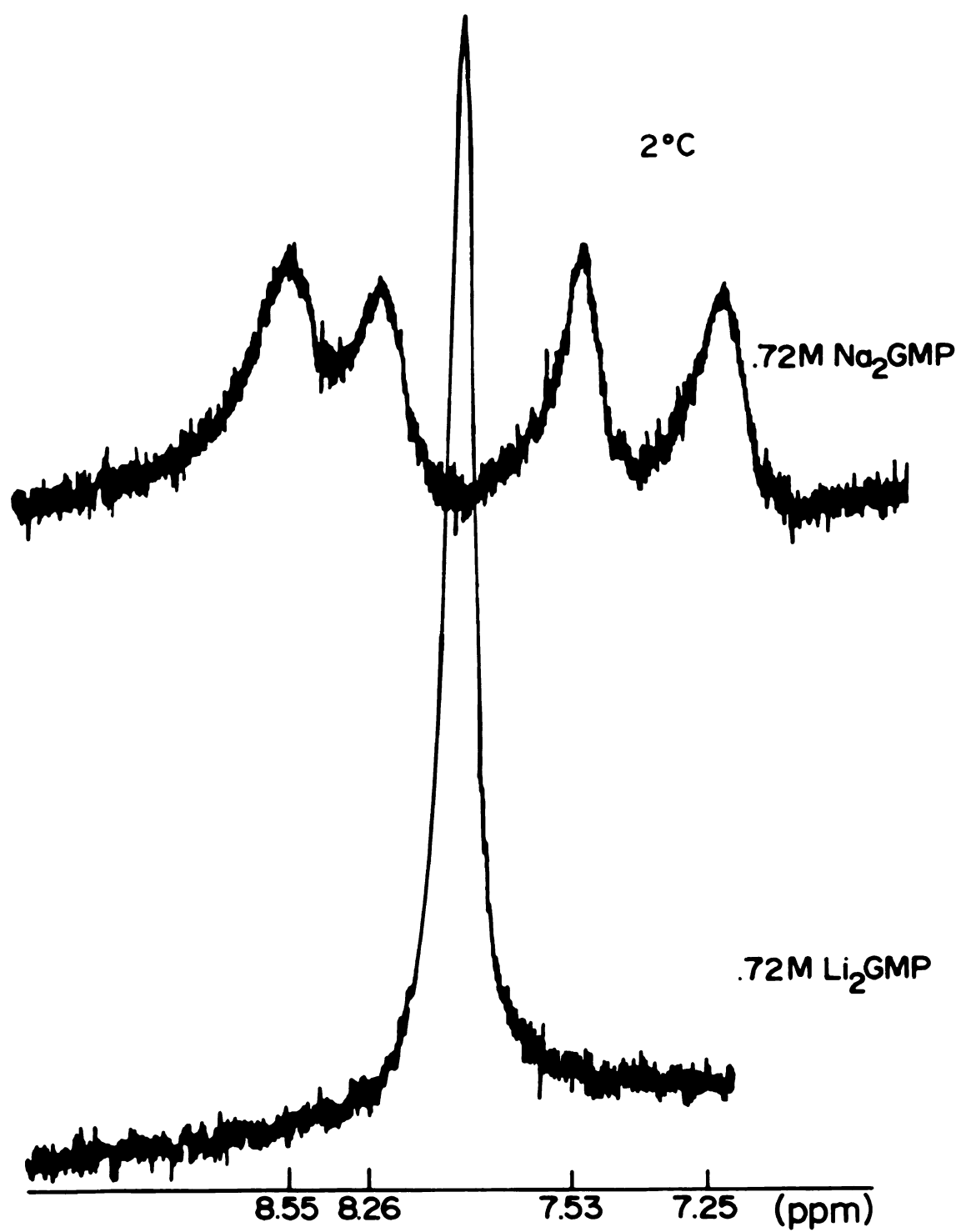


Figure 74. A temperature profile of 0.72 M Na<sub>2</sub>GMP from 2-30° C.

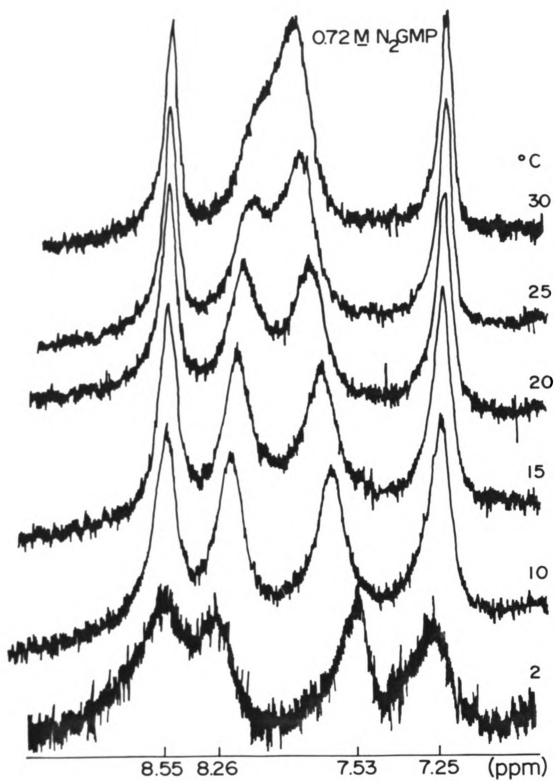


Figure 75. A temperature profile of 0.72 M Na<sub>2</sub>GMP from 35-45° C.

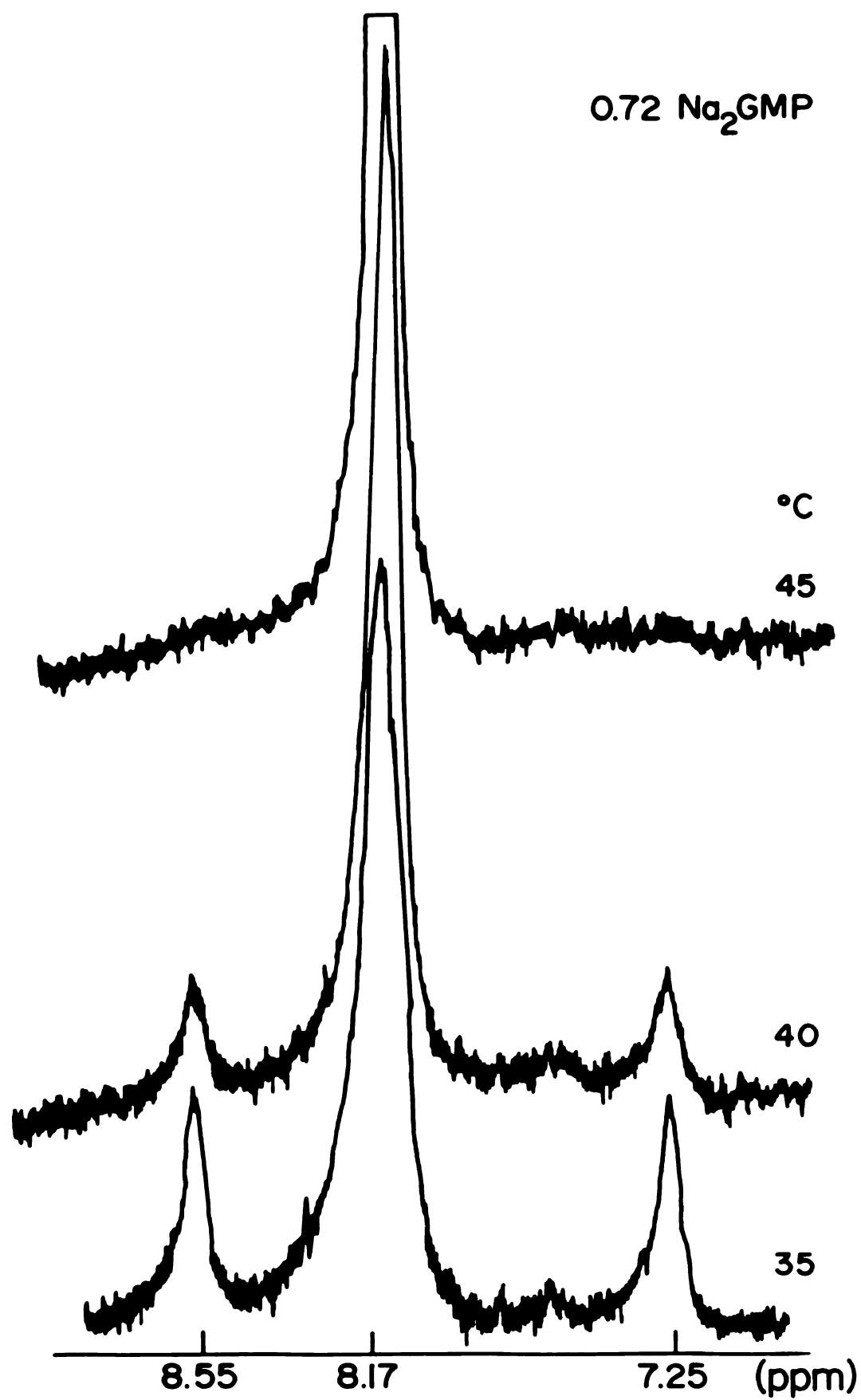


Figure 76. A temperature profile of a 0.72 M  $\text{GMP}^{2-}$  solution containing 12.5%  $\text{Na}^+$  and 87.5%  $\text{Li}^+$ .



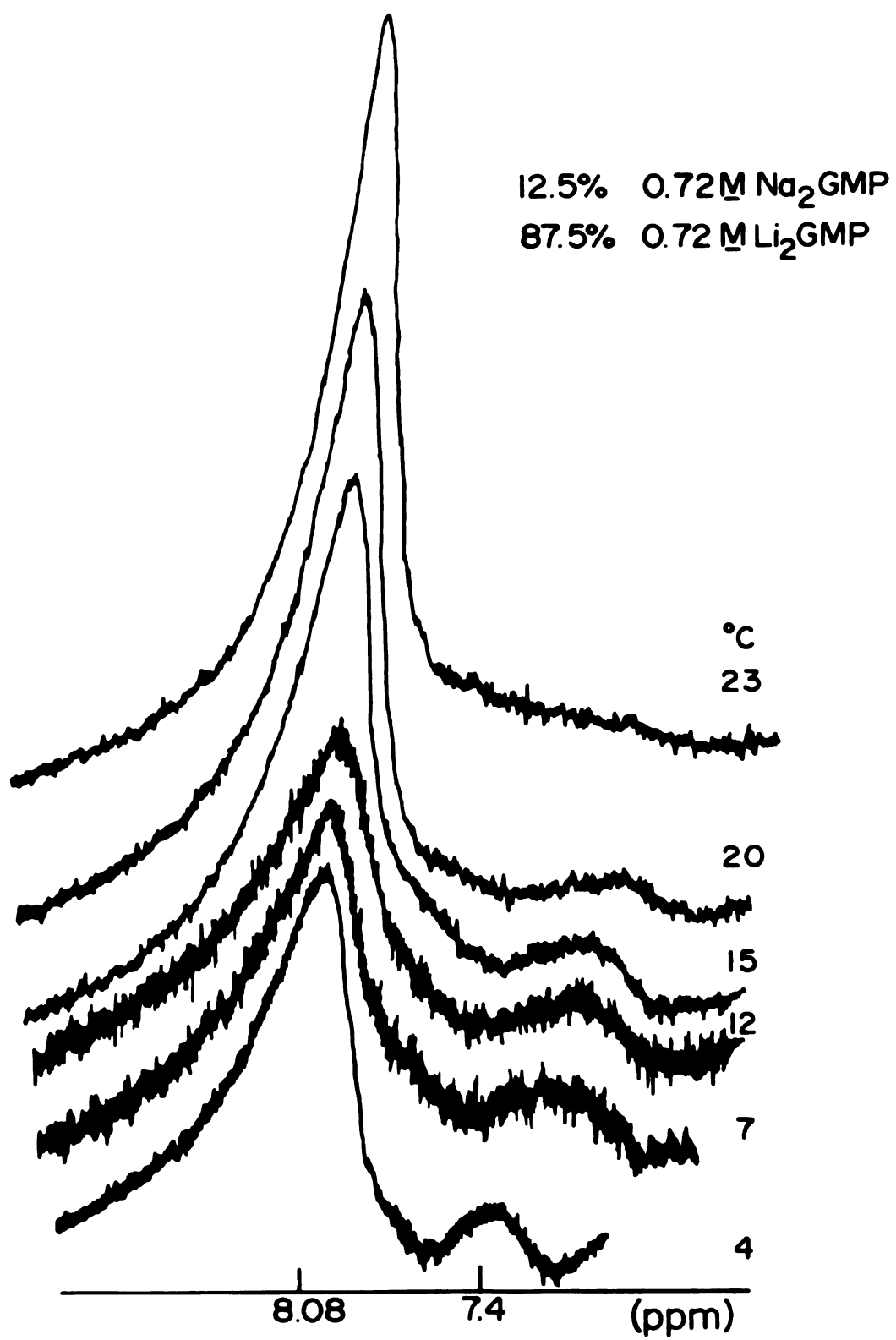


Figure 77. A temperature profile of a 0.72 M  $\text{GMP}^{2-}$  solution containing 25%  $\text{Na}^+$  and 75%  $\text{Li}^+$ .

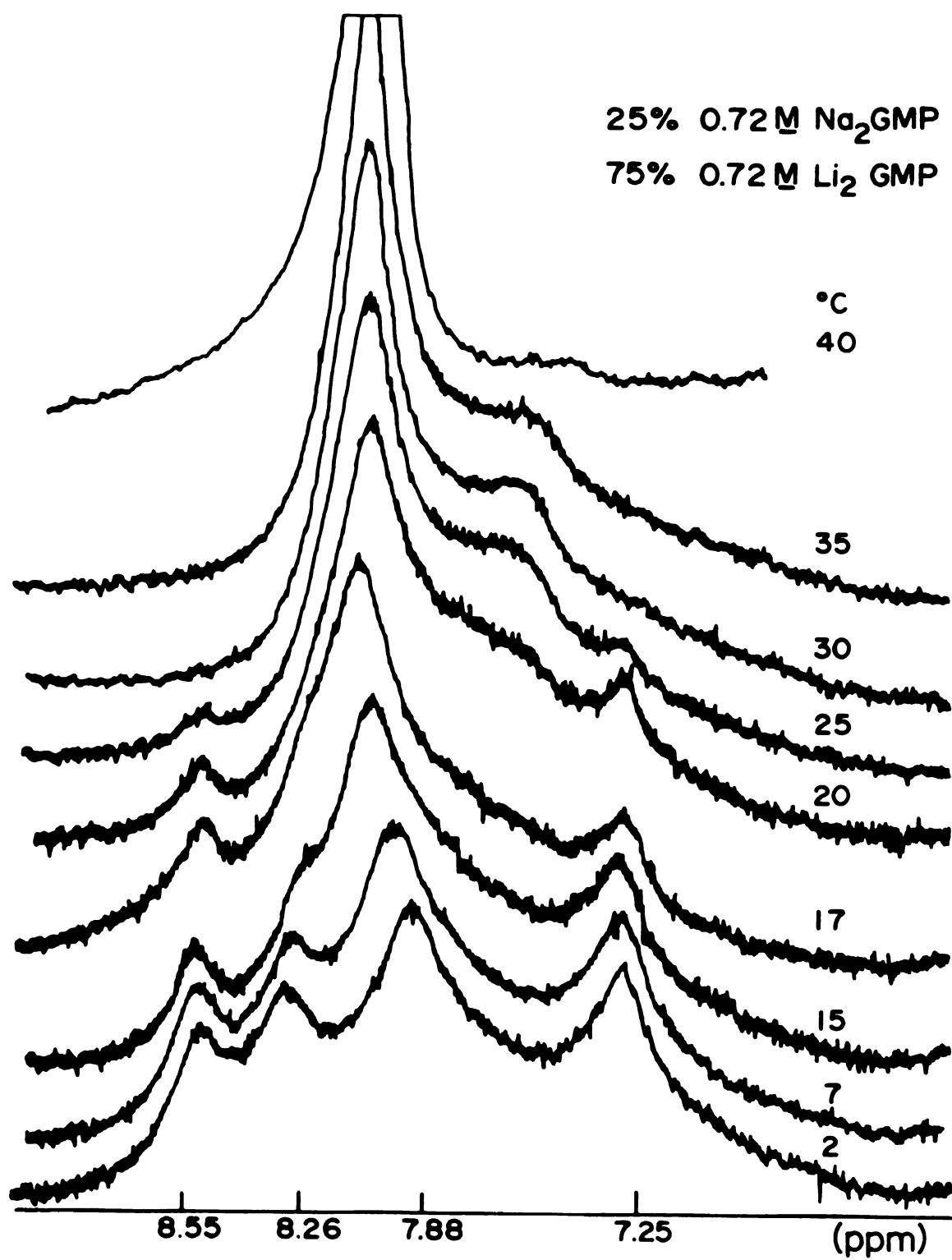


Figure 78. A temperature profile from 2-30° C of a 0.72 M GMP<sup>2-</sup> solution containing 37.5% Na<sup>+</sup> and 62.5% Li<sup>+</sup>.

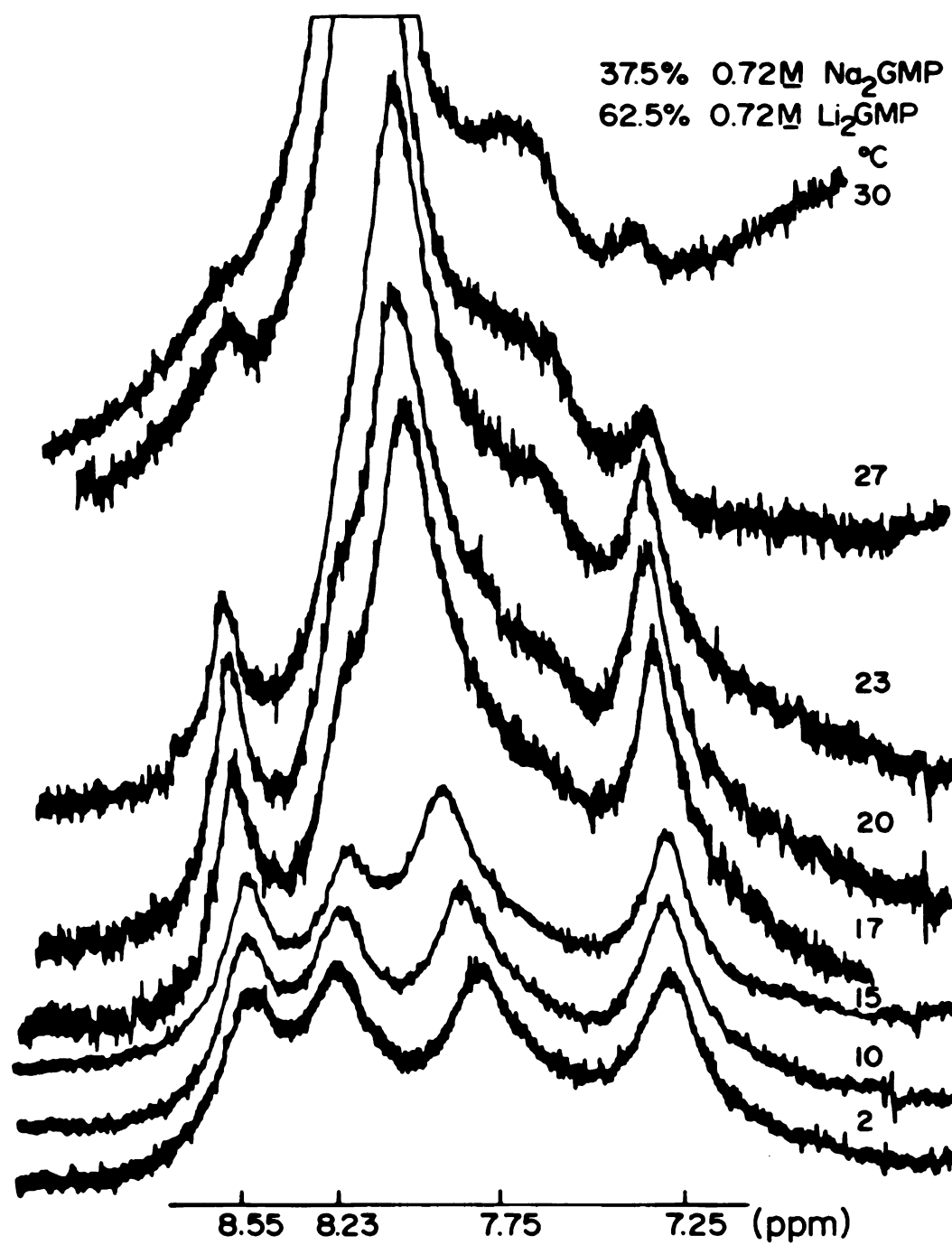


Figure 79. A temperature profile from 35-45° C of a 0.72 M  $\text{GMP}^{2-}$  solution containing 37.5%  $\text{Na}^+$  and 62.5%  $\text{Li}^+$ .

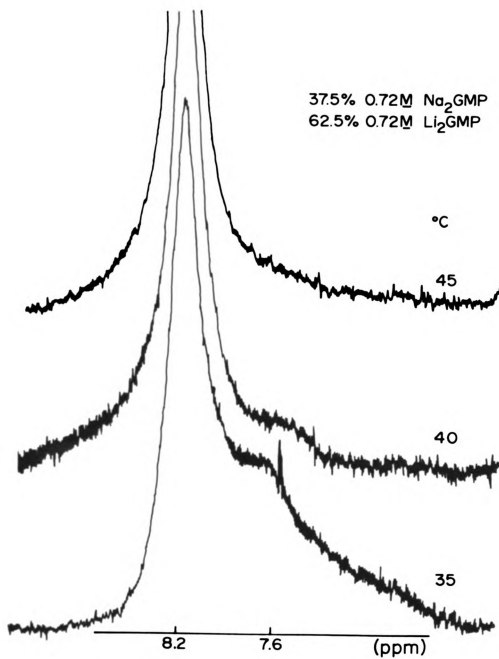


Figure 80. A temperature profile of a 0.72 M  $\text{GMP}^{2-}$  solution containing 50%  $\text{Na}^+$  and 50%  $\text{Li}^+$ .



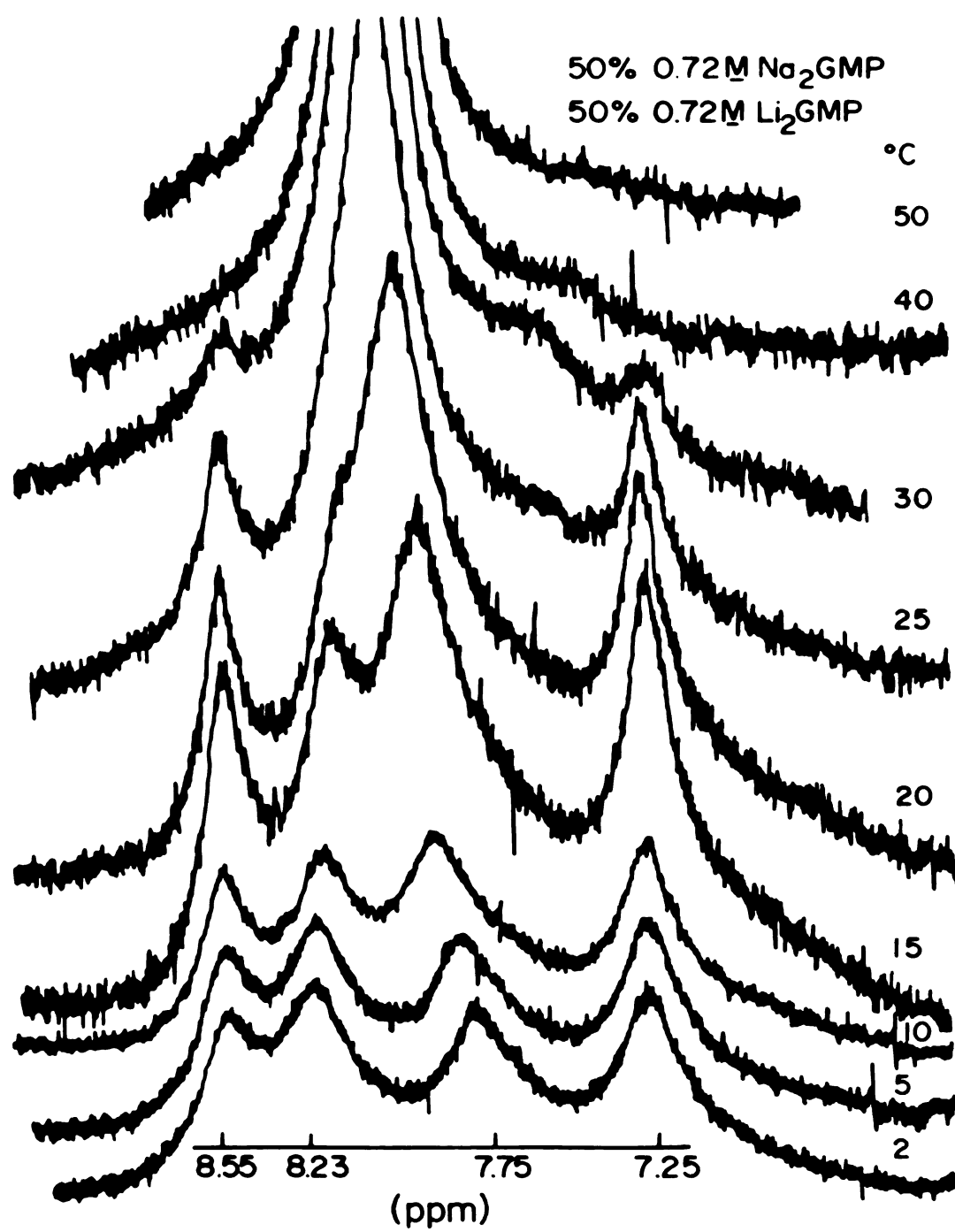


Figure 81. 0.72 M  $\text{GMP}^{2-}$  solutions containing different ratios of  $\text{Na}^+$  to  $\text{Li}^+$  at  $2^\circ \text{C}$ .

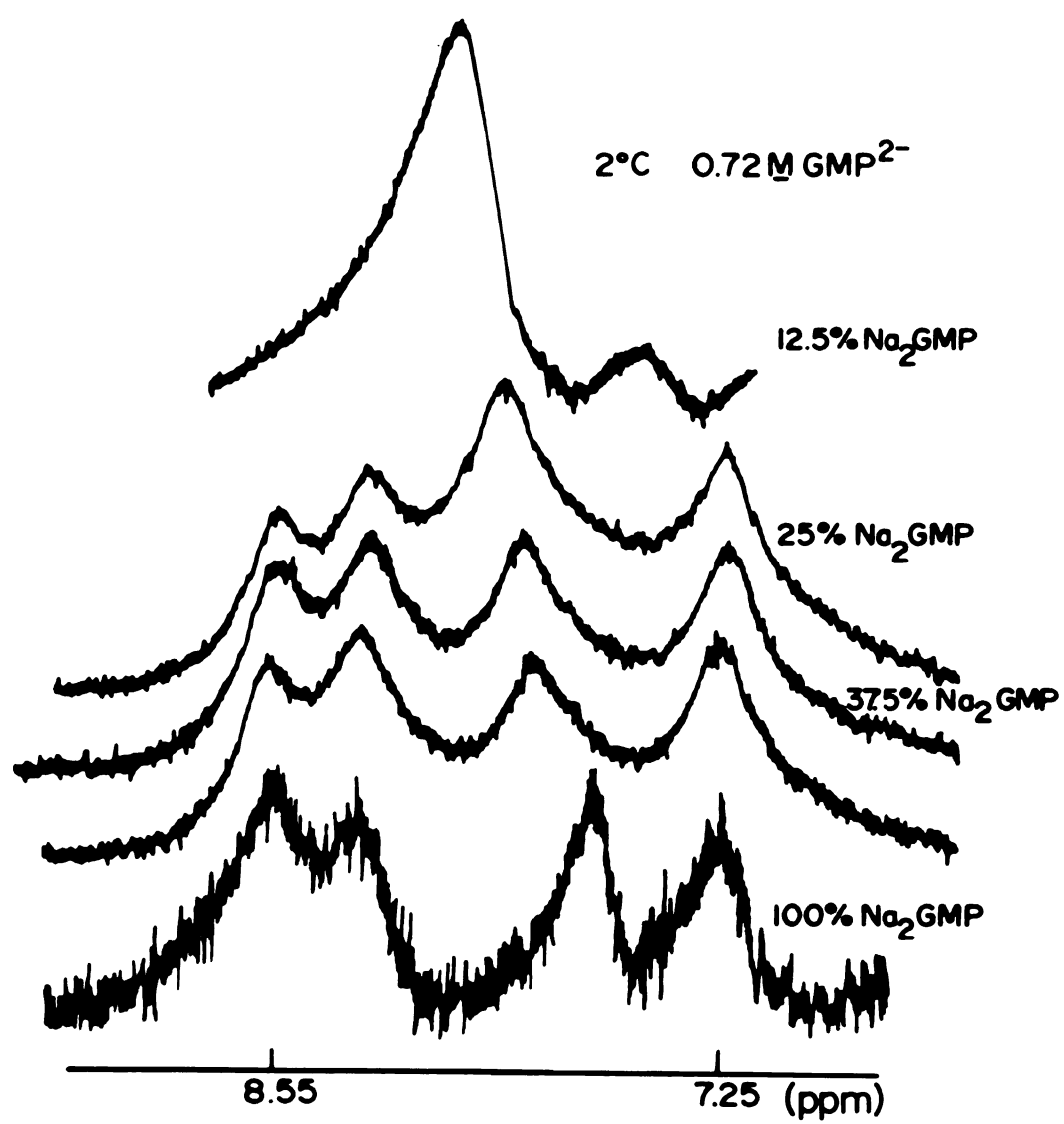


Figure 82. 0.72 M  $\text{GMP}^{2-}$  solutions containing different ratios of  $\text{Na}^+$  to  $\text{Li}^+$  at 15° C.

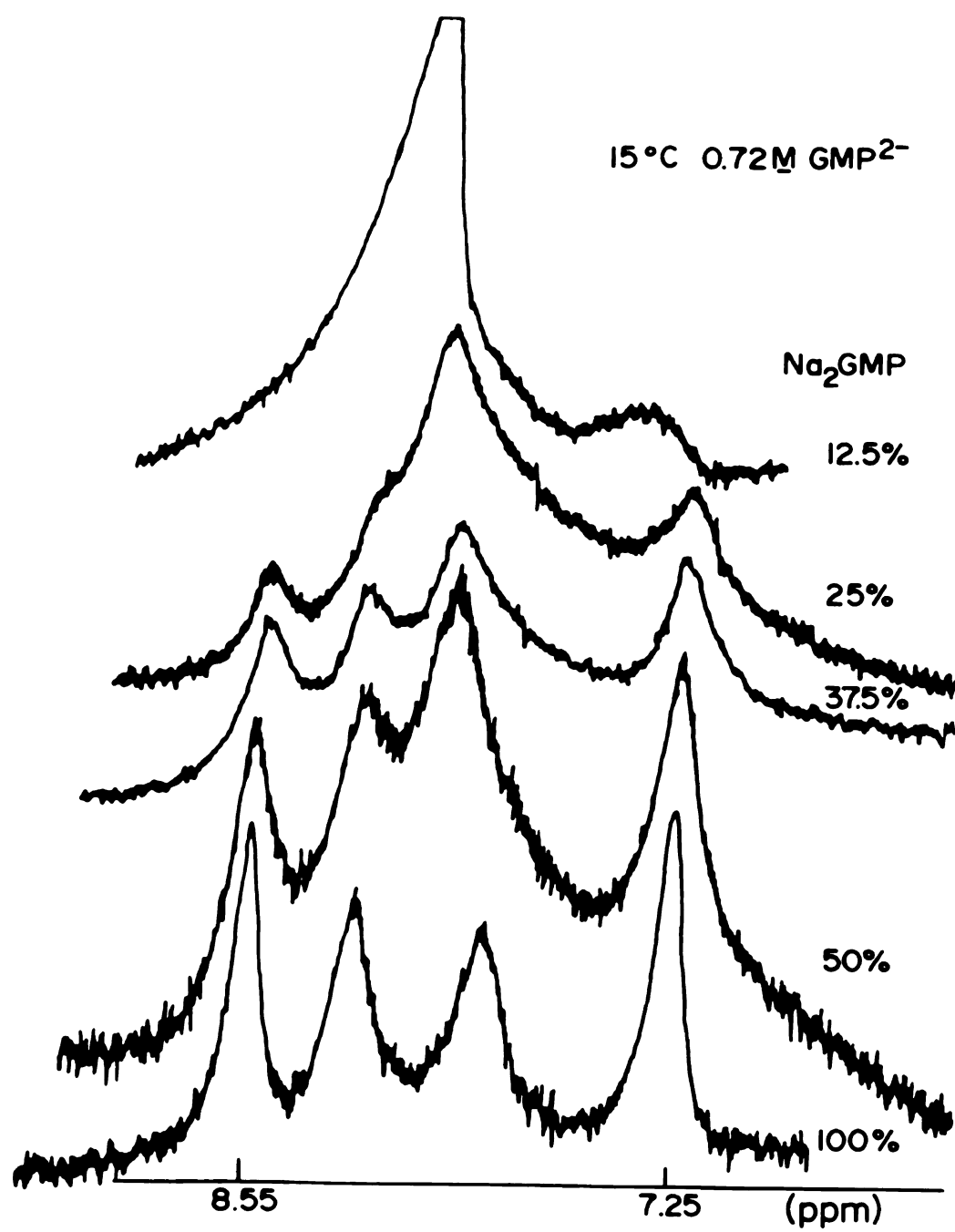


Figure 83. 0.72 M  $\text{GMP}^{2-}$  solutions containing different ratios of  $\text{Na}^+$  to  $\text{Li}^+$  at 20° C.

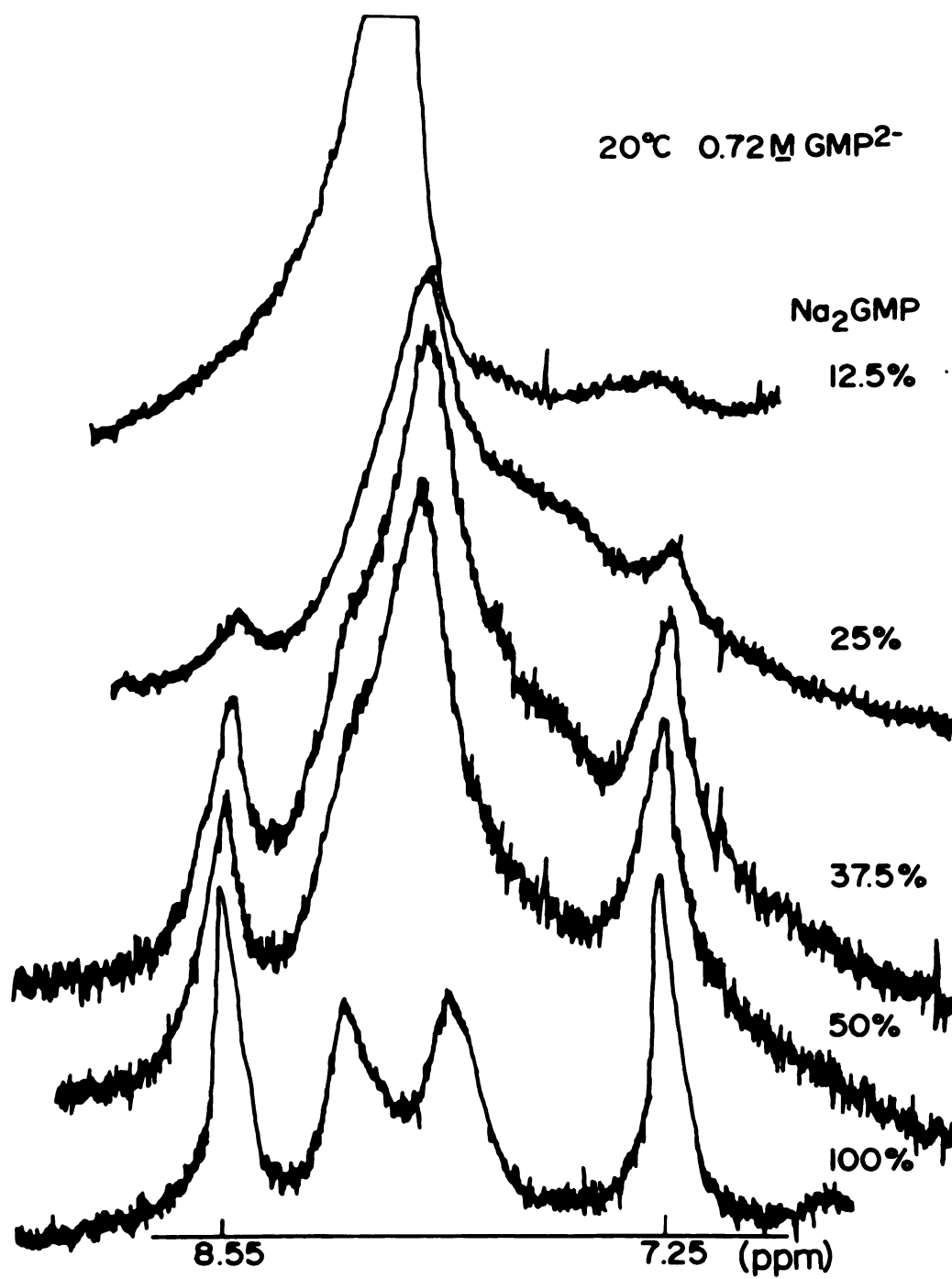
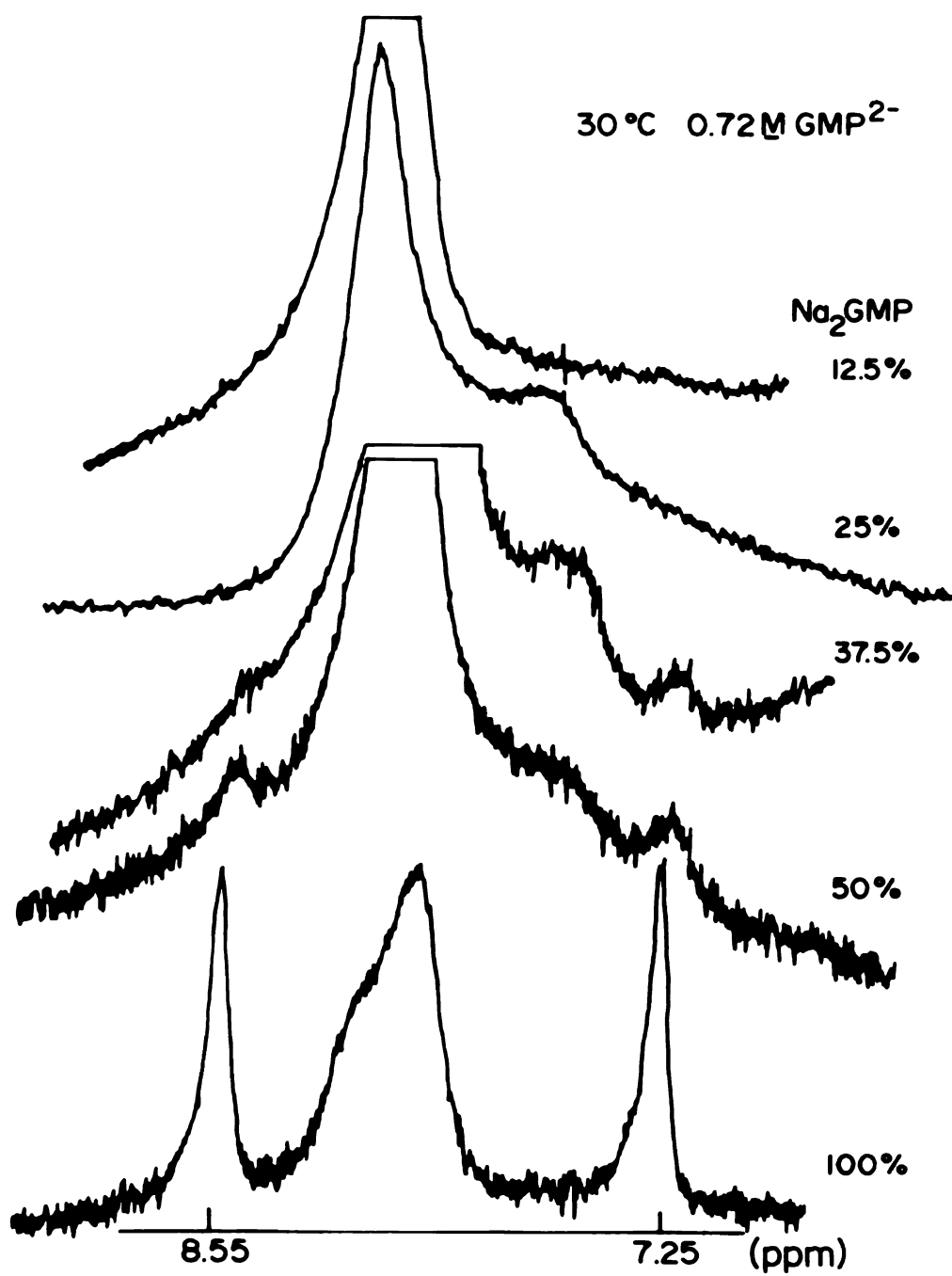


Figure 84. 0.72 M  $\text{GMP}^{2-}$  solutions containing different ratios of  $\text{Na}^+$  to  $\text{Li}^+$  at  $30^\circ \text{C}$ .





## APPENDIX B

Figure 85. A 0.76 M Na<sub>2</sub>GMP solution containing 10% Tl<sup>+</sup> at 2° C.

